# MOLECULAR STUDIES ON THE ENERGY-TRANSDUCING ATP SYNTHASE

A Thesis

Submitted for the Degree

of

Doctor of Philosophy

of

The Australian National University

Andrew John William Rodgers
October, 1995

Membrane Biochemistry Group
Division of Biochemistry and Molecular Biology
John Curtin School of Medical Research
Australian National University

NO PAGE 160. TEXT O.K.

# STATEMENT

The work described in this Thesis was performed by the author, except where specifically stated in the text

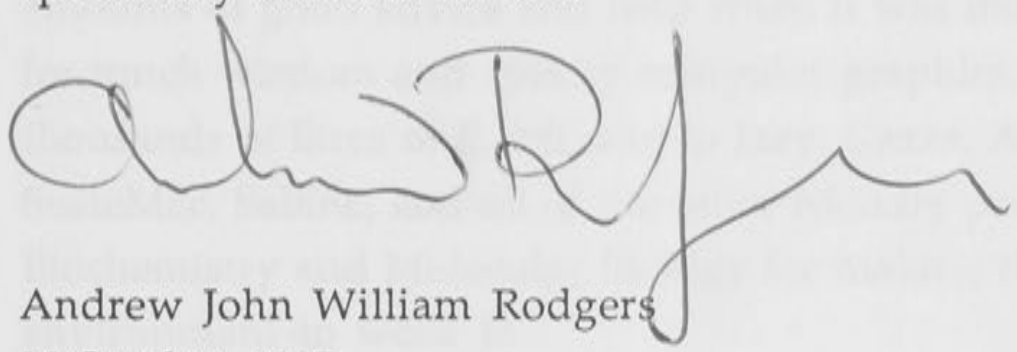

Andrew John William Rodgers
30 October, 1995

# ACKNOWLEDGEMENTS

First and foremost, I wish to thank my supervisors, Professor Graeme Cox and Dr. Susan Howitt, for advice, support and understanding above and beyond the call of duty. My deepest gratitude goes to both of you.

Thankyou to the wonderful co-habitants of the students lab, where the music is loud, the gossip is spicy, the plants are hungry and the science is on the cutting edge; thankyou to Brett for cross-country ski trips, the best way to put the troubles of difficult experiments as far to the back of the mind as possible; to Louise for being a kind and generous guru, and for the supply of Toblerones marking the Aussies continued dominance over the Kiwis in every sporting arena; and to Robyn for always being 110% Robyn.

Thanks to everyone in the Membrane Biochemistry Group, the best group a student could ever hope to be part of. Thanks to Lyndall for vast amounts of good advice and help when it was most needed, to Frank Gibson for much wisdom and spekky computer graphics, to Russell for countless thousands of litres of *E. coli*, and to Izzy, Gazza, Aunty Di, Bazza, Shelley, SusieMac, Sabine, and all of the other friendly people of the Division of Biochemistry and Molecular Biology for making the place such a happy environment to work in.

Thankyou to close friends for support and companionship and fun group-houses; Tony Willis, Steven Hoy, Susan Downing, Judy Toman (and her wonderful family), Jimmy Popple, Paula Fearn, Ian Collins, Ailsa Carruthers, Juliet Fisher and Kerrin Anderson, to name but a few.

Thanks and no thanks to the players, coaching staff and administration of the Geelong Football Club, for the ecstasy of four grand-final appearances in the last seven years, and the agony of no premierships.

Thankyou to my parents and sisters for their love, and for hanging in there with emotional support whilst wondering what would become of me, and for Sunday night roast dinners so that at least once a week mum would know I've eaten properly!

Last but not least, thankyou to sweet Sonja, for love and patience over the last eighteen months; I hope I can repay your kindness.

# ABSTRACT

Three sections of work are described in this thesis. The first section was concerned with the expression of spinach chloroplast $F_OF_1$-ATPase subunits in *E. coli*, to test whether these might be able to functionally replace homologous *E. coli* subunits. The second section was concerned with the expression of spinach chloroplast, cyanobacterial and *E. coli* $F_OF_1$-ATPase subunits as fusion proteins with glutathione-S-transferase (GST), along with combinations of other $F_OF_1$-ATPase subunits, with the aim of purifying multi-subunit complexes. The third section involved a detailed examination of the biochemical and physical properties of wild-type and mutant forms of the hydrophilic domain of the *E. coli b*-subunit.

Complementation experiments involved the plasmid-borne expression of genes encoding spinach chloroplast $F_OF_1$-ATPase subunits in mutant *E. coli* strains deficient in the corresponding subunit. This was carried out in the hope that an experimental system could be developed to probe the structure and function of the foreign subunit in a functional hybrid $F_OF_1$-ATPase complex. However, none of the chloroplast subunits complemented to a significant degree. Results confirmed reports from other workers that chloroplast subunits $CF_OII$ and γ are unable to functionally replace homologous *E. coli* subunits, but that the δ-subunit could complement, albeit poorly. An outcome from the complementation analysis was the correction of a report in the literature claiming that chloroplast subunit $CF_OI$ could functionally replace the *E. coli b*-subunit. This was shown conclusively not to be the case.

Studies involving the expression of spinach chloroplast $F_OF_1$-ATPase subunits as fusions with GST were hampered by the insolubility of most of the fusions in *E. coli*. However, the GST-chloroplast ε-subunit fusion was found to be soluble and the further refinement of purification procedures should yield valuable structural information on this protein. Studies on fusions of GST and cyanobacterial $F_OF_1$-ATPase subunits met with greater success. Fusions of the γ-subunit and the hydrophilic domains of the *b*- and *b´*-subunits were found to be soluble and could be purified by glutathione affinity chromatography. Interestingly, the cyanobacterial δ-subunit was found to possibly play a role in stabilising the structure of the hydrophilic domain of the *b*-subunit.

Studies on *E. coli* $F_OF_1$-ATPase subunits expressed as GST fusions were primarily aimed initially at the investigation of interactions between the hydrophilic domain of the *b*-subunit and $F_1$-subunits proposed to exist according to models for assembly and functional mechanism of the enzyme (Cox *et al.*, 1981; 1984; 1986). The α- and β-subunits were found to co-purify with a fusion of GST and the *b*-subunit hydrophilic portion, suggesting that the α-, β- and *b*-subunits may interact *in vivo*.

Using the GST fusion expression system, large quantities of wild-type and mutant (A128D) forms of the *b*-subunit hydrophilic domain were prepared in high purity. The mutation A128D had been shown to cause loss of $F_OF_1$-ATPase function *in vivo* by disrupting assembly (S. M. Howitt,personal communication). In a previous study of the wild-type form of the *b*-subunit hydrophilic portion (Dunn, 1992), this protein was found to be dimeric and highly extended in structure, was capable of binding to the $F_1$-ATPase, and was found to have a high content of α-helical secondary structure. Results in this study confirm these findings, and show that a single mutation, A128D, is sufficient to prevent dimerisation of the *b*-subunit hydrophilic portion, to prevent binding to the $F_1$-ATPase, and to decrease significantly the amount of α-helical secondary structure. Hydrodynamic measurements suggest that the wild-type dimeric protein has double the axial ratio of the mutant monomeric protein. In an attempt to reconcile these findings with information presently available regarding the structure of the *E. coli* $F_OF_1$-ATPase, a new model for the structure and function of the *b*-subunit is presented. The model for rotational catalysis proposed by Cox *et al.* (1986) is modified such that the *b*-subunit interacts with the α-, β- and *c*-subunits to form the stator, rather than forming part of the inner rotating complex with the *a*-, γ-, δ- and ε-subunits.

# TABLE OF CONTENTS

## CHAPTER 1

### INTRODUCTION



## CHAPTER 2

### MATERIALS AND METHODS

# CHAPTER 3

## COMPLEMENTATION STUDIES ON GENES ENCODING SPINACH CHLOROPLAST ATP SYNTHASE SUBUNITS EXPRESSED IN *E. coli.*

# CHAPTER 4

## STUDIES ON SPINACH CHLOROPLAST AND *SYNECHOCOCCUS* R2 ATP SYNTHASE SUBUNITS EXPRESSED AS FUSION PROTEINS WITH GLUTATHIONE-*S*-TRANSFERASE

# CHAPTER 5

## STUDIES ON *ESCHERICHIA COLI* ATP SYNTHASE SUBUNITS EXPRESSED AS FUSION PROTEINS WITH GLUTATHIONE-*S*-TRANSFERASE

# CHAPTER 6

## PHYSICAL CHARACTERISATION OF WILD-TYPE AND MUTANT FORMS OF THE SOLUBLE PORTION OF THE *E. coli b*-SUBUNIT



# CHAPTER 7

# CHAPTER 1

# INTRODUCTION

## 1.1 Introduction

The metabolism of all living cells includes processes and enzymic reactions which would be thermodynamically unfavourable without the input of free energy. These include mechanical work, the transport of molecules and ions, and the synthesis of macromolecules from simple precursors. To overcome the thermodynamic barrier, most of these reactions are coupled with a highly exergonic reaction, the hydrolysis of the β–γ phosphodiester bond of adenosine 5′-triphosphate (ATP). The hydrolysis of ATP yields about 30 kJ/mol at pH 8, 1 mM $Mg^{2+}$ (Rosing and Slater, 1972).

The need to maintain an adequate pool of ATP for growth and activity requires that all cells possess an efficient system for regenerating ATP from the products of its hydrolysis, ADP and $P_i$. A small fraction of total ATP synthesis may be accounted for by substrate level phosphorylation, in which ATP is formed as a by-product of metabolic reactions such as those in gycolysis (Nicholls and Ferguson, 1992). By far the majority of ATP synthesised in cells is generated by the processes of oxidative phosphorylation (which occurs in many prokaryotes and the mitochondria of eukaryotes) and photophosphorylation (which occurs in photosynthetic organisms; Nicholls and Ferguson, 1992).

Oxidative phosphorylation is the process by which the synthesis of ATP is coupled to the oxidation of reduced co-factors such as NADH or $FADH_2$, or metabolic intermediates such as succinate or α-glycerophosphate. In the closely related process of photophosphorylation, energy for ATP synthesis is derived from the absorption of light.

## 1.2 Coupling Factors and the ATPase

The chemiosmotic hypothesis of Mitchell (1961) proposed that the endergonic synthesis of ATP is coupled to the exergonic oxidation/reduction reactions of the electron transport chains of energy transducing membranes via the formation of a proton electrochemical gradient ($\Delta\mu_{H^+}$) across the membrane. Electrons derived either from the oxidation of substrates (in the case of oxidative phosphorylation) or the excitation of photosynthetic reaction centres (in the case of photophosphorylation) are transferred sequentially to components of the electron transport chain of higher redox potential. In non-photosynthetic electron transport chains the ultimate electron acceptor is usually molecular oxygen, which is reduced to water. A schematic diagram of the *E. coli* electron transport chain is shown in Figure 1.1. Non-cyclic electron flow in photosynthetic electron transport chains results in the reduction of $NADP^+$ to form NADPH (Nicholls and Ferguson, 1992). A schematic diagram of the chloroplast electron transport chain is shown in Figure 1.2.

Experiments employing bacterial extracts (Pinchot, 1953) and mitochondrial extracts (Pullman *et al.*, 1958; Penefsky *et al.*, 1959) demonstrated that the oxidation of NADH could be 'uncoupled' from ATP synthesis if a certain protein (or proteins) were removed from the membranes by mechanical disruption or washing with low ionic strength buffers. The NADH oxidase activity was found to be associated with the membrane (particulate fraction). Although neither the membrane nor soluble fractions possessed ATP synthase activity, ATP hydrolase (ATPase) activity was found in the soluble fraction. When the soluble fraction was added to the membrane fraction in the presence of $Mg^{2+}$ ions, 'coupling' between the NADH oxidase and ATP synthase activities was restored, and the soluble fraction was therefore said to contain a 'coupling factor' (Pinchot, 1953; Penefsky *et al.*, 1959). Purification of the ATPase activity from the soluble mitochondrial fraction by Pullmann *et al.* (1960) and Linnane and Titchener (1960) led to the demonstration by Penefsky *et al.* (1960) that the 'coupling factor' and the ATPase were one and the same species. It was later demonstrated by Prairie *et al.* (1963) that ATP hydrolysis by the intact membrane-associated enzyme could drive the reduction of $NAD^+$ by succinate via the electron transport chain. The 'coupling factor' was therefore shown to be capable both of using energy from a proton electrochemical gradient to synthesise ATP, and of using energy from ATP hydrolysis to establish a proton gradient.

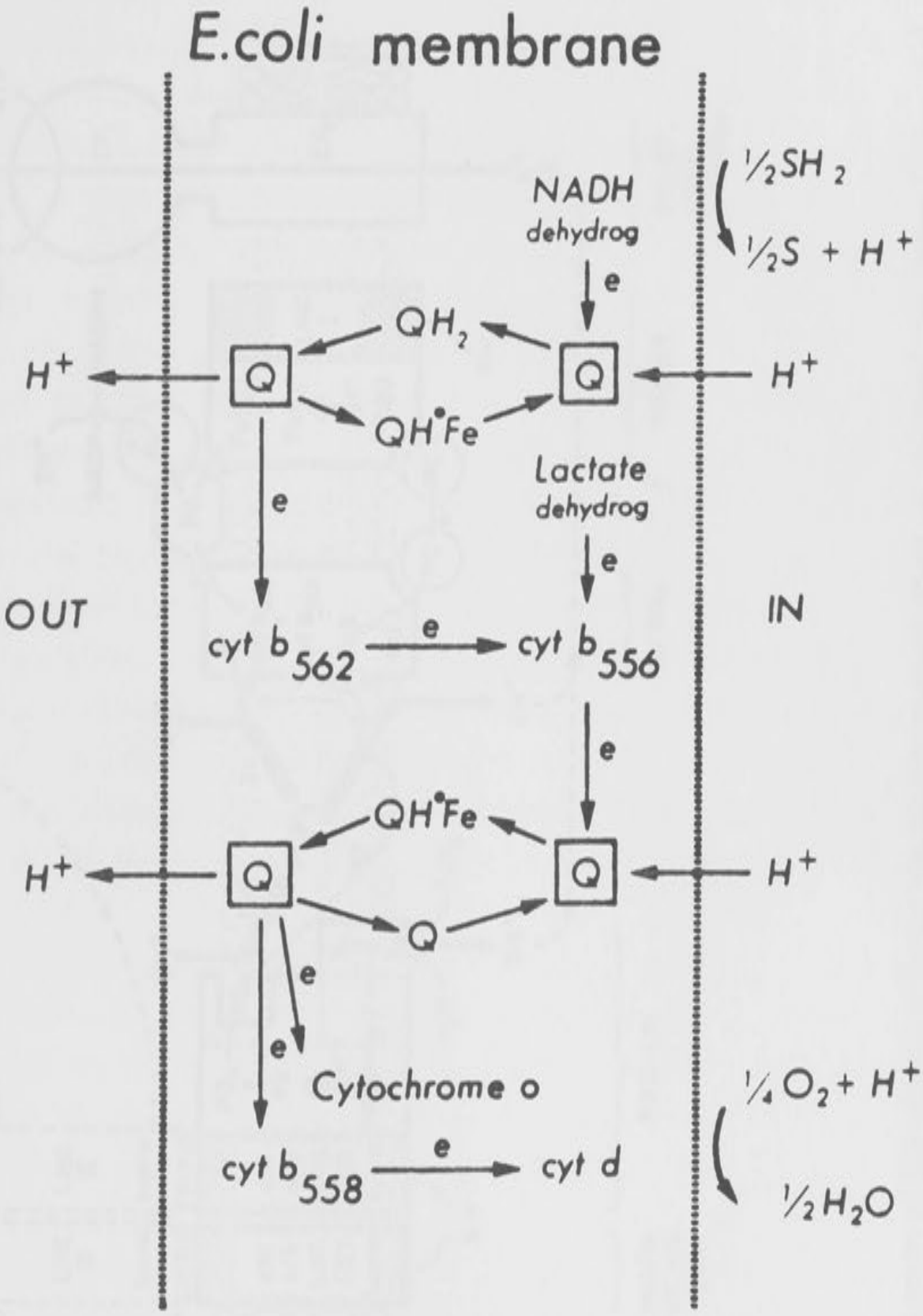


**Figure 1.1**: Schematic diagram of the electron transport chain of *E. coli* (from Downie and Cox, 1978). The oxidation of respiratory substrates leads to cyclical reductions and oxidations of ubiquinone at the inner and outer faces of the bacterial plasma membrane, respectively, causing protons to be translocated. Molecular oxygen is the terminal electron acceptor in the respiratory process. cyt = cytochrome; $SH_2$ = reduced substrate; S = oxidised substrate; Q = ubiquinone; e = electron.

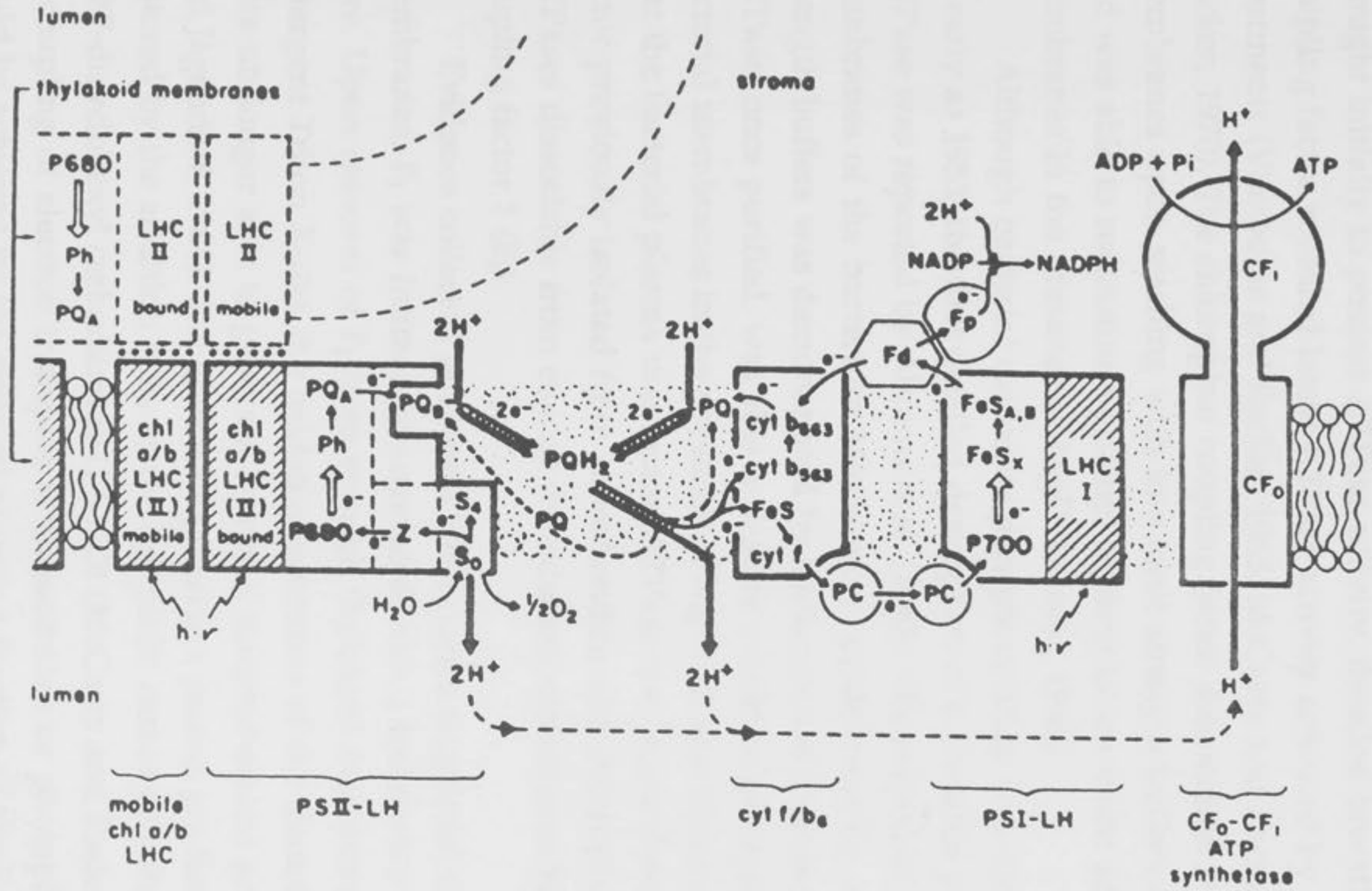


Fig. 1.2 Schematic diagram of the photosynthetic electron transport chain of chloroplasts (from Dilley *et al.*, 1987).

The coupling factor was first isolated from spinach chloroplast thylakoid membranes by Jagendorf and Smith (1962) and Avron (1963). Although not thought initially to possess ATPase activity, detailed investigation of the coupling factor revealed latent ATPase activity activated by a variety of treatments (Vambutas and Racker, 1965; McCarty and Racker, 1968; Farron and Racker, 1970). The chloroplast coupling factor dissociated from the thylakoid membranes upon washing with low ionic strength buffers containing EDTA, and was able to reconstitute photophosphorylation when added to the membranes in the presence of $Mg^{2+}$ (Avron, 1963).

Although bacterial oxidative phosphorylation was described by Pinchot as early as 1953, the first detailed description of a bacterial plasma membrane ATPase was reported by Abrams *et al.* (1960). The release of an ATPase from membranes of the bacterium *Micrococcus lysodeikticus* by washing in low ionic strength buffers was demonstrated by Ishikawa and Lehninger (1962). This ATPase, once purified, was able to restore oxidative phosphorylation to the bacterial membranes in the presence of $Mg^{2+}$. It was therefore demonstrated that the bacterial plasma membrane ATPase was equivalent to the coupling factor previously isolated from mitochondria and chloroplasts. These soluble ATPases dissociable from energy transducing membranes became known as coupling factor 1 ($F_1$).

Evidence collected in several laboratories suggested that in intact membranes, $F_1$ was intimately associated with a membrane-integral proton pore. Upon removal of $F_1$ from spinach thylakoid membranes by the non-ionic detergent Triton X-100, the oxidative processes of the electron transport chain were no longer able to generate a proton electrochemical gradient (Neumann and Jagendorf, 1964). The ability to generate a proton gradient was, however, restored by the addition of $F_1$ or the lipophilic carboxylate-reactive compound N,N'-dicyclohexyl carbodiimide (DCCD) (McCarty and Racker, 1966; 1967). The uncoupling of electron transport from oxidative or photophosphorylation could be achieved by the removal of only a fraction of the $F_1$ complexes associated with the mitochondrial or spinach chloroplast membranes, and ATP synthesis could be restored by the addition of inactivated $F_1$ or low levels of DCCD or oligomycin (Lee and Ernster, 1965; McCarty and Racker, 1967; Racker and Horstman, 1967). The ability of oligomycin to block mitochondrial membrane proton permeability caused the membrane bound proton pore to

become known as $F_O$ (as it possessed an oligomycin sensitivity conferring factor).

Although $F_OF_1$-ATPases are widely distributed, occurring in bacteria, chloroplasts and mitochondria, the overall structure of the complex from all sources is remarkably similar. Despite variation in the total number of component subunits, structural similarity and and amino acid sequence homology between enzymes point to a common mechanism of action (Senior, 1990). Two major types of complex organisation may be considered. The first is the more simple type found in bacteria and chloroplasts. Here the $F_1$ sector carrying the nucleotide binding and catalytic properties, and the $F_O$ sector containing the proton channel, are clearly demarcated. The $F_1$ sectors all contain five different subunits, named α, β, γ, δ and ε in order of decreasing molecular weight. The $F_O$ sectors from most bacteria contain three subunits named *a*, *b* and *c*, although some photosynthetic bacteria possess a fourth subunit named *b´*. The four chloroplast $F_O$ subunits are named $CF_O$I-IV (Cox *et al.*, 1992). The second more complex type of enzyme structure is found in mitochondria, where in addition to the $F_1$ and $F_O$ sectors there exist a number of subunits whose interaction with the membrane is less well defined. These subunits have been denoted $F_A$ (associated components) and may serve to make functional links between $F_O$ and $F_1$ (Nagley, 1988).

## 1.3 The *E. coli* $F_OF_1$-ATPase

### *1.3.1 Identification and Purification of the E. coli $F_1$-ATPase*

A membrane associated ATPase activity in *E. coli* was first described by Solomon (1962), and was studied in detail by Evans (1969; 1970). Both the membrane-bound and solubilised ATPase activity was found to be $Mg^{2+}$ or $Ca^{2+}$ dependent, and could be inhibited by chaotropic anions, monovalent cations and DCCD (Evans, 1970). Similarities between the properties of the bacterial enzyme and those previously reported for the mitochondrial coupling factor led to the suggestion that the bacterial enzyme was important in oxidative phosphorylation and active transport at the plasma membrane (Evans, 1970).

The *E. coli* $F_1$-ATPase is cold labile (Evans, 1970), but the addition of methanol to 20% (v/v) (Kobayashi and Anraku, 1972) or glycerol to 20% (v/v) (Davies and Bragg, 1972) or 50% (v/v) (Kobayashi and Anraku, 1972) to buffers used in the preparation and storage of the enzyme stabilises the purified $F_1$.

### 1.3.2 *Identification and Purification of the E. coli $F_O$ sector*

Studies similar to those carried out with mitochondrial and chloroplast membranes established the existence of a membrane bound proton channel as a component of the 'coupling factor'/ATPase in *E. coli*. DCCD inhibits the membrane bound $F_1$ and weakly inhibits dissociated (soluble) $F_1$ (Evans, 1970; Roisin and Kepes, 1972). Using pH dependent fluorescence quenching of acridine dyes, it was demonstrated that *E. coli* membranes from which $F_1$ had been removed cannot maintain a proton electrochemical gradient across the membrane, and that addition of $F_1$ or DCCD restored membrane energisation (Nieuwenhuis *et al.*, 1973; Tsuchiya and Rosen, 1975).

The reagent *para*-aminobenzamidine (PAB) causes $F_1$ to remain bound to *E. coli* membranes, even after washing with low ionic strength buffers containing EDTA (Cox *et al.*, 1978; Downie *et al.*, 1979a). By adding PAB to buffers used in the solubilisation and ion-exchange chromatography steps, Friedl *et al.* (1979) were able to prepare 80% pure $F_OF_1$, containing three identifiable polypeptide components. This complex could be reconstituted into proteoliposomes, where it catalysed uncoupler- and DCCD sensitive ATP dependent proton pumping as measured by quenching of acridine dye fluorescence (Friedl *et al.*, 1979).

### 1.3.3 *Subunit composition of the E. coli $F_OF_1$-ATPase.*

SDS-polyacrylamide gel electrophoresis of the *E. coli* $F_1$-ATPase resolves five distinct subunits, designated α, β, γ, δ and ε in order of decreasing molecular weight. According to the gel electrophoresis, these subunits have the following molecular weights:- α: 54,000-60,000; β: 52,000-56,000; γ: 32,000-35,000; δ: 21,000 and ε: 11,000-13,000 (from the review of Downie *et al.*, 1979b). Molecular weights predicted from the amino acid sequences of the subunits, as deduced from the nucleotide sequence of the *unc* operon (from the reviews of Futai and Kanazawa, 1983; Walker *et al.*, 1984) are listed in Table 1.1.

The subunit stoichiometry of the $F_1$-ATPase is generally accepted to be $\alpha_3\beta_3\gamma\delta\varepsilon$ (Senior, 1990). This ratio has been determined using a variety of techniques, including the incorporation of $^{14}C$-labelled amino acids (Bragg and Hou, 1975), and [$^{35}S$]sulphate or [U-$^{14}C$]glucose (Foster and Fillingame, 1982), and measuring the radioactivity in slices excised from SDS-PAGE gels. Labelling of the β-subunits with [$^{14}C$]DCCD (Satre *et al.*, 1982) and decoration of the α-subunits with monoclonal antibodies (Lunsdorf *et al.*, 1984) indicate that

**TABLE 1.1**

Subunit composition, genetic specification and stoichiometry of $F_OF_1$-ATPases from *E. coli*, spinach chloroplast and the cyanobacterium *Synechococcus* 6301. Subunits are aligned horizontally according to perceived relationships based on sequence homology or other structural predictions.

| | *E. coli* | | | | Spinach chloroplast | | | | *Synechococcus* 6301 | | | |
|---|---|---|---|---|---|---|---|---|---|---|---|---|
| Sector | Subunit | Gene[a] | Stoichio-metry[b] | Subunit mass (kDa)[a] | Subunit | Gene | Stoichio-metry[d] | Subunit mass (kDa) | Subunit | Gene[h] | Stoichio-metry | Subunit mass (kDa)[h] |
| $F_1$ | α | *uncA* | 3 | 55.3 | α | *atpA*[c] | 3 | 55.5[c] | α | *atpA* | ? | 54.1 |
| | β | *uncD* | 3 | 50.2 | β | *atpB*[c] | 3 | 53.9[c] | β | *atpB* | ? | 52.2 |
| | γ | *uncG* | 1 | 31.5 | γ | *atpC*[f] | 1 | 35.7[f] | γ | *atpC* | ? | 34.8 |
| | δ | *uncH* | 1 | 19.3 | δ | *atpD*[e] | 1 | 20.4[e] | δ | *atpD* | ? | 19.5 |
| | ε | *uncC* | 1 | 15.0 | ε | *atpE*[c] | 1 | 14.7[c] | ε | *atpE* | ? | 14.7 |
| $F_O$ | *a* | *uncB* | 1 | 30.3 | $CF_OIV$ | *atpI*[c] | 1 | 25.0[c] | *a* | *atpI* | ? | 29.0 |
| | *b* | *uncF* | 2 | 17.2 | $CF_OI$ | *atpF*[c] | 1 | 19.0[c] | *b* | *atpF* | ? | 18.7 |
| | *b´* | - | - | - | $CF_OII$ | *atpG*[g] | 1 | 16.5[g] | *b´* | *atpG* | ? | 17.7 |
| | *c* | *uncE* | 6-12 | 8.3 | $CF_OIII$ | *atpH*[c] | 6-12 | 8.0[c] | *c* | *atpH* | ? | 8.0 |

References: (a) Walker *et al.*, 1985, (b) reviewed in Senior (1990), (c) Hudson *et al.* (1987), (d) reviewed in Glaser and Norling (1991), (e) Hermans *et al.* (1988), (f) Miki *et al.* (1988), (g) Herrmann *et al.* (1993), (h) Cozens and Walker (1987)

these subunits are each present in three copies per $F_1$. Experiments aimed at finding an optimal ratio of α-, β- and γ-subunits required for binding to $F_1$-depleted membranes show that maximum specific activity was reconstituted when the purified subunits were mixed in the ratio $\alpha_3\beta_3\gamma$ (Dunn and Futai, 1980), while one copy each of the δ- and ε-subunits per complex are necessary for maximal reconstitution (Sternweis and Smith, 1977; Sternweis, 1978).

Mutant *E. coli* strains deficient in any of the genes encoding the five $F_1$ subunits are unable to carry out oxidative phosphorylation, indicating that each subunit is required for activity *in vivo* (Downie *et al.*, 1979b; 1980; Humbert *et al.*, 1983). These results are consistent with those from reconstitution experiments with individual purified $F_1$ subunits, showing that all five subunits are required for proper binding to $F_O$, and for reconstitution of ATP-driven proton pumping and ATP synthesis (Dunn and Heppel, 1981). The minimum subunit requirement for normal ATPase activity is $\alpha_3\beta_3\gamma$, but both the δ- and ε-subunits are required for proper binding to $F_O$ (Dunn and Heppel, 1981).

The separation of subunits from purified preparations of the *E. coli* $F_OF_1$-ATPase by SDS-PAGE yields, in addition to the five $F_1$ subunits, three polypeptide components of the $F_O$ (Friedl *et al.*, 1979; Foster and Fillingame, 1982), and by measuring the incorporation of radioactivity in labelled cells, a molar ratio of $a_1b_2c_{10\pm1}$ was estimated (Foster and Fillingame, 1982). Results from numerous cross-linking experiments (Sebald *et al.*, 1982; Aris and Simoni, 1983; Hermolin *et al.*, 1983) are compatible with this stoichiometry. The *a*-subunit appears to present in a single copy because no more than one copy of this protein was observed in any cross-linked species, while cross-linked *b*-subunit dimers, *c*-subunit dimers, *ab* heterodimers and $ab_2$ complexes were observed. Genetic analysis by Jans *et al.* (1985) confirms the presence of at least two copies of the *b*-subunit per $F_O$ complex. The mutant alleles of the *uncF* gene(*uncF469* and *uncF476*), encoding the *b*-subunit, prevented assembly of the ATPase complex when present in isolation in a partial diploid strain of *E. coli*. When, however, the two alleles were both present, an active enzyme was assembled. The mutations appear to interfere with inter-subunit interactions important at different stages of an integrated assembly pathway (see section 1.3.8 below), and the observation that the presence of both mutant alleles overcame the individual effects indicates the presence of at least two copies of the *b*-subunit per complex.

Evidence from various sources shows that all three $F_O$ subunits are required for a functional complex. Genetic analysis shows that mutations in any of the three genes encoding $F_O$ subunits may abolish activity *in vivo* (Cox *et al.*, 1973; Downie *et al.*, 1979c; Downie *et al.*, 1981), and experiments involving reconstitution of individual purified $F_O$ subunits into liposomes demonstrated that all three subunits are required for the formation of a proton pore that binds $F_1$ (Schneider and Altendorf, 1984; 1985).

### *1.3.4 Genetics of the E. coli $F_OF_1$-ATPase: the unc operon*

Mutant *E. coli* strains unable to carry out oxidative phosphorylation are unable to grow on oxidisable but non-fermentable substrates such as succinate or D-lactate, although they are capable of growth on glucose. The first strain with these characteristics was reported by Butlin *et al.* (1971), and the genetic locus of the mutation was designated *unc* to signify the uncoupling of electron transport from ATP synthesis. The locus maps at minute 84 on the *E. coli* chromosome (von Meyenburg *et al.*, 1982; Nielsen *et al.*, 1984). Although a number of alternative designations for the *unc* locus have been proposed, this name remains in popular use and has been adopted in this thesis.

The ability to isolate mutants defective in the $F_OF_1$-ATPase by screening for the inability to grow on succinate as sole carbon source (the $suc^-$ phenotype), and the observation that normal alleles are usually dominant in partial diploid strains (Gibson *et al.*, 1977a) assisted in the characterisation of many further *unc* mutations. Mutant alleles of all eight structural genes encoding subunits of the $F_OF_1$-ATPase have been identified (Gibson *et al.*, 1977b; Gibson *et al.*, 1978; Fayle *et al.*, 1978; Senior *et al.*, 1979a; Downie *et al.*, 1979a; 1979c; 1980; 1981; Humbert *et al.*, 1983).

Determination of the nucleotide sequence of the operon (Gay and Walker, 1981a; 1981b; Kanazawa *et al.*, 1981a; 1981b; 1981c; 1982; Hansen *et al.*, 1981; Mabuchi *et al.*, 1981; Nielsen *et al.*, 1981; Saraste *et al.*, 1981) along with biochemical and genetic studies, showed that the eight genes encoding the eight subunits of the *E. coli* $F_OF_1$-ATPase are translated from a single polycistronic message in the order *uncBEFHAGDC* . Gene-polypeptide relationships (see Table 1.1) were established by *in vitro* transcription-translation experiments (Brusilow *et al.*, 1981; Downie *et al.*, 1980; 1981), two-dimensional SDS-PAGE analysis of the complex from mutant strains (Fayle *et al.*, 1978; Senior *et al.*, 1979a; 1979b) and protein sequencing of subunits (Walker and Gay, 1983).

Sequence analysis of the *unc* operon (Kanazawa *et al.*, 1981b; Gay and Walker, 1981b) revealed an open reading frame upstream of the *uncB* gene, designated *uncI*, which would encode a largely hydrophobic 127-amino acid protein. Strains in which the *uncI* gene is disrupted by Tn10 insertion (von Meyenburg *et al.*, 1982) or deletion mutagenesis (Gay, 1984) are not different phenotypically to wild-type strains other than a 10% reduction in growth yield of the deletion strain in limiting concentrations of glucose. This was suggested to indicate a possible role for the *uncI* gene product in facilitating assembly of the $F_OF_1$-ATPase complex (Gay, 1984). The *in vivo* expression of *uncI* is very low, at best 10 to 20 times less than for *uncB* (Solomon *et al.*, 1989), probably due to very weak translational initiation efficiency (Schneppe *et al.*, 1991).

Differences in the efficiency of translation initiation appear to control the levels at which each of the *unc* genes is expressed, such that subunits are synthesised in amounts roughly consistent with the stoichiometry of the complex (McCarthy, 1988). In particular, the presence of a 30 bp region immediately upstream of the start codon for the *uncE* gene causes the *c*-subunit to be translated at high rates, and also promotes the efficient translation of other genes (McCarthy, 1988). The rates at which some *unc* genes are expressed appear also to depend on whether sequences from the preceding gene are also present. This 'translational coupling' has been shown to occur between the gene pairs *uncEF*, *uncFH*, *uncHA* and *uncAG* (Hellmuth *et al.*, 1991; Pati *et al.*, 1992). Secondary structure in mRNA around the *uncH* translation initiation region contributes to the particularly low expression levels of this gene (Pati *et al.*, 1992). The efficiency of ribosome binding upstream of the *uncA* gene is influenced by mRNA secondary structure in the *uncA* translation initiation region, which in turn is affected by the presence of ribosomes translating *uncH* and mutations in the *uncH* gene (Rex *et al.*, 1994).

### *1.3.5 Nucleotide-binding and enzymic properties of the E.coli $F_OF_1$-ATPase.*

Early studies aimed at locating catalytic sites within particular subunits by labelling the *E. coli* $F_1$-ATPase with chemically reactive substrate analogues (Nelson *et al.*, 1974; Futai *et al.*, 1974; Verheijen *et al.*, 1978; Lunardi *et al.*, 1979; Bragg *et al.*, 1981) established that nucleotide binding sites were present on both the α- and β-subunits, without resolving which of these were catalytically active. Six ATP binding sites were subsequently identified (Cross and Nalin, 1982; Wise *et al.*, 1983; Perlin *et al.*, 1984), of which three are catalytically active.

Bound ATP at these sites exchanges rapidly with free nucleotides, and the binding is dependent on $Mg^{2+}$ (Cross and Nalin, 1982). ATP bound at the other three (non-catalytic) sites does not exchange rapidly with free nucleotides, and the binding is not dependent on $Mg^{2+}$ (Cross and Nalin, 1982; Wise *et al.*, 1983).

ATP and ADP bind to both isolated α- (Dunn and Futai, 1980) and isolated β- (Issartel and Vignais, 1984) subunits. ATP binds to the isolated α-subunit with very high affinity, without a requirement for $Mg^{2+}$, and once bound only exchanges very slowly with free nucleotide (Rao *et al.*, 1987). The binding sites on the α-subunits therefore appear to be the non-catalytic ATP binding sites (Senior, 1988). This is consistent with information from the recently published high-resolution structure of the bovine heart mitochondrial $F_1$-ATPase, which shows nucleotide binding sites at the interfaces between the α- and β-subunits, with the catalytic sites predominantly in the β-subunits and the non-catalytic sites predominantly in the α-subunits (Abrahams *et al.*, 1994). Weber *et al.* (1993) substituted residue Y331 in the catalytic site of the β-subunit with tryptophan so that fluorescence quenching could be used to probe nucleotide binding, and showed that maximal ATP hydrolysis occurs with all three catalytic sites occupied. Following mutagenesis of the α-, β-, δ- and γ-subunits to produce an $F_1$ free of tryptophan residues (Wilke-Mounts *et al.*, 1994), Weber *et al.* (1994) introduced the mutations αR365W and βY354W so that nucleotide binding in all six sites could be probed. Occupancy of the non-catalytic sites was shown not to be required for ATP hydrolysis (Weber *et al.*, 1994).

Although adenine nucleotides (ATP and ADP) are the preferred substrates for proton pumping and oxidative phosphorylation, guanine and inosine nucleotides can be utilised and may be physiological substrates (Perlin *et al.*, 1984; Wise and Senior, 1985). Both $Mg^{2+}$ and $Ca^{2+}$ are good co-factors, but $Mg^{2+}$ is most likely to be employed *in vivo* (Senior, 1990). Other divalent metal cations known to be able to act as co-factors are $Co^{2+}$, $Mn^{2+}$ and $Ni^{2+}$ (Hanson and Kennedy, 1973; Perlin *et al.*, 1984; Smith *et al.*, 1985). The $K_M$ for Mg-ATP is 0.29 mM and the turnover number is approximately 30-50 $s^{-1}$, depending on the reaction conditions (Roisin and Kepes, 1972; Hanson and Kennedy, 1972; Perlin *et al.*, 1984), because the rate is pH-dependent and varies with the ratio of $Mg^{2+}$ to ATP (Evans, 1969). Inhibitors of the *E. coli* $F_OF_1$-ATPase include citreoviridin (Satre *et al.*, 1980) aureovertin (Satre *et al.*, 1978; 1980), which specifically binds to the β-subunit (Dunn and Futai, 1980) and venturicidin, which binds the *c*-

subunit (Perlin *et al.*, 1985). The enzyme is inactivated by DCCD, which binds specifically to residues Asp-61 of the *c* subunit (Hoppe and Sebald, 1984) and Glu-192 of the β-subunit (Yoshida *et al.*, 1982) and 4-chloro-7-nitrobenzofurazan (Nbf; Wise *et al.*, 1981). Azide inhibits ATP hydrolysis when the substrate concentration is sufficient to allow steady-state cooperative ("multisite") activity, but not when substrate concentation is low (during "unisite" activity; Wise *et al.*, 1984; Noumi *et al.*, 1987). Sulphydryl-specific reagents do not inhibit the enzyme (Roisin and Kepes, 1972; Hanson and Kennedy, 1973; Futai *et al.*, 1974).

*1.3.6 Gross structure of the E.coli $F_OF_1$-ATPase.*

The crystal structure of the bovine mitochondrial $F_1$-ATPase has been determined by X-ray diffraction at 2.8Å resolution (Abrahams *et al.*, 1994). For two reasons, this structure is likely to provide an accurate guide to the architecture of $F_1$-ATPases from all species. Firstly, high levels of amino acid sequence homology exist between equivalent subunits, particularly among the α- and β-subunits which are directly involved in catalysis (Senior, 1990). Secondly, predicted secondary structures of equivalent subunits appear to be highly conserved (Cox *et al.*, 1992).

The crystal structure determined by Abrahams *et al.* (1994) shows the $F_1$ to be a flattened sphere 80Å high and 100Å across. The three α- and three β-subunits are arranged alternately around a central α-helix 90Å long formed by the C-terminal amino acids of the γ-subunit. The lower half of this helix forms a coiled-coil with a second α-helix composed of N-terminal amino acids of the γ-subunit. Each of the α- and β-subunits possesses a six-stranded β-barrel on the top face of the $F_1$ (facing away from the membrane). These domains interact to form a continuous 24-stranded β-sheet around the top of the structure which may be important in holding these subunits together (Abrahams *et al.*, 1994).

The basic shape of the *E. coli* $F_1$-ATPase determined by cryoelectron microscopy appears to be similar to the high-resolution structure of the bovine heart mitochondrial $F_1$-ATPase discussed above. The *E.coli* $F_1$ appears to be a roughly spherical complex, approximately 95Å in diameter (Gogol *et al.*, 1989a). The three α- and three β- subunits, each approximately 90x30Å, form a hexagonal barrel with a compact protein density including part of the γ-subunit partly obstructing the central cavity (Gogol *et al.*, 1989a; Capaldi *et al.*, 1994).

Labelling of the α-subunit with monoclonal antibodies showed that the α- and β-subunits alternate to form the hexagon (Gogol *et al.*, 1989b).

*1.3.7 Structure/ function models for subunits of the* E.coli $F_OF_1$-*ATPase.*

i) The *a*-subunit: Analysis of the hydropathy profile of the *a*-subunit (Figure 1.3) indicates five likely transmembrane α-helices. Four appear to contain residues 40-60, 100-120, 145-165 and 240-260 approximately, while the fifth helix is less clearly defined by the hydropathy profile. The results from membrane topological analysis by Lewis *et al.* (1990) using alkaline phosphatase 'sandwich' fusions were interpreted by these workers as supporting an eight-helix model, but appear to be also consistent with a five-helix structure (Cox *et al.*, 1992; see Figure 1.3).

Extensive mutational analysis of the *a*-subunit in many laboratories has identified many amino acid residues important in proton translocation and stabilisation of the correctly folded structure. Residues R210 (Lightowlers *et al.*, 1987; Cain and Simoni, 1989), E219 (Lightowlers *et al.*, 1988; Cain and Simoni, 1988) and H245 (Cain and Simoni, 1986; Lightowlers *et al.*, 1987; Vik and Simoni, 1987; Cain and Simoni, 1988) have been shown to be critical for proton conduction (see Figure 1.4). The deleterious effects of the mutation R210Q may be partly overcome by the mutation Q252R, indicating that these residues are close (Hatch *et al.*, 1995). Similar analysis suggests that V50 is close to R210 (Howitt and Cox, 1992), and that G218 is close to H245 (Hartzog and Cain, 1994). A cluster of charged residues (D44, D124 and R140) on the periplasmic side of putative α-helices 1, 2 and 3 appear to be involved in stabilising *a*-subunit structure, possibly via the formation of salt-bridges. These interactions between amino acid residues in different parts of the *a*-subunit are consistent with a five-helix *a*-subunit model (Howitt *et al.*, 1990; 1993).

ii) The *b*-subunit possesses a short (22 residue) segment at the N-terminus which is highly hydrophobic and predicted to traverse the membrane. The remainder of the molecule (126 residues) is hydrophilic, and is predicted from the amino acid sequence to be largely α-helical (Senior *et al.*, 1983; Walker *et al.*, 1984; see Figure 1.3). A water-soluble fragment of the *b*-subunit is liberated following treatment of $F_1$-depleted membranes with trypsin (Perlin *et al.*, 1983). Pre-binding of $F_1$ prevents proteolysis by trypsin, suggesting a probable role for the *b*-subunit in binding $F_1$ to $F_O$ (Perlin *et al.*, 1983).

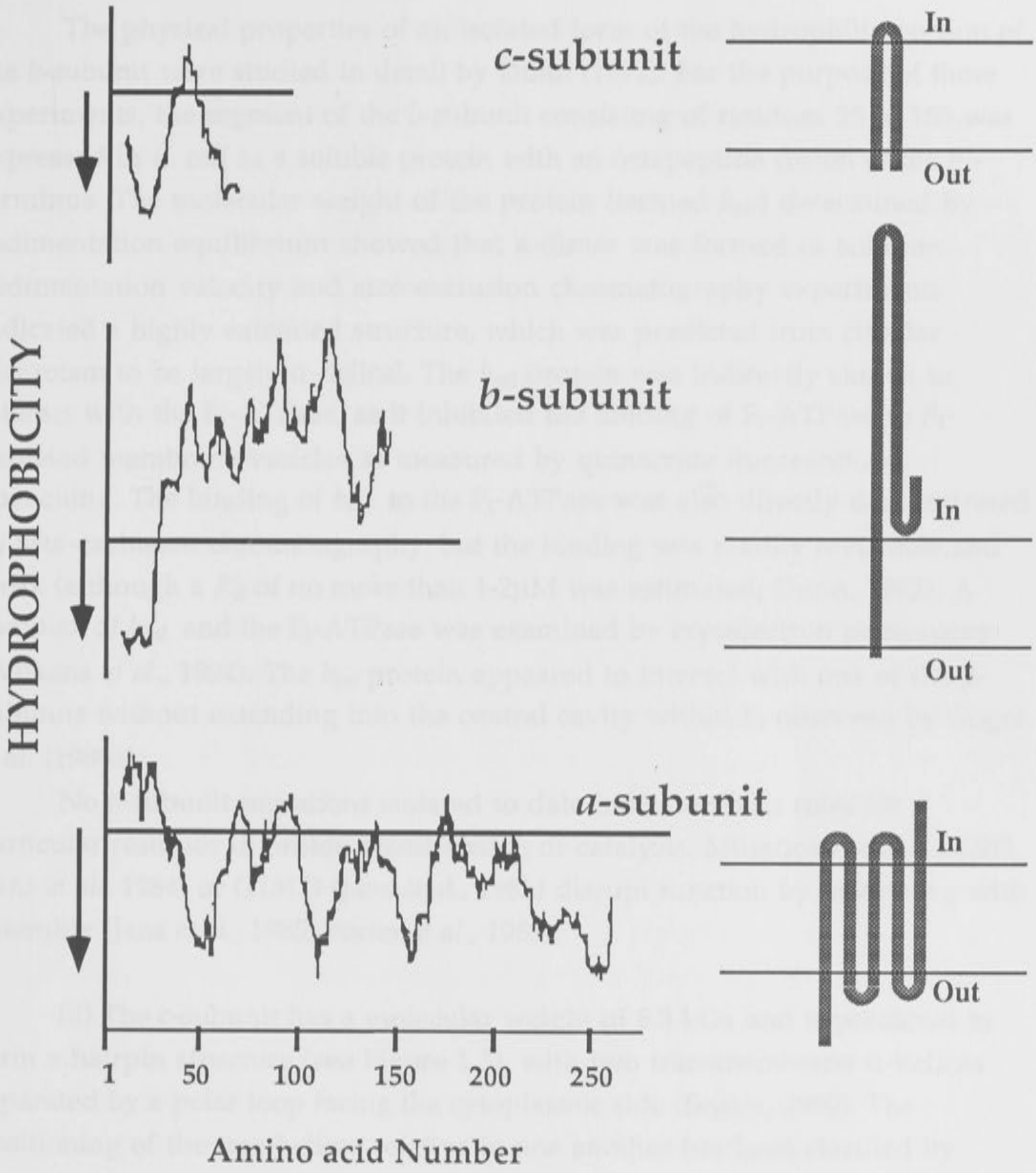


**Figure 1.3**: Left: Hydropathy profiles of the *c*-, *b*- and *a*-subunits of the *E. coli* $F_OF_1$-ATPase calculated using the GES scale (Engelman *et al.*, 1986), with a window of 19 amino acids.

Right: Structural models for these subunits based on hydropathy profiles and secondary structure predictions. "In" and "out" refer to the cytoplasmic and periplasmic sides of the membrane, respectively. Structures depicted for the *c*- and *b*-subunits are as predicted by Senior (1983), while the five transmembrane α-helix model for the *a*-subunit is as predicted by Cox *et al.* (1992).

The physical properties of an isolated form of the hydrophilic portion of the *b*-subunit were studied in detail by Dunn (1992). For the purpose of these experiments, the segment of the *b*-subunit consisting of residues 25 to 156 was expressed in *E. coli* as a soluble protein with an octapeptide fusion at the N-terminus. The molecular weight of the protein (termed $b_{sol}$) determined by sedimentation equilibrium showed that a dimer was formed in solution. Sedimentation velocity and size exclusion chromatography experiments indicated a highly extended structure, which was predicted from circular dichroism to be largely α-helical. The $b_{sol}$ protein was indirectly shown to interact with the $F_1$-ATPase, as it inhibited the binding of $F_1$-ATPase to $F_1$-depleted membrane vesicles as measured by quinacrine fluorescence quenching. The binding of $b_{sol}$ to the $F_1$-ATPase was also directly demonstrated by size-exclusion chromatography, but the binding was readily reversible and weak (although a $K_d$ of no more than 1-2μM was estimated; Dunn, 1992). A complex of $b_{sol}$ and the $F_1$-ATPase was examined by cryoelectron microscopy (Wilkens *et al.*, 1994). The $b_{sol}$ protein appeared to interact with one of the β-subunits without extending into the central cavity within $F_1$ observed by Gogol *et al.* (1989a).

No *b*-subunit mutations isolated to date indicate direct roles for particular residues in proton translocation or catalysis. Mutations such as G9D (Jans *et al.*, 1984) or G131D (Jans *et al.*, 1985) disrupt function by interfering with assembly (Jans *et al.*, 1985; Porter *et al.*, 1985).

iii) The *c*-subunit has a molecular weight of 8.3 kDa and is predicted to form a hairpin structure (see Figure 1.3), with two transmembrane α-helices separated by a polar loop facing the cytoplasmic side (Senior, 1990). The positioning of the two helices relative to one another has been clarified by analysis of *c*-subunit mutants. The deleterious effects of an amino acid substitution in the C-terminal helix (P64L) may be partially overcome by a second substitution (A20P) in the N-terminal helix, indicating that these residues are in close proximity (Fimmel *et al.*, 1983). Similarly, the effects of the mutation D61G may be partially overcome by the substitution A24D, suggesting that these residues also are close (Miller *et al.*, 1990). Analysis of third-site revertants with these mutations and further improved function suggests that residues A217, I221 and L224 in the *a*-subunit are proximal to D61 and A24 in the *c*-subunit (Fraga *et al.*, 1994).

The residue D61 in the *c*-subunit has been shown to be critical for proton translocation through $F_O$ (see Figure 1.4). The mutations D61G (Hoppe *et al.*, 1980) and D61N (Hoppe *et al.*, 1982) block proton translocation, even when a mixture of mutant and wild-type *c*-subunits are present. Proton transport is inactivated by the reaction of DCCD at D61 with only one copy of the *c*-subunit per complex (Hermolin and Fillingame, 1989). These data suggest that all of the approximately 10 copies of the *c*-subunit per complex are required for proton translocation.

iv) The α-subunit has a molecular weight of 55.3 kDa and is the largest protein species in the $F_OF_1$-ATPase complex. Three functional regions are apparent in the α-subunit sequence (Senior, 1990). Firstly, the N-terminal 30 amino acid residues are involved in membrane binding. Removal of N-terminal residues with proteases (Dunn *et al.*, 1980) or the mutation G29D (Maggio *et al.*, 1988) causes defective binding of the δ-subunit within the complex, which thereby prevents or weakens binding of $F_1$ to $F_O$. Secondly, a region encompassing residues 160-340 was proposed by Maggio *et al.* (1987) to form the nucleotide-binding domain, on the basis of secondary structure predictions and sequence homology with other nucleotide-binding proteins, although residues K175 and T176 appear to also be important in stabilising subunit/subunit interactions (Jounouchi *et al.*, 1993). Thirdly, the residues 345-376 appear to be involved in the transmission of conformational changes across the interface between the α-subunits and the β-subunits where the catalytic sites are located. Mutations in this region strongly inhibit ATPase activity by $F_1$ in multisite catalytic mode with lesser or no effect on activity in unisite mode (Wise *et al.*, 1981; Senior *et al.*, 1984; Wise *et al.*, 1984; Soga *et al.*, 1989) and therefore appear to prevent the signalling of positive catalytic cooperativity and negative binding cooperativity between catalytic sites on the β-subunits (Senior, 1990).

v) The β-subunits have molecular weights of 50.2 kDa and contain the catalytic sites of the $F_OF_1$-ATPase complex. The nucleotide-binding domain appears from the presence of the Walker "A" and "B" motifs (Walker *et al.*, 1982a) and secondary structure predictions to be formed by residues 140-335 approximately (Duncan *et al.*, 1986; Senior, 1988). Mutational analysis has shown that residue K155 in the "A" sequence is involved in ATP binding and

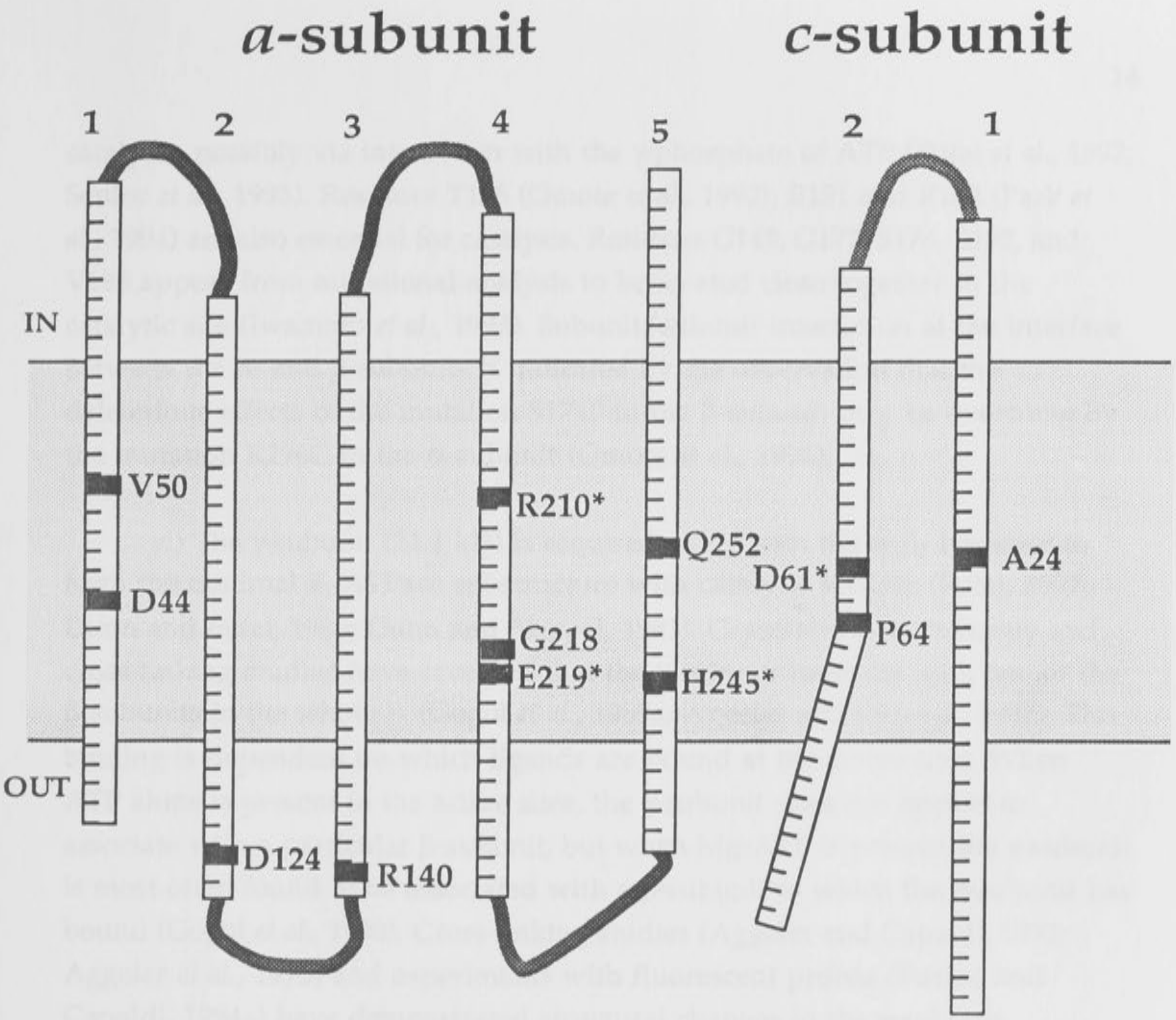


**Figure 1.4**: Proposed arrangement of transmembrane α-helices of the *a*- and *c*-subunits of the *E. coli* $F_OF_1$-ATPase (from Hatch *et al.*, 1995). The interacting amino acid residues described in section 1.3.7 are indicated. Residues involved in proton translocation are marked with stars. Proline-64 of the *c*-subunit is predicted to cause a kink in the second transmembrane α-helix.

catalysis, possibly via interaction with the γ-phosphate of ATP (Futai *et al.*, 1992; Senior *et al.*, 1993). Residues T156 (Omote *et al.*, 1992), E181 and R182 (Park *et al.*, 1994) are also essential for catalysis. Residues G149, G172, S174, E192, and V198 appear from mutational analysis to be located close together in the catalytic site (Iwamoto *et al.*, 1993). Subunit/subunit interaction at the interface between the α- and β-subunits is indicated by the observation that the deleterious effects of the mutation S174F in the β-subunit may be overcome by the mutation R296C in the α-subunit (Omote *et al.*, 1994).

vi) The γ-subunit (31.4 kD) is required along with the $\alpha_3\beta_3$ hexamer to form the minimal $F_1$-ATPase substructure with catalytic activity (Futai, 1977; Dunn and Futai, 1980; Dunn and Heppel, 1981). Cryoelectron microscopy and cross-linking studies have revealed that the γ-subunit interacts with one of the β-subunits in the whole $F_1$ (Gogol *et al.*, 1989a; Aggeler and Capaldi, 1992). This binding is dependent on which ligands are bound at the active sites. When ATP alone is present in the active sites, the γ-subunit does not appear to associate with a particular β-subunit, but when Mg-ATP is present the γ-subunit is most often found to be associated with a β-subunit to which the ε-subunit has bound (Gogol *et al.*, 1990). Cross-linking studies (Aggeler and Capaldi, 1992; Aggeler *et al.*, 1993) and experiments with fluorescent probes (Turina and Capaldi, 1994a) have demonstrated structural changes in the γ-subunit dependent on nucleotide binding at the catalytic sites. The structural changes induced by ATP binding are reversed upon hydrolysis of the substrate (Turina and Capaldi, 1994b).

The mutation M23K in the N-terminal region of the γ-subunit causes uncoupling of ATPase and proton pumping activities (Shin *et al.*, 1992), but these effects may be suppressed by second-site mutations in the C-terminal region at residue 242 and between residues 269 and 280 (Nakamoto *et al.*, 1993). Second-site mutations between residues 18 and 35 in the N-terminal region and between 236 and 246 in the C-terminal regions are also able to suppress the uncoupling effects of the mutations Q269E and T273V in the C-terminal region, suggesting that these three regions form interacting segments essential for coupling (Nakamoto *et al.*, 1995). The N- and C-terminal regions are predicted to be α-helical in structure, and probably extend into the $\alpha_3\beta_3$ barrel observed in cryoelectron microscopy experiments (Capaldi *et al.*, 1994) This is consistent with the crystal structure of the bovine mitochondrial $F_1$-ATPase (Abrahams *et*

*al.*, 1994). The middle region, predicted to consist mainly of β-turn and β-sheet structures, appears from protease digestion and labelling experiments to lie outside the $\alpha_3\beta_3$ barrel, and is involved in binding the ε-subunit (Tang *et al.*, 1994).

vii) The δ-subunit (19.3kD) is required for binding of the $F_1$-ATPase to $F_O$ (Bragg *et al.*, 1973; Sternweis and Smith, 1977; Dunn and Heppel, 1981; Jounouchi *et al.*, 1992). The protein is predicted from size-exclusion chromatography to be highly elongated, and from circular dichroism spectra to be highly α-helical (Sternweis and Smith, 1977). Protease digestion and chemical labelling experiments suggest that the N- and C-terminal parts of the δ-subunit associate with $F_1$, while the central part of the protein is separate from the main mass of $F_1$ (Mendel-Hartvig and Capaldi, 1991b).

Site-directed mutagenesis has been used extensively to study the structure and function of the δ-subunit. Experiments involving the labelling of two cysteine residues (64 and 140) indicate that these residues are in close proximity and may be involved in binding of the δ-subunit to other subunits (Ziegler *et al.*, 1994). Digestion of $F_1$ with trypsin to remove approximately 20 residues from the C-terminus of the δ-subunit abolishes coupling between ATPase and proton pumping activities, even though binding to $F_O$ is unaffected (Mendel-Hartvig and Capaldi, 1991b). The substitution of residue D161 with proline (Stack and Cain, 1994) or the substitution of G150 with threonine, proline or aspartate (Hazard and Senior, 1994) causes loss of enzyme function by disrupting assembly, while the substitution G150N abolishes coupling without disrupting assembly (Hazard and Senior, 1994). These results indicate an important role for the C-terminus of the δ-subunit in energy coupling in the $F_OF_1$-ATPase complex.

viii) The ε-subunit (15kD) is predicted to be globular in shape (Sternweis and Smith, 1980). The ε-subunit is essential for binding of $F_1$ to $F_O$ (Sternweis, 1978), although only the N-terminal 78 residues are required for this function (Kuki *et al.*, 1988). The ε-subunit inhibits ATPase activity of the purified $F_1$ (Laget and Smith, 1979) but not of the $F_OF_1$-ATPase complex (Sternweis and Smith, 1980). This inhibition is mediated by the binding of the ε-subunit to the C-terminal domain of one of the β-subunits (Tozer and Dunn, 1987; Dunn *et al.*, 1987b; 1990; Dallmann *et al.*, 1992), and appears to impair the rate of product

release from the catalytic site (Dunn *et al.*, 1987a; Wood *et al.*, 1987). As determined by rates of trypsin cleavage and the degree of cross-linking to the β-subunit, the conformation of the ε-subunit is dependent on which ligands are present in the catalytic sites (Mendel-Hartvig and Capaldi, 1991a).

The ε-subunit binds strongly to the γ-subunit with a $K_d$ of approximately 3 nM (Dunn, 1982), which has enabled a complex of these subunits to be purified and crystallised (Cox *et al.*, 1993). Mutational analysis and cross-linking experiments indicate that the highly conserved residue H38 of the ε-subunit is close to the γ-subunit without interacting directly with that subunit (Skakoon and Dunn, 1993a) and that portions of the C-terminal domain interact with a β-subunit near an α/β interface (Skakoon and Dunn, 1993b).

Analysis by Zhang *et al.* (1994) of suppressor mutations indicates a close proximity between residue E31 of the ε-subunit and residue Q42 in the polar loop of residues in the *c*-subunit of $F_O$ predicted to lie outside the membrane facing the cytoplasmic side. These workers found that the effects of the *c*-subunit mutation Q42E, which causes uncoupling of catalysis and proton translocation, could be suppressed by the substitution of E31 in the ε-subunit by glycine, valine or lysine. Residue E31 lies in a highly conserved region of the ε-subunit (LaRoe and Vik, 1992).

### *1.3.8 Assembly of the E. coli $F_OF_1$-ATPase complex*

Any proposal for assembly of the $F_OF_1$-ATPase complex must take into account the need to never allow an open proton channel to form, which would collapse $\Delta\mu_{H^+}$ and inhibit growth. For this reason , the original proposal of Sternweis and Smith (1977) in which the complex assembles from pre-formed $F_1$ and $F_O$ components seems unlikely. An 'integrated membrane assembly pathway' has, however, been proposed (see Figure 1.5) which prevents the formation of a proton permeable $F_O$ at any stage (Cox *et al.*, 1981; Cox and Gibson, 1987). Evidence for this comes from the study of mutants deficient in the α- and β-subunits. Two-dimensional SDS-PAGE of membrane proteins isolated from these strains revealed that the *b*-subunit was not incorporated into the membrane, and indicated that both the α- and β- subunits are required for this process (Cox *et al.*, 1981). Studies involving the expression of $F_O$ genes from high copy number plasmids in *unc* deletion strains (Aris *et al.*, 1985; Fillingame *et al.*, 1986) suggest that $F_1$ subunits are not required for the assembly of a functional $F_O$ in the membrane, but the physiological relevance

of experiments where the expression levels of the $F_O$ genes are much higher than those which normally occur is questionable (Hermolin and Fillingame, 1995).

A plasmid carrying all of the *unc* genes was constructed by Brusilow (1987) in which the *uncA* and *uncG* genes were fused so as to produce an inactive α/γ fusion. An *unc* deletion strain carrying this plasmid is capable of growth, but the induction of α-subunit synthesis from a second plasmid increases membrane proton permeability and impairs growth (Pati and Brusilow, 1989). These results indicate that the α-subunit is required for correct assembly of the $F_O$ and are consistent with a mechanism of integrated assembly.

The original proposal by Cox *et al.* (1981) for an integrated assembly pathway suggested that both the *a*- and *c*-subunits assembled in the membrane prior to the α- and β- dependent insertion of the *b*-subunit (see Cox *et al.*, 1981 and Figure 1.5). If, however, subunits *b* and *c* incorporate independently of subunit *a* and and are required for membrane insertion of subunit *a* as proposed by Hermolin and Fillingame (1995), incorporation of the *a*-subunit may not occur until after the *c*-, *b*-, β- and α-subunits are incorporated.

## 1.4 The Chloroplast $F_OF_1$-ATPase

### *1.4.1 Identification and Purification of the Chloroplast $F_OF_1$-ATPase*

Like its mitochondrial and bacterial counterparts, the chloroplast $F_OF_1$-ATPase consists of a dissociable water soluble ATPase and a membrane-intrinsic proton channel, designated $CF_1$ and $CF_O$ respectively. The enzyme is located in the stromal lamellae and in the exposed regions of grana stacks in thylakoid membranes (Andersson and Anderson, 1980), and in etioplasts of non-photosynthetic plant tissue (Nechushtai and Nelson, 1985). The $CF_1$-ATPase dissociates from the thylakoid membranes upon washing with low ionic strength buffers containing EDTA, and is able to reconstitute photophosphorylation when added to the membranes in the presence of $Mg^{2+}$ (Avron, 1963). Thylakoid membranes from which $CF_1$ has been removed show high proton conductivity (Neumann and Jagendorf, 1964), which is prevented by the binding of $CF_1$ (McCarty and Racker, 1966; Schmid *et al.*, 1976) or DCCD (McCarty and Racker, 1967).

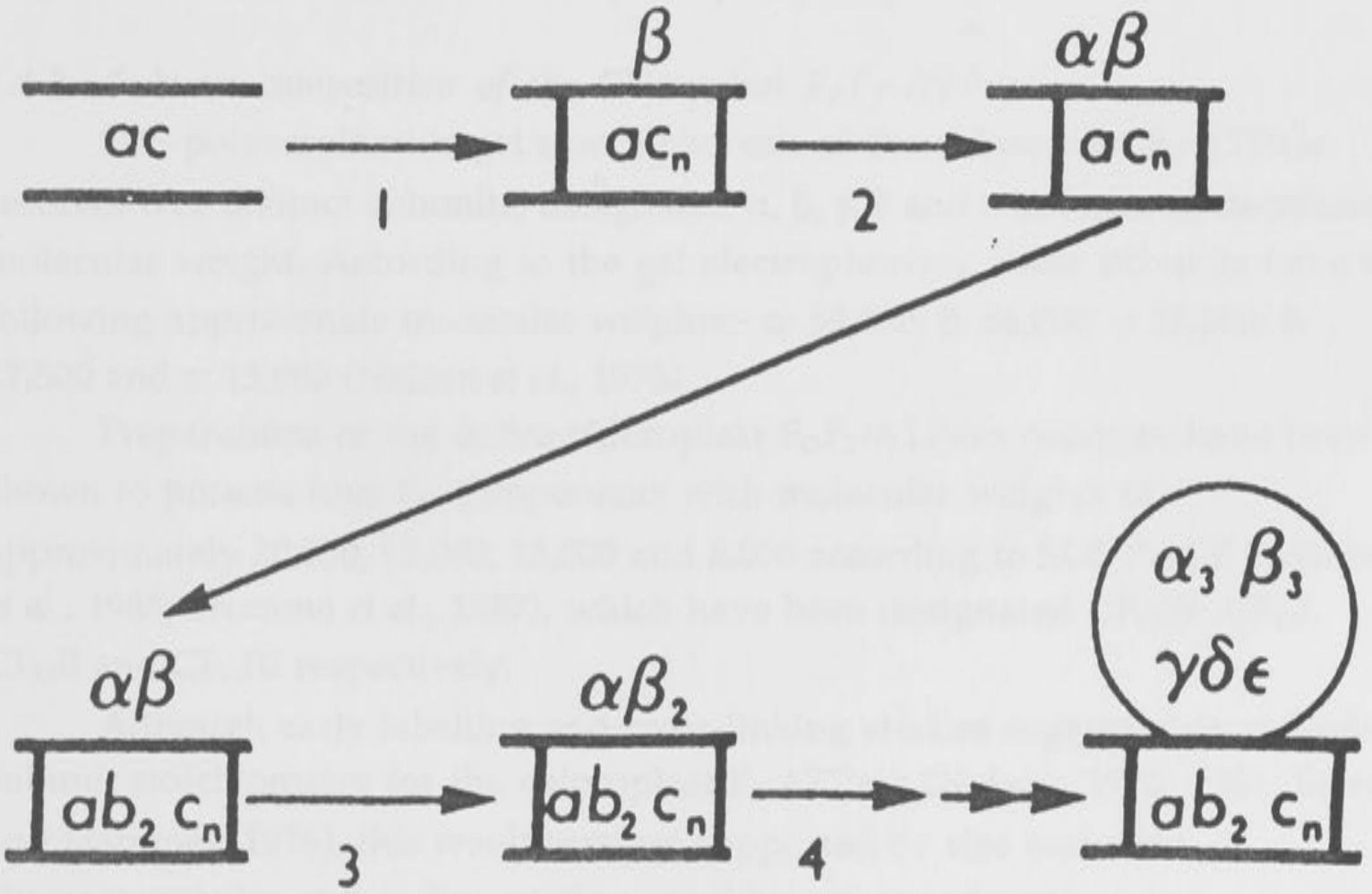


**Figure 1.5**: Outline of the integrated membrane assembly pathway for the *E. coli* $F_OF_1$-ATPase, in which incorporation of the the α- and β-subunits of the $F_1$-ATPase is required before completion of the $F_O$ sector and subsequent completion of the $F_1$ sector (Cox *et al.*, 1981). Taken from Cox and Gibson (1987).

Lien and Racker (1971) purified $CF_1$ in high yield from the soluble extract after washing thylakoid membranes with low ionic strength buffers containing EDTA, using ion-exchange and sucrose density gradient sedimentation.

Isolation of the entire chloroplast $F_OF_1$-ATPase complex from spinach thylakoids was first reported by Carmeli and Racker (1973). Purer preparations were subsequently shown to be capable of photophosphorylation when reconstituted into phospholipid vesicles containing bacteriorhodopsin (Winget *et al.*, 1977; Dewey and Hammes, 1981; Takabe and Hammes, 1981; Krupinski and Hammes, 1986) or photosystem I (Hauska *et al.*, 1980). Younis and Winget (1977) reconstituted purified $CF_O$ from $CF_1$-depleted thylakoid membranes into phospholipid vesicles with bacteriorhodopsin. $CF_1$ bound to $CF_O$ and restored DCCD-sensitive photophosphorylation.

### *1.4.2 Subunit composition of the Chloroplast $F_OF_1$-ATPase.*

SDS-polyacrylamide gel electrophoresis of the chloroplast $F_1$-ATPase resolves five distinct subunits, designated $\alpha$, $\beta$, $\gamma$, $\delta$ and $\varepsilon$ in order of decreasing molecular weight. According to the gel electrophoresis, these subunits have the following approximate molecular weights:- $\alpha$: 59,000; $\beta$: 56,000; $\gamma$: 37,000; $\delta$: 17,500 and $\varepsilon$: 13,000 (Nelson *et al.*, 1973).

Preparations of the entire chloroplast $F_OF_1$-ATPase complex have been shown to possess four $F_O$ components with molecular weights of approximately 20,000, 15,000, 13,000 and 8,000 according to SDS-PAGE (Westhoff *et al.*, 1985; Fromme *et al.*, 1987), which have been designated $CF_OIV$, $CF_OI$, $CF_OII$ and $CF_OIII$ respectively.

Although early labelling and cross-linking studies suggested an $\alpha_2\beta_2\gamma\delta\varepsilon_2$ subunit stoichiometry for the chloroplast $F_1$-ATPase (Nelson, 1976; 1981; Baird and Hammes, 1976), this result was not supported by size exclusion chromatography and sedimentation equilibrium experiments using *Chlamydomonas reinhardi* $CF_1$, from which a ratio of $\alpha_3\beta_3\gamma\delta\varepsilon$ was calculated (Merchant *et al.*, 1983). An $\alpha_3\beta_3\gamma\delta\varepsilon$ stoichiometry was also proposed by Süss and Schmidt (1982), who grew broad bean *(Vicia faba)* in an atmosphere enriched with $^{14}CO_2$, and measured the distribution of radioactivity in the subunits separated by SDS-PAGE. These workers also calculated that one copy each of $CF_OI$ and $CF_OII$ and five copies of $CF_OIII$ were present per $F_OF_1$-ATPase complex.

Electron microscopy studies of $CF_1$ by Boekema *et al.* (1990) show that like the *E. coli* and mitochondrial enzymes, the α- and β-subunits are in a hexagonal arrangement, with an asymmetric mass in the centre formed by the minor subunits. The γ-subunit appears to lie in the centre of the hexagon with subunits δ and ε located between γ and a pair of α- and β-subunits.

### *1.4.3 Genetics of the Spinach Chloroplast $F_OF_1$-ATPase*

As is the case with all chloroplast multi-subunit enzyme complexes characterised thus far, some subunits of the spinach chloroplast $F_OF_1$-ATPase are encoded by genes in the cell nucleus, and others by genes on the chloroplast genome. Most chloroplast proteins are nuclear encoded, are translated in the cytoplasm from polyadenylated mRNA, and transported into the chloroplast (Gillham *et al.*, 1978; Chua and Schmidt, 1979; Nelson and Cidon, 1984), while the remainder are chloroplast encoded and are translated within the organelle (Ellis, 1977).

The labelling of isolated chloroplasts using radioactive precursors [$^{35}$S]-methionine or [$^{3}$H]-leucine (Mendiola-Morgenthaler *et al.*, 1976; Doherty and Gray, 1980; Nelson *et al.*, 1980) and treatment of pea shoots with cycloheximide, which affects synthesis of nuclear-encoded proteins but not chloroplast encoded proteins (Bouthyette and Jagendorf, 1978) showed that genes for the α-, β-, ε-, $CF_OI$ and $CF_OIII$ subunits are located on the chloroplast genome. Analysis of mutant rye plants, affected in the 70S ribosome such that expression of chloroplast genes is temperature-sensitive (Bieckmann and Feierabend, 1985), and *in vitro* transcription/translation experiments using cytoplasmic polyadenylated mRNA as template (Westhoff *et al.*, 1981; 1985) confirmed that the δ-, γ- and $CF_OII$ subunits are nuclear-encoded.

Mapping of the spinach chloroplast genome located the genes encoding the β and ε subunits adjacent to the gene encoding the large subunit of ribulose bisphosphate carboxylase/oxygenase (Westhoff *et al.*, 1981), while the genes encoding the α, $CF_OI$ and $CF_OIII$ subunits were mapped to a region approximately 40kb away (Alt *et al.*, 1983; Westhoff *et al.*, 1985). Sequencing of the genes encoding the β- and ε-subunits (designated *atpB* and *atpE*, respectively; see Table 1.1) revealed that the genes overlap, such that the initiation codon for the *atpE* gene formed part of the termination codon for *atpB* (Zurawski *et al.*, 1982). The *atpBE* gene cluster is transcribed to a dicistronic mRNA with the same gene order as the corresponding *E. coli unc* genes.

The spinach chloroplast genes encoding the $CF_OIV$, $CF_OIII$, $CF_OI$ and α-subunits (designated *atpI, atpH, atpF* and *atpA* respectively) were sequenced and found to be in the order *atpIHFA*, which is the same as that of the *E. coli unc* operon except that the gene encoding the δ-subunit is absent (Alt *et al.*, 1983; Hudson *et al.*, 1987). Genes in this cluster are expressed at different levels in different plant tissues, due to tissue-specific factors (Green and Hollingsworth, 1994). The amino acid sequence of $CF_OI$ is predicted from a cDNA clone as the *atpF* gene is interrupted by a large intron (Hudson *et al.*, 1987).

The nuclear genes from spinach encoding the γ-, δ- and $CF_OII$ subunits (designated *atpC, atpD* and *atpG*, respectively) have been cloned in cDNA form (Tittgen *et al.*, 1986). The cDNA clones of *atpC, atpD* and *atpG* hybridise to mRNA which, when translated in vitro, give rise to precursors with molecular weights of 45,000, 27,500, and 23,000 respectively. The precursors are taken up by isolated chloroplasts, and processed to mature forms with molecular weights of 37,000, 19,500 and 16,000 respectively (Tittgen *et al.*, 1986). The *atpG* gene appears to be a duplication of the chloroplast *atpF* gene and represents the first instance of one copy of a duplicated plastid locus being phylogenetically translocated to the nucleus (Herrmann *et al.*, 1993). Sequences covering the coding regions for mature form of the γ-subunit (Miki *et al.*, 1988), and the entire precursors of the γ-subunit (Mason and Whitfeld, 1990), the δ-subunit (Hermans *et al.*, 1988) and subunit $CF_OII$ (Herrmann *et al.*, 1993) have been published.

The predicted molecular weights of the spinach chloroplast $F_OF_1$-ATPase subunits, based on the amino acid sequences derived from nucleotide sequencing (Zurawski *et al.*, 1982; Hudson *et al.*, 1987; Miki *et al.*, 1988; Hermans *et al.*, 1988; Herrmann *et al.*, 1993), are listed in Table 1.1.

### *1.4.4 Physical and Enzymic properties of the Chloroplast $F_1$-ATPase*

The coupling factor ($CF_1$) first isolated from spinach chloroplast thylakoid membranes was initially thought not to possess ATPase activity (Jagendorf and Smith, 1962; Avron, 1963), although detailed investigation of its properties revealed latent ATPase activity activated by a number of treatments including heat (Vambutas and Racker, 1965; Farron and Racker, 1970), partial tryptic proteolysis (Vambutas and Racker, 1965) and dithiothreitol (DTT) (McCarty and Racker, 1968). The molecular weight of spinach $CF_1$ was

estimated to be between 325,000 and 430,000 according to sedimentation equilibrium analytical centrifugation (Farron, 1970; Moroney *et al.*, 1983). Based on deduced primary sequences, $CF_1$ with an $\alpha_3\beta_3\gamma\delta\varepsilon$ stoichiometry is predicted to have a molecular weight of 399,000.

Activated $CF_1$ hydrolyses ATP four times faster than GTP or ITP, while CTP and UTP are inactive as substrates (Vambutas and Racker, 1965). $Ca^{2+}$ is the preferred cation for $CF_1$, giving at least thirty fold higher ATPase activity than $Ni^{2+}$, $Mg^{2+}$, $Mn^{2+}$, $Co^{2+}$ or $Sr^{2+}$ (Vambutas and Racker, 1965), although the membrane-bound enzyme uses $Mg^{2+}$ preferentially (McCarty and Racker, 1968). The $K_M$ for $Ca^{2+}$ATP is approximately 0.8 mM (Nelson, 1976). Sulphydryl-specific reagents do not inhibit the $CF_1$-ATPase (Vambutas and Racker, 1965; Deters *et al.*, 1975).

*1.4.5 Structure/ function models for subunits of the chloroplast $F_OF_1$-ATPase.*

i) Subunit $CF_OI$ has a hydropathy profile similar to the *E. coli b*-subunit, although these proteins share only 19% similarity at the amino acid sequence level (Hudson *et al.*, 1987). $CF_OI$ has a short (28 residue) segment at the N-terminus which is highly hydrophobic and predicted to traverse the membrane, while the remainder of the molecule (121 residues) is hydrophilic and contains many charged residues (Hudson *et al.*, 1987).

Comparison of the amino acid sequence of $CF_OI$ as predicted from the sequence of the *atpF* gene and the N-terminal sequence of the isolated subunit reveals that a 17 amino acid leader sequence is cleaved from the precursor protein (184 residues in length) to yield the mature subunit (Bird *et al.*, 1985; Hudson *et al.*, 1987). The leader peptide may act to guide correct insertion of $CF_OI$ into the thylakoid membrane (Hudson *et al.*, 1987).

ii) The $CF_OII$ subunit precursor has 222 amino acid residues which includes 147 residues for the mature protein (molecular weight 16.5 kDa) and a transit sequence of 75 residues (molecular weight 8.0 kDa; Herrmann *et al.*, 1993). The hydropathy profile of the mature $CF_OII$ is similar to those of the *E. coli b*-subunit and $CF_OI$, but $CF_OII$ is not able to functionally replace the *E. coli b*-subunit (Schmidt, 1992). Spinach $CF_OII$ shares 29% amino acid sequence homology with the *E. coli b*-subunit, but has negligible homology with spinach $CF_OI$ (Herrmann *et al.*, 1993). The precursor subunit is imported into the chloroplast, processed and assembled in the thylakoid membrane via a bipartite

(import/thylakoid-targeting) transit peptide. There is no cleavage site for the stroma protease, suggesting a different method of membrane integration from $CF_oI$ (Herrmann *et al.*, 1993).

iii) Subunit $CF_oIII$ is a small (81 residue) hydrophobic protein with a hydropathy profile very similar to the *E. coli c*-subunit , although sequence identity is only 30% (Hudson *et al.*, 1987). Spinach $CF_oIII$ cannot functionally replace the *E. coli c*-subunit (Burkovski *et al.*, 1990). Like the *E. coli c*-subunit, $CF_oIII$ is predicted to form a hairpin structure, with two transmembrane α-helices separated by a short hydrophilic loop. As in *c*-subunit equivalent proteins from all species studied thus far, a DCCD-reactive acidic residue (E61 in $CF_oIII$) is positioned near the centre of the second transmembrane helix. This residue is essential for proton translocation through $F_o$ in *E. coli* (Hoppe *et al.*, 1980; 1982), raising the possibility that E61 in $CF_oIII$ may also play a role in proton conduction through the $CF_o$ complex. Interestingly, a kink in the second transmembrane α-helix of the *E. coli c*-subunit caused by a proline residue is also present in $CF_oIII$, the only difference being that in $CF_oIII$ the proline occurs in the first transmembrane α-helix. A significant role for the kink is suggested by the isolation of an *E. coli* double mutant in which the deleterious effects caused by the loss of the proline in the second helix are partially reversed by the mutation of a residue to a proline in the first helix (Fimmel *et al.*, 1983).

$CF_oIII$ may also be involved in the binding of $CF_1$ to $CF_o$. Using modified chromatographic procedures, Feng and McCarty (1990a) prepared $CF_oF_1$ depleted subunits $CF_oI$, $CF_oII$ and $CF_oIV$, leaving a complex of $CF_1$ and $CF_oIII$. A stable $CF_1/CF_oIII$ complex was purified, from which $CF_oIII$ dissociated upon treatment with EDTA (Wetzel and McCarty, 1993a; b).

iv) Subunit $CF_oIV$ (247 residues) has a hydropathy profile similar to the *E. coli a*-subunit (Hudson *et al.*, 1987). Although overall amino acid sequence similarity is low, significant homology between these subunits is found near the C-terminus, where many of the *a*-subunit residues known to be essential for proton translocation through the *E. coli* $F_o$ are located (Hudson *et al.*, 1987; Cox *et al.*, 1992). It therefore seems likely that $CF_oIV$ would play a role in proton conduction through $CF_o$, although Feng and McCarty (1990b) propose $CF_oIV$ to be merely involved in organisation and/or stabilisation of $CF_o$.

v) The $CF_1$ α- and β-subunits are much more highly conserved than the other $CF_OF_1$-ATPase subunits. The α-subunit (507 residues) shares 51% sequence identity with the *E. coli* α-subunit (Hudson *et al.*, 1987), while the $CF_1$ β-subunit (498 residues) shares 67% sequence identity with the *E. coli* β-subunit (Zurawski *et al.*, 1982). The spinach $CF_1$ α-subunit is partially able to functionally replace the equivalent *E. coli* subunit (Lill *et al.*, 1993). The $CF_1$ β-subunit was reported not able to functionally replace the equivalent *E. coli* subunit (Munn *et al.*, 1991; Lill *et al.*, 1993), but was shown to be able to substitute for the *E. coli* β-subunit in its role in allowing assembly of the *b*-subunit into the membrane (Cox *et al.*, 1981; Munn *et al.*, 1991). More recently, the cloned gene encoding the spinach chloroplast β-subunit has been shown to restore $F_OF_1$-ATPase function in an *E. coli* strain in which the *uncD* gene had been deleted (Chen *et al.*, 1995).

Binding studies with 2-azido-ATP indicate six nucleotide binding sites per $CF_1$ complex, all involving the three β-subunits, although three may occur at α/β subunit interfaces (Xue *et al.*, 1987a). As with *E. coli* $F_1$, there appear to be three catalytic and three non-catalytic nucleotide binding sites. Binding of 2-azido-ATP at non-catalytic sites resulted in labelling of $CF_1$ residue βY385 by an ATP or an ADP moiety, while binding at catalytic sites resulted in labelling of βY362 by only an ADP moiety (Xue *et al.*, 1987b).

vi) The $CF_1$ γ- and ε-subunits are poorly conserved in comparison to the other $CF_OF_1$-ATPase subunits. The spinach γ-subunit precursor (40.0 kDa) has 364 amino acid residues which includes 323 residues for the mature protein (molecular weight 35.7 kDa) and a transit sequence of 41 residues (Miki *et al.*, 1988; Mason and Whitfeld, 1990). The mature γ-subunit shares 33% sequence identity with the *E. coli* γ-subunit (Miki *et al.*, 1988), while the spinach $CF_1$ ε-subunit (134 residues) shares 26% sequence identity with the *E. coli* ε-subunit (Zurawski *et al.*, 1982). Neither of these subunits is able to functionally replace the equivalent *E. coli* subunit (Lill *et al.*, 1993). Spinach $CF_1$-γ contains four cysteine residues, two of which (C199 and C205) are capable of forming a disulphide bond (McCarty, 1992). These two residues form part of an extra domain not present in the *E. coli* γ-subunit (Miki *et al.*, 1988).

The $CF_1$ γ- and ε-subunits play a crucial role in the regulation of $CF_OF_1$-ATPase activity, both in terms of $\Delta\mu_{H^+}$ induced activation of the enzyme and redox modulation of activity. These processes account for the approximately

100 fold difference in catalytic rate observed between dark and illuminated thylakoid membranes, and prevent the wasteful hydrolysis of ATP in the dark (McCarty, 1992). As is the case with the *E. coli* $F_1$, the ε-subunit is an inhibitor of $CF_1$-ATPase activity (Richter *et al.*, 1984), and appears to bind $CF_1$ predominantly via the γ-subunit (McCarty, 1992). Neither the $CF_1$ δ- nor ε-subunits are required for $CF_1$ binding to $CF_O$, as they are in *E. coli* (Andreo *et al.*, 1982; Patrie and McCarty, 1984; Xiao and McCarty, 1989; Feng and McCarty, 1990). Removal of the ε-subunit from $CF_1$ has been shown to expose the γ-subunit domain that bears the redox-active thiols to reduction by DTT (Richter *et al.*, 1985) and thioredoxin (Dann and McCarty, 1992). One of the steps in the transformation of $CF_OF_1$ from its lowest to highest activity states involves a $\Delta\mu_{H+}$ induced activation of the enzyme. Generation of $\Delta\mu_{H+}$ causes conformational changes in the ε-subunit (Richter and McCarty, 1987) which weaken interaction between it and the γ-subunit, thereby reducing the inhibitory effects of the ε-subunit (McCarty, 1992). The second mechanism by which $CF_OF_1$ activity is controlled involves redox regulation. The redox-active pair of cysteine residues (C199 and C205 in spinach $CF_1$-γ) form a disulphide bond in the dark (McCarty, 1992). Upon illumination, an increased flux of electrons from photosystem I increases the pool of reduced thioredoxin, which in turn reduces the C199/C205 disulphide bond (Mills *et al.*, 1980; Mills and Mitchell, 1982; Soterupoulos *et al.*, 1992). The resulting changes in γ-subunit conformation decrease the affinity of ε-subunit binding approximately 20 fold (Soterupoulos *et al.*, 1992). The effect of the thiol reduction on the inactivated enzyme is to decrease the energy required for activation (Junesch and Gräber, 1987). Upon return to darkness, the binding of ADP to a $CF_1$ nucleotide binding site of the reduced activated enzyme causes rapid deactivation without causing the γ-subunit disulphide bond to reform. The oxidation of the sulphydryls occurs more slowly by an unknown mechanism (McCarty, 1992).

viii) The spinach δ-subunit precursor (27.6 kDa) has 257 amino acid residues which includes 187 residues for the mature protein (molecular weight 20.5 kDa) and a transit sequence of 70 residues (molecular weight 7.2kDa; Hermans *et al.*, 1988). The mature $CF_1$ δ-subunit shares little sequence identity with the *E. coli* δ-subunit, but appears from comparison of hydropathy profiles to be homologous (Hermans *et al.*, 1988).

The $CF_1$ δ-subunit has been suggested to play a role in coupling proton translocation to ATP synthesis (Engelbrecht and Junge, 1990). As mentioned above, neither the $CF_1$ δ- nor ε-subunits are required for $CF_1$ binding to $CF_O$, as they are in *E. coli* (Andreo *et al.*, 1982; Patrie and McCarty, 1984; Xiao and McCarty, 1989; Feng and McCarty, 1990). The δ-subunit may, however, bind to $CF_O$ and block the proton pore (Engelbrecht and Junge, 1990). Cross-reconstitution experiments using $CF_1$-depleted thylakoid membranes have also shown that the hybrid constructs $CF_1$(-δ)+ *E. coli* δ and *E. coli* $F_1$(-δ)+ chloroplast δ diminish proton flow through $CF_O$, and that $CF_1$(-δ) + *E. coli* δ does the same on the *E. coli* $F_O$, although the hybrid ATPases are not able to carry out ATP synthesis (Engelbrecht and Junge, 1990).

### 1.5 The *Synechococcus* $F_OF_1$-ATPase

The cyanobacteria are unique among prokaryotes in that they possess chlorophyll *a*, and carry out photosynthesis involving non-cyclic electron flow (Nicholls and Ferguson, 1992). As with plants and eukaryotic algae, water is used as the primary electron donor and oxygen is evolved (Stanier and Cohen-Bazire, 1977). The photosynthetic apparatus are located in thylakoid membranes which are continuous with the plasmalemma but form physically distinct specialized structures (Carr and Whitton, 1982). Signal peptides play an important role in targeting cyanobacterial proteins to the correct membrane region (Mackle and Zilinskas, 1994). The $F_OF_1$-ATPase occurs in both the thylakoids and the plasmalemma. Cyanobacteria synthesize ATP by photophosphorylation when illuminated, but most are able to carry out oxidative phosphorylation in the dark to enable the organism to at least survive (Matthijs and Lubberding, 1988).

The organisation and sequences of genes encoding $F_OF_1$-ATPase subunits from the cyanobacteria *Synechococcus* 6301 (Cozens and Walker, 1987), *Synechocystis* 6803 (Lill and Nelson, 1991) and *Synechococcus* 6716 (van Walraven *et al.*, 1993) have been determined. In *Synechococcus* 6301 and *Synechocystis* 6803, genes for four $F_O$ components (the *a*-, *c*-, *b*´- and *b*-subunits) and three $F_1$ components (the δ-, α- and γ-subunits) were found to be linked, and separated from another cluster containing the genes for the $F_1$ β- and ε-subunits. In the thermophile *Synechococcus* 6716, the gene for the γ-subunit is separate from the large operon, and thus lies at a third site (van Walraven *et*

*al.*, 1993). These gene orders are related to those found both in *E. coli* and in chloroplasts, but the presence of the genes for the $F_1$ β- and ε-subunits in a separate cluster most resembles the organisation found in chloroplasts. The presence in the cyanobacterial $F_O$ of two components with structures closely resembling the *E. coli b*-subunit (the *b'*- and *b*-subunits) indicates a close relationship with $CF_O$, which also contains two apparent *b*-subunit equivalents, $CF_OI$ and $CF_OII$. These findings, along with sequence comparisons, appear to support the theory that chloroplasts arose by endosymbiosis of an ancient photosynthetic bacterium from which cyanobacteria are descended (van Walraven *et al.*, 1993).

Comparisons of the sequences of cyanobacterial $F_OF_1$-ATPase genes with those from other sources confirm previously observed patterns in which the α- and β-subunit sequences are well conserved, while the γ-, δ-, ε-, *a*- and *b*-subunit sequences tend to be poorly conserved (Walker *et al.*, 1985). The cyanobacterial *c*-subunit sequences are moderately conserved with those from the *E. coli c*-subunit and tend to be well conserved with chloroplast $CF_OIII$ (van Walraven *et al.*, 1993).

As discussed above, a sequence region in the chloroplast $F_1$ γ-subunit containing two redox-active cysteine residues plays an important role in regulating $CF_OF_1$ activity. Alignment of sequences from all cyanobacterial γ-subunits published thus far indicates that this regulatory sequence is absent in cyanobacteria (van Walraven *et al.*, 1993; Wernegrune *et al.*, 1994). Using site-directed mutagenesis, Wernegrune *et al.* (1994) inserted the chloroplast sequence into the *Synechocystis* 6803 γ-subunit. The ATPase activity of the mutant enzyme was considerably lower than wild-type, but increased upon treatment with DTT.

### 1.6 Proposed Catalytic and Coupling Mechanisms of $F_OF_1$-ATPases

A model for an energy-dependent binding change mechanism for ATP synthesis by $F_OF_1$-ATPases, based on kinetic experiments involving hydrolysis of ATP by soluble $F_1$, was initially proposed by Boyer *et al.*, (1973) and refined by Cross (1981). According to this model, $F_1$ possesses three chemically identical but conformationally distinct interacting catalytic sites. The first site (O) has very low affinity for ligands and is catalytically inactive. The second site (L) has loose binding for ligands and is catalytically inactive. The third site (T) has tight binding for ligands and is catalytically active. The reaction is proposed to

involve three steps (see Figure 1.6). Firstly, the substrates ADP and inorganic phosphate ($P_i$) bind to the L binding site. Secondly, an energy-dependent conformational change converts the L site to a T site, the T site to an O site, and the O site to an L site. Thirdly, ATP is formed at the T site, and ATP dissociates from the O site. These steps would then be repeated twice to complete a full catalytic cycle (Cross, 1981).

If the mechanism proposed by Cross (1981) is correct, the three catalytic sites must be structurally equivalent but differ in conformation at any instant. The high resolution crystal structure of $F_1$ from bovine heart mitochondria reported by Abrahams *et al.* (1994) confirms that the three catalytic β-subunits differ in conformation and in the bound nucleotide. This structure shows an α-helical domain of the γ-subunit extending asymmetrically into the centre of a hexagonal ring formed by alternating α- and β-subunits. Cyclical interconversion of the conformational states of the catalytic β-subunits as proposed by Cross (1981) may therefore occur in the intact $F_1F_O$-ATPase complex via rotation of the $\alpha_3\beta_3$ subassembly relative to the γ-subunit (Abrahams *et al.*, 1994).

The mechanism proposed by Cross (1981) also predicts that the primary step for which the input of free energy is required is not the synthesis of ATP from ADP and $P_i$, but the release of ATP from the catalytic site where it forms spontaneously. Evidence for this has primarily been collected from experiments involving the hydrolysis of ATP by submitochondrial particles in the presence of $H_2{}^{18}O$, and measuring the amounts of $^{18}O$ incorporated into $P_i$ (Boyer, 1993). The exchange of $^{18}O$ is greater than that which could be accounted for by ATP hydrolysis alone, and continues even when an uncoupler is present to stop net ATP synthesis, indicating that $\Delta\mu_{H^+}$ is not required for the reversible formation of ATP from ADP and $P_i$ (Rosing *et al.*, 1977). At very low concentrations of ATP consistent with unisite catalysis, tightly bound ATP becomes more loosely bound when respiration is initiated by the addition of succinate or NADH, suggesting that the release of ATP is an energy-requiring step during steady-state oxidative phosphorylation (Hackney and Boyer, 1978). When present at higher concentrations (during multisite catalysis) ATP appears to occupy one or more lower affinity catalytic sites, which causes conformational changes allowing hydrolysis of ATP and release of products from the high affinity site at a much accelerated rate. The $F_1$-ATPase therefore

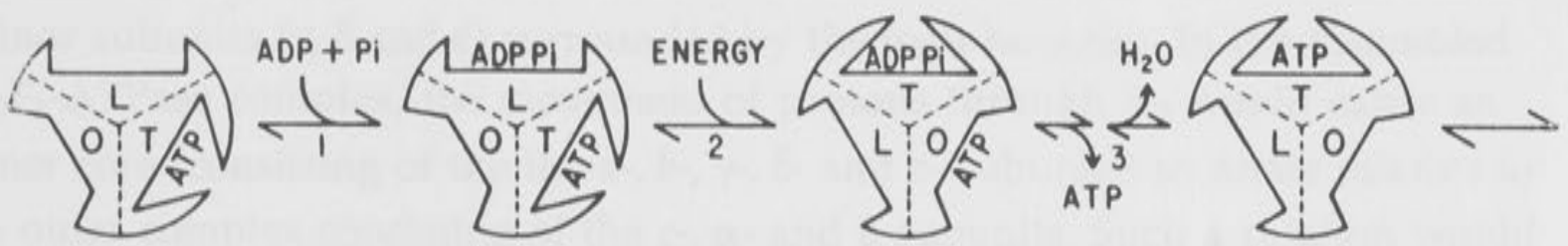


**Figure 1.6**: The cyclic energy-dependent binding change mechanism for ATP synthesis proposed by Cross (1981). According to this model, $F_1$ possesses three chemically identical but conformationally distinct interacting catalytic sites (Open, Loose and Tight). The reaction is proposed to involve three steps. Firstly, the substrates ADP and inorganic phosphate ($P_i$) bind to the L binding site. Secondly, an energy-dependent conformational change converts the L site to a T site, the T site to an O site, and the O site to an L site. Thirdly, ATP is formed at the T site, and ATP dissociates from the O site. One third of the full reaction cycle is shown.

exhibits negative co-operativity with respect to substrate binding but positive co-operativity of catalysis.

Any proposed mechanism for the coupling of ATPase activity to proton pumping, or the movement of protons down an electrochemical gradient to ATP synthesis, must take into account all relevant information regarding the quaternary structure of the $F_OF_1$-ATPase complex. The cyclical interconversion of catalytic sites in the mechanism proposed by Cross (1981) implied that rotational movement of some subunits relative to others in the complex may be involved. Early suggestions regarding rotational catalysis (Boyer and Kohlbrenner, 1981; Gresser *et al.*, 1982) made no predictions regarding the roles to be played by particular subunits or how such a mechanism could be reconciled with the existing structural information. A more detailed model for rotational catalysis was proposed by Cox *et al.* (1984; 1986). This model proposes that $F_O$ assembles as a ring of *c*-subunits about a central core consisting of the *a*-subunit and the two *b*-subunits (see Figure 1.7), and that $F_1$ would consist of the minor subunits (γ, δ and ε) surrounded by the $\alpha_3\beta_3$ hexagon. In the assembled $F_OF_1$-ATPase complex, the movement of protons through $F_O$ would cause an inner core (consisting of the the *a*-, *b*-, γ-, δ- and ε- subunits) to rotate relative to an outer complex consisting of the *c*-, α- and β-subunits. Such a rotation would satisfy the cyclical conformational changes which were proposed by Cross (1981) to be associated with catalysis.

The proposal for rotational catalysis outlined above is consistent with many experimental observations. The dominance of some mutant *uncE* alleles (coding for the *c*-subunit; Friedl *et al.*, 1980) and the inactivation of proton transport by reaction of DCCD with only one copy of the *c*-subunit per complex (Hermolin and Fillingame, 1989) are compatible with this model. The fact that there is only a single copy of the *a*-subunit, and that proton translocation requires it to interact with many *c*-subunits, supports the model. By determining rates of trypsin cleavage and degree of cross-linking to the β-subunit in isolated $F_1$, Mendel-Hartvig and Capaldi (1991a) showed that the ε-subunit undergoes conformational changes depending on which ligands are bound to the enzyme. They suggest that the observed affinity of the ε-subunit for the one particular β-subunit carrying out ATP hydrolysis is reversed upon $P_i$ release. This could induce the movement of the ε-subunit (and the rest of the inner complex) on to the next β-subunit (one third of a rotation) concomitant

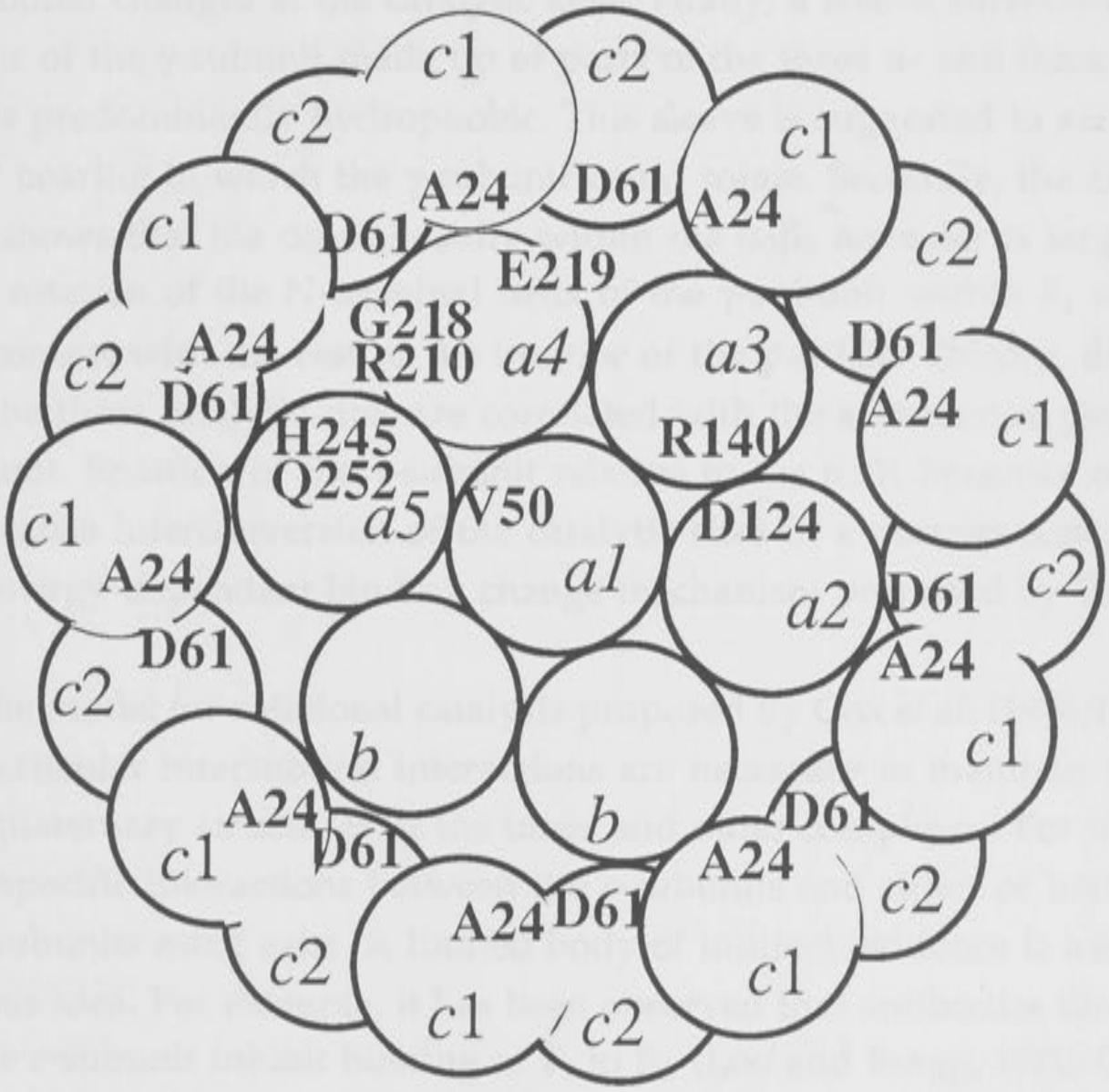


**Figure 1.7**: A proposed arrangement for the packing of transmembrane α-helices within the *E. coli* $F_O$ sector (from Hatch *et al.*, 1995). The five transmembrane α-helices of the *a*-subunit, and the single transmembrane helix from each of the two *b*-subunits, are placed within a ring of *c*-subunits. The interacting amino acid residues described in section 1.3.7 are indicated.

with the transport of protons and movement of the *a*- and *b*-subunits relative to the *c*-subunits in a manner consistent with rotational catalysis.

The high resolution crystal structure of $F_1$ from bovine heart mitochondria reported by Abrahams *et al.* (1994) is clearly compatible with the rotational catalysis model proposed by Cox *et al.* (1984; 1986). Abrahams *et al.* (1994) make several pertinent observations which support the idea that rotation of the γ-subunit relative to the $\alpha_3\beta_3$ hexamer may cause cyclical conformational changes at the catalytic sites. Firstly, a sleeve surrounding the C-terminus of the γ-subunit made up of parts of the three α- and three β-subunits is predominantly hydrophobic. This sleeve is suggested to act as a molecular bearing in which the γ-subunit could rotate. Secondly, the crystal structure shows that the central cavity within the $\alpha_3\beta_3$ hexamer is large enough to permit rotation of the N-terminal helix of the γ-subunit within $F_1$ with minimal contact with the rest of the interior of the particle. Thirdly, differences between the three catalytic sites are correlated with the asymmetric position of the γ-subunit. Rotation of the γ-subunit relative to the $\alpha_3\beta_3$ hexamer could therefore cause interconversion of the catalytic sites in a manner compatible with the energy-dependent binding change mechanism proposed by Cross (1981).

If the model for rotational catalysis proposed by Cox *et al.* (1984;1986) is correct, particular intersubunit interactions are necessary to maintain the separate quaternary structures of the inner and outer complexes. For the outer complex, specific interactions between the *c*-subunits and either or both of the α- and β-subunits must exist. A limited body of indirect evidence is available to support this idea. For example, it has been observed that antibodies directed against the *c*-subunit inhibit binding of $F_1$ to $F_O$ (Loo and Bragg, 1982; Girvin *et al.*, 1989; Deckers-Hebestreit and Altendorf, 1992), and may displace $F_1$ bound to $F_O$ (Deckers-Hebestreit and Altendorf, 1992). Certain mutations in the polar loop region of the *c*-subunit weaken $F_1$ binding (Mosher *et al.*, 1985; Miller *et al.*, 1989; Fraga and Fillingame, 1989), and partially reconstituted $F_O$ sectors bind some $F_1$ in a *c*-subunit-dependent manner (Schneider and Altendorf, 1985). Weak but significant labelling of α- and β-subunits by lysine-specific reagents directed to the polar head groups of the lipid bilayer suggest the close proximity of these subunits to the membrane (Aggeler *et al.*, 1987). The absence, however, of direct evidence for *c*/α or *c*/β interactions remains a significant weakness of the rotational model.

Evidence for intersubunit interactions within the inner complex appears to be more substantial. Both the δ-subunit and the cytoplasmic domain of the *b*-subunit are predicted from Chou-Fasman sequence analysis (Senior, 1983; Walker *et al.*, 1982b; 1984) and circular dichroism spectroscopy (Sternweis and Smith, 1977; Dunn, 1992) to be highly α-helical. It was suggested by Sternweis and Smith (1977) and Walker *et al.* (1984) that these subunits combine through helix-helix interactions to form the stalk visible in electron micrographs of the $F_OF_1$ complex (most clearly seen in the cryoelectron micrographs reported by Gogol *et al.* (1989a)). Although no evidence for specific interactions between the *E. coli b*- and δ-subunits has been reported, zero-length crosslinking between spinach chloroplast subunits $CF_1\delta$ and $CF_OI$ (one of the two $CF_O$ subunits equivalent to the *E. coli b*-subunit) has been demonstrated (Beckers *et al.*, 1992). Cross-linking studies involving $F_O$ subunits have yielded $b_2$, *ab* and $ab_2$ species (Hermolin *et al.*, 1983), as would be predicted from the proposed model. The finding of cross-linked heterodimers of γδ (Aris and Simoni, 1983) and γε (Bragg and Hou, 1976; 1980; Aris and Simoni, 1983) are also in agreement with the model, although these findings do not preclude other possible mechanisms. The strong γε interaction observed following *in vitro* mixing of the purified subunits (Dunn, 1982) and the γ-subunit-dependence of the inhibitory action of the ε-subunit (Sternweis and Smith, 1977; Larson and Smith, 1977) suggest that these proteins interact in the native enzyme. Dunn (1982) was not able, however, to isolate a complex of the γ-, δ- and ε-subunits following gel-sieve chromatography of mixtures of the purified subunits, and a role for the *b*-subunit in holding these subunits together must be postulated if the model for the inner complex is to be sustained.

It is clear from the evidence discussed above that some of the crucial intersubunit interactions predicted by the rotational catalysis model of Cox *et al.* (1986) have yet to be demonstrated. To test the model, further experimentation aimed at isolating and characterising the relevant multisubunit complexes must be carried out.

**1.7 Aims of the Project**

*i) Complementation Studies and Experiments with Hybrid Enzymes*: In vitro cross-reconstitution experiments have shown that some hybrid assemblies containing *E. coli* and PS3 (a thermophilic bacterium) $F_1$ α-, β- and γ-subunits, and all assemblies of these subunits from *E. coli* and *Salmonella typhimurium*, have ATPase activity (Futai *et al.*, 1980; Takeda *et al.*, 1982; Hsu *et al.*, 1984). It has also been shown that the purified *E. coli* and spinach chloroplast β-subunits can reconstitute ATPase activity and and a low level of photophosphorylation in chromaphores from the photosynthetic bacterium *Rhodospirillum rubrum* depleted in β-subunits (Gromet-Elhanan *et al.*, 1985; Richter *et al.*, 1986). Das and Ljungdahl (1993) reconstituted $F_1$ stripped membrane vesicles from *Clostridium thermoautotrophicum* and *E. coli* with $F_1$ from both bacteria. Reconstituted complexes exhibited ATPase activity but did not support ATP synthesis or ATP-dependent proton pumping. Following the reconstitution of partially $CF_1$-depleted chloroplast $CF_OF_1$ATPase complexes into liposomes, the addition of $F_1$ from the thermophilic bacterium PS3 restored greater ATP-dependent proton uptake than the addition of $CF_1$ (Galmiche *et al.*, 1994).

Genetic complementation analysis allows the assembly and function of hybrid enzyme complexes to be tested *in vivo*. For example, Kaim and Dimroth (1994) transformed an *E. coli* mutant deficient in the entire *unc* operon with a plasmid containing the genes encoding the *a-*, *c-*, *b-*, and δ-subunits of the $Na^+$-dependent $F_OF_1$ATPase of *Propionigenium modestum* and the genes encoding the *E. coli* α, γ, β and ε subunits. The transformants showed $Na^+$-dependent growth on succinate as sole carbon source. Xie *et al* (1993) reported that *Chlorobium limicola* β- and ε-subunits complemented *E. coli* mutants defective in the corresponding subunits, indicating that the hybrid enzyme formed from subunits of the two bacteria is active in ATP synthesis. Genes encoding the α- and β-subunits from *Bacillus megaterium* could complement some*E. coli uncA* and *uncD* mutations, depending on which other *B. megaterium* genes were also expressed (Hawthorne and Brusilow, 1986; Scarpetta *et al.*, 1991). Complementation of a particular *E. coli* β-subunit mutant by the *B. megaterium* β- or β- and ε-subunits produced obligately aerobic *E. coli* cells (Scarpetta *et al.*, 1991). More recently, the cloned gene encoding the spinach chloroplast β-subunit has also been shown to complement the *E. coli uncD* gene (Chen *et al.*, 1995). Burkovski *et al* (1994) reported that a chimaeric protein

comprising the seven N-terminal amino acid residues from spinach chloroplast $CF_oIII$ and the remaining part of the *E. coli c*-subunit was able to replace the wild-type *E. coli c*-subunit, although hybrid proteins with 13 and 33 N-terminal amino acids of $CF_oIII$ were not functional.

Lill *et al.* (1993) expressed genes encoding all of $F_1$-ATPase subunits from both spinach chloroplasts and the cyanobacterium *Synechocystis* sp. PCC 6803 in *E. coli*. Each of the recombinant subunits formed inclusion bodies within the cells. The α-subunits from both sources, the cyanobacterial β-subunit, the δ-subunits from both sources and the ε-subunits from both sources restored the ability to grow on succinate as sole carbon source of *E. coli* mutant strains affected in the cooresponding subunit. Neither of the γ-subunits were able to complement a defective *uncG* gene, however.

Much of the literature discussed in previous sections describes how the analysis of mutants has led to a greater understanding of the structure and function of $F_oF_1$-ATPase complexes from many species, and in particular from *E. coli*. Genetic complementation and cross-reconstitution experiments involving the mixing of subunits from different species may be considered extreme forms of mutagenesis where, depending on the degree of homology between the equivalent 'normal' and 'foreign' subunit, from almost none to almost all amino acids have been altered. To provide useful information, such experiments must usually lead to the formation of an active or partially active enzyme in which one or more subunits are replaced by their 'foreign' equivalents, or at least to the formation of an inactive enzyme in which the 'foreign' subunits have correctly assembled. In this way, successful genetic complementation and cross-reconstitution experiments provide valuable information about which subunits, or which domains, regions or residues within subunits, are important to the structure, function or assembly of the enzyme complex. Site-directed mutagenesis of the 'foreign' subunit(s) may then provide futher or more detailed information.

The aim of the first section of work described in this thesis was to test whether particular spinach chloroplast $F_oF_1$-ATPase subunits might be able to functionally replace the homologous *E. coli* subunits. This may be carried out by firstly cloning spinach chloroplast genes into *E. coli* expression vectors, then transforming mutant *E. coli* strains affected in the relevant subunit with the appropriate plasmid. Assays may then be carried out to assess whether a functional hybrid $F_oF_1$-ATPase had assembled in the cell. If any of the spinach

chloroplast subunits were found to be able to replace the homologous *E. coli* subunit, site-directed mutagenesis and other experiments could then be carried out to probe the structure and function of the foreign subunit in the hybrid complex.

Munn (1988) expressed genes encoding spinach chloroplast subunits α, β, ε, $CF_OIII$, $CF_OIV$ and the precursor to $CF_OI$ in mutant *E. coli* strains, and none of these subunits was found to be able to functionally replace the corresponding *E. coli* subunit. The expression of subunit $CF_OIII$ in an *uncE* mutant *E. coli* strain was also reported by Burkovski *et al.*, (1990), and was found not to be able to functionally replace the *E. coli c*-subunit. At the time of the work described by Munn (1988), clones for the three nuclear encoded spinach $F_OF_1$-ATPase subunits (δ, γ and $CF_OII$) were not available to this laboratory. These clones were subsequently obtained, allowing further complementation studies described in this work.

*ii) Investigation of intersubunit interactions within $F_OF_1$-ATPase complexes*: As discussed in section 1.6, confirmation of the rotational model for the mechanism of the $F_OF_1$-ATPase requires that defined interactions occur between particular subunits. To test this, relevant subunits were expressed as fusions with the enzyme glutathione-S-transferase (GST). Fusion proteins produced in this way may be purified rapidly by affinity chromatography under non-denaturing conditions. Once purified, the fusion protein may be specifically cleaved to remove the GST component, allowing the protein of interest to be studied.

The mild conditions under which GST-fusion proteins may be purified allow protein/protein interactions to be investigated. If genes encoding other proteins of interest are cloned downstream of the gene encoding the fusion protein, these genes may be expressed at high levels along with the gene for the fusion protein. The fusion protein may then be purified and analysed to determine whether any of the gene products with which it was expressed co-purify with it. These techniques are used to investigate of interactions between $F_OF_1$-ATPase subunits from *E. coli*, spinach chloroplast and the cyanobacterium *Synechococcus* R2.

*iii) Studies on the structure and function of purified wild-type and mutant soluble domains of the E. coli b-subunit:* As explained in section 1.6, the hypothesis for rotational catalysis proposed by Cox *et al.* (1984; 1986) requires that strong and specific interactions exist between the *b*-subunit of $F_O$ and the minor $F_1$ subunits $\gamma$, $\delta$ and $\varepsilon$. The cytoplasmic domain of the *b*-subunit has been shown to bind $F_1$ (Dunn, 1992; Wilkens *et al.*, 1994), and must certainly play a central role in the coupling of proton translocation through $F_O$ and catalysis in $F_1$. A section of work in this thesis is devoted to analysing the physical properties of purified wild-type and mutant proteins corresponding to the *b*-subunit cytoplasmic domain, with the aim of better understanding the molecular architecture and coupling mechanism of the *E. coli* $F_OF_1$-ATPase.

# CHAPTER 2

# MATERIALS AND METHODS

## 2.1 Chemicals and enzymes

All chemicals used in this work were of analytical reagent grade or better, and were obtained from the following sources:

Ajax Chemicals (Auburn, NSW, Australia):

Acetic acid (glacial), boric acid, calcium chloride, ethanol, ethylenediamine-*N, N, N´, N´*-tetraacetic acid (EDTA), ferric chloride, glucose, glycine, magnesium acetate, magnesium sulphate, manganous sulphate, methanol, potassium acetate, sodium acetate, sodium chloride, sodium cyanide, sodium hydroxide, sodium succinate, trichloroacetic acid (TCA), urea, zinc sulphate

Amersham (Amersham, UK)

[$^{35}$S]-methionine, [$^{35}$S]dATPαS

AMRAD Pharmacia Biotechnology (Melbourne, Australia)

Isopropyl-β-D-thiogalactoside (IPTG), T7 DNA polymerase-based sequencing kit

Aldrich-Chemie (Steinheim, Germany):

*para*-amino benzamidine

AT Biochem (Malvern, PA, USA):

Long Ranger modified acrylamide/bis-acrylamide stock solution for DNA sequencing gels

BDH (Poole, UK):

Ammonium persulphate, glycerol, poly(ethyleneglycol)- average mol. wt. approx 6000 (PEG-6000), sodium dodecylsulphate (SDS), sucrose

Bio-Rad (CA, USA)

Assay reagent for Bradford method protein estimation

Boehringer Mannheim (Mannheim, Germany):

All restriction endonucleases and buffers, calf intestinal alkaline phophatase (CIAP) and buffer, deoxynucleotide 5´-triphosphates, *Taq* DNA Polymerase and buffer, terminal transferase and buffer

Calbiochem (La Jolla, CA, USA):

N-tris(hydroxymethyl)methyl-2-aminoethanesulphonic acid (TES)

Difco Laboratories (Detroit, MI, USA):

Bacto-agar, Bacto-tryptone, beef extract, casamino acids, yeast extract

Eastman Kodak (Rochester, NY, USA):

Coomassie Blue R250, β-mercaptoethanol

Fluka Chemie (Buchs, Switzerland):

2-aminocaproic acid (ε-aminocaproic acid, EACA)

Merck (Darmstadt, Germany):

L-arginine

Promega Corporation (Madison, WI, USA):

Miniprep DNA purification resin, PCR DNA purification resin, DNA clean-up purification resin, T4 DNA ligase and buffer, *E. coli* S30 extract system for circular DNA (*in vitro* transcription/ translation system)

Sigma Chemical (St. Louis, MO, USA):

Adenosine 5´-triphosphate (ATP), agarose, atebrin, bromophenol blue, caesium chloride, carbonyl cyanide *m*-chlorophenylhydrazone (CCCP), chloramphenicol, dithiothreitol (DTT), ethidium bromide, ethyleneglycol bis(β-aminoethyl ether)*N, N, N´, N´*,-tetraacetic acid (EGTA), glutathione, glutathione insolubilised on cross-linked 4% beaded agarose, human thrombin, *N*-2-hydroxyethylpiperazine-*N´*-2-ethanesulphonic acid (HEPES), β-nicotinamide adenine dinucleotide (reduced form) (NADH), rubidium chloride, *N, N, N´, N´*,-tetramethylethylenediamine (TEMED), thiamine, 2,2,2-trifluoroethanol, tricine, tris(hydroxymethylaminomethane) (Tris), Triton X-100

Stratagene (La Jolla, CA, USA):

*Pfu* DNA polymerase and buffer

**2.2 Media**

*i) 56 minimal medium*: The minimal medium employed for bacterial cell culture was similar to medium 56, described by Monod *et al.*, (1951), and contained (per litre) 10.6 g potassium hydrogen orthophosphate, 6.1 g sodium dihydrogen orthophosphate, 0.2 g magnesium sulphate and 2.0 g ammonium sulphate. This was prepared as a five-times concentrated stock containing 0.05% chloroform, and was diluted to the correct concentration prior to use.

Trace element stock solution (Gibson *et al.*, 1977a), prepared at 1000 times concentration, was added to 56 minimal medium immediately prior to use, to give final concentrations of 1.78 μM ferric chloride, 2.45 μM calcium chloride, 1.0 μM manganous sulphate, 13.9 μM zinc sulphate, 0.68 μM cobaltous sulphate and 4.69 μM boric acid.

56 minimal medium containing trace elements was sterilised by autoclaving at 121 °C for 45 min. Glucose or succinate was added to a final concentration of 33 mM, and thiamine was added to 1 μM. Additional growth factors were added, where required, to the following final concentrations: 0.7 mM L-arginine, 30.0 μM 2,3-dihydroxybenzoate and 0.2 mM uracil.

ii) *Luria medium*: Luria broth (Luria and Burrous, 1957) consisted of (per litre) 10 g Bacto-tryptone, 5 g yeast extract and 5 g sodium chloride, adjusted to pH 7.0 with aqueous 10 M sodium hydroxide. It was sterilised by autoclaving at 121 °C for 45 min, then supplemented with either glucose or glycerol to a final concentration of 33 mM.

iii) *2YTmedium*: 2YT medium consisted of (per litre) 16 g Bacto-tryptone, 10 g yeast extract and 5 g sodium chloride, adjusted to pH 7.0 with aqueous 10 M sodium hydroxide. It was sterilised by autoclaving at 121 °C for 45 minutes.

iv) *MG medium*: MG medium contained (per litre) 10 g beef extract, 10 g peptone, 3 g yeast extract and 5 g sodium chloride, adjusted to pH 7.5 with 10 M aqueous 10 M sodium hydroxide. MG medium was sterilised by autoclaving at 121 °C for 45 min, then supplemented with glucose to a final concentration of 33 mM.

v) *Solid media*: Solid Luria and MG media were prepared by the addition of Bacto-agar, 20 g per litre, to the liquid media prior to sterilisation. Solid 56

medium into sterile plastic petrie dishes and allowing it to set at room temperature.

vi) *Antibiotics*: Stock solutions of ampicillin were prepared at a concentration of 100 mg/ mL, and added to media at a final concentration of 100 µg/mL. Stock solutions of chloramphenicol were prepared at 60 mg/mL in ethanol, and added to media to a final concentration of 100 µg/mL.

## 2.3 Bacterial Strains and Plasmids

The genotypes of all relevant bacterial strains and plasmids used in this work are described where mentioned in the text or in cited references. Bacterial strains and selected plasmids are listed in Tables 2.2 and 2.3, respectively.

i) *Storage of strains*. Short-term storage of strains was on solid medium, at 4°C. For long term storage of strains, a freshly-grown lawn of bacteria on solid medium was resuspended in Luria broth containing 30% glycerol, and stored in screw-cap vials at -20 °C.

ii) *Growth Measurements in Liquid Media*. The cell density of liquid cell cultures was measured as turbidity, against a blank of the liquid medium, using a Klett-Summerson colourimeter (Klett Manufacturing, NY, USA). Cell densities are expressed as Klett units, where $10^8$ cells/mL is approximately equivalent to a reading of 40 Klett units.

## 2.4 Growth on succinate media

The ability of strains to carry out oxidative phosphorylation was tested by determining their capacity for growth on minimal medium containing succinate as sole carbon source. Strains to be tested were streaked onto succinate plates and incubated at 37 °C for up to three days. Succinate plates contained 33

mM sodium succinate in 56 minimal medium supplemented with trace elements (see section 2.2), 0.5% casamino acids (Difco), required growth factors, antibiotics where appropriate and 2% Bacto-agar (Difco).

**2.5 Measurement of Aerobic Growth Yield in Limiting Glucose**

The ability of bacterial strains to carry out oxidative phosphorylation was measured by their aerobic growth in medium containing limiting glucose. The growth yield medium contained 56 minimal salts, trace elements, 5 mM glucose, 4% Luria broth and growth supplements plus antibiotics where appropriate.

The strain of interest was inoculated from a freshly grown plate into 10 mL of growth medium and grown in a water bath with vigorous shaking at 37°C. The cell density in Klett units was measured at various times and the maximal cell density reached by each culture was recorded.

**2.6 Small-Scale Plasmid Preparations**

Small-scale preparations of plasmid DNA were carried out using the Magic and Wizard Minipreps DNA Purification Systems (Promega Corporation, Madison, WI, USA), according to instructions set out in the technical bulletin supplied by the manufacturer. These are summarised below:

1.5 mL of stationary phase *E. coli* culture was transferred to a 1.5 mL polypropylene microcentrifuge tube. Cells were pelleted by centrifugation for 1 min at 14,000 x *g* in an Eppendorf microcentrifuge. Growth medium was poured off and discarded. The tube was briefly centrifuged to bring any remaining growth medium to the bottom of the tube, and this was removed with a pipette. The cell pellet was resuspended in 200 µL of cell resuspension solution (50 mM Tris-HCl (pH 7.5), 10 mM EDTA, 100 mg/mL RNase A). The cells were then lysed by the addition of cell lysis solution (0.2 M NaOH, 1% SDS), followed by gentle mixing by repeated invertion of the tube. 200 mL of neutralisation solution (1.32 M potassium acetate, pH 4.8) was added, and the contents of the tube mixed by vortexing. The fluffy white precipitate was pelleted by centifugation at 14,000 x *g* in an Eppendorf microcentrifuge for 5 minutes. The supernatant was transferred to a fresh microcentrifuge tube using a pipette. 800 µL of Magic or Wizard Minipreps DNA purification resin was added, and the contents mixed by repeated inversion of the tube. A 2.5 mL sterile disposable syringe was prepared for use by removing the plunger. A

Magic or Wizard minicolumn was attached to the syringe barrel by the luer-lock extension. The mixture of crude DNA and resin was transferred to the syringe barrel. The syringe plunger was then slowly inserted, and the slurry pushed into the minicolumn. The syringe was detached from the minicolumn and the plunger removed from the syringe. The syringe barrel was then reattached to the minicolumn. 2 mL of column wash solution (84 mM NaCl, 8.4 mM Tris-HCl (pH 7.5), 2 mM EDTA, 55% v/v ethanol) was poured into the syringe barrel. The syringe plunger was re-inserted into the syringe barrel, and the wash solution pushed gently through the minicolumn. The syringe was removed and the minicolumn transferred to a 1.5 mL microcentrifuge tube. The tube was then centrifuged at 14,000 x *g* for 20 seconds in an Eppendorf microcentrifuge to dry the resin. The minicolumn was transferred to a fresh 1.5 mL microcentrifuge tube. 50 µL of pre-heated (65°C) water was then added, and allowed to stand for 1 min. The minicolumn was then centrifuged at 14,000 x *g* in an Eppendorf microcentrifuge to elute the DNA solution, which was collected in the microcentrifuge tube.

### 2.7 Large-Scale Preparation of Plasmid DNA

The method used for the large-scale preparation of plasmid DNA was essentially that of Selker *et al.*, (1977). The strain bearing the plasmid of interest was grown to stationary phase in 1 litre of growth medium (either 56 medium with trace elements or Luria broth) containing glucose, any other necessary supplements and the appropriate antibiotic, with vigorous shaking at 200 cycles per minute for aeration. Cells were pelleted by centrifugation for 5 minutes at 8,000 x*g* at 4°C, growth medium was discarded, and the cell pellet resuspended in a buffer containing 50 mM Tris-HCl (pH 8.0) and sucrose (25% w/v). 8 mL of lysozyme solution (10 mg/mL in 0.25 M Tris-HCl, pH 8.0) was then added. The cell suspension was swirled gently and stored on ice for 5 minutes to allow spheroplast formation. 4 mL of 0.25 M EDTA (pH 8.0) was added, with swirling, and the cells incubated on ice for 5 min. 32 mL of Triton lysis buffer (50 mM Tris-HCl (pH 8.0), 62.5 mM EDTA, 0.3% v/v Triton X-100) was added to lyse the spheroplasts. The suspension was stirred for 5 minutes. Cell debris was pelleted by centrifugation for 20 mins at 48,000 x *g* at 4°C, and the supernatant carefully removed. One quarter volume of 5M NaCl was added, with stirring, followed by one quarter volume of 50% PEG-6000 in 50 mM Tris-HCl (pH 8.0). This was mixed gently on ice, and left on ice for between 30 minutes and 2 hours to allow

precipitation of the DNA. The precipitate was collected by centrifugation for 5 minutes at 3,000 x *g* at 4°C, and the supernatant poured off. The pellet was then resuspended in 7mL TE buffer (10 mM Tris-HCl (pH 8.0), 1 mM EDTA), and 7.0 mL was removed to a Sorvall SE12 centrifuge tube. 7.2 g CsCl was added, the tube sealed with parafilm, and the salt dissolved by repeated inversion of the tube. The tube was centrifuged for 20 minutes at 2,300 x *g* at room temperature, and the layer of protein at the top of the tube scooped off carefully with a spatula. The solution was then transferred to a 50Ti centrifuge tube (16 x 76 mm, Beckman Instruments) and 300 µL of 10 mg/mL ethidium bromide solution added. The tubes were filled with paraffin oil, sealed, and centrifuged at 140,000 x *g* at 15°C for between 42 and 72 hours to allow the CsCl density gradient to come to equilibrium. Two bands, a heavy band below a much lighter one, were normally observed. The lower of the two bands, being the plasmid DNA band, was removed by inserting an 18 gauge needle attached to a 2.5 mL syringe into the side of the centrifuge tube, unsealing the top of the tube, and drawing the band out into the syringe. The solution was immediately extracted 5 times with isopropanol (stored over NaCl-saturated TE) to remove the ethidium bromide. CsCl was removed by twice dialysing the solution against 1 litre of TE buffer at 4°C. The plasmid DNA was stored in sterile tubes at 4°C.

**2.8 Digestion of Plasmid DNA with Restriction Endonuclease Enzymes**

DNA in water was mixed with ten-times concentrated restriction buffer as specified by the manufacturer to give a final one-times concentration. When more than one enzyme was used and different buffers recommended for each enzyme, charts supplied by Boehringer Mannheim and/or Promega Corporation listing percentages of maximal activity observed in each buffer were consulted. From this information, an appropriate buffer was selected. Approximately 5 units of restriction enzyme were normally added, and the incubation carried out for 1-2 hrs at 37°C (30°C for incubations with *Sma*I).

If removal of the enzyme and/or transfer to a different buffer was required following digestion, DNA was purified using Magic or Wizard DNA Clean-Up systems (Promega Corporation, Madison, WI, USA) according to instructions set out in the technical bulletin supplied by the manufacturer. These are summarised below:

800 mL of Magic or Wizard DNA Clean-Up resin was added to the DNA solution to be purified in a 1.5 mL microcentifuge tube, and the contents mixed by repeated inversion of the tube. A 2.5 mL sterile disposable syringe was prepared for use by removing the plunger. A Magic or Wizard minicolumn was attached to the syringe barrel by the luer-lock extension. The mixture of DNA and resin was transferred to the syringe barrel. The syringe plunger was then slowly inserted, and the slurry pushed into the minicolumn. The syringe was detached from the minicolumn and the plunger removed from the syringe. The syringe barrel was then reattached to the minicolumn. 2 mL of 80% isopropanol was poured into the syringe barrel. The syringe plunger was re-inserted into the syringe barrel, and the wash solution pushed gently through the minicolumn. This washing procedure was then repeated. The syringe was removed and the minicolumn transferred to a 1.5 mL microcentrifuge tube. The tube was then centrifuged at 14,000 x *g* for 20 seconds in an Eppendorf microcentrifuge to dry the resin. The minicolumn was allowed to stand in air for 5 mins to allow all traces of isopropanol to evaporate. The minicolumn was transferred to a fresh 1.5 mL microcentrifuge tube. 50 µL of pre-heated (65°C) water was then added, and allowed to stand for 1 min. The minicolumn was then centrifuged at 14,000 x *g* in an Eppendorf microcentrifuge to elute the DNA solution, which was collected in the microcentrifuge tube.

**2.9 Removal of 5´ Phosphate Groups from Linear DNA Fragments**

When DNA ligations involving insertion of a fragment into a vector cut with a single enzyme were attempted, 5´ phosphate groups were removed to prevent ligation of the vector fragment to itself (recircularisation). This was carried out by incubating the linear vector fragments with calf-intestinal alkaline phosphatase (CIAP) (Boehringer Mannheim, Mannheim, Germany) in CIAP buffer (50 mM Tris-HCl (pH 8.5), 0.1 mM EDTA) at 50°C for 1-2 hours.

Following the dephosphorylation reaction, CIAP was removed by purifying the DNA solution using Magic or Wizard DNA Clean-Up systems, as described in section 2.8 above.

**2.10 Ligation of DNA fragments**

*i) Cohesive-end ligation*: To the DNA in a 1.5 mL polypropylene microcentrifuge tube were added 3 µL of ten-times concentrated ligation buffer, and water to a total volume of 30 µL. The ligation buffer consists of 30 mM Tris-HCl (pH 7.8), 10 mM $MgCl_2$, 10 mM DTT and 0.5 mM ATP. The tube was heated to 65°C for 1 minute then cooled to room temperature. Approximately 10 units of T4 DNA ligase (Promega Corporation, Madison, WI, USA) were added and mixed by gently pipetting the solution up and down. The reaction was left to proceed for 6-12 hours at room temperature. If the ligation reaction mix was to be used for transformation of *E. coli* cells by electroporation, the purification of the DNA into water was required. This was carried out using Magic or Wizard DNA Clean-Up systems, as described in section 2.8 above.

*ii) Blunt-end ligation*: Blunt-end ligations were carried out using the same method as for cohesive-end ligations except that the reaction was carried out at 16°C for 16-20 hours.

**2.11 Transformation of *E. coli* Cells**

*i) Electroporation*: Transformation of bacterial cells were routinely carried out by electroporation, using a method based on that of Dower *et al.* (1988).

To 200 mL of Luria broth in a 1 litre baffled conical flask was added 2 mL of a stationary phase culture of the strain to be transformed. The cells were grown at 37°C, with vigorous shaking for aeration, to a cell density of approximately 120 Klett units. The flask was cooled on ice for 20 minutes, and the cells collected in sterile polypropylene centrifuge tubes by centrifugation at 4,300 x *g* at 4°C for 10 minutes. The cells were washed consecutively three times in 1 mM Hepes buffer (pH 7.0), and once in 50 mL of this buffer also containing 10% v/v glycerol. The cells were then resuspended in 1 mL Hepes buffer (pH 7.0) with 10% v/v glycerol. The cells were ready for electroporation at this stage but could also be stored frozen at -70°C for several months.

To 50 µL of washed cells in a 1.5 mL polypropylene microcentrifuge tube was added 1-10 µL of transforming DNA (the volume depending on the concentration of the DNA and/or other solutes, given that the success of the electroporation method depends on very low conductivity in the cell/DNA mixture). The mixture was transferred to an 0.2 cm electrode gap electroporation cuvette (Bio-Rad, Hercules, CA, USA), and subjected to an

approximately 4.8 ms electrical pulse at a field strength of 400 V/cm. Immediately, 1 mL of pre-warmed (37°C) SOC medium (Luria broth supplemented with 33 mM glucose, 2.5 mM KCl, 10 mM $MgCl_2$ and 10 mM $MgSO_4$) was added. The cells were transferred to a 15 mL polypropylene tube and incubated at 37°C for 1 hour. The cells were then transferred to a 1.5 mL polypropylene tube, and collected by centrifugation at 14,000 x *g* for 1 minute.

If the cells were to be plated out on rich media plates (Luria or MG), the cells were resuspended in approximately 50 µL of SOC medium, transferred directly to the surface of the plate, and spread over the entire surface using a bent sterile glass rod. If the cells were to be plated out on minimal (56) medium, the cells were resuspended in 1 mL of 56 medium, and pelleted by centrifugation at 14,000 x *g* for 1 minute. The cells were then resuspended in approximately 50 µL of 56 medium, transferred to the surface of the plate, and spread over the entire surface using a bent sterile glass rod.

*ii) Hanahan Method*: Following DNA manipulations involving M13 RF DNA such as site-directed mutagenesis reactions (see section 2.16 below) or the subcloning of DNA fragments into M13 RF DNA (see section 2.10 above), cells of *E. coli* strain TG1 were transformed using a method based on that of Hanahan (1983). The method follows that recommended in the technical notes accompanying the oligonucleotide-directed *in vitro* mutagenesis system of Amersham (Amersham, UK). The genotype for TG1 is also listed here.

Strain TG1 was grown in 200 mL of SOC medium (Luria broth supplemented with 33 mM glucose, 2.5 mM KCl, 10 mM $MgCl_2$ and 10 mM $MgSO_4$)with vigorous shaking for aeration, to a cell density of approximately 120 Klett units. The cells were transferred to sterile 50 mL polypropylene centrifuge tubes, and placed on ice for 15 minutes. The cells were pelleted by centrifugation at 4,300 x *g* at 4°C for 10 minutes, and the supernatant discarded. The cells were resuspended in 64 mL of transformation buffer #1 (30 mM potassium acetate (pH 5.8), 100 mM RbCl, 50 mM $MnCl_2$, 10 mM $CaCl_2$, 15% w/v glycerol), and placed on ice for 15 minutes. The cells were pelleted by centrifugation at 4,300 x *g* at 4°C for 10 minutes, and the supernatant discarded. The cell pellet was resuspended in 16 mL of transformation buffer #2 (10 mM MOPS (pH 6.8), 10 mM RbCl, 75 mM $CaCl_2$, 15% w/v glycerol). The cells were ready for transformation at this stage but could also be stored frozen at -70°C for several months.

300 µL of resuspended competent cells were transferred to a pre-chilled 15mL sterile polypropylene tube. 10-30 µL of transforming DNA was added (depending on the DNA concentration), and mixed in gently by swirling the tube. The cells were incubated on ice for 40 minutes, then heat-shocked for 45 seconds at 42°C. The cells were then placed on ice for 5 minutes. 4 mL of molten (42°C) Luria top agar (Luria broth containing 0.7% Bacto-agar) was then added, and mixed by rolling the tube by hand. The mixture was then poured onto plates of solid Luria medium and allowed to set at room temperature. The plates were then inverted and incubated at 37°C for 16 hours.

**2.12 Agarose Gel Electrophoresis of DNA**

Gels were prepared with agarose concentrations of between 0.8% and 1.2% in TAE buffer (40 mM Tris-acetate (pH 8.0), 1 mM EDTA), depending on the sizes of DNA fragments to be examined. Agarose was dissolved by boiling the buffer for approximately 3 minutes in a microwave oven. Molten agarose solution was allowed to cool to approximately 65°C before pouring into horizontal trays with tape at each end. A comb with 16 3 mm x 1 mm teeth (IBI/ Kodak Eastman, New Haven, CT, USA) was suspended in the molten agarose to a depth of approximately 5 mm to form sample loading wells (although if larger wells were required for preparative electrophoresis these were created by taping comb teeth together). The gel was allowed to set at room temperature, and the comb was removed.

The reservoirs of the electrophoresis apparatus (IBI/ Kodak Eastman, New Haven, CT, USA) were filled with TAE buffer such that the gel was overlaid to a depth of approximately 4 mm. DNA samples were prepared for electrophoresis by adding one eighth volume of bromophenol blue loading solution (0.05% w/v bromophenol blue, 50 mM EDTA, 15% w/v sucrose). Most gels involved determination of sizes of linear DNA fragments, for which 1kb DNA ladder (Gibco BRL, MD, USA) was used as standard. 16 µL of sample was loaded into the sample wells using an automatic pipette (Gilson Instruments, France) and the gels electrophoresed at 200 mA for approximately 1 hour at room temperature. Gels were then removed from the apparatus and stained by soaking in a solution of ethidium bromide (100 µg/mL) for 20 minutes. Gels were then washed briefly in water, and the DNA bands visualised using a transilluminator (IBI/ Kodak Eastman, New Haven, CT, USA). Permanent

images of gels were recorded using a Novaline video camera gel documentation system.

**2.13 Purification of DNA Fragments Excised from Agarose Gels**

DNA fragments were separated by agarose gel electrophoresis and visualised as described in the previous section. The DNA band was excised from the gel using a sterile scalpel, and transferred to a 1.5 mL microcentrifuge tube wrapped in aluminium foil to protect the sample from light. 1 mL of Magic or Wizard DNA Clean-Up resin (Promega Corporation, Madison, WI, USA) was then added. The tube was placed in a 65°C bath for approximately 10 seconds, then inverted repeatedly at room temperature. This procedure was repeated until the agarose had dissolved in the resin. The resin was washed and DNA eluted from the resin as described in section 2.8 above.

**2.14 Preparation and Phosphorylation of Oligonucleotides**

The synthetic oligonucleotides used in this work were synthesised and deprotected by staff of the Biomolecular Resource Facility, Australian National University, using an Applied Biosystems 380B DNA Synthesiser. Oligonucleotides were produced on 0.2 µmol scale, employing 5´-dimethoxytrityl-nucleoside-β-cyanoethyl-phosphoramidite chemistry. They were deprotected by heating in air-tight vials at 55 °C for 9-12 hours.

Ammonia was removed from the deprotected oligonucleotides by freeze-drying overnight. The samples were then reconstituted in 800 µL TE buffer, and placed, if necessary, in short term storage at 4 °C or long term storage at -20 °C.

The protocol for site-directed mutagenesis (see section 2.x below) requires that oligonucleotides be 5´- phosphorylated. Approximately 10µg of oligonucleotide was added to 30µL of T4 polynucleotide kinase (PNK) buffer (70 mM Tris-HCl (pH 7.6), 10 mM $MgCl_2$, 5 mM DTT, 1 mM ATP). 2 units of T4 PNK (Promega Corporation, Madison, WI, USA) were then added, and the reaction allowed to proceed at 37°C for 30 minutes. The reaction was stopped by heating the enzyme at 65°C for 15 minutes to inactivate the enzyme. The 5´-phosphorylated oligonucleotide was stored at -20 °C.

The sequences of all synthetic oligonucleotides used in this work are listed in Table 2.1.

**TABLE 2.1**

Sequences of synthetic oligonucleotides used in this work. Bases differing from the normal sequence are underlined.

| Name | Sequence |
|---|---|
| AR1 | 5´- CGTTTTCTAGGGTCACTGAGGATCCGCCATGAGTTTCG -3´ |
| AR2 | 5´- ACCCCTCTCACCCTCTGGTACCTCTAACCCTACCGAGGACTAGCCATGGAAATCGAGAAA -3´ |
| AR3 | 5´- ATACAAATTTCACATTAAGGATCCAAAACTTAAAAA -3´ |
| AR4 | 5´- CTCAATAAAAAAAATAGAATTCATTTAGAAG -3´ |
| AR5 | 5´- TAATTGTAGGTACCATTTTTTTGTTT -3´ |
| AR6 | 5´- TTTTGAAACAAAAAAATGGTACCTACAATTAAATAG -3´ |
| AR7 | 5´- GGAGTGTTAAGTGATGGTACCGATAATCGAAAACAG -3´ |
| AR8 | 5´- CTCACCGCCAAATCTAGAGGCTGAGCTCTTGGAGGACGCATGATGGACTCCACCGCTAGC -3´ |

**TABLE 2.1 (continued)**

Sequences of synthetic oligonucleotides used in this work. Bases differing from the normal sequence are underlined.

| Name | Sequence |
|---|---|
| AR9 | 5′- GTTTTTTTTAAATTCGAGCTC -3′ |
| AR10 | 5′- CCAAACAACGCCAGCATGCTCCCCTAGACAAACCGAGGACAATGCATGAACCTCCGTGAGCTA -3′ |
| AR11 | 5′- CCCTAGACAAACCGAGGAGAATTCATGAACCTCCGTGAGC -3′ |
| AR12 | 5′- CCATATTGTAAAAACGAATTCATTAATCAAACACATGC -3′ |
| AR13 | 5′- CCCAATTCTGGAGTTCGAACAAGATCCTGC -3′ |
| AR14 | 5′- GCAGGATCTTGTTCGAACTCCAGAATTGGG -3′ |
| AR15 | 5′- GGAGAGCAAATTGGATCCATGACCTTAAAT -3′ |
| AR16 | 5′- CGCTCAAGGCGCACTCCCGGGCTGGATAATGTTTTTTGCG -3′ |

**TABLE 2.1 (continued)**

Sequences of synthetic oligonucleotides used in this work. Bases differing from the normal sequence are underlined.

| Name | Sequence |
|---|---|
| AR17 | 5′- GTCACGATGAATTCCCGGGGATCAACGCGGAACCAGATCCG -3′ |
| AR18 | 5′- GGATCCCCGGGCGTGTCGACTGAAACAAACTGGAGGAATTAAATGACCTTAAATCTTTGTGTACTG -3′ |
| AR19 | 5′- GGTTATGATTATTCGGACGCGGCCGCCGACTGGTTACG -3′ |
| AR20 | 5′- CCCCTAGACAAACCGAGGAGGATCCATGAACCTCCGTGAGC -3′ |
| AR21 | 5′- CCAAAAATAAGTAAGTACAAGGATCCATATTGTAAAAAC -3′ |
| AR22 | 5′- GGAAAGGGATCCTTAAGTGAT -3′ |
| AR23 | 5′- AGAGGAATTCGTTTTAACTGAAACAAACTGGAGACTGTCATGCTTGACAAGATATACTAC -3′ |
| AR24 | 5′- ATACAAATTTCACATTAAGGATCTAGAACTTAAAAACC -3′ |

**TABLE 2.1 (continued)**

Sequences of synthetic oligonucleotides used in this work. Bases differing from the normal sequence are underlined.

| Name | Sequence |
|---|---|
| AR25 | 5′- CTGTTCCTTATGTTCGGATCCGACAAGATATAC -3′ |
| AR26 | 5′- ACGCTGGACTGTGGCGAATTCGCCCTCCTGACAG -3′ |
| AR27 | 5′- CGACGGCCAGTGCCAGAATTCAGAAGGCATTCAGG -3′ |
| AR28 | 5′- GGCCGCCCAACAGCTCTAGATCGATCGCAGCT -3′ |
| AR29 | 5′- CAAGAAACCGCGCCCGAATTCACTCAA -3′ |
| AR30 | 5′- GGATCCCCGGGCGTGTCGACTGAAACAAACTGGAGGAGACCATGAGCCTGACTGTCCGCG -3′ |
| AR31 | 5′- TTATTATTATTGCGGCCGCATTCAGGATCAAACGCTGACTAGACCACCCGC -3′ |
| AR32 | 5′- CGGCGCCGCTTTTTGGAGGGATCCATGGCAAACCTCAAGGCG -3′ |

**TABLE 2.1 (continued)**

Sequences of synthetic oligonucleotides used in this work. Bases differing from the normal sequence are underlined.

| Name | Sequence |
|---|---|
| AR33 | 5′- CGCTCTTGCCTTTAGATCCGCAAGGCTTGG -3′ |
| AR34 | 5′- CCAAGCCTTGCGGATCTAAAGGCAAGAGCG -3′ |
| AR35 | 5′- GGATCCCCGGGCGTGTCGACTGAAACAAACTGGAGGACTTTGCCATGACGAGCACTTCTC -3′ |
| AR36 | 5′- CGTCGGGTCTGATGCTAACCGCGGCCGCGTAATTCCGGTGG -3′ |
| AR37 | 5′- GGAACTCACCGAGATCGTCCCGGGGGCCGCCGC -3′ |
| AR38 | 5′- GCAGCGGTGCGCGGCCGCGGTAGATCCCCAGTTAAGCTTCGCTACCCG -3′ |
| AR39 | 5′- GGTCATTGATGGAAGCTTACGCGGTCGTCTTGAGCG -3′ |
| AR40 | 5′- CCTCTTGTCCCTGCGGCCGCCCCTAAGGAAGCCGCC -3′ |

**TABLE 2.1 (continued)**

Sequences of synthetic oligonucleotides used in this work. Bases differing from the normal sequence are underlined.

| Name | Sequence |
|---|---|
| AR41 | 5´- GAAGTACGTATGGGATCCTTAATGGCCAGCCATC -3´ |
| AR42 | 5´- ATCCTGGACGTTGCTGGC -3´ |

**TABLE 2.2**
Bacterial strains used and referred to in this work.

| Strain | Genotype | Reference |
|---|---|---|
| AN802 | *uncC424 argH purE entA xyl+ rpsL recA nal$^R$* | Gibson *et al.*, 1977 |
| AN818 | *uncD409 argH purE entA xyl+ rpsL recA nal$^R$* | Cox *et al.*, 1978 |
| AN943 | *uncE429 argH purE entA rpsL recA nal$^R$* | Downie *et al.*, 1981 |
| AN1124 | *uncA450 argH purE entA xyl+ rpsL recA nal$^R$* | Senior *et al.*, 1979 |
| AN1273 | *uncG428 argH purE entA xyl+ rpsL recA nal$^R$* | Downie *et al.*, 1980 |
| AN1440 | *uncF469 argH purE entA xyl+ rpsL recA nal$^R$* | Downie *et al.*, 1981 |
| AN1460 | pAN45/ *unc413::Mu argH purE entA xyl+ rpsL recA nal$^R$* | Downie *et al.*, 1980 |
| AN1521 | *uncF476 argH purE entA rpsL recA nal$^R$* | Downie *et al.*, 1981 |
| AN2015 | *uncH241 argH purE entA rpsL recA nal$^R$* | Jans *et al.*, 1984 |
| AN2191 | pAN257/ *uncF469 argH purE entA xyl+ rpsL recA nal$^R$* | Jans *et al.*, 1985 |
| AN2192 | pAN257/ *uncF476 argH purE entA xyl+ rpsL recA nal$^R$* | Jans *et al.*, 1985 |
| AN2401 | pAN51/ *uncF469 argH purE entA xyl+ rpsL recA nal$^R$* | Schmidt *et al.*, 1990 |
| AN2704 | pAN423/ *uncF469 argH purE entA xyl+ rpsL recA nal$^R$* | Schmidt *et al.*, 1990 |

**TABLE 2.2 (continued)**

| Strain | Genotype | Reference |
|---|---|---|
| AN2840 | pAN495/ *uncB402 argH purE entA xyl+ rpsL recA nal$^R$* | Howitt *et al.*, 1988 |
| AN2936 | pAN573/ *uncF469 argH purE entA xyl+ rpsL recA nal$^R$* | This Work |
| AN2987 | pUC18/ *uncF469 argH purE entA xyl+ rpsL recA nal$^R$* | This Work |
| AN3347 | pGroESL/ *lacZ(am) trp(am) pho(am) supC$^{ts}$ rpsL mal(am)* | This Work |
| AN3781 | pAN1126/ *uncH241 argH purE entA xyl+ rpsL recA nal$^R$* | This Work |
| AN3782 | pAN1127/ *uncH241 argH purE entA xyl+ rpsL recA nal$^R$* | This Work |
| AN3783 | pUC18/ *uncH241 argH purE entA xyl+ rpsL recA nal$^R$* | This Work |
| AN3784 | pAN1128/ *uncE429 argH purE entA rpsL recA nal$^R$* | This Work |
| AN3785 | pAN1128/ *uncF469 argH purE entA rpsL recA nal$^R$* | This Work |
| AN3786 | pAN1128/ *uncH241 argH purE entA rpsL recA nal$^R$* | This Work |
| AN3791 | pUC19/ *uncG428 argH purE entA rpsL recA nal$^R$* | This Work |
| AN3792 | pAN1130/ *uncG428 argH purE entA rpsL recA nal$^R$* | This Work |
| AN3793 | pAN1131/ *uncG428 argH purE entA rpsL recA nal$^R$* | This Work |

**TABLE 2.2 (continued)**

| Strain | Genotype | Reference |
|---|---|---|
| AN3797 | pAN1133/ pGroESL/ *lacZ(am) trp(am) pho(am) supC$^{ts}$ rpsL mal(am)* | This Work |
| AN3798 | pAN1007/ pGroESL/ *lacZ(am) trp(am) pho(am) supC$^{ts}$ rpsL mal(am)* | This Work |
| AN3799 | pAN573/ *uncF476 argH purE entA rpsL recA nal$^{R}$* | This Work |
| AN3800 | pAN573/ *uncF515* Cm$^{R}$/ *uncF469 argH purE entA rpsL recA nal$^{R}$* | This Work |
| AN3801 | pUC18/ *uncF476 argH purE entA rpsL recA nal$^{R}$* | This Work |
| AN3802 | pUC18/ *uncF515* Cm$^{R}$/ *uncF469 argH purE entA rpsL recA nal$^{R}$* | This Work |
| AN3803 | pAN1128/ *uncF476 argH purE entA rpsL recA nal$^{R}$* | This Work |
| AN3804 | pAN1128/ *uncF515* Cm$^{R}$/ *uncF469 argH purE entA rpsL recA nal$^{R}$* | This Work |
| AN3805 | pAN1139/ *uncF469 argH purE entA rpsL recA nal$^{R}$* | This Work |
| AN3806 | pAN1139/ *uncF476 argH purE entA rpsL recA nal$^{R}$* | This Work |
| AN3809 | pAN1140/ *uncF469 argH purE entA rpsL recA nal$^{R}$* | This Work |
| AN3810 | pAN1140/ *uncF476 argH purE entA rpsL recA nal$^{R}$* | This Work |
| AN3811 | pAN1140/ *uncF515* Cm$^{R}$/ *uncF469 argH purE entA rpsL recA nal$^{R}$* | This Work |

**TABLE 2.2 (continued)**

| Strain | Genotype | Reference |
|---|---|---|
| AN3812 | pAN1144/ *uncF469 argH purE entA rpsL recA* $nal^R$ | This Work |
| AN3818 | pAN495/ *uncF469 argH purE entA rpsL recA* $nal^R$ | This Work |
| AN3819 | pAN1140/ *uncF476 argH purE entA rpsL recA* $nal^R$ | This Work |
| AN3820 | pAN174/ *uncF469 argH purE entA rpsL recA* $nal^R$ | This Work |
| AN3821 | pAN174/ *uncF469 argH purE entA rpsL recA* $nal^R$ | This Work |
| AN3826 | pAN1053/ pGroESL/ *lacZ(am) trp(am) pho(am)* $supC^{ts}$ *rpsL mal(am)* | This Work |
| AN3827 | pAN1069/ pGroESL/ *lacZ(am) trp(am) pho(am)* $supC^{ts}$ *rpsL mal(am)* | This Work |
| AN3830 | pAN974/ pGroESL/ *lacZ(am) trp(am) pho(am)* $supC^{ts}$ *rpsL mal(am)* | This Work |
| AN3831 | pAN1052/ pGroESL/ *lacZ(am) trp(am) pho(am)* $supC^{ts}$ *rpsL mal(am)* | This Work |
| AN3832 | pAN1149/ pGroESL/ *lacZ(am) trp(am) pho(am)* $supC^{ts}$ *rpsL mal(am)* | This Work |
| AN3833 | pAN1024/ pGroESL/ *lacZ(am) trp(am) pho(am)* $supC^{ts}$ *rpsL mal(am)* | This Work |
| AN3840 | pAN1055/ pGroESL/ *lacZ(am) trp(am) pho(am)* $supC^{ts}$ *rpsL mal(am)* | This Work |
| AN3842 | pAN1156/ pGroESL/ *lacZ(am) trp(am) pho(am)* $supC^{ts}$ *rpsL mal(am)* | This Work |

**TABLE 2.2 (continued)**

| Strain | Genotype | Reference |
|---|---|---|
| AN3843 | pAN1157/ pGroESL/ *lacZ(am) trp(am) pho(am) supC$^{ts}$ rpsL mal(am)* | This Work |
| AN3844 | pAN1158/ pGroESL/ *lacZ(am) trp(am) pho(am) supC$^{ts}$ rpsL mal(am)* | This Work |
| AN3845 | pAN1159/ pGroESL/ *lacZ(am) trp(am) pho(am) supC$^{ts}$ rpsL mal(am)* | This Work |
| AN3846 | pAN1160/ pGroESL/ *lacZ(am) trp(am) pho(am) supC$^{ts}$ rpsL mal(am)* | This Work |
| AN3848 | pAN1162/ pGroESL/ *lacZ(am) trp(am) pho(am) supC$^{ts}$ rpsL mal(am)* | This Work |
| AN3849 | pAN1163/ pGroESL/ *lacZ(am) trp(am) pho(am) supC$^{ts}$ rpsL mal(am)* | This Work |
| AN3850 | pAN1165/ pGroESL/ *lacZ(am) trp(am) pho(am) supC$^{ts}$ rpsL mal(am)* | This Work |
| DH5α | *endA1 hsdR17* ($r_K^- m_K^+$) *supE44 thi-1 recA1 gyrA* ($Nal^R$) *relA1 Δ(lacZYA-argF U169 deoR(ϕ80dlacΔ(lacZ)M15)* | CLONTECH Laboratories, Palo Alto, California |

**TABLE 2.3**

Selected plasmids used and referred to in this work

| Plasmid | Genotype | Reference |
|---|---|---|
| pGroESL | *groES*$^+$ *groEL*$^+$ | Goloubinoff *et al.*, 1989 |
| pAN45 | Cm$^R$ Tc$^S$ *uncB*$^+$*E*$^+$*F*$^+$*H*$^+$*A*$^+$*G*$^+$*D*$^+$*C*$^+$ | Downie *et al.*, 1980 |
| pAN51 | Cm$^R$ Tc$^S$ *uncB*$^+$*E*$^+$*F*$^+$*H*$^+$*A*$^+$ | Downie *et al.*, 1980 |
| pAN257 | Cm$^R$ Tc$^S$ *uncB*$^+$*E*$^+$*F515H*$^+$*A*$^+$ | Jans *et al.*, 1985 |
| pAN423 | Ap$^R$ *atpF*cDNA | Schmidt *et al.*, 1990 |
| pAN495 | Cm$^R$ Tc$^S$ *uncB*$^+$*E*$^+$*F*$^+$ | Howitt *et al.*, 1988 |
| pAN573 | Ap$^R$ modified *atpF*cDNA | This Work |
| pAN1126 | Ap$^R$ modified *atpD*cDNA | This Work |
| pAN1128 | Ap$^R$ *uncB*$^+$*E*$^+$*F*$^+$ | This Work |
| pAN1131 | Ap$^R$ modified *atpC*cDNA | This Work |
| pAN1139 | Cm$^R$ Tc$^S$ *uncB*$^+$*E*$^+$*atpF'uncF'* | This Work |
| pAN1140 | Ap$^R$ modified *atpG*cDNA | This Work |
| pAN1144 | Ap$^R$ modified atpFcDNA + modified *atpD*cDNA | This Work |

**2.15 Preparation of M13 Single-Stranded DNA**

Single-stranded DNA was prepared from M13 clones using a method based on that described in the technical notes accompanying the oligonucleotide-directed *in vitro* mutagenesis system of Amersham (Amersham, UK).

50 mL of 2YT medium in a 200 mL baffled conical flask was inoculated with 1mL of fresh stationary phase culture of *E. coli* strain TG1 and either a single plaque picked from a plate as an agar plug by a sterile pasteur pipette or 10 µL of phage stock of an M13 clone. The culture was incubated to stationary phase at 37°C with vigorous shaking for aeration, then transferred to a 50 mL polypropylene centrifuge tube. The cells were pelleted by centrifugation at 4300 x *g* at 4°C for 10 minutes. 40 mL of supernatant was transferred to a fresh tube, and mixed with 10 mL of PEG-6000 in 2.5 M NaCl. The tube was left to stand at room temperature for 15 minutes to allow aggregation of phage particles. The suspension was transferred to two 50 mL polypropylene centrifuge tubes, and the phage particles pelleted by centrifugation at 4,300 x *g* at 4°C for 10 minutes. The supernatant was poured off and discarded. The tubes were centrifuged at 4,300 x *g* at 4°C for 1 minute to bring any remaining supernatant to the bottom of the tubes, and this was drawn off with a pasteur pipette and discarded. The phage pellets were resuspended in 2 mL of TE buffer, and transferred to six 1.5 mL polypropylene microcentrifuge tubes. The tubes were centrifuged at 14,000 x *g* in an Eppendorf microcentrifuge to pellet any remaining cells. The supernatants were carefully removed to six fresh ultracentrifuge tubes. 150 µL of TE-saturated phenol was added to each of the tubes, which were vortexed vigorously for 1 minute. 150 µL of 24:1 chloroform/isoamyl alcohol was added to each of the tubes, which were again vortexed vigorously for 1 minute. The tubes were then centrifuged at 14,000 x *g* in an Eppendorf microcentrifuge to separate the phases. The upper (aqueous) layer from each tube was transferred to a fresh microcentrifuge tube. The phenol/chloroform/isoamyl alcohol extraction was then repeated as described above, and the aqueous layer from each tube transferred to a fresh microcentrifuge tube. To remove any remaining traces of phenol, 500 mL of water-saturated diethyl ether was added to each of the tubes, which were vortexed vigorously. The upper (ether) layer was removed and remaining traces of dissolved ether were removed by heating the tubes with their lids open at 65°C for 5 minutes.

To precipitate the DNA, 30 µL of 3M sodium acetate (pH 6.0) and 800 µL of ethanol were added to each of the tubes, which were left in a -70°C freezer for 15 minutes. The tubes were centrifuged at 14,000 x *g* for 15 minutes in an Eppendorf microcentrifuge to pellet the DNA. The pellets were washed with 800 µL of -20°C ethanol, dried under vacuum, then resuspended in a total combined volume of 200 µL of TE buffer.

The optical density of the solution at 260nm was measured. Using the formula of 1 $OD_{260}$ unit being equivalent to 40 mg/mL of single-stranded DNA (Sambrook *et al.*, 1989), the yield of single-stranded DNA was estimated.

**2.16 Site-Directed Mutagenesis**

Site-directed mutagenesis was carried out using the Oligonucleotide-directed *in vitro* Mutagenesis System Version 2.1 and the Sculptor *in vitro* Mutagenesis System of Amersham (Amersham, UK), using methods based on the work of Eckstein and co-workers (Taylor *et al.*, 1985a; b; Nakamaye and Eckstein, 1986; Sayers *et al.*, 1988). The protocols are described in the handbooks accompanying the kits, and are summarised below:

*i) Annealing of mutant oligonucleotide to single-stranded DNA template*: Single-stranded DNA template, 5´-phosphorylated mutant oligonucleotide and annealing buffer concentrate were combined in a 1.5 mL microcentrifuge tube. The tube was placed in a beaker of heated water (80°C), which was allowed to cool to 37°C over a time period of approximately 45 minutes. The tube was centrifuged briefly to collect condensate at the bottom of the tube, then placed on ice for 5 minutes.

*ii) Synthesis and ligation of the mutant DNA strand*: To the annealing reaction were added $MgCl_2$ solution and nucleotide mix "#1" (version 2.1 kit) or "A" (Sculptor kit). The mixes contain the phosphothioate analogue of dCTP, along with dGTP, dATP, dTTP and ATP.

If kit version 2.1 was used, 6 units of the Klenow fragment of DNA polymerase I and 6 units of T4 DNA ligase were added, and the reaction allowed to proceed overnight at room temperature.

If the Sculptor kit was used, 0.8 units of T7 polymerase and 2.5 units of T4 ligase were added. The reaction was allowed to proceed at room temperature for 10 minutes, followed by 30 minutes at 37°C. The enzymes were then inactivated by heating the tube at 80°C for 15 minutes.

*iii) Removal of single-stranded (non-mutant) DNA:* If kit version 2.1 was used, single-stranded (non-mutant) DNA was removed by filtration through nitrocellulose. Following the reaction for the synthesis and ligation of the mutant DNA strand, the ionic strength of the solution was raised by the addition of NaCl. The sample was then added to the upper chamber of the disposable filter unit, which was centrifuged in a bench-top swinging bucket centrifuge. The centrifugation causes the sample to pass through a pair of nitrocellulose membranes, which bind the single-stranded (non-mutant) DNA. The double-stranded heteroduplex DNA passes through to the collection tube below, because double-stranded DNA does not bind at this ionic strength. The double-stranded DNA was ethanol precipitated and resuspended in appropriate buffer for the next step.

If the Sculptor kit was used, the sample was digested with T5 exonuclease, which specifically degrades single-stranded and nicked double-stranded DNA, but does not degrade closed circular double stranded DNA (Sayers and Eckstein, 1990).

*iv) Nicking of the non-mutant strand of DNA:* Restriction endonuclease *Nci*I was added to the sample from the previous step. The heteroduplex is nicked by *Nci*I, which will not cleave the phosphothioate linkage of the mutant strand (Nakamaye and Eckstein, 1986).

*v) Digestion of the non-mutant strand:* Exonuclease III was added to digest away the nicked non-mutant strand. Exonuclease III leaves approximately 800 bp of double-stranded DNA (Nakamaye and Eckstein, 1986), allowing the resynthesis of the second strand.

*vi) Resynthesis and ligation of the second strand*: $MgCl_2$ and nucleotide mix "#2" (kit version 2.1) or "A" (Sculptor kit) were added to the sample from the previous step. The mixes contain dGTP, dATP, dTTP, dCTP and ATP. DNA polymerase I and 2 units of T4 DNA ligase were then added.

If kit version 2.1 was used, the reaction was allowed to proceed overnight at room temperature. If the Sculptor kit was used, the reaction was left to proceed at 37°C for 1 hour.

*vii) Transformation of competent cells and analysis of mutant progeny*: 300 µL of competent *E. coli* TG1 cells were transformed with reaction mix following the resynthesis and ligation of the second strand, using the method described in section 2.x above. Screening for mutant progeny was carried out by preparing single-stranded DNA from single plaques (as described in section 2.x

above) and sequencing this DNA (as described in section 2.x below). In addition, where the mutagenesis involved the insertion or deletion of a restriction site, RF DNA was prepared, digested with the appropriate enzyme, and analysed by agarose gel electrophoresis.

**2.17 DNA Sequencing**

Sequencing of both single-stranded and double-stranded DNA was carried out using the T7 Sequencing Kit of Pharmacia (Uppsala, Sweden), which employs the dideoxy chain termination method of Sanger *et al.*, (1977). The exact details of the protocol are described in the handbook accompanying the kit. A summary of the method is described below:

*i) Annealing of the primer to the template*: For sequencing of single-stranded DNA, the concentration of the template was adjusted to approximately 0.2 μg/μL. The concentration of the primer (synthetic oligonucleotide) was adjusted to 0.8 μM. 10 μL of template DNA, 2 μL of primer solution and 2 μL of annealing buffer (suppied in the kit) were combined in a 1.5 mL polypropylene microcentrifuge tube. The tube was placed in a beaker of heated (80°C) water, which was allowed to cool to room temperature over the course of approximately 45 minutes.

For sequencing of double-stranded DNA, the template was denatured prior to annealing of the primer. The concentration of the template was adjusted to approximately 0.2 μg/μL. In a 1.5 mL microcentrifuge tube, 8 μL of template was mixed with 2 μL of 2 M NaOH, and left to stand at room temperature for 10 minutes. 3 μL of 3 M sodium acetate (pH 4.8) and 7 μL of water were then added. 60μL of ethanol was added, and the tube left in a -70 °C freezer for 20 minutes. The DNA was pelleted by centrifugation at 14,000 x *g* for 15 minutes. The pellet was washed with chilled (-20 °C) ethanol, dried under vacuum, and dissolved in 10 μL water.

To the 10 μL of denatured DNA was added 2 μL of annealing buffer and 2 μL of primer (0.8 μM). The tube was incubated at 37°C for 20 minutes, then at room temperature for 15 minutes.

*ii) Labelling Reaction*: A mixture of dGTP, dTTP and dCTP (supplied with the kit) and [$^{35}$S]dATPαS (approximately 10 μCi) were added to the tube containing the annealed template and primer. T7 DNA polymerase was then added to initiate strand extension and labelling of the DNA, and the reaction was left to proceed for 5 minutes at room temperature.

*iii) Chain-termination (sequencing) reactions*: The chain-termination reactions were commenced by transferring aliquots from this tube into four labelled tubes, each containing one of the dideoxynucleoside-5´-triphosphates (ddGTP, ddATP, ddTTP or ddCTP) and each of the four deoxynucleoside-5´-triphosphates (dGTP, dATP, dTTP and dCTP). The tubes were incubated at 37°C for 5 minutes, then the reaction was halted by the addition of stop solution (formamide/EDTA/xylene cyanol/bromophenol blue; supplied in the kit).

The electrophoresis gels used for DNA sequencing were prepared using Long Ranger Gel solution (AT Biochem, Malvern, PA, USA), which is stated by the manufacturer to contain a modified acrylamide (modification not specified), a comonomer and a cross-linker (both unspecified). To prepare 50 mL of gel solution, 21 g of urea was dissolved in 6 mL 10x TBE (Tris-Borate-EDTA) buffer, 5 mL Long Ranger Gel concentrate and water to 50 mL. One liter of 10x TBE buffer contains 108 g Tris base, 55 g boric acid and 40 mL 0.5M EDTA, adjusted to pH 8.0. The final concentration of TBE buffer in the gel solution was set at 1.2x, as recommended by the Long Ranger Gel solution manufacturer. Polymerisation of the gel was initiated by the addition of 25 µL TEMED and 300 µL of 10% ammonium persulphate.

Electrophoresis gels were run in a Base Runner Nucleic Acid Sequencer (IBI/Eastman Kodak, New Haven, CT, USA), between 21.6cm x 45 cm or 21.6cm x 60cm glass plates. To prepare a gel, the mirrored glass plate was placed on a bench in a horizontal position, and 0.4 mm spacers placed along the long edges. Gel-Slick solution (IBI/Eastman Kodak, New Haven, CT, USA) was applied to the non-mirrored plate to prevent polymerised gel adhering to this plate following electrophoresis. Gel solution (to which TEMED and ammonium persulphate had just been added) was poured onto the mirrored plate whilst the non-mirrored plate was slid along its length. Once a uniform film of gel solution was formed between the two aligned plates, an 0.4 mm spacer was placed at the top of the gel, and the plates clamped together. Polymerisation of the gel was allowed to proceed for one hour at room temperature.

Following polymerisation of the gel, the top spacer and clamps were removed, and the plates placed into the Base Runner apparatus with the non-mirrored plate facing outwards. Buffer tanks, each of 500 mL capacity, were placed at the top and bottom of the plates, and filled with 1x TBE buffer. The gel was pre-run at 30 W (for 21.6 cm x 45 cm plates) or 45 W (for 21.6 cm x 60 cm

plates) for 30 minutes to warm the gel to running temperature. A sharkstooth comb was then placed at the top of the gel to form 32 loading wells.

The samples were heated at 100°C for 2 minutes to denature the strands, and 3μL from each sample added to a loading well. The gel was electrophoresed at 30W (for 21.6 cm x 45 cm plates) or 45W (for 21.6 cm x 60 cm plates) for up to 5 hours, depending on the length of sequence to be read. Where appropriate, samples were loaded twice, with loadings separated by two hours, to read the maximum length of sequence. Ninety minutes before the expected finish of the electrophoresis, 50 mL of 3 M sodium acetate was added to the bottom buffer tank. This has the effect of compressing bands at the bottom of the gel, and thus increases the length of readable sequence that may be obtained from the gel.

The gel was removed from the plates by adhesion to 3MM chromatography paper (Whatman), covered with plastic film, and dried under vacuum at 80°C for 2 hours. Autoradiography was carried out by placing the dried gel in a cassette facing a piece of Hyperfilm MP autoradiography film (Amersham). The film was exposed for 20-25 hours, then developed in an X-omat M20 automatic processor (Eastman Kodak).

### 2.18 Polymerase Chain Reaction

The polymerase chain reaction (PCR) was used to amplify large amounts of a specific DNA fragment of defined length and sequence from small amounts of template DNA. The PCR primers used in this work normally had restriction enzyme sites incorporated into their sequences to facilitate subcloning of the final PCR product.

The thermostable DNA polymerase used in the early parts of the work was *Taq* polymerase (Chien *et al.*, 1976) supplied by Boehringer Mannheim, using the incubation buffer provided by the manufacturer: Tris-HCl, 10mM (pH 8.3 at 20°C); 1.5 mM $MgCl_2$, 50 mM KCl. The high base incorporation error rate associated with this enzyme ($2.0 \times 10^{-5}$; Lundberg *et al.*, 1991) required, however, that all subcloned products be sequenced to confirm the nucleotide sequence. Later work employed the *Pfu* polymerase isolated from *Pyrococcus furiosis* , supplied by Stratagene, which has been shown to have a 12-fold lower error rate ($1.6 \times 10^{-6}$; Lundberg *et al.*, 1991). The incubation buffer provided by the manufacturer was used: Tris-HCl, 20mM (pH 8.2 at 20°C); 2 mM $MgCl_2$, 10 mM KCl, 6 mM $(NH_4)_2SO_4$; 0.1% Triton X-100, 10 μg/mL nuclease-free BSA.

The reactions contained 200 mM dNTPs, 0.5 mM primers, 1-100 ng template DNA and 2-5 units of the relevant polymerase. Reactions were carried out by firstly incubating for 5 minutes at 94°C to denature the template DNA. Thirty cycles were then used with the following temperatures and time intervals: 94°C, 1 minute; 45-65°C (normally 5°C below the lower of the calculated annealing temperatures of the two primers), 2 minutes; 72°C, 3 minutes. This was followed by a 10 minute incubation at 72°C to allow completion of strand synthesis. Reaction conditions to achieve maximum product yield were optimised by altering the annealing temperature, and adjusting the $MgCl_2$ concentration in the range 1-3 mM.

**2.19 Addition of Dideoxythymidine 3´ Overhangs to Linearised DNA Vectors**

As descibed in the previous section, restriction sites were incorporated into PCR primers for subsequent digestion and cloning of the PCR products. It was not possible, however, to clone one of the products described in this work in this way (see section 3.x). In this case, an alternative method involving the direct cloning of PCR products was employed, based on the protocol described by Holton and Graham (1991). The method is based on the observation that *Taq* polymerase normally adds a single non template-directed deoxyadenosine residue to the 3´ end of duplex PCR products (Clarke, 1988), and that vectors may be constructed for the direct cloning of PCR products which possess such overhangs. This is carried out by digesting the vector with a restriction enzyme which generates blunt ends, then "tailing" the vector using dideoxythymidine (ddT). The use of ddT ensures the addition of only a single thymidine residue. The vector ends thus generated have a single 3´-overhanging thymidine residue which lacks a 3´-hydroxyl group, and cannot therefore form a phosphodiester bond. The other strand can, however, ligate to other DNA strands as it possesses a 5´- phosphate group. The ddT tailed vector can ligate directly to a PCR product possessing a 3´-overhanging adenosine residue at both ends by forming phosphodiester bonds between the 5´-phosphate groups of the vector and the 3´-hydroxyl groups of the overhanging adenosine residue (Holton and Graham, 1991).

2 µg of the vector pUC19 were digested with *Sma*I (see section 2.x above), which generates a linear fragment with blunt ends. The DNA was purified using the Magic DNA Clean-Up System (Promega Corporation, Madison, WI, USA). The tailing reaction was carried out using terminal transferase and buffer

from Boehringer Mannheim (Mannheim, Germany). The *Sma*I digested linear DNA was tailed in a total volume of 40 µL containing 25 mM Tris-HCl (pH 6.6), 200 mM potassium cacodylate, 250 µg/mL BSA, 1.5 mM $CoCl_2$, 10 mM ddT (Pharmacia, Uppsala, Sweden), using 100 units of terminal transferase for 1 hour at 37°C. The DNA was purified using the Magic DNA Clean-Up System (Promega Corporation, Madison, WI, USA).

The ligation of the PCR product into the ddT tailed vector was carried out as described in section 2.10 above.

**2.20 *In vitro* Transcription/ Translation**

The *E . coli* S30 Extract System for Circular DNA (Promega Corporation, Madison, WI, USA) was used to confirm the expression of genes cloned into plasmid vectors. Only plasmids purified using caesium chloride equilibrium density gradient centrifugation (see section 2.x) were used as templates for this procedure.

To 3 µg of plasmid DNA in a 1.5 mL polyproylene centrifuge tube were added the following kit components: 5 µL amino acid mixture minus methionine, 20 µL S30 premix without amino acids, 15 µL S30 extract and water to a total volume of 49 mL. 1 µL of [$^{35}$S]-methionine solution (15 µCi/µL) was then added, and the reaction allowed to proceed at 37°C for 2 hours. The reaction was stopped by placing the tube on ice. The reaction mix could be placed at -70°C for storage at this stage.

To precipitate protein following the *in vitro* transcription/translation reaction, 20 µL of acetone was added to a 5 µL sample of the reaction, and the tube left on ice for 15 minutes. The tube was then centrifuged at 14,000 x *g* for 5 minutes to pellet the protein. The supernatant was removed and discarded, and the pellet dried under vacuum.

The pellet was resuspended in 20 µL of 2x tricine gel SDS loading buffer (45 mM Tris-HCl (pH8.45), 24% glycerol, 4% SDS, 0.005% Coomassie Blue G and 0.005% Phenol Red), and heated at 100°C for 5 minutes. The tube was then centifuged at 14,000 x *g* for 1 minute. 10 µL of sample were loaded on a pre-poured acrylamide gradient gel (Novex, San Diego, CA, USA) for analysis by SDS-Polyacrylamide Gel Elecrophoresis (see section below).

Following electrophoresis, the gel was removed by adhesion to 3MM chromatography paper (Whatman), covered with plastic film, and dried under vacuum at 60°C for 2 hours. Autoradiography was carried out by placing the

dried gel in a cassette facing a piece of Hyperfilm MP autoradiography film (Amersham). The film was exposed for 12-20 hours, then developed in an X-omat M20 automatic processor (Eastman Kodak).

**2.21 SDS-Polyacrylamide Gel Elecrophoresis (SDS-PAGE)**

Two systems were used for SDS-Polyacrylamide Gel Elecrophoresis (SDS-PAGE) of protein samples in this work. Rapid routine analysis of protein samples was usually carried out using the Pharmacia Phastgel system. When higher band resolution was considered necessary, electrophoresis was carried out using a Novex system with pre-poured gels.

*i) Electrophoresis using the Pharmacia Phastgel system*: The Phastgel system employs 0.45mm gels attached to a hard plastic cover. The gels used in this work contained a 6% acrylamide stacking buffer followed by an 8-25% acrylamide gradient. The running buffer was composed of 112mM Tris-acetate (pH 6.4). Electrodes were connected to both ends of the gel via 2% agarose buffer strips containing 200 mM tricine, 200 mM Tris and 0.55% SDS (pH 8.1). Samples were loaded onto the gel using a saw-toothed comb with grooves in the teeth. The teeth were dipped into drops of the samples to be loaded. Approximately 1 μL of sample is drawn into the groove by capillary action. The comb is then lowered onto the surface of the gel to apply the samples. Electrophoresis was carried out at 10mA constant current for approximately 25 minutes.

The staining and destaining of Phastgels are controlled by an integrated development unit, and take place in a sealed chamber. The gel is first stained with staining solution (0.1% Coomassie R350 in 30% methanol, 10% acetic acid), washed three times in destaining solution (30% methanol, 10% acetic acid), then washed in preserving solution (5% glycerol, 10% acetic acid).

*ii)Electrophoresis using the Novex system*: Electrophoresis was carried out according to the method of Laemmli (1970). Pre-poured 4-20% acrylamide gradient gels buffered with Tris-Glycine (Novex, San Diego, CA, USA) were run in the Novex XCell-II apparatus. The running buffer was composed of 24mM Tris base (pH 8.3), 192 mM glycine, 0.1% SDS. The 2x loading buffer was composed of 40mM Tris-HCl (pH 6.8), 10% (w/v) glycerol, 1.6% SDS, 4% β-mercaptoethanol. Electrophoresis was carried out at a constant voltage of 125V for approximately 100 minutes.

**2.22 Protein Determinations**

*i) Bradford Protein Assays:* Routine analysis of protein concentration was carried out using the Bio-Rad protein assay system, based on the dye-binding assay method of Bradford (1976). All assays were carried out in duplicate, employing a standard curve of 0, 25, 50, 75 and 100 µg of bovine serum albumin (BSA). The dye concentrate provided with the kit was diluted with four volumes of deionised distilled water and filtered using a Sartorius 0.22 µm filter. 100 µL of the samples to be assayed or BSA standards was mixed thoroughly with 5 mL of the diluted dye reagent, and transferred to disposable plastic cuvettes. After a time period of between 2 and 5 minutes, the absorbance at 595 nm was measured, and protein concentrations calculated by reference to the BSA standard curve.

*ii) Amino Acid Analysis:* Accurate determinations of protein concentration were carried out by quantitative amino acid analysis. Samples were hydrolysed by incubation in 6 N HCl (with 0.1% phenol) at 110°C for 24 hours. Analyses were performed using a Hewlett-Packard AminoQuant Series II (Hewlett-Packard Australia Ltd, North Ryde, NSW) amino acid analyser coupled to an HP1046 fluorescence detector. Primary amino acids were subjected to pre-column derivatisation with orthophtaldehyde (OPA) and secondary amino acids with 9-fluorenylmethyl chloroformate (FMOC). The assistance of Greg de Plater (Biomolecular Resource Facility, ANU) with the operation of the amino acid analyzer is gratefully acknowledged.

**2.23 Large-Scale Bacterial Cultures**

Bulk fermentation vessels were used to grow *E. coli* cultures of between 10 L and 80 L. The strain to be grown in bulk fermentation was grown overnight on solid Luria medium supplemented with 33 mM glucose and the appropriate antibiotics.

This culture was used to inoculate one 1 L liquid culture per 10 L of culture to be grown in large-scale, supplemented with 33 mM glucose or glycerol and the appropriate antibiotics. These cultures were grown overnight at 37°C to stationary phase in 2 L baffled conical flasks, aerated by orbital shaking. This culture was used to inoculate the 14 L glass pot of the fermenter (New Brunswick Scientific, NJ, USA), containing 9 L of the same medium.

Cultures were grown with vigorous aeration (12 L air/min), to the required cell density.

The cultures were pumped into a refrigerated cart and cooled to 4°C, and the cells then harvested by centrifugation at 20,000 rpm in a Sharples centrifuge (Pennwalt Corporation, PA, USA).

**2.24. Preparation of Membrane and Cytoplasm Fractions and Preparation of the *E. coli* $F_1$-ATPase.**

Cells from a large-scale culture were resuspended in STEM buffer, approximately 3mL per gram of cells (wet weight). STEM buffer contains 110 mM TES (pH 7.0), 250 mM sucrose and 20 mM magnesium acetate. When necessary, the protease inhibitors ε-amino caproic acid (EACA; Alkjaersig *et al.*, 1959) and *para*-aminobenzamidine (PAB; Mares-Guia *et al.*, 1965) were added at concentrations of 40 mM and 6 mM, respectively.

Cells were sedimented by centifugation at 4000 x g for 15 mins at 4°C, and the supernatant discarded. The cell pellet was then resuspened in STEM buffer, approximately 2 mL per gram of cells (wet weight). The cells were then disrupted in a Sorvall RIBI French pressure cell (Ivan Sorvall, CT, USA) by passage through an aperture at 137 MP operating pressure. Unlysed cells and cell debris were removed by centrifugation for 30 minutes at 39,000 x g at 4 °C. The supernatant, containing both membrane vesicles and the soluble cytoplasmic fraction, was collected.

Membrane vesicles were separated from the cytoplasm by ultracentrifugation at 4°C for two hours at $3.6 \times 10^5 \times g$. The cytoplasm was removed and stored, if necessary, at -20°C. The membranes were washed by resuspending the pellet in a buffer containing 50 mM TES (pH 7.0), 15 % (v/v) glycerol, 40 mM EACA and 6 mM PAB, and centrifuging for one hour at 4°C at $3.6 \times 10^5 \times g$. The pellet was then washed twice in 5 mM TES buffer (pH 7.0) supplemented with 15% (v/v) glycerol, 40 mM EACA, 6 mM PAB, 0.5 mM EDTA and 0.5 mM DTT, by resuspension and resedimentation 4°C for one hour at $3.6 \times 10^5 \times g$. About 70% of the protein is removed from the membranes by this process, but the PAB causes retention of the $F_1$-ATPase on the membranes (Cox et al., 1978). The washed membranes were resuspended in 5 mL of the same 5 mM TES buffer and stored at -20°C.

If the membranes were to be used for preparation of the *E. coli* $F_1$-ATPase, or if stripped membranes were required for atebrin fluorescence quenching

assays, membranes were washed three times as described above in 5 mM TES buffer (pH 7.0) supplemented with 15% (v/v) glycerol, 40 mM EACA, 0.5 mM EDTA and 0.5 mM DTT (but no PAB) by resuspension and resedimentation at 4°C for one hour at $3.6 \times 10^5 \times g$. The washing in low ionic strength buffers in the absence of PAB causes solubilisation of the $F_1$-ATPase. To collect the crude preparation of the $F_1$-ATPase, the combined supernatants from the washing procedure were pooled and concentrated to a volume of less than 5 mL using a Centriprep 10 concentrator (Amicon, MA, USA). To collect the stripped membranes, the final pellet was resuspended in 5 mL of the 5 mM TES buffer described above (and lacking PAB) and stored at -20°C.

The crude $F_1$-ATPase preparation was purified by size-exclusion HPLC when required for the laboratory, but no work using HPLC-purified $F_1$-ATPase is described in this thesis.

**2.25 Purification of soluble glutathione-S-transferase (GST) fusion proteins, thrombin cleavage and isolation of the non-GST moiety**

A twenty litre culture of the required strain in Luria broth supplemented with 33 mM glycerol and 100 µg/mL ampicillin was grown with aeration to a cell density of 200 Klett units. Production of the fusion protein was induced by the addition of IPTG to a concentration of 0.1 mM, and the strain cultured for a further two hours before being collected by centrifugation (see section 2.23 above).

The cells were washed once, by suspension in STEM buffer (see section 2.24 above), followed by sedimentation by centrifugation. The cell pellet was resuspended in STEM buffer (3 mL per gram wet weight of cells), disrupted, and unlysed cells and cell debris removed as described in section 2.24 above. The supernatant, containing both membrane vesicles and the soluble cytoplasmic fraction, was collected.

Glutathione agarose beads were prepared as follows. A mass of 0.35 g of beads, corresponding to 5 mL volume of swollen beads, was swollen in 15 mL water for 30 minutes and collected by centrifugation for 30 seconds in a bench-top centrifuge. The supernatant was carefully removed and the the beads washed twice in STEM buffer, by resuspension and centrifugation.

The beads were mixed with the cell extract containing the soluble cytoplasmic fraction in a 600 mL flat-sided flask, which was rocked gently on a platform for three hours at 4 °C. The mixture was transferred to 50 mL

polypropylene centrifuge tubes and the beads collected by centrifugation for 30 seconds in a bench-top centrifuge. The supernatant, containing unbound protein, was carefully removed and the the beads washed four times with 100 mL STEM buffer, by resuspension and centrifugation.

The beads were resuspended in a total of 20 mL STEM buffer in two 50 mL polypropylene centrifuge tubes. The bound fusion protein was cleaved by treatment with human thrombin, at 10 NIH units per mL of suspension, for four hours at 25 °C while the tubes were gently rocked on a platform. This treatment releases the non-GST moiety of the fusion protein, while the GST moiety remains bound to the beads. The beads were collected by centrifugation for 30 seconds in a bench-top centrifuge. The supernatant, containing the desired protein, was carefully removed, and normally concentrated to a volume of approximately 5 mL using a Centriprep 10 concentrator (Amicon, MA, USA).

**2.26. Atebrin Fluorescence Quenching Assays of Membranes**

The electrochemical proton gradient ($\Delta\mu_{H^+}$) between the inside and outside of inverted membrane vesicles was assayed by atebrin fluorescence quenching (Haddock and Downie, 1974), using a Shimadzu RF5000 spectrofluorophotometer and DR-15 controller unit (Shimadzu, Kyoto, Japan). The excitation wavelength was 450 nm, the emission wavelength was 520 nm, with 5nm bandwidths. Detection of emission was at 90° to excitation. Cuvettes were 10 x 10mm with four optical faces.

To 2mL of Hepes buffer (10 mM Hepes (pH 7.5), 300 mM KCl, 5 mM $MgCl_2$) was added 50-150 mL of membrane suspension, and the cuvette was placed into the spectrofluorophotometer compartment. The machine was zeroed, and the recording of fluorescence was commenced. Atebrin (quinacrine dihydrochloride) was added to a concentration of 5 μM, and the contents of the cuvette were mixed thoroughly.

The NADH-dependent fluorescence quench assays the electrochemical proton gradient across the membrane due to proton pumping by the electron transport chain. NADH was added to the cuvette to a concentration of 2 mM, and the contents mixed thoroughly. When the fluorescence quench reached its maximum level and began to decrease, due to depletion of oxygen in the sample, the electron transport chain activity was terminated by the addition of the cytochrome *c* oxidase inhibitor NaCN to a final concentration of 2.5 mM.

The sample was left for sufficient time for fluorescence to return to maximal levels. ATP was added to a final concentration of 1 mM to measure the electrochemical proton gradient across the membrane due to proton pumping coupled to ATP hydrolysis by the $F_OF_1$-ATPase. When this quench reached its maximal level, the uncoupler CCCP (carbonyl cyanide *m*-chlorophenylhydrazone) was added to a final concentration of 4 mM, and fluorescence returned to its maximal level.

To calibrate the amount of active inverted membrane vesicles present in the assay it was necessary to vary the volume of membranes added, such that the NADH- dependent fluorescence quench began to decrease due to oxygen depletion at a time within 5 seconds of 1 minute after the addition of the NADH. If the time of oxygen depletion occurred too early or too late, the assay was aborted, and begun again with a lesser or greater amount of membranes.

**2.27 Mass Spectrometry**

A VG Analytical TOFSPEC Time-of-Flight (TOF) matrix-assisted laser desorption mass spectrometer (LDMS, Fisons Instruments, Manchester, UK) was employed for determining accurate masses of proteins. The principle of TOF mass analysis is based on the observation that ions of different masses which leave the ion source at the same time take different times to reach the detector when subjected to an accelerating potential, V, according to the following equation where z = charge, v = ion velocity ($ms^{-1}$) and m = ion mass (D) (Jennings and Dolnikowski, 1990):

$$v = 1.39 \times 10^4 (zV/m)^{1/2}$$

For each analysis, 1 µL of analyte (approximately 0.01 pmol) in 40% $CH_3CN$/0.009% TFA containing standard (0.75 pmol/µL equine cardiac myoglobin) was spotted onto the target (an inert metal substrate) followed by 1 µL of sinapinic acid matrix in $CH_3CN$. The target was allowed to dry for 1 hour before being introduced into the vacuum. The TOF-LDMS was used in positive ion detection mode. Following ion detection, ionization pulses were stopped to prevent sample consumption, and acquisition was switched from repetitve to averaged. Ionization was then continued until the average peak height began to decline (generally following 50 ionization pulses). The assistance of Dr. Peter

Milburn (Biomolecular Resource Facility, ANU) with the operation of the mass spectrometer is gratefully acknowledged.

**2.28 Circular Dichroism Spectroscopy**

Circular dichroism spectra were collected using a Jasco 720 Spectropolarimeter (Japan Spectroscopic Co., Ltd) purged with nitrogen, controlled by an Osborne MPRII peronal computer. The quartz cell had a pathlength of 0.1 cm. The instrument was calibrated prior to each set of scans by measuring the CD of (+)10-camphorsulfonic acid at 290.5 nm. The assistance of Dr. Michael Morris (Department of Biochemistry, University of Sydney) with the operation of the CD spectropolarimeter is gratefully acknowledged.

**2.29 Size-Exclusion High-Performance Liquid Chromatography**

HPLC was carried out on a dual-pump Bio-Rad gradient module fitted with titanium $^{1}/_{16}$" tubing. Detection was carried out using a Linear Instruments Uvis-204 ultraviolet/visible absorbance detector. Operation was under the control of a Bio-Rad model 700 Chromatography Data Station.

The size-exclusion (gel sieve) HPLC employed a TosoHaas TSK-G-3000-SW column (600 x 7.5 mm). Calibration between elution time and molecular weight was carried out using Bio-Rad Gel Filtration Standards (bovine thyroglobulin, 670 kD ; bovine γ-globulin, 158 kD; chicken ovalbumin, 44 kD; horse myoglobin, 17 kD; cyanocobalamin, 1350 D). Flow rate was routinely 1 mL/min. Detection was at 280 nm, or 215 nm for when the protein of interest contained no aromatic amino acid residues.

**2.30 Analytical Ultracentrifugation**

Sedimentation equilibrium and velocity experiments were carried out using a Beckman Optima XL-A analytical ultracentrifuge using 12 mm path length cells with carbon-filled double sector centrepieces. Data was analyzed using the standard programs supplied with the instrument. These were XLAEQ and XLAMW in the case of sedimentation equilibrium experiments and XLAVEL in the case of sedimentation velocity experiments.

**2.31 Precision Density Determinations**

Precision density determinations were carried out using a DMA O2C digital precision densitometer (Anton Paar K. G., Graz, Austria).

# CHAPTER 3

# COMPLEMENTATION STUDIES ON GENES ENCODING SPINACH CHLOROPLAST ATP SYNTHASE SUBUNITS EXPRESSED IN *E. coli.*

## 3.1 Introduction.

The aim of work described in this chapter was to test whether certain spinach chloroplast ATP synthase subunits might be able to functionally replace the homologous *E. coli* subunits. If any of the spinach chloroplast subunits were found to be able to replace the homologous *E. coli* subunit, site-directed mutagenesis and other experiments could then be carried out to probe the structure and function of the foreign subunit in the hybrid complex. Complementation analysis was carried out by firstly cloning spinach chloroplast genes into *E. coli* expression vectors, then transforming mutant *E. coli* strains affected in the relevant subunit with the appropriate plasmid. Assays were then carried out to assess whether a functional hybrid $F_OF_1$-ATPase had assembled in the cell.

Complementation analysis requires the choice of appropriate mutant *E. coli* strains in which to express the spinach chloroplast $F_OF_1$-ATPase subunits. Many of the characterised *unc* mutant alleles code for altered subunits which are able to assemble with the wild-type subunits to form inactive complexes. If a wild-type subunit formed in a partial diploid has to compete with mutant (including foreign) subunits for assembly, the mutation may have partial dominant effects (for example, see Gibson *et al.* (1977b) and Jans *et al.* (1983)). When complementation is to be analysed, it is therefore appropriate wherever possible to choose mutant *E. coli* strains that either lack the relevant $F_OF_1$-ATPase subunit completely, or express a subunit unable to assemble with the other subunits.

During the progress of this work, the complementation of several mutant *E. coli unc* genes by genes encoding chloroplast and cyanobacterial subunits was observed by Lill *et al.* (1993). The expression of spinach

chloroplast subunit $CF_oII$ in a *b*-subunit deficient mutant *E. coli* strain was also described. This subunit was found not to be able to replace the *E. coli b*-subunit (Schmidt, 1992).

Although some of the aims of the work described in this chapter are covered by information presented by Lill *et al.* (1990) and Schmidt (1992), novel experiments in which the complementation of combinations of $CF_o$ subunits were carried out, and more detailed assays were performed. Results are presented to complement those reported by Lill *et al.* (1993) and Schmidt (1992).

**3.2 Background to work on the *atpF* gene encoding subunit $CF_oI$ of the spinach chloroplast ATP synthase.**

Sequencing of chloroplast genomic DNA has revealed that the coding region of the *atpF* gene consists of a 142bp exon and a 407 bp exon separated by a 767bp intron. The predicted amino acid sequence encoded by the first exon starting at residue 18 correlates with the N-terminal amino acid sequence of the purified $CF_oI$ subunit, suggesting that the $CF_oI$ subunit is processed (Hudson *et al.*, 1987).

Although the amino acid sequence of the *E. coli b*-subunit shows little identity with that of the spinach chloroplast $CF_oI$ subunit (19%), the hydrophobicity profiles of the two subunits are very similar (see Fig 1.3 and Hudson *et al.*, 1987). To test whether the *atpF* gene can complement mutations in the *uncF* gene encoding the *E. coli b* subunit, *E. coli* strains carrying suitable mutations affecting the *uncF* gene are required. The strains used in this work are AN1440 and AN1521, which carry the *uncF469* and *uncF476* alleles repectively on their chromosomes, and AN2192, which carries the *uncF515* allele on a multicopy plasmid in the *uncF469* background strain AN1440.

The *uncF469* allele specifies a nonsense mutation with a stop codon replacing the codon for Tryptophan-26 in the *b*-subunit. Strain AN1440 therefore produces only a severely truncated *b*-subunit, and is unable to grow on succinate as sole carbon source. Membranes from AN1440 have maximal atebrin fluorescence quenching activity before and after washing with buffers of low ionic strength and are therefore proton impermeable. These membranes also have no ATPase activity or ATP dependent atebrin fluorescence quenching activity. No *b*-subunit is visible when membranes from AN1440 are analysed by two-dimensional gel electrophoresis. Low levels of the α- and β- subunits are visible, but the minor subunits (γ, δ and

ε) and the other α- and β- subunits are unable to assemble in AN1440 (Jans *et al.*, 1984).

The *uncF476* allele specifies a missense mutation which replaces glycine-9 of the *b*-subunit with aspartate. Strain AN1521, which carries this allele, is incapable of growth on succinate as sole carbon source. The mutant *b*-subunit is not assembled into the membrane in haploid strains carrying the *uncF476* allele, but if the mutant allele is incorporated into a multicopy plasmid then some assembly of the mutant *b*-subunit occurs. Such plasmids confer the ability to grow on succinate as sole carbon source on strains AN1440 or AN1521 (Jans *et al.*, 1984). The observation that partial assembly of the mutant *b*-subunit was dependent on expression from a multicopy plasmid was a factor in the choice of the pUC vectors (which replicate to 500-700 copies per cell; Sambrook *et al.*, 1989) for use in the complementation studies described in this chapter. These vectors (described by Viera and Messing, 1982) were also chosen for the range of restriction sites in the multiple cloning region and the ease of screening for recombinants by histochemical means (Sambrook *et al.*, 1989). When cloned in the correct orientation, the expression of genes inserted into the multiple cloning region in these vectors is under the control of the *lac* promoter (Sambrook *et al.*, 1989).

The *uncF515* allele specifies a missense mutation which replaces glycine-131 of the *b*-subunit with aspartate. The allele is carried by plasmid pAN257 (*uncB*$^+$*E*$^+$*F515H*$^+$*A*$^+$*cap*$^R$). When strain AN1440 is transformed with pAN257, the resulting strain (AN2191) is unable to grow on succinate as sole carbon source. The *uncF515* allele therefore does not complement the *uncF469* allele. The *uncF515* allele does, however, complement the *uncF476* allele. When strain AN1521 is transformed with pAN257, the resulting strain (AN2192) is able to grow on succinate as sole carbon source (Jans *et al.*, 1985). This finding of intragenic complementation suggested that it would be worth while to test for complementation of $CF_oI$ and $CF_oII$ in a range of different host strains.

A 1.67 kb *Eco*RI/*Hin*dIII fragment derived from spinach chloroplast cDNA and covering the entire *atpF* coding region and part of the *atpA* gene, which was isolated by Dr. Alan Munn in this laboratory, was used for this work. This fragment was subcloned into the *Eco*RI and *Hin*dIII sites of the polylinker in pUC8 to create the plasmid pAN423 . Using minicell labelling experiments with [$^{35}$S]-methionine, the expression of the $CF_oI$ precursor protein was demonstrated (Munn, 1988). When used to transform strain AN1440, plasmid pAN423 did not confer the ability to grow on succinate as

sole carbon source. The spinach chloroplast *atpF* gene in unprocessed form therefore did not complement the mutant *E. coli uncF* gene, and the $CF_oI$ precursor was therefore shown not to be able to replace the *E. coli b*-subunit and assemble with normal *E. coli* subunits to form a functional $F_oF_1$-ATPase (Munn, 1988).

The inability of *E. coli* to specifically cleave the the 17 amino acid residue leader sequence at the N-terminus of the $CF_oI$ may have prevented the unprocessed *atpF* gene from complementing the *uncF469* mutation, possibly due to the leader sequence interfering with the assembly of the $CF_oI$ precursor into a functional $F_oF_1$-ATPase complex. To investigate whether the mature $CF_oI$ protein could functionally replace the *E. coli b* subunit, site-directed mutagenesis was carried out on the cloned *atpF* gene to introduce a new start site at the position corresponding to the N-terminus of the mature $CF_oI$ protein, and to introduce appropriate *E. coli* translation start signals upstream of the new start site. These experiments are described below.

### 3.3 The subcloning and site-directed mutagenesis of the *atpF* gene

The 1.67kb *Eco*RI/*Hin*dIII fragment carrying the entire *atpF* coding region was subcloned from pAN423 into the *Eco*RI and *Hin*dIII sites of M13mp19 RF DNA, creating clone M13mp19:*atpF*. Site-directed mutagenesis was then carried out to modify the sequence in three ways:

Firstly, a new methionine initiation codon was introduced at a position corresponding to the known start of the mature protein.

Secondly, a suitable ribosome binding site for the initiation of translation in *E. coli* was placed in the region immediately upstream from the new start site. Most highly expressed *E. coli* genes possess a sequence of nucleotides 5-15 bases upstream from the AUG start codon which shows homology to the 3′ terminal region of the *E. coli* 16S ribosomal RNA (Shine and Dalgarno, 1974). Alterations in the Shine-Dalgarno sequence and the spacing between the sequence and the start codon can lead to a 1000-fold variation in the level of expression of the gene (Guarente *et al.*, 1980; Chang *et al.*, 1980; Shepard *et al.*, 1982; Whitehorn *et al.*, 1985; Luck *et al.*, 1986; Curry and Tomich, 1988). In order to maximise potential expression of the mature $CF_oI$ subunit in *E. coli*, the Shine-Dalgarno sequence GAGGA was introduced in the region 10 to 5 bases upstream from the new start codon.

Thirdly, an in-frame stop codon was required upstream from the regulatory signals to terminate prematurely translation of the $CF_oI$ precursor. Oligonucleotide AR-1 was constructed by G. Schmidt in this

laboratory with a sequence identical to this region except for these modifications (see Table 2.1).

Using single-stranded DNA of clone M13mp19:*atpF* as template, site-directed mutagenesis was carried out using oligonucleotide AR-1 as the mutagenic primer. Single stranded DNA was prepared from several isolates and sequenced using the M13 universal sequencing primer. RF DNA was prepared from an isolate carrying the desired mutations, and this clone was named mp19*atpF*AR-1. The 1.67kb fragment carrying the modified *atpF* gene was then subcloned from the RF DNA into *Eco*RI and *Hin*dIII sites of pUC18 to create plasmid pAN573 (see Fig 3.1; referred to below in genotypic descriptions as "mCF$_O$I").

Plasmid pAN573 was used to transform strains AN1440, AN1521 and AN2191 to ampicillin resistance, creating strains AN2936 (mCF$_O$I/*uncF469*), AN3799 (mCF$_O$I/*uncF476*) and AN3800 (mCF$_O$I/*uncF469/uncF515*) respectively.

### 3.4 Construction of positive and negative control strains for complementation analysis with *uncF* mutant strains

To serve as a positive control for complementation analysis with *uncF* mutant strains, a pUC18 derived plasmid was constructed which expresses the wild-type *uncF* gene, and when transformed into the *uncF* mutant background strains is able to restore the ability to grow on succinate as sole carbon source. Plasmid pAN51 (described by Downie *et al.*, 1980), was cut with *Bam*HI and *Eco*RI to yield a 1.5kb fragment with the *unc* genes*E, F* and *H*. The subcloning of this fragment into the *Bam*HI and *Eco*RI sites of both pUC18 and pUC19 was attempted. The orientation of the polylinker in these vectors is such that if expression of the genes were to be under the control of the *lac* promoter, pUC19 must be the vector of choice. However, the subcloning of the fragment into pUC18 yielded a plasmid (named pAN1128) which conferred upon strain AN1440 the ability to grow on succinate minimal medium, whereas the the subcloning of the fragment into pUC19 yielded a plasmid which did not. This may have been due to the deleterious overexpression of one or more of the *unc* genes.

Plasmid pAN1128 used to transform the *uncE429* background strain AN943 and the *uncH421* background strain AN2015, creating strains AN3784 and AN3786 respectively. These strains were able to grow on succinate minimal medium. Plasmid pAN1128 was therefore chosen as an appropriate positive control for complementation analysis involving mutant *uncF* and *uncH* background strains. Plasmid pAN1128 was used to

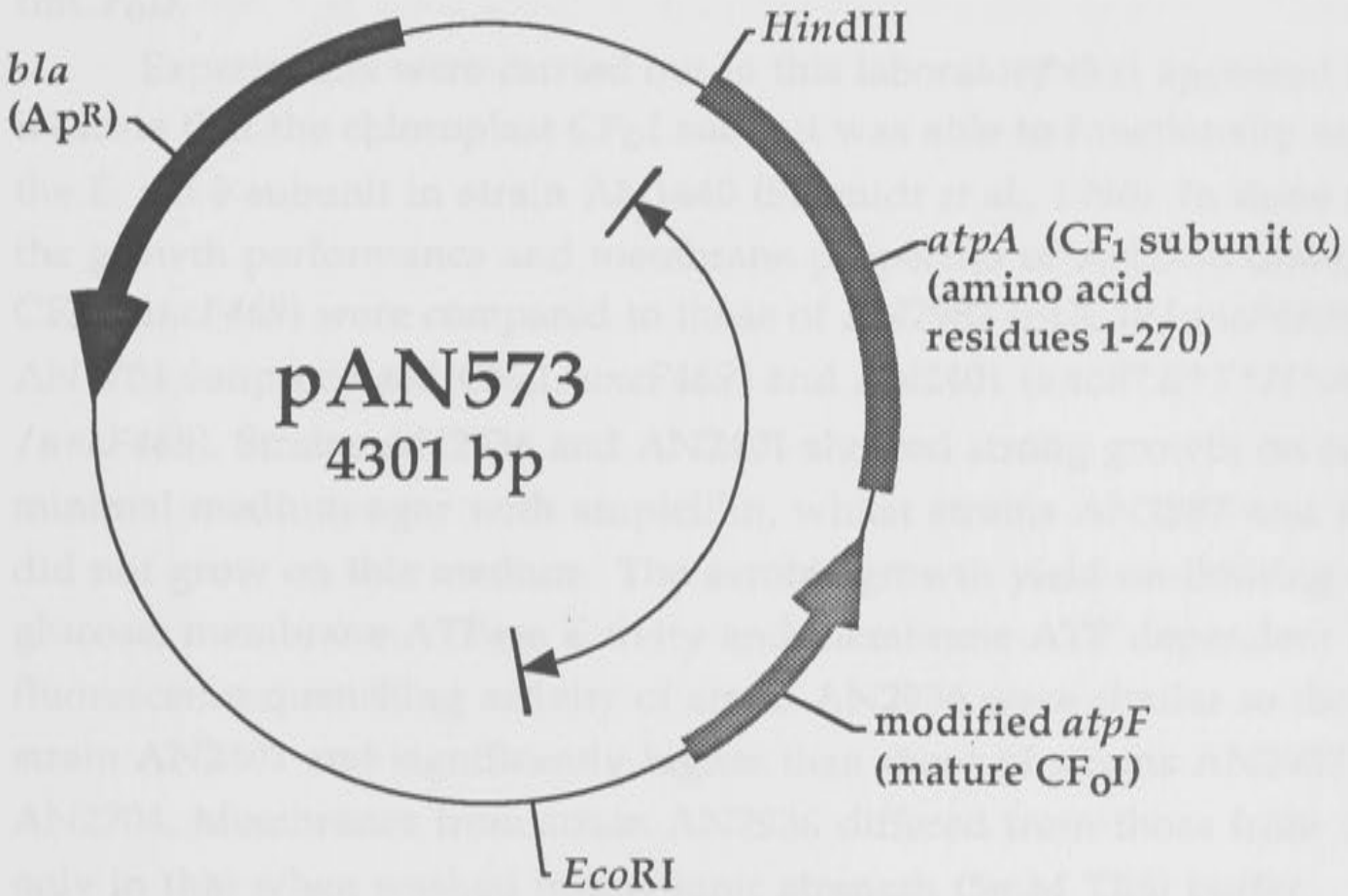


**Figure 3.1**: Plasmid pAN573, carrying a 1.67kb fragment with the modified *atpF* gene encoding the mature form of spinach chloroplast subunit $CF_0I$, cloned into the *Eco*RI and *Hin*dIII sites of pUC18.

transform strains AN1440, AN1521 and AN2191 to create strains AN3785, AN3803 and AN3804. Strains AN3785 and AN3803 were able to grow on succinate minimal medium with ampicillin, and strain AN3804 was able to grow on this medium with chloramphenicol also present.

To construct negative controls for complementation analysis involving mutant *uncF* background strains, the vector pUC18 was used to transform strains AN1440, AN1521 and AN2192, creating the strains AN2987, AN3801 and AN3802 respectively.

### 3.5 Growth properties of *uncF* mutant strains carrying plasmid pAN573 ($mCF_oI$).

Experiments were carried out in this laboratory that appeared to indicate that the chloroplast $CF_oI$ subunit was able to functionally replace the *E. coli b* subunit in strain AN1440 (Schmidt *et al.*, 1990). In these studies, the growth performance and membrane properties of AN2936 (mature $CF_oI$/*uncF469*) were compared to those of AN2987 (pUC18/*uncF469*), AN2704 (unprocessed $CF_oI$/*uncF469*) and AN2401 (*uncB*$^+$*E*$^+$*F*$^+$*H*$^+$*A*$^+$ /*uncF469*). Strains AN2936 and AN2401 showed strong growth on succinate minimal medium agar with ampicillin, whilst strains AN2987 and AN2704 did not grow on this medium. The aerobic growth yield on limiting (5 mM) glucose, membrane ATPase activity and membrane ATP dependent atebrin fluorescence quenching activity of strain AN2936 were similar to those of strain AN2401 and significantly higher than those of strains AN2987 and AN2704. Membranes from strain AN2936 differed from those from AN2401 only in that when washed in low ionic strength (5mM TES) buffer, membranes form strain AN2936 were significantly more proton permeable. The results of these studies clearly suggested, however, that subunit $CF_oI$ could functionally replace the *E. coli b*-subunit.

Based on this finding, a series of site-directed mutagenesis experiments were carried out to alter amino acid residues in $CF_oI$ conserved with the *b* subunit. The aim of these experiments was to determine which of these residues may be important to the function of the hybrid complex in which $CF_oI$ had been substituted for the *b* subunit. It was hoped that this information may help to elucidate important interactions involved in the structure of the hybrid and wild-type $F_oF_1$-ATPase complexes.

Single-stranded DNA was isolated from clone mp19*atpF*AR-1. Using this DNA as a template, site-directed mutagenesis was carried out to alter twelve amino acid residues in $CF_oI$: Leucine-10→Alanine; Phenylalanine-27→Isoleucine; Phenylalanine27→Tyrosine; Leucine36→Asparagine;

Isoleucine47→Asparagine; Alanine66→Serine; Alanine75→Serine; Glutamine113→Leucine; Glutamate115→Glutamine; Arginine124→Glutamine; Glutamine130→Leucine; Alanine161→Serine; and Arginine165→Glutamine. A single clone was isolated following each of the site-directed mutagenesis reactions, each carrying the desired mutation as determined by sequencing. RF DNA was prepared from all of the clones, each cut with the enzymes *Eco*RI and *Hin*dIII, and subcloned into the *Eco*RI and *Hin*dIII sites of the vector pUC18. The twelve pUC based plasmids carrying the mutant *atpF* genes were each used to transform strain AN1440. The twelve strains thus created were streaked out on solid succinate minimal medium with ampicillin, but none was able to grow. These observations suggested that the original finding that strain AN2936 was able to grow on succinate minimal medium may have been erroneous, possibly due to contamination of this strain with a low copy-number plasmid carrying the wild-type *uncF* gene. To test this idea, plasmid DNA was prepared from a liquid culture of strain AN2936 and analysed by agarose gel electrophoresis. In addition to the band of plasmid pAN573, another fainter band was visible, which was excised from the gel. DNA purified from the excised gel fragment was used to transform AN1440. The resulting strain was streaked out on succinate minimal medium agar containing either ampicillin or chloramphenicol. Strong growth was observed on the agar plate containing chloramphenicol, but no growth was observed on the plate containing ampicillin. The contaminating plasmid which conferred resistance to chloramphenicol and the ability to grow on succinate on strain AN1440 was identified following further analysis as pAN495 (Howitt *et al.*, 1988), which carries the wild-type *unc* genes *B*, *E* and *F* .

Measurements of growth yield in limiting (5mM) glucose were carried out using the method described in section 2.5. The abilities of each strain to grow on solid succinate minimal medium are described using the following symbols: -, no growth; +/- , poor but significant growth; +, growth; ++, growth to high yields. The succinate growth experiments were also repeated with 0.1 mM IPTG present in the medium to increase expression from the *lac* promoter:

| Strain | Growth on succinate | Growth on succinate with 0.1 mM IPTG | Growth Yield in 5mM glucose (Klett Units) |
|---|---|---|---|
| AN2987 (pUC18/AN1440) | - | - | 131 |
| AN3801 (pUC18/AN1521) | - | - | 132 |
| AN3802 (pUC18/ *uncF469/uncF515*) | - | - | 130 |
| AN2936 (mCF$_O$I/AN1440) | - | - | 133 |
| AN3799 (mCF$_O$I/AN1521) | - | - | 134 |
| AN3800 (mCF$_O$I/ *uncF469/uncF515*) | - | - | 126 |
| AN3785 (pAN1128/AN1440) | ++ | ++ | 214 |
| AN3803 (pAN1128/AN1521) | ++ | ++ | 216 |
| AN3804 (pAN1128/ *uncF469/uncF515*) | ++ | ++ | 213 |

The similarity in growth properties of AN2936 (mCF$_O$I/*uncF469*), AN3799 (mCF$_O$I/*uncF476*) and AN3800 (mCF$_O$I/*uncF469/uncF515*) to the uncoupled negative control strains indicates that when expressed from the vector pUC18, the modified *atpF* gene does not complement the mutant *uncF* alleles, and that the mature CF$_O$I subunit cannot replace the *E. coli b*-subunit and assemble with the other *E. coli* subunits to form a functional F$_O$F$_1$-ATPase.

**3.6 Background to work on the *atpG* gene encoding the $CF_oII$ subunit of the spinach chloroplast ATP synthase.**

The isolation and sequencing of cDNA clones covering the entire coding region for the $CF_oII$ subunit of the spinach chloroplast ATP synthase was described by Herrmann *et al.*, (1993). One of these clones was made available to this laboratory, providing the opportunity to test whether the spinach chloroplast $CF_oII$ subunit could functionally replace the *E. coli b* subunit in an appropriate mutant *E. coli* strain. During the progress of this work, the complementation testing of processed spinach chloroplast subunit $CF_oII$ in AN1440 was reported (Schmidt, 1992). When expressed from the vector pDS12, this subunit was found not to be able to replace the *E. coli b*-subunit.

The mature spinach $CF_oII$ subunit and the *E. coli b* subunit share only 29% amino acid sequence identity, but homology between the subunits is indicated by a highly conserved pattern of secondary structural elements (Herrmann *et al.*, 1993). To test whether the *atpG* gene can complement mutations in the *uncF* gene encoding the *E. coli b* subunit, *E. coli* strains carrying suitable mutations affecting the *uncF* gene are required. The strains used in this work are AN1440, AN1521 and AN2191, described previously in section 3.2.

As discussed above, the inability of *E. coli* to specifically cleave the N-terminal leader sequence possessed by some chloroplast $F_oF_1$-ATPase proteins may prevent complemention of the *unc* mutations by homologous spinach *atp* genes. The reading frame of 222 amino acid residues for the $CF_oII$ precursor includes 147 residues for the mature protein (molecular weight 16.5 kD) and a transit sequence of 75 residues (molecular weight 8.0 kD) (Herrmann *et al.*, 1993). To investigate whether the mature $CF_oII$ subunit could functionally replace the *E. coli b* subunit when expressed from a pUC vector, site-directed mutagenesis was carried out on the *atpG* gene to allow expression of the mature protein. These experiments are described below.

**3.7 The subcloning and site-directed mutagenesis of the *atpG* gene encoding the $CF_oII$ subunit of the spinach chloroplast ATP synthase.**

Plasmid pSocCF$_o$II, carrying a fragment covering the entire coding sequence for the precursor to $CF_oII$ inserted in the *Eco*RI site of the vector pBluescript, was a generous gift of Prof. R. G. Herrmann, Munich.

Using pSocCF$_o$II DNA as template, the polymerase chain reaction was used to amplify a 420bp fragment encoding the mature $CF_oII$. The 5′

oligonucleotide used in the amplification (AR-2) introduced a new start codon at the position corresponding to the N-terminus of the mature $CF_oII$ protein, the concensus Shine-Dalgarno ribosome binding sequence (see section 3.3 above) upstream of the new start site, and a restriction site for *Kpn*I (see Table 2.1). The 3′ end complementary strand oligonucleotide used in the amplification reaction was AR-3, which has a sequence complementary to the region 7-42 bases 3′ of the *atpG* stop codon, except that a site for *Bam*HI was incorporated into the sequence 20-26 bases 3′ of the *atpG* stop codon.

The 420bp amplified fragment was digested with the enzymes *Kpn*I and *Bam*HI. The subcloning of the fragment into the *Kpn*I and *Bam*HI sites of pUC18 was attempted several times using the method described in section 2.10, but without success. All colonies screened carried the vector pUC18 without the desired insert.

The subcloning of the PCR fragment carrying the modified *atpG* gene was successfully carried out using an alternative method reported by Holton and Graham (1991), and described in detail in section 2.19. The vector pUC19 was digested with the enzyme *Sma*I, to linearize the DNA leaving "blunt" ends. The uncut PCR product carrying the modified *atpG* gene was then subcloned directly into the vector. Plasmid preparations from several colonies were digested with *Eco*RI and analysed by agarose gel electrophoresis to determine the orientation of the insert in the vector. Two colonies yielded plasmids with the insert in the correct orientation for expression of the modified *atpG* gene from the *lac* promoter. One of these was chosen for further work and was named pAN1140 (see Fig 3.2; referred to below in genotypic descriptions as "$mCF_oII$"). Four colonies yielded plasmids with the insert in the incorrect orientation for expression of the modified *atpG* gene from the *lac* promoter. One of these was chosen for further work (see section 3.10 below) and was named pAN1141.

Using the M13 universal forward and reverse sequencing primers, the entire modified *atpG* gene in plasmid pAN1140 ($mCF_oII$) was sequenced. Apart from the directed mutations, the sequence matched exactly that described by Herrmann *et al.* (1993). Plasmid pAN1141 was not sequenced at this stage but the *atpG* gene in a plasmid from which it was derived was sequenced and found to be also completely wild-type apart from desired directed mutations (see section 3.10 below).

Plasmid pAN1140 ($mCF_oII$) was used to transform strains AN1440*(uncF469)*, AN1521 *(uncF476)* and AN2191 *(uncF469/uncF515)* to

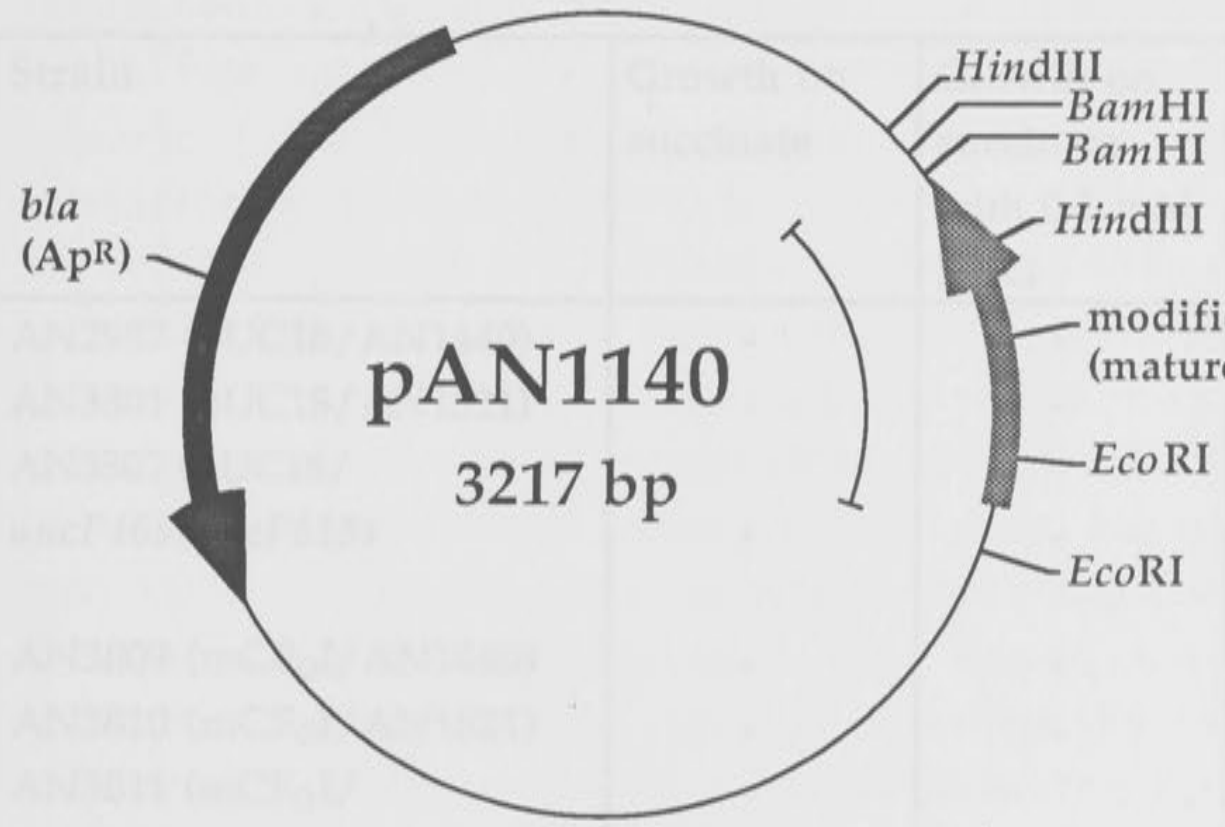


**Figure 3.2**: Plasmid pAN1140, carrying a 420bp fragment with the modified *atpG* gene encoding the mature form of spinach chloroplast subunit $CF_oII$, cloned into the *Sma*I site of pUC19.

ampicillin resistance to give strains AN3809, AN3810 and AN3811 respectively.

### 3.8 Growth properties of *uncF* mutant strains carrying plasmid pAN1140 ($mCF_oII$).

Measurements of growth yield in limiting (5mM) glucose were carried out using the method described in section 2.5. The abilities of each strain to grow on solid succinate minimal medium are described using the following symbols: -, no growth; +/- , poor but significant growth; +, growth; ++, growth to high yields. The succinate growth experiments were also repeated with 0.1 mM IPTG present in the medium to increase expression from the *lac* promoter:

| Strain | Growth on succinate | Growth on succinate with 0.1 mM IPTG | Growth Yield in 5mM glucose (Klett Units) |
|---|---|---|---|
| AN2987 (pUC18/AN1440) | - | - | 131 |
| AN3801 (pUC18/AN1521) | - | - | 132 |
| AN3802 (pUC18/ *uncF469/uncF515*) | - | - | 130 |
| AN3809 ($mCF_oI$/AN1440) | - | - | 135 |
| AN3810 ($mCF_oI$/AN1521) | - | - | 135 |
| AN3811 ($mCF_oI$/ *uncF469/uncF515*) | - | - | 127 |
| AN3785 (pAN1128/AN1440) | ++ | ++ | 214 |
| AN3803 (pAN1128/AN1521) | ++ | ++ | 216 |
| AN3804 (pAN1128/ *uncF469/uncF515*) | ++ | ++ | 213 |

The growth properties of strains AN3809 ($mCF_oII$/*uncF469*), AN3810 ($mCF_oII$/*uncF476*) and AN3811 ($mCF_oII$/*uncF469/uncF515*) closely resemble those of the negative control strains AN2987 (pUC18/*uncF469*), AN3801 (pUC18/*uncF476*) and AN3802 (pUC18/*uncF469/uncF515*). These results indicate that the spinach chloroplast subunit $CF_oII$ cannot replace

the *E. coli b* subunit and assemble with the other *E. coli* subunits to form a functional $F_OF_1$-ATPase, confirming the observation of Schmidt (1992).

**3.9 Construction of a plasmid carrying both the *atpF* and *atpG* genes encoding the $CF_OI$ and $CF_OII$ subunits of the spinach chloroplast ATP synthase.**

Although the $F_OF_1$-ATPase of *E. coli* possesses two copies of the *b*-subunit (Senior, 1990), the enzyme complex from spinach chloroplasts appears to have one copy each of $CF_OI$ and $CF_OII$ (Herrmann *et al.*, 1993). Interactions between the two proteins may be important for the correct folding of the individual subunits and assembly into a functional $F_OF_1$-ATPase. Neither $CF_OI$ nor $CF_OII$ alone were capable of replacing the *E. coli b*-subunit and assembling with the other *E. coli* subunits to form a functional $F_OF_1$-ATPase (see above). To test whether both subunits together could replace the pair of *b*-subunits, a plasmid was constructed to co-express both the modified *atpF* and *atpG* genes.

Plasmid pAN573 ($mCF_OI$) carries the modified *atpF* gene on an *Eco*RI/*Hin*dIII insert in pUC18. Because the *Eco*RI and *Hin*dIII sites are at the extreme 5′ and 3′ ends of the polylinker in pUC18 respectively, no other restriction sites were available for subcloning into this plasmid (or from this plasmid into another already carrying the *atpG* gene). Using the polymerase chain reaction, a 652bp fragment carrying the entire modified *atpF* gene was amplified, with restriction sites at the 5′ and 3′ ends convenient for subcloning. The 5′ primer used was oligonucleotide AR4 which has a sequence identical to the region 88 to 59 bases upstream of the $CF_OI$ start codon, except that an *Eco*RI site is introduced in the bases 72 to 66 upstream of the start codon. The 3′ primer used was oligonucleotide AR5, which has a sequence complementary to a region 7-42 bases downstream of the *atpF* stop codon, except that a *Kpn*I site is introduced in bases 21-26 downstream of the *atpF* stop codon. The amplified fragment was digested with *Eco*RI and *Kpn*I, and inserted into the *Eco*RI and *Kpn*I sites of pUC18. This plasmid was named pAN1142. The entire coding region of the modified *atpF* gene was sequenced and found to be completely wild-type apart from desired directed mutations previously described (section 3.4 above).

Plasmid pAN1141, which is described above, carries the modified *atpG* gene encoding the mature $CF_OII$ subunit inserted in the *Sma*I site of pUC19, although the orientation is incorrect for expression of the gene from the *lac* promoter. This plasmid was digested with the enzymes *Kpn*I and *Xba*I, and the DNA fragments separated by agarose gel electrophoresis. The

550bp fragment carrying the modified *atpG* gene was excised from the gel and purified using the method described in section 2.8.

Plasmid pAN1142 was digested with the enzymes *Kpn*I and *Xba*I. The 550bp fragment carrying the modified *atpG* gene was then ligated into these sites, creating plasmid pAN1144 (see Fig 3.3; referred to below in genotypic descriptions as "mCF$_O$I + mCF$_O$II"). This plasmid now carries both the modified *atpF* and *atpG* genes, encoding the mature CF$_O$I and CF$_O$II subunits respectively, and both in the correct orientation for expression from the *lac* promoter of pUC18.

Plasmid pAN1144 was used to transform strain AN1440 *(uncF469)*to create strain AN3812 (mCF$_O$I + mCF$_O$II/*uncF469*).

### 3.10 Growth properties of an *uncF* mutant strain carrying plasmid pAN1144 (mCF$_O$I + mCF$_O$II).

Measurements of growth yield in limiting (5mM) glucose were carried out using the method described in section 2.5. The abilities of each strain to grow on solid succinate minimal medium are described using the following symbols: -, no growth; +/- , poor but significant growth; +, growth; ++, growth to high yields. The succinate growth experiments were also repeated with 0.1 mM IPTG present in the medium to increase expression from the *lac* promoter:

| Strain | Growth on succinate | Growth on succinate with 0.1 mM IPTG | Growth Yield in 5mM glucose (Klett Units) |
|---|---|---|---|
| AN2987 (pUC18/*uncF469*) | - | - | 131 |
| AN3812 (mCF$_O$I + mCF$_O$II/*uncF469*) | - | - | 130 |
| AN3785 (pAN1128/*uncF469*) | ++ | ++ | 214 |

The growth properties of strain AN3812 (mCF$_O$I + mCF$_O$II/*uncF469*) closely resemble those of the negative control strain AN2987 (pUC18/*uncF469*). These results indicate that when expressed from the same plasmid, the spinach chloroplast subunits CF$_O$I and CF$_O$II cannot replace the *E. coli b*-subunits and assemble with the other *E. coli* subunits to form a functional F$_O$F$_1$-ATPase.

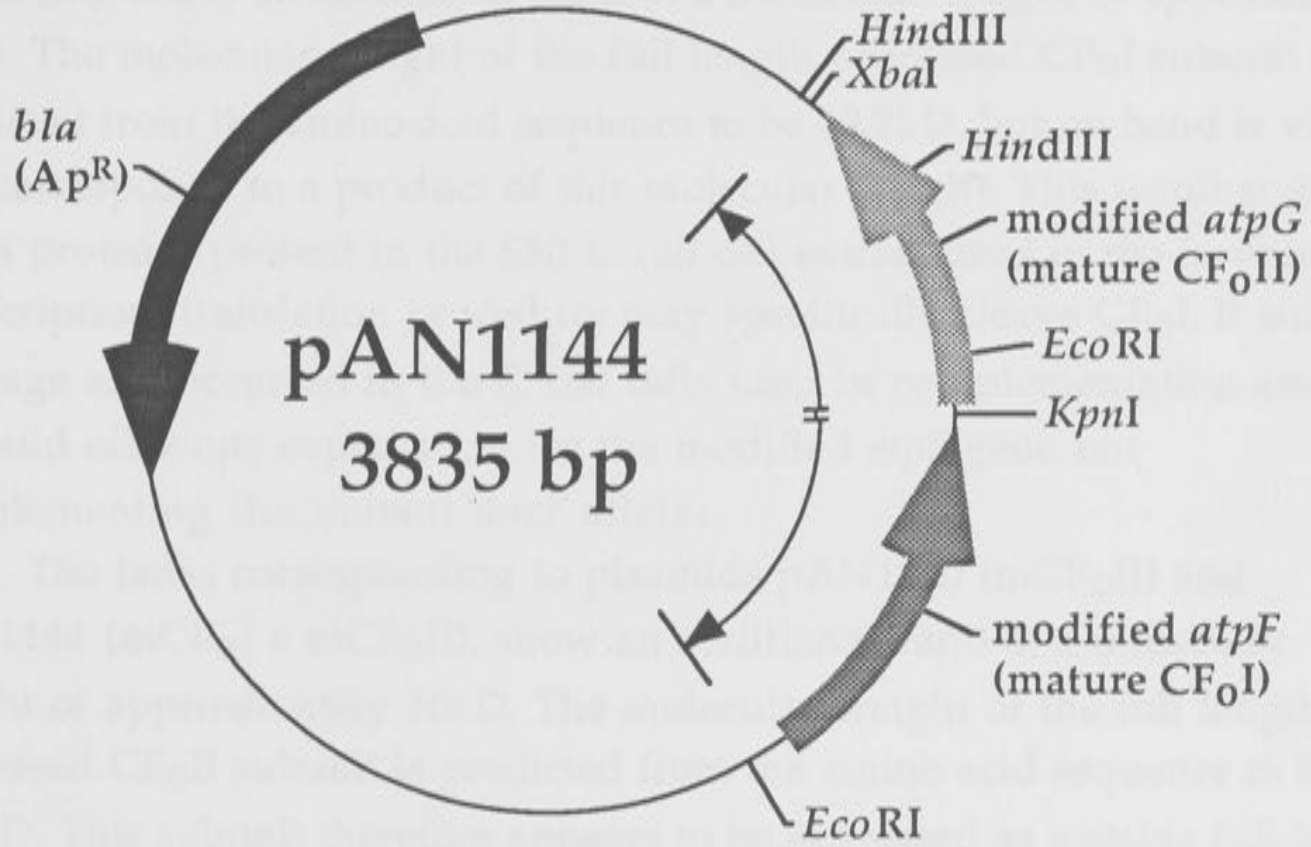


**Figure 3.3**. Plasmid pAN1144, which carries a 1.1 kb fragment with the modified *atpF* gene, encoding the mature form of subunit $CF_oI$, and the modified *atpG* gene, encoding the mature form of subunit $CF_oII$, cloned into the *Eco*RI and *Xba*I sites of the vector pUC18.

**3.11 Analysis of gene expression from plasmids pUC18, pAN573, pAN1140 and pAN1144 using *in vitro* transcription/ translation**

The expression of the genes from plasmids pUC18, pAN573 ($mCF_oI$), pAN1140 ($mCF_oII$) and pAN1144 ($mCF_oI$ + $mCF_oII$) was analysed by *in vitro* transcription/translation using the method described in section 2.20. The gel autoradiograph from this experiment is shown in Fig 3.4.

When compared to the lane with translation products from pUC18, the lanes corresponding to plasmids pAN573 ($mCF_oI$) and pAN1144 ($mCF_oI$ + $mCF_oII$), show an additional band at a molecular weight of approximately 13kD. The molecular weight of the full length processed $CF_oI$ subunit is predicted from the amino acid sequence to be 19.2kD, but no band is visible that corresponds to a product of this molecular weight. This result suggests that a protease present in the S30 *E. coli* cell extract used in the *in vitro* transcription/translation procedure may specifically cleave $CF_oI$. If such cleavage also occurred in the *E. coli* cells used in complementation analysis it would offer one explanation for the modified *atpF* gene not complementing the mutant *uncF* alleles.

The lanes corresponding to plasmids pAN1140 ($mCF_oII$) and pAN1144 ($mCF_oI$ + $mCF_oII$), show an additional band at a molecular weight of approximately 16kD. The molecular weight of the full length processed $CF_oII$ subunit is predicted from the amino acid sequence to be 15.4kD. This subunit therefore appears to be expressed as a stable full-length product in the *in vitro* transcription/translation system.

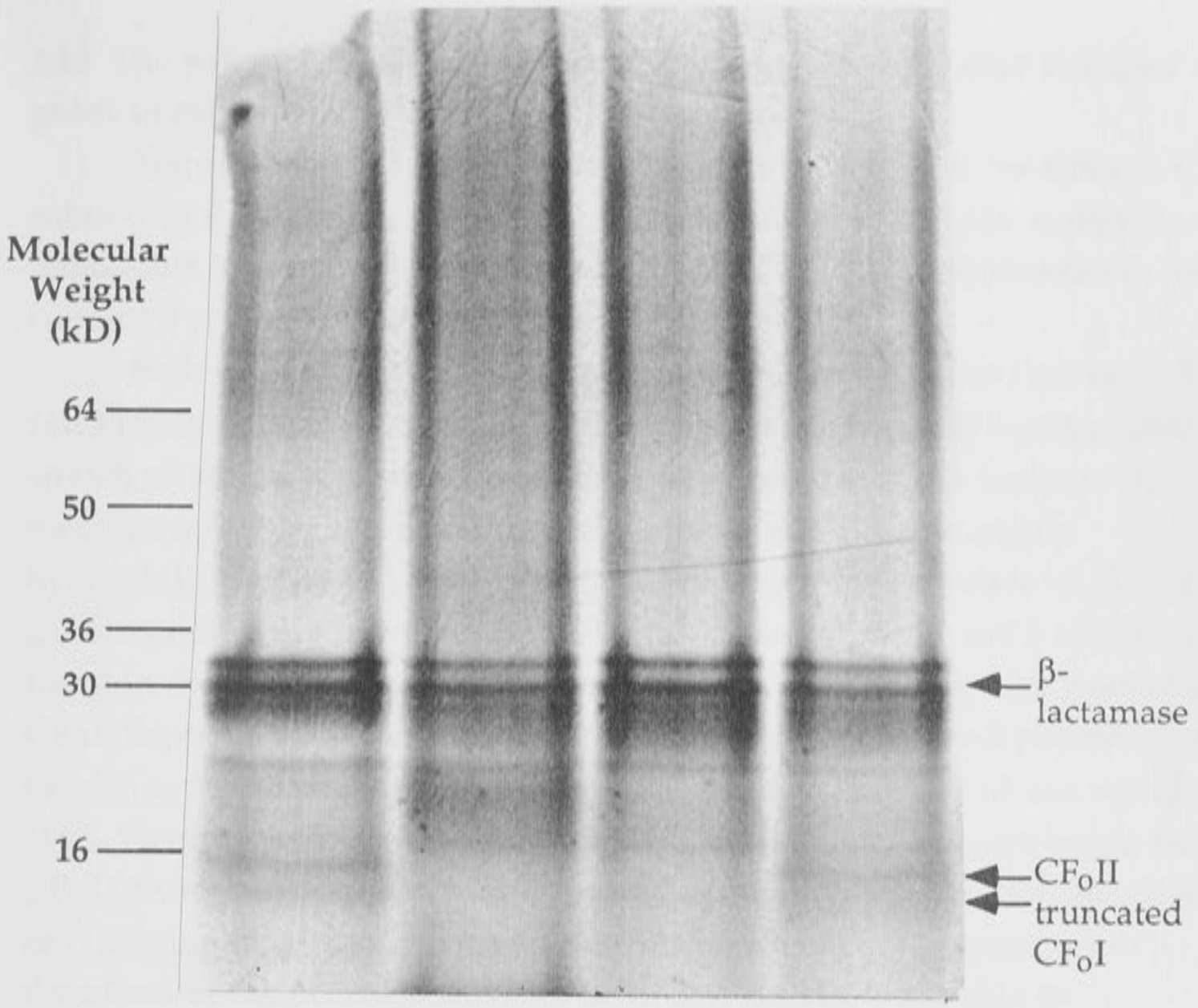


**Fig. 3.4:** Autoradiograph of SDS-PAGE gel to analyse gene expression from plasmids pUC18, pAN573 (mCF$_o$I/pUC18), pAN1140 (mCF$_o$II/pUC18)and pAN1144 (mCF$_o$I + mCF$_o$II/pUC18) using *in vitro* transcription/ translation.
Lane 1: Expression products from plasmid pAN1144 (mCF$_o$I + mCF$_o$II/pUC18)
Lane 2: Expression products from plasmid pUC18
Lane 3: Expression products from plasmid pAN573 (mCF$_o$I/pUC18)
Lane 4: Expression products from plasmid pAN1140 (mCF$_o$II/pUC18)

**3.12 The subcloning and site-directed mutagenesis of the *atpF* and *uncF* genes to construct a hybrid $CF_oI$/*b* subunit protein.**

The apparent susceptibility to proteolytic cleavage of the spinach $CF_oI$ subunit in the *E. coli* cells used for complementation analysis makes it impossible to conclude that $CF_oI$ could not functionally replace the *E. coli b*-subunit if it were stable in the cell.

Both $CF_oI$ and the *E. coli b* subunit have two sequence regions with contrasting physical properties, with a short predominantly hydrophobic stretch of amino acids near the N-terminus predicted to be traverse the membrane, while the remainder of the protein is predominantly hydrophilic. A plasmid was constructed in which the sequence of the *uncF* gene encoding the membrane traversing portion of the *E. coli b* subunit was fused to the sequence of the *atpF* gene encoding the hydrophilic portion of $CF_oI$. Experiments to test whether the hybrid $CF_oI$/*b* subunit protein might be able to functionally replace the whole *E. coli b* were carried out with two aims. Firstly, it was hoped that the hybrid protein may be more stable than $CF_oI$ (given that this protein is apparently susceptible to degradation in *E. coli*, judging from the *in vitro* transcription/translation experiments described in the previuos section). Secondly, if $CF_oI$ is not able to functionally replace the *E. coli b*-subunit because the hydrophobic N-terminus of $CF_oI$ is unable to assemble into the membrane with the wild-type *E. coli* subunits, and the hybrid protein is able to functionally replace the *E. coli b*-subunit, this would give valuable information regarding inter-subunit interactions within the $F_1$ sector of the $F_oF_1$-ATPase complex.

This laboratory possesses a plasmid with a 4.5kb fragment carrying the *unc* genes *B, E, F, H* and *A*, inserted into the *Hin*dIII site of the polylinker in M13mp19. Site-directed mutagenesis was carried out on single-stranded DNA of this clone. A restriction site for the enzyme *Kpn*I was introduced into the *uncF* gene, thereby replacing leucine-29 and methionine-30 of the *E. coli b* subunit with glycine and threonine respectively. These residues lie adjacent to the junction between hydrophobic and hydrophilic regions in the *b* subunit amino acid sequence (see Fig 1.3). The mutagenesis was directed by oligonucleotide AR6 (see table 2.1)

Following the mutagenesis procedure, RF DNA was isolated from several independent clones, digested with the enzyme *Kpn*I, and analysed by agarose gel electrophoresis. Several clones showed a single 6.5kb band consistent with a *Kpn*I site having been introduced into the sequence, and one of these was chosen for further work. DNA from this clone was digested with the enzymes *Hin*dIII and *Cla*I, and the 2.2kb fragment carrying

the wild-type *unc* genes *B* and *E* and the mutated *uncF* gene was subcloned into the *Hin*dIII and *Cla*I sites of the vector pAN174 (described in section 3.5 above). This plasmid was named pAN1138.

Oligonucleotide AR7 was constructed with a sequence identical to a region of the *atpF* gene except that a *Kpn*I site was introduced which would result in isoleucine residues at positions 51 and 52 in $CF_OI$ changing to glycine and threonine respectively. These residues lie adjacent to the junction between hydrophobic and hydrophilic regions in the $CF_OI$ amino acid sequence (see Table 2.1).

Using oligonucleotides AR7 and AR6 as primers and pAN573 DNA as template, the polymerase chain reaction was used to amplify a 420bp fragment of the *atpF* gene encoding the 'hydrophilic domain' of $CF_OI$. The amplified fragment was digested with *Kpn*I, and ligated into the *Kpn*I site of pAN1138. Restriction analysis identified a clone with the insert in the correct orientation. The entire hybrid *uncF/atpF* gene was sequenced (see section 2.17) and both portions found to have the correct wild-type sequences, apart from the codons for glycine and threonine created in the course of adding the *Kpn*I site at the junction point of the sequences. This plasmid was named pAN1139 (see Fig 3.5; referred to below in genotypic descriptions as $b/CF_OI$ hybrid), and was used to transform strains AN1440 and AN1521 to create strains AN3805 and AN3806 respectively.

Positive control strains for complementation analysis were constructed by transforming strains AN1440 and AN1521 with plasmid pAN495, which carries the wild-type *unc* genes *B*, *E* and *F* on a 2.2kb fragment cloned into the *Hin*dIII and *Cla*I sites of the vector pAN174. These strains were named AN3818 and AN3819 respectively. Negative control strains were constructed by transforming strains AN1440 and AN1521 with pAN174, creating strains AN3820 and AN3821.

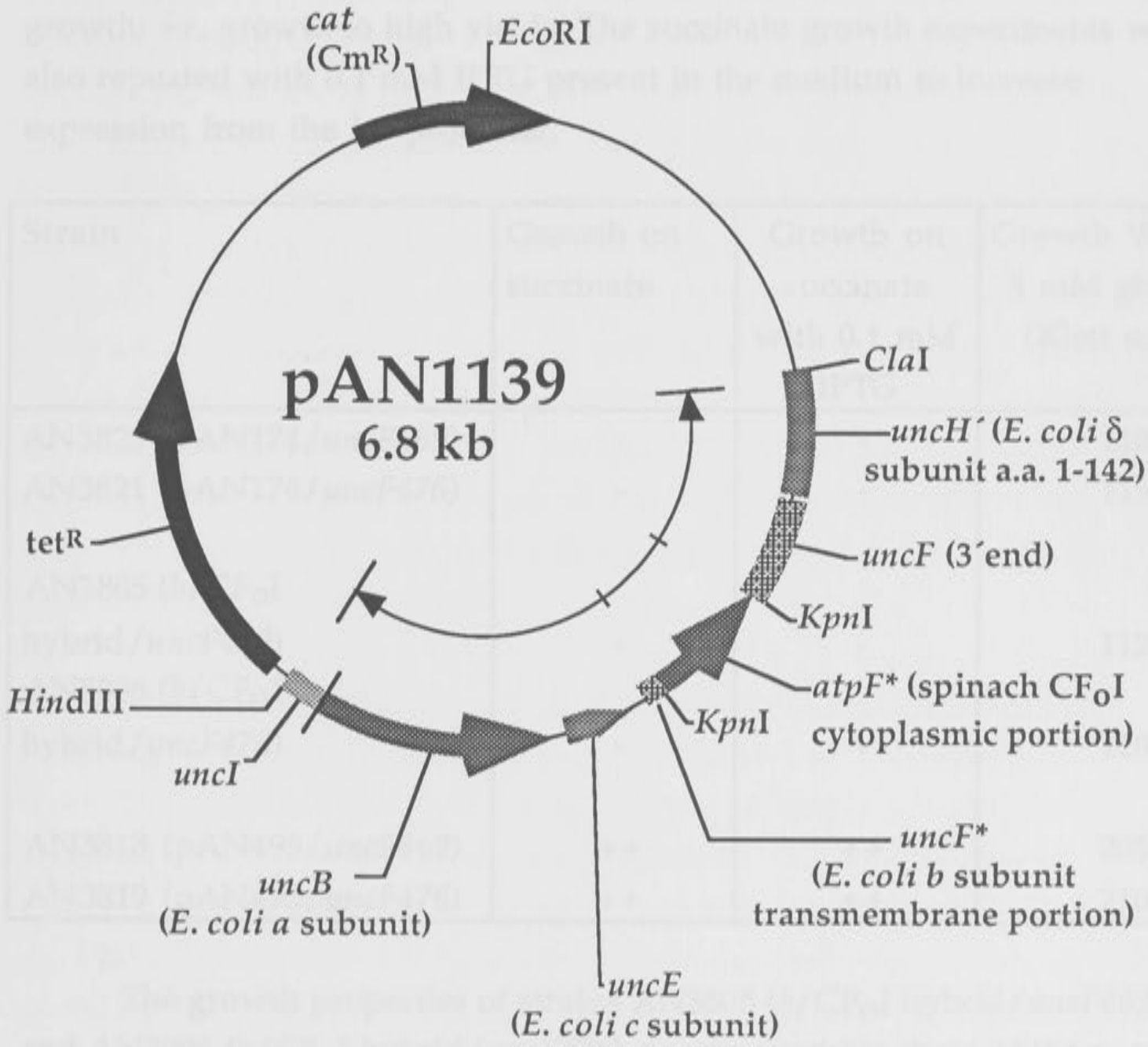


**Figure 3.5:** Plasmid pAN1139, carrying the *E. coli unc* genes *B* and *E*, and a fusion of the *uncF* gene and the spinach chloroplast *atpF* gene. This gene encodes a hybrid protein with the transmembrane domain of the *E. coli b*-subunit and the hydrophilic portion of the spinach chloroplast subunit $CF_0I$.

**3.13 Growth properties of *uncF* mutant strains carrying plasmid pAN1139 (*b*/$CF_oI$ hybrid).**

Measurements of growth yield in limiting (5mM) glucose were carried out using the method described in section 2.5. The abilities of each strain to grow on solid succinate minimal medium are described using the following symbols: -, no growth; +/- , poor but significant growth; +, growth; ++, growth to high yields. The succinate growth experiments were also repeated with 0.1 mM IPTG present in the medium to increase expression from the *lac* promoter:

| Strain | Growth on succinate | Growth on succinate with 0.1 mM IPTG | Growth Yield in 5 mM glucose (Klett units) |
|---|---|---|---|
| AN3820 (pAN174/*uncF469*) | - | - | 110 |
| AN3821 (pAN174/*uncF476*) | - | - | 119 |
| AN3805 (*b*/$CF_oI$ hybrid/*uncF469*) | - | - | 112 |
| AN3806 (*b*/$CF_oI$ hybrid/*uncF476*) | - | - | 118 |
| AN3818 (pAN495/*uncF469*) | ++ | ++ | 205 |
| AN3819 (pAN495/*uncF476*) | ++ | ++ | 210 |

The growth properties of strains AN3805 (*b*/$CF_oI$ hybrid/*uncF469*) and AN3806 (*b*/$CF_oI$ hybrid/*uncF476*) closely resemble those of the negative control strains AN3820 (pAN174/*uncF469*) and AN3821 (pAN174/*uncF476*). These results indicate that the hybrid protein consisting of the *E. coli b* subunit transmembrane portion and the hydrophilic portion of the spinach chloroplast subunit $CF_oI$ cannot replace the *E. coli b*-subunit and assemble with the other *E. coli* subunits to form a functional $F_oF_1$-ATPase.

**3.14 Background to work on the *atpD* gene encoding the δ-subunit of the spinach chloroplast ATP synthase.**

The isolation and sequencing a cDNA clone covering the entire coding region for the δ subunit of the spinach chloroplast ATP synthase was described by Hermans *et.al* (1988). This clone (pSocCF$_1$δ) was made available to this laboratory, providing the opportunity to test whether the spinach chloroplast δ subunit could functionally replace the *E. coli* δ subunit in an appropriate mutant *E. coli* strain. The mature spinach δ subunit and the *E. coli* δ subunit share little sequence identity at the amino acid level (14%), but homology between the subunits is indicated by a highly conserved pattern of secondary structural elements (Hermans *et al.*, 1988).

To test whether the *atpD* gene encoding the spinach δ subunit can complement mutations in the *uncH* gene encoding the *E. coli* δ subunit, an*E. coli* strain carrying a suitable mutation affecting the *uncH* gene is required. The strain used in this work is AN2015, which carries the *uncH241* allele, isolated by Humbert *et al.* (1983). This allele encodes a severely truncated δ-subunit, due to the replacement of the codon for tryptophan-28 by a stop codon.

**3.15 The subcloning and site-directed mutagenesis of the *atpD* gene encoding the δ-subunit of the spinach chloroplast ATP synthase.**

The predicted molecular weight of the precursor of the spinach δ subunit is 27.7kD, which includes a predicted 7.2kD transit peptide involved in the transport of the precursor into the chloroplast (Hermans *et al.*, 1988). It was necessary to modify by site-directed mutagenesis the clone encoding the precursor such that the mature protein could be expressed in *E. coli*:

Firstly, a new methionine initiation codon was introduced at a position corresponding to the known start of the mature protein.

Secondly, a Shine-Dalgarno *E. coli* ribosome binding site was introduced 10-5 bases upstream from the new start site (see section 3.3 above).

Thirdly, because the polymerase chain reaction was to be used in producing a fragment with the mutated sequence, a restriction site was added upstream of the stop codon. The recognition sequence for *Xba*I was chosen for this purpose. Oligonucleotide AR-8 was constructed with a sequence identical to this region except for changes specifying these modifications (see Table 2.1).

Using pSocCF$_1$δ DNA as template, polymerase chain reaction was carried out with oligonucleotide AR8 at the 5′ end of the fragment and the M13 reverse primer at the 3′ end. A 650 bp fragment covering the entire coding region of the modified *atpD* gene was amplified, and digested with the enzymes*Xba*I and*Eco*RI. The fragment was cloned into the *Xba*I and *Eco*RI sites of pUC19 to create plasmid pAN1126 (see Fig 3.6; referred to below in genotypic descriptions as "m.chl.δ"). In this vector the insert is in the correct orientation for the expression of the modified *atpD* gene from the *lac* promoter. The entire modified *atpD* gene carried by plasmid pAN1126 was sequenced as described in section 2.17, and was found to match the published sequence of Hermans *et al.* (1988), apart from the desired directed mutations. Plasmid pAN1126 was used to transform strain AN2015 (*uncH241*) to create strain AN3781.

To serve as a positive control, plasmid pAN1128, which carries the *unc* genes *E, F* and *H* (see section 3.4 above), was used to transform strain AN2015 to create AN3786. To serve as a negative control, pUC18 was used to transform strain AN2015 to create AN3783.

**3.16 Growth properties of strains with the *uncH241* mutant background.**

Measurements of growth yield in limiting (5mM) glucose were carried out using the method described in section 2.5. The abilities of each strain to grow on solid succinate minimal medium are described using the following symbols: -, no growth; +/- , poor but significant growth; +, growth; ++, growth to high yields. The succinate growth experiments were also repeated with 0.1 mM IPTG present in the medium to increase expression from the *lac* promoter:

| Strain | Growth on succinate | Growth on succinate with 0.1 mM IPTG | Growth Yield in 5mM glucose (Klett Units) |
|---|---|---|---|
| AN3783 (pUC18/*uncH241*) | - | - | 112 |
| AN3786 (pAN1128/*uncH241*) | ++ | ++ | 205 |
| AN3781 (m.chl.δ/*uncH241*) | +/- | +/- | 111 |

The ability of strain AN3781 (m.chl.δ/*uncH241*) to grow weakly on solid succinate medium indicates that this strain is able to carry out

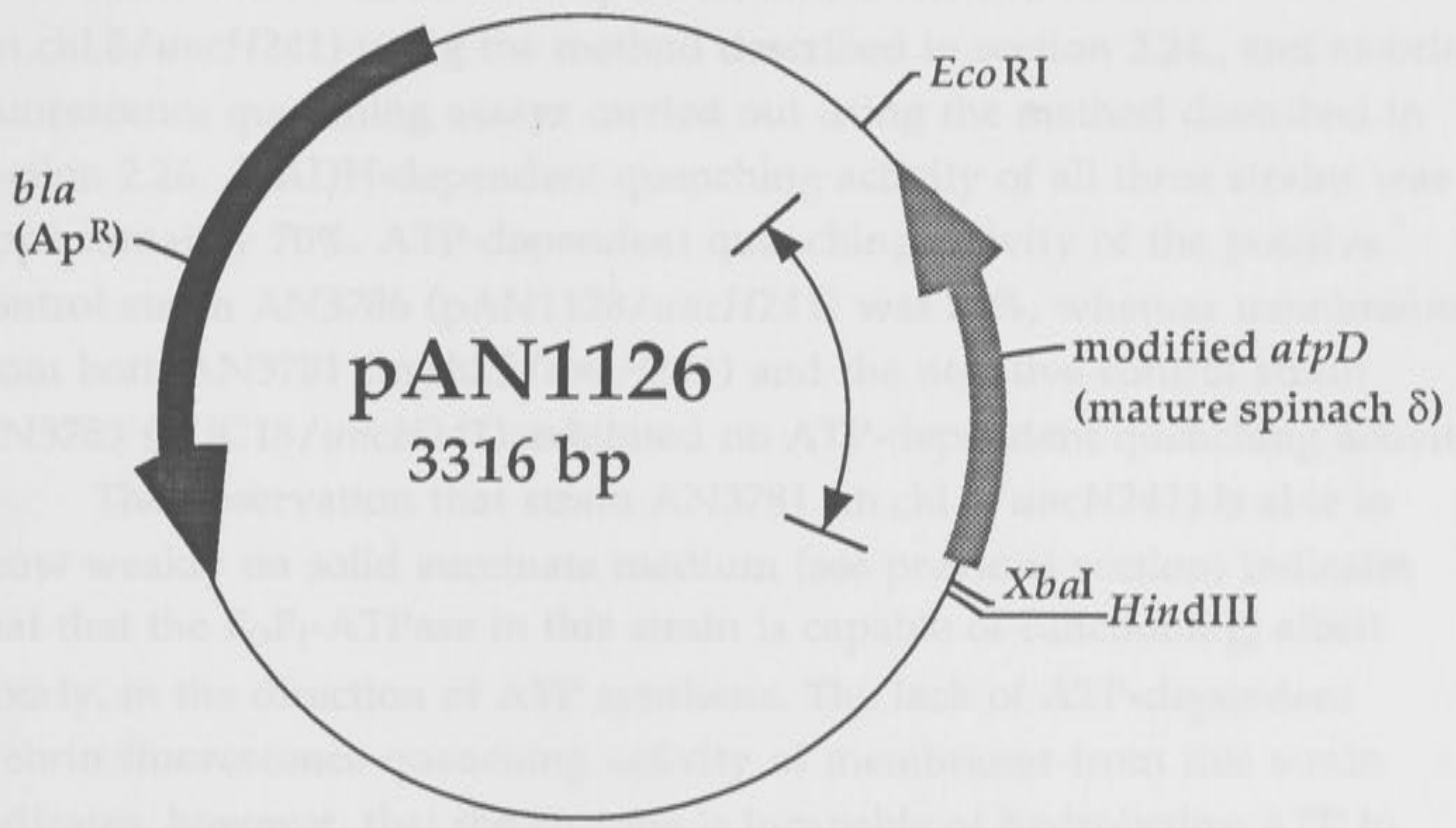


**Figure 3.6:** Plasmid pAN1126, carrying a 650bp fragment with the modified *atpD* gene, encoding the mature form of spinach chloroplast $F_OF_1$-ATPase subunit δ, cloned into the *Xba*I and *Eco*RI sites of pUC19.

oxidative phosphorylation, but growth is impaired in comparison to the wild-type strain AN3786 (pAN1128/*uncH241*). The determinations of growth yield in limiting glucose indicate, however, that this strain is not able to metabolise glucose to produce cell mass any more efficiently than the negative control strain AN3783 (pUC18/*uncH241*).

**3.17 Membrane atebrin fluorescence quenching activities of strains with the *uncH241* mutant background**

Membranes were prepared from strains AN3786 (pAN1128/*uncH241*), AN3783 (pUC18/*uncH241*), and AN3781 (m.chl.δ/*uncH241*) using the method described in section 2.24., and atebrin fluorescence quenching assays carried out using the method described in section 2.26. NADH-dependent quenching activity of all three strains was approximately 70%. ATP-dependent quenching activity of the positive control strain AN3786 (pAN1128/*uncH241*) was 75%, whereas membranes from both AN3781 (m.chl.δ/*uncH241*) and the negative control strain AN3783 (pUC18/*uncH241*) exhibited no ATP-dependent quenching activity.

The observation that strain AN3781 (m.chl.δ/*uncH241*) is able to grow weakly on solid succinate medium (see previous section) indicates that that the $F_OF_1$-ATPase in this strain is capable of functioning, albeit poorly, in the direction of ATP synthesis. The lack of ATP-dependent atebrin fluorescence quenching activity of membranes from this strain indicates, however, that the enzyme is incapable of hydrolyzing ATP to pump protons across the membrane. It is not possible to determine, however, whether the hybrid $F_OF_1$-ATPase complex remains assembled following preparation of membranes, and the lack of ATP-dependent atebrin fluorescence quenching activity may be due to the instability of the hybrid complex in the *in vitro* assay.

**3.18 Background to work on the *atpC* gene encoding the γ-subunit of the spinach chloroplast ATP synthase.**

The isolation and sequencing of a cDNA clone covering the coding region for the mature γ-subunit of the spinach chloroplast ATP synthase were reported by Miki *et al.*, (1988), although cDNA clones covering the coding region for the entire precursor protein were first described by Mason and Whitfeld (1990). These clones were made available to this laboratory, providing the opportunity to test whether the spinach chloroplast γ-subunit could functionally replace the *E. coli* γ-subunit in an appropriate mutant *E. coli* strain.

To test whether the *atpC* gene encoding the spinach γ-subunit can complement mutations in the *uncG* gene encoding the *E. coli* γ-subunit, an*E. coli* strain carrying a suitable mutation affecting the *uncG* gene is required. The strain used in this work is AN1273, which carries the *uncG428* allele, isolated by Downie *et al.*, (1979). The *uncG428* allele has the tryptophan-106 codon of the γ-subunit replaced by the stop codon TGA (D. Webb, personal communication), causing the γ-subunit to be severely truncated. Strain AN1273 is not able to grow on succinate minimal medium, indicating a loss of function of the $F_OF_1$-ATPase.

**3.19 The subcloning and site-directed mutagenesis of the *atpC* gene.**

Two spinach cDNA clones covering the coding region for the entire γ-subunit precursor were generously supplied by Dr. Paul Whitfeld (CSIRO, Canberra) for this work, each inserted into the *Eco*RI site of pUC18. When joined the clones cover a region from 5 bases upstream from the initiation methionine of the γ-subunit precursor to 222 bases downstream of the stop codon, a total of 1325bp (see diagram). The plamid carrying the insert with bases 1 to 857 was designated γA/pUC18, and the plasmid carrying the insert with bases 858 to 1325 was designated γB/pUC18.

The plasmid γB/pUC18 was cut with the restriction enzyme *Eco*RI, and the γ subunit gene fragment was subcloned into the *Eco*RI site of M13 mp19 RF DNA. Restriction analysis identified a clone with the insert in the correct orientation for the vector to produce single-stranded DNA of the complementary strand of the γ-subunit gene fragment. This clone was designated γBmp19.

To facilitate the subcloning of the *Eco*RI/*Eco*RI fragment carrying the 5′end of the γ subunit gene, the removal by site-directed mutagenesis of the *Eco*RI site at the 3′end of the fragment carried by γBmp19 was required. For

this purpose, oligonucleotide AR9 was constructed with a sequence identical to this region except that the G at the 5′end of the *Eco*RI recognition sequence was changed to A (see Table 2.1). Following the mutagenesis reactions, RF DNA was prepared from several isolates, digested with the enzyme *Eco*RI and analysed by agarose gel electrophoresis. A clone which gave a single band size of 7.7 kb was identified, consistent with an *Eco*RI site having been removed. Single-stranded DNA was prepared, and the clone was sequenced with the M13 reverse primer. Analysis of the sequence confirmed that the *Eco*RI site which had been at the 3′ end of the insert had been removed as expected. This clone was designated γBmp19:91-20.

The plasmid γA/pUC18 was cut with *Eco*RI, and the fragment carrying the 5′ end of the γ-subunit gene was subcloned into the *Eco*RI site of γBmp19:91-20 using methods described in section 2.10. Restriction analysis identified a clone with the fragment carrying the 3′ end of the gene inserted downstream and in the same orientation as the 5′ end of the gene already present in the vector. This clone now carried the entire coding region for the precursor protein of the γ-subunit gene in a single continous fragment, and was designated γmp19:AR9.

**3.20 Mutagenesis of the γ-subunit of the spinach chloroplast ATP synthase using polymerase chain reaction and subcloning of the amplification product.**

The predicted molecular weight of the precursor of the γ-subunit is 40 kD, which includes a 4kD transit peptide involved in the transport of the precursor into the chloroplast (Mason and Whitfeld, 1990). There is no known mechanism by which the bacterium *E. coli* could cut the precursor specifically to yield the mature γ-subunit found in the spinach chloroplast. It was therefore necessary to modify by site-directed mutagenesis the clone encoding the precursor such that the mature protein could be expressed in *E. coli*. Three modifications were necessary:

Firstly, a new methionine initiation codon was introduced at a position corresponding to the known start of the mature protein.

Secondly, the concensus Shine-Dalgarno *E. coli* ribosome binding site was introduced 10-5 bases upstream from the new start site (see section 3.3 above).

Thirdly, because the polymerase chain reaction was to be used in producing a fragment with the mutated sequence, a restriction site was added upstream of the stop codon. The recognition sequence for *Sph*I was

chosen for this purpose. Oligonucleotide AR10 was constructed with a sequence identical to this region except for changes indicated (see Table 2.1). Using γmp19:AR9 DNA as template, polymerase chain reaction was carried out with oligonucleotide AR10 as the 5′ end primer and the M13 reverse primer at the 3′ end. A 1.1kb fragment covering the entire coding region of the modified *atpC* gene was amplified, and digested with the enzymes *Sph*I and *Bam*HI. The fragment was cloned into the *Sph*I and *Bam*HI sites of pUC19, to create plasmid pAN1131 (see Fig. 3.7; referred to below in genotypic descriptions as "m.chl.γ"). The entire modified *atpC* gene carried by plasmid pAN1131 was sequenced. The sequence matched that published by Mason and Whitfeld (1990), apart from the desired directed mutations. Plasmid pAN1131 was used to transform strain AN1273 to create strain AN3793.

**3.21 Construction of positive and negative control strains for complementation analysis with the *uncG* mutant strain AN1273.**

To serve as a positive control for complementation analysis with the *uncG* mutant strain AN1273, a plasmid was constructed carrying the wild-type *uncG* gene in the vector pUC19. Plasmid pAN734 carries the *uncG* gene downstream of the *uncC* gene (encoding the *E. coli* ε subunit) fused to the gene for glutathione-*S*-transferase from *Schistosoma japonicum*. This plasmid was digested with the enzymes *Bam*HI and *Eco*RI, and the resulting fragments were separated by agarose gel elecrophoresis. The 1.4kb fragment carrying the *uncC* and *uncG* genes was excised from the gel, and subcloned into the *Bam*HI and *Eco*RI sites of the vector pUC19 using the method described in section 2.10. This plasmid was named pAN1130, and used to transform strain AN1273 to create strain AN3792.

To serve as a negative control for complementation analysis with the *uncG* mutant strain AN1273, the vector pUC19 was used to transform this strain to create strain AN3791.

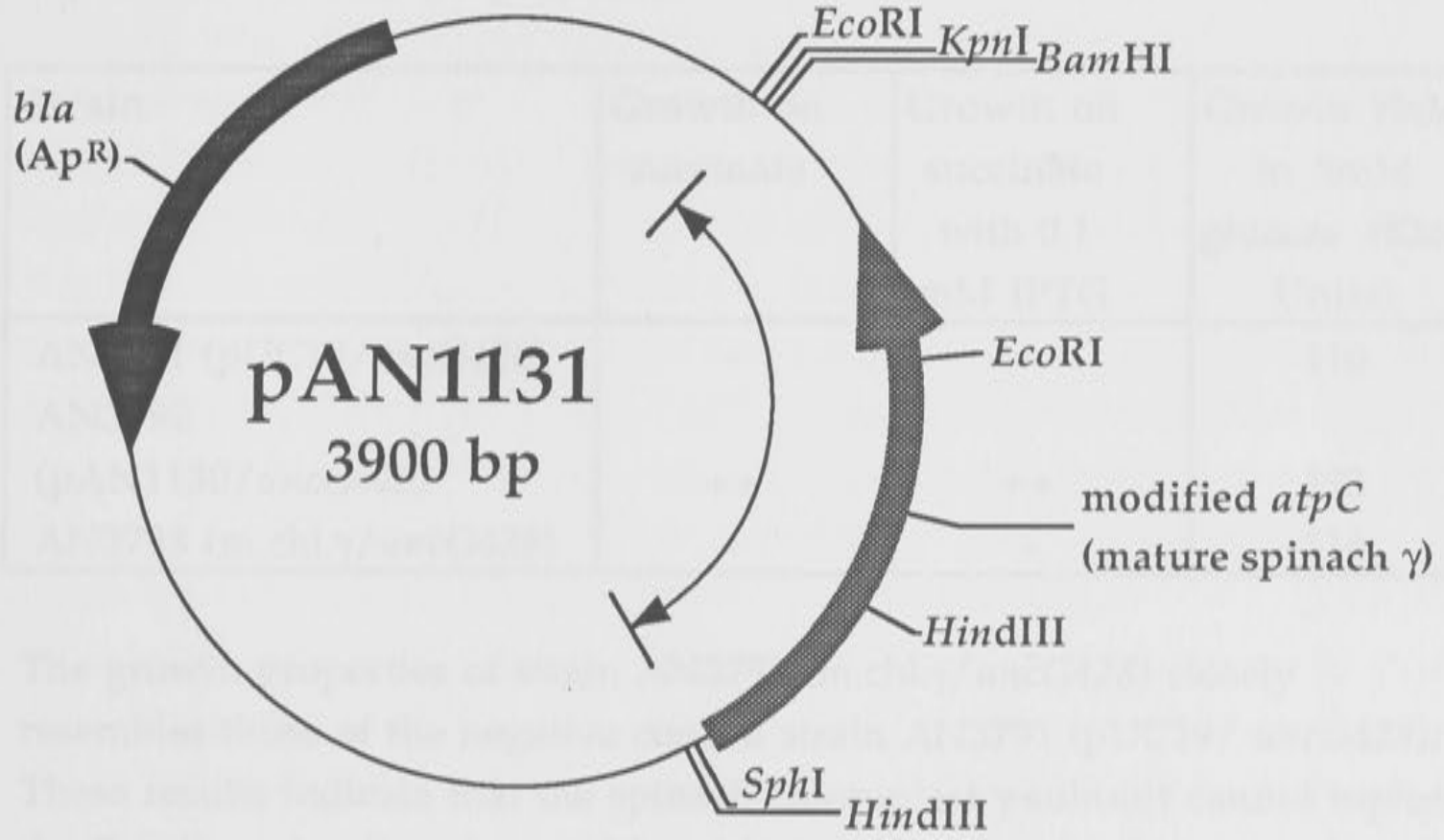


**Figure 3.7:** Plasmid pAN1131, carrying a 1.1kb fragment with the modified *atpC* gene, encoding the mature form of the spinach chloroplast $F_OF_1$-ATPase γ subunit, cloned into the *Sph*I and *Bam*HI sites of pUC19.

**3.23 Growth properties of the strains AN3791 (pUC19/*uncG428*), AN3792 (pAN1130/*uncG428*) and AN3793 (m.chl.γ/*uncG428*)**

Measurements of growth yield in limiting (5mM) glucose were carried out using the method described in section 2.5. The abilities of each strain to grow on solid succinate minimal medium are described using the following symbols: -, no growth; +/- , poor but significant growth; +, growth; ++, growth to high yields. The succinate growth experiments were also repeated with 0.1 mM IPTG present in the medium to increase expression from the *lac* promoter:

| Strain | Growth on succinate | Growth on succinate with 0.1 mM IPTG | Growth Yield in 5mM glucose (Klett Units) |
|---|---|---|---|
| AN3791 (pUC19/*uncG428*) | - | - | 110 |
| AN3792 (pAN1130/*uncG428*) | ++ | ++ | 193 |
| AN3793 (m.chl.γ/*uncG428*) | - | - | 114 |

The growth properties of strain AN3793 (m.chl.γ/*uncG428*) closely resembles those of the negative control strain AN3791 (pUC19/ *uncG428*). These results indicate that the spinach chloroplast γ-subunit cannot replace the *E. coli* γ-subunit and assemble with the other *E. coli* subunits to form a functional $F_OF_1$-ATPase, confirming the observation of Lill *et al.* (1993).

### 3.24 Discussion

The findings that neither of the spinach chloroplast subunits $CF_oI$ nor $CF_oII$ are able to functionally replace the *E. coli b*-subunit corrects a report in the literature in which it was claimed that CFoI was able to replace the b-subunit in the *E. coli* $F_oF_1$-ATPase. The very low levels of sequence homology between the three subunits in any pairwise comparison suggest that functional replacement is unlikely. A heterodimer of $CF_oI$ and $CF_oII$ appears to carry out the same function in the chloroplast $F_oF_1$-ATPase complex as the *b*-subunit homodimer in the *E. coli* complex (Glaser and Norling, 1991). This may mean that during the course of evolution, compensating mutations in $CF_oI$ and $CF_oII$ may allow these subunits to assemble correctly when both present but may prevent either of them individually replacing the *E. coli b*-subunit in a functional complex. This was the case with $CF_oI$ even when the N-terminal transmembrane domain was replaced with the equivalent *E. coli b*-subunit sequence to assist correct packing of $CF_oI$ with the *E. coli a*- and *c*-subunits in the membrane. Results from *in vitro* transcription/translation analysis suggest that proteases present in the S30 *E. coli* cell extract may cleave $CF_oI$. It is possible that proteolysis of $CF_oI$ also occurred in the *E. coli* cells used in complementation analysis, and that the full length protein did not have a chance to assemble with the *E. coli* subunits. It is therefore difficult to assess the inherent ability of $CF_oI$ to functionally substitute for the *E. coli b*-subunit.

Results show that a combination of $CF_oI$ and $CF_oII$ is not able to replace the *b*-subunit heterodimer. This may be due to the inability of the N-terminal domains of $CF_oI$ and $CF_oII$ to pack correctly with the *E. coli a*- and *c*-subunits in the membrane, to disrupted interactions between the cytoplasmic domains and $F_1$ subunits, or to proteolysis of $CF_oI$ as previously discussed. An experiment is planned in which a fusion of the *E. coli b*-subunit N-terminal transmembrane domain with the $CF_oII$ cytoplasmic domain is to be expressed with the fusion of the *E. coli b*-subunit transmembrane domain with the $CF_oI$ cytoplasmic domain. This experiment may provide information as to whether disrupted interactions between the cytoplasmic domains and the *E. coli* $F_1$ subunits are responsible for the failure of the complementation experiments.

Results presented above indicate the spinach chloroplast δ-subunit is barely able to replace the equivalent *E. coli* subunit. The *uncH* mutant strain carrying the gene for the chloroplast δ-subunit is able to grow only weakly on succinate as sole carbon source, does not catabolise glucose to produce

cell mass any more efficiently than the negative control strain, and membranes do not exhibit ATP-dependent atebrin fluorescence quenching activity. The observation that *E. coli* δ-subunit is able to partially replace the chloroplast δ-subunit in reconstitution experiments with δ-depleted $CF_1$, but not *vice versa* (Engelbrecht *et al.*, 1989), indicates that the chloroplast δ-subunit does not easily assemble with *E. coli* $F_1$ subunits. The partial success of genetic complementation experiments suggests, however, that some chloroplast δ-subunit is able to assemble with *E. coli* subunits during *de novo* synthesis of the enzyme complex *in vivo*.

The results reported by Lill *et al.* (1993), which also show that the spinach chloroplast δ-subunit was found to poorly substitute for the *E. coli* δ-subunit, reveal that expression levels are important to the outcome of complementation analysis. In these studies, genes for all five $F_1$-ATPase subunits from spinach chloroplast and the cyanobacterium *Synechcystis* sp. PCC 6803 were subcloned into pJLA expression vectors containing λ $p_R p_L$ promoters in tandem (Schauder *et al.*,1987). The promoters are controlled by a temperature-sensitive repressor (cIts857), which allows expression levels to be controlled by alterations in incubation temperature. Transcriptional initiation is very effectively repressed at 28-30°C, while full induction is achieved at 42°C (Schauder *et al.*,1987). The α-, δ- and ε-subunits from both sources were able to complement the corresponding mutant *E. coli* subunits, although no complementation was observed with γ-subunits from either source. Interestingly, the chloroplast δ-subunit was better able to complement at lower temperatures, indicating that excessive expression was deleterious to the cell. Similarly, low-level expression of the spinach chloroplast β-subunit allowed this protein to be expressed in soluble form in *E. coli*, resulting in complementation of an *uncD* deletion mutation, whereas high-level expression yielded entirely insoluble protein incapable of complementation (Chen *et al.*, 1995). The spinach chloroplast β-subunit had previously been shown not to complement an *uncD* mutation when expressed from a pUC vector (Munn *et al.*, 1991). These results highlight the advantages of carrying out complementation analysis using vectors from which the expression of foreign proteins may be easily controlled, so that a variety of different expression levels may be tested.

The high resolution crystal structure of the bovine mitochondrial $F_1$ shows that the γ-subunit occupies a central position within the $F_1$ complex, and appears to move extensively within a tight cavity during catalysis (Abrahams *et al.*, 1994). The γ-subunit is likely to have a large number of

contact points with other subunits. The structure and function of $F_1$ may therefore be particularly sensitive to alterations in size and shape of the γ-subunit. The chloroplast γ-subunit shares only 33% sequence homolgy with the equivalent *E. coli* subunit, and has an extra domain responsible for redox modulation which is absent in the *E. coli* subunit (see section 1.4.5 above). The chloroplast subunit is almost 5 kD larger than the *E. coli* subunit, and the extra size might be expected to sterically hinder the packing of subunits within the *E. coli* $F_1$. These factors may explain the failure of the spinach chloroplast γ-subunit to complement in the *uncG* mutant *E. coli* strain.

# CHAPTER 4

# STUDIES ON SPINACH CHLOROPLAST AND *SYNECHOCOCCUS* R2 ATP SYNTHASE SUBUNITS EXPRESSED AS FUSION PROTEINS WITH GLUTATHIONE-*S*-TRANSFERASE

## 4.1 Introduction

The aim of work described in this chapter was to investigate interactions between subunits of the $F_OF_1$-ATPases from chloroplasts and cyanobacteria, with the goal of better understanding the quaternary structure of the complex. As discussed in Chapter 1 of this thesis, the subunit architecture of the enzyme is directly relevant to the mechanism of catalysis and its coupling to proton transport across the membrane. The identification of inter-subunit interactions therefore provides valuable information from which structure and function models may be constructed.

The rotational model proposed by Cox *et al.* (1986) for the mechanism of the *E. coli* $F_OF_1$-ATPase requires that defined interactions occur between particular subunits. Specifically, the minor subunits of the $F_1$ ($\gamma$, $\delta$ and $\varepsilon$) are proposed to interact with the polar domain of the *b*-subunit, which is predicted to extend away from the cytoplasmic face of the membrane (Senior, 1983). Experiments described in this chapter involve the co-expression of the homologues of these subunits from spinach chloroplast and the cyanobacterium *Synechococcus* R2, either alone or in combination. Co-purification of proteins expressed together would then constitute evidence for specific interaction between them *in vivo*.

Structure/function studies of proteins and protein complexes require that the proteins of interest be produced in large amounts whilst retaining native structure, and be amenable to rapid and efficient purification using non-denaturing methods that do not expose the proteins to degradation.

The over-expression of genes from recombinant plasmids in *E. coli* provides a method for producing large amounts of protein, although incorrect folding and degradation by proteolytic enzymes which recognise abnormal proteins prevent useful amounts of the native protein from being purified in some cases (Marston, 1986). One method of overcoming the lability of proteins over-expressed in *E. coli* has been to fuse the gene of interest to another which is known to produce a stable product (Marston, 1986). Examples of this have included the expression of polypeptides as fusions with all or part of the *lacZ* gene encoding *E. coli* β-galactosidase (Gray *et al.*, 1982; Koenen *et al.*, 1982; Rüther and Müller-Hill, 1983), and all or part of the *trpE* gene encoding anthranilate synthase (Kleid *et al.*, 1981; Stanley and Luzio, 1984). The technique of producing fusion proteins provides an additional advantage when the properties of the second component allow the fusion product to be easily purified by affinity chromatography (Nilsson *et al*, 1985; Marston *et al.*, 1986), and where the protein of interest may be specifically cleaved from the second component, allowing its isolation (Nagai and Thogersen, 1984; Marston *et al.*, 1986; Smith and Johnson, 1988).

This chapter describes the attempted expression and purification of spinach chloroplast and *Synechococcus* R2 ATP synthase subunits, fused to the C-terminus of Sj26, the enzyme glutathione-S-transferase of the parasitic helminth *Schistosoma japonicum* (Smith *et al*, 1986; 1988). Derivatives of the plasmid pGEX, developed by Smith and Johnson (1988), were used in these experiments. The pGEX plasmids contain the *tac* promoter (Amman *et al.*, 1983; De Boer *et al.*, 1983), followed by the complete coding sequence for Sj26 (Smith *et al.*, 1986; 1987). In the pGEX-2 series plasmids, the normal termination codon is replaced by a polylinker containing unique recognition sites for *Bam*HI, *Sma*I (*Xma*I) and *Eco*RI, and followed by TGA termination codons in all three reading frames. Plasmids of the pGEX-4 series are identical except that the polylinker contains unique recognition sites for *BamHI*, *Eco*RI, *Sma*I (*Xma*I), *Sal*I, *Xho*I and *Not*I. In both cases, the region immediately upstream of the polylinker encodes the thrombin recognition sequence from bovine factor XIII, -Leu-Val-Pro-Arg-Gly- (Mikuni *et al.*, 1973; Nakamura *et al.*, 1974; Chang, 1985). The cloning of a gene of interest into the polylinker in the correct reading frame therefore gives rise to a plasmid capable of expressing a thrombin cleavable fusion protein. All pGEX plasmids also contain the ampicillin resistance ($Ap^R$) gene encoding β-lactamase, *ori* (the pBR322 origin of replication) and a fragment of the *lac* operon containing the over-expressed *lacI*$^q$ allele of the *lac* repressor and part of *lacZ*. The presence in pGEX vectors of the *lacI*$^q$ allele

allows transformation of the plasmid into a variety of *E. coli* host strains, including those lacking the *lacI*$^q$ allele on their chromosomes, and maintaining of effective repression of transcription from the *tac* promoter until such time as a *lac* inducer such as IPTG is added to the *E. coli* culture (Messing, 1983).

It has been found that fusion proteins expressed from the pGEX plasmids are usually resistant to *in vivo* proteolytic degradation and are often found in the soluble fraction of lysed cells, but these characteristics often depend on the nature of the introduced component of the fusion system (Smith and Johnson, 1988; Koland *et al.*, 1990). A major advantage of producing GST fusion proteins is they are easily purified from cell lysates using affinity chromatography on immobilised reduced glutathione. If desired, the fusion protein may then be eluted competitively from the affinity medium with free reduced glutathione (Smith and Johnson, 1988), a process which is mild and may be achieved under physiological conditions of pH and ionic strength. The eluted protein may then be incubated with thrombin to yield free GST and the protein of interest. Alternatively, thrombin may be added directly to the affinity medium to which the fusion protein is bound. The fusion protein is then cleaved, and the protein of interest may be separated from the affinity medium whilst leaving free GST bound to the affinity medium.

The mild conditions under which GST-fusion proteins may be purified make the pGEX system ideal for the study of protein-protein interactions in *E. coli*. In these studies, genes encoding other proteins of interest, along with appropriate translation signals, are cloned into one or more of the restriction enzyme sites in the polylinker, downstream of the gene encoding the fusion protein. Upon induction, these genes may then be expressed at high levels from the *tac* promoter, along with the gene for the fusion protein. The fusion protein may then be purified as described above, and analysed to determine whether any of the other gene products co-purify with it. This technique has been successfully used in this laboratory to purify a complex of the γ- and ε-subunits of the *E. coli* $F_OF_1$-ATPase (Cox *et al.*, 1993). In these studies, a GST-γ-subunit fusion was expressed along with the ε-subunit, and the two proteins co-purified as a complex.

The *Schistosoma japonicum* GST enzyme exists as a stable dimer when expressed in *E. coli* (G. B. Cox, personal communication), but interaction between the GST moieties of fusion proteins expressed from pGEX vectors is likely to be sterically hindered by the presence of the introduced protein moiety. If dimerization is an important factor in the

stability of GST expressed in *E. coli* , the presence of a second unfused GST molecule may assist stabilization of GST fusion proteins expressed in the pGEX system. Experiments carried out in this laboratory have shown that the use of a modified form of the pGEX vectors not available from the commercial supplier improves the solubility of GST-fusion proteins in many cases. The modified pGEX vectors possess a second copy of the Sj26 GST gene, preceded by it's own *tac* promoter, cloned into restriction sites downstream of the GST gene to which introduced genes of interest are fused (details of construction are described below). When the influenza virus membrane proteins M2 and NB are expressed as GST fusion proteins from unmodified pGEX vectors in *E. coli*, the fusion proteins precipitate with the cell debris following disruption of the cells. When, however, the same proteins are expressed from modified pGEX vectors with the second copy of the GST gene, the proteins localize almost exclusively in the membrane fraction (N. Sunstrom, personal communication). When expressed as a GST fusion protein from the unmodified pGEX-2T vector, an extramembranous portion of the α-subunit of the human $GABA_A$ receptor precipitates with the cell debris following disruption of the cells, and cannot be solubilised with non-denaturing detergents. Expressed from the modified pGEX vector, however, the fusion protein precipitates with the cell debris, but may easily be solubilised with the detergent Triton X-114 (L. Tierney, personal communication). Given the apparent benefits to the stability of GST fusion proteins of having a second GST gene expressed from the plasmids, modified pGEX vectors were extensively used for the later experiments described in this work.

As discussed in section 1.3.4 above, differences in the efficiency of translation initiation at different sites in the *E. coli unc* operon appear to play an important role in determining the relative amounts of $F_OF_1$-ATPase subunits that are synthesized (McCarthy *et al.*, 1985). Measurement of the rates of synthesis of cloned genes encoding the *c*, *b* and δ subunits of the *E. coli* $F_OF_1$-ATPase show that the rate of synthesis of subunit *c* is at least six times that of subunit *b*, and 18 times that of subunit δ. Maximal expression of the *uncE* gene, encoding the *c* subunit, is dependent on the presence of a sequence of approximately 30bp upstream of the ATG initiation codon, and thus appears to enhance the rate of translation initiation (McCarthy *et al.*, 1985). This is consistent with the observation that the *c* subunit is present in approximately 10 copies per $F_OF_1$-ATPase complex, whilst the *b* subunit and δ subunit are present in only two copies and one copy per complex respectively (Foster and Fillingame, 1982). Vectors have been described

which incorporate the *uncE* pregenic region to enhance the efficiency of translation of recombinant proteins in *E. coli* (Schauder *et al.*, 1987). In order to maximise the level of translation of proteins to be co-expressed with GST fusion proteins from pGEX vectors, the 30bp *uncE* pregenic region was inserted immediately upstream of their respective genes wherever possible. This was aimed at maximising the potential for the fusion and other expressed proteins to interact *in vivo*, and for protein-protein complexes to be successfully purified.

The background strain used in all experiments is AN3347 (pESL/ *lacZ(am) trp(am) pho(am) supC$^{ts}$ rpsL mal(am))*, which contains the plasmid pESL, obtained originally as a kind gift from Dr. George Lorimer, Du Pont Corporation. This plasmid carries genes for the *E. coli* heat-shock proteins (chaperonins) groES and groEL, under the control of the *lac* promoter (Goloubinoff *et al.*, 1989). Co-expression of these proteins was shown to be required for the correct assembly of *Anacystis nidulans* ribulose bisphosphate carboxylase oligomers expressed in *E. coli* (Goloubinoff *et al.*, 1989), and was included in the background strain to maximise the possibility of correct folding of the foreign proteins to be expressed.

## EXPRESSION OF SPINACH CHLOROPLAST ATP SYNTHASE SUBUNITS AS FUSION PROTEINS WITH GLUTATHIONE-*S*-TRANSFERASE

### 4.2 Background to studies on the γ- and ε-subunits of the spinach chloroplast $F_OF_1$-ATPase.

The γ- and ε-subunits of the spinach chloroplast $F_1$-ATPase are known to interact (Feng and McCarty, 1990; Soteropoulos *et al.*, 1992; Soteropoulos *et al.*, 1994). The nature and strength of this interaction is central to the mechanism of light regulation of the chloroplast $F_OF_1$-ATPase *in vivo* (see section 1.4.5 and McCarty, 1992). The γ- and ε-subunits of the *E. coli* $F_1$-ATPase interact strongly *in vitro* (Dunn, 1982). Cox *et al.* (1993) expressed a fusion of GST and the *E. coli* γ-subunit with the *E. coli* ε-subunit, and showed that the ε-subunit co-purified with the fusion. Part of the work described in this chapter involves the construction of plasmids expressing genes for these subunits from spinach chloroplast, and the attempted purification of a γ/ε complex. The purified complex could then be analysed using a variety of techniques including circular dichroism spectroscopy, analytical ultracentrifugation and X-ray crystallography with the aim of determining structure. Because the redox state of reactive thiols in the γ-subunit affect the nature of interaction with the ε-subunit (McCarty, 1992), comparisons between physical properties of the complex under reducing and non-reducing conditions would be particularly informative.

### 4.3 Construction of a plasmid co-expressing a GST-spinach chloroplast ε fusion with the spinach chloroplast γ-subunit.

*i) Subcloning of the modified atpC gene into pAN787*: The plasmid described in this section was derived from the vector pAN787, constructed by L. Tierney in this laboratory. This vector has a 30bp *Bam*HI-*Eco*RI fragment, carrying a modified *uncE* pregenic region inserted into the *Bam*HI and *Eco*RI sites of the vector pGEX-2T. This insert differs from the wild-type *uncE* pregenic region only in that the *Eco*RI recognition sequence GAATTC occupies the last six bases of the sequence.

Plasmid pAN1131 contains a 1.1 kb fragment carrying the entire coding sequence for the modified *atpC* gene, encoding the mature γ-subunit of the spinach chloroplast $F_OF_1$-ATPase, inserted into the *Sph*I and *Bam*HI sites of the vector pUC19 (see section 3.20). For insertion into the vector pAN787 immediately downstream of the *uncE* pregenic region, an *Eco*RI site is required in the six bases immediately preceding the ATG start codon for the mature γ subunit. The presence, however, of an *Eco*RI site within the

modified *atpC* coding region, 723 bases downstream of the ATG start codon, complicates the subcloning of the fragment. A two-step process employing the polymerase chain reaction was used to remove the *Eco*RI site. Oligonucleotide AR11 was designed with a sequence identical to the region from 24 bases upstream of the start codon to 16 bases into the gene, except that the recognition sequence for *Eco*RI, GAATTC, is introduced in the six bases immediately upstream of the start codon. Oligonucleotide AR12 was designed with a sequence complementary to the region from 9 bases upstream from the TGA stop codon to 26 bases downstream from the stop codon, except that the recognition site for *Eco*RI is introduced in the bases 6 to 12 bases downstream of the stop codon. Two oligonucleotides of complementary sequence, AR13 and AR14 were designed with a sequence straddling the internal *Eco*RI site, except that base 725 of the gene (A) is changed to G. This alters codon 241 from GAA to GAG, thus retaining glutamate as the amino acid at this position.

Using plasmid pAN1131 as template and oligonucleotides AR11 and AR14 as primers, polymerase chain reaction was carried out with *Pfu* polymerase to amplify a 768bp fragment encoding the 5′ end of the *atpC* gene. Using the same template and polymerase, oligonucleotides AR13 and AR12 were then used to amplify a 283bp fragment encoding the 3′ end of the gene. The two amplification products were purified as described in section 2.13., mixed along with primers AR11 and AR12, heated to 94° C, and cooled slowly to allow annealing of complementary regions at the ends of the fragments. Species where the region at the 3′ end of the coding strand of the large fragment have annealed to the region at the 3′ end of the complementary strand of the small fragment may then serve as templates for the synthesis of full length (~1.05kb) fragments encoding the entire modified *atpC* gene, with the desired mutations removing the internal *Eco*RI site, and placing *Eco*RI sites at the 3′ and 5′ ends of the gene. In the presence of primers AR11 and AR12, the full length fragment was amplified. This fragment was digested with the enzyme *Eco*RI, and subcloned into the *Eco*RI site of plasmid pAN787. Restriction analysis identified a clone with the insert in the correct orientation for the *atpC* gene to run in the same direction as the gene for GST. This plasmid was named pAN1132.

*ii) Subcloning of the atpE gene into plasmid pAN1132:* Plasmid pAN420, constructed by A. Munn in this laboratory, contains a 580 bp fragment carrying the entire coding sequence for the *atpE* gene, encoding the ε-subunit of the spinach chloroplast $F_OF_1$-ATPase, inserted into the *Pst*I and

*Bam*HI sites of the vector pUC9. This plasmid was digested with the enzymes *Pst*I and *Bam*HI, and the 580bp fragment cloned into the *Pst*I and *Bam*HI sites in the vector M13 mp18, using the method described in section 2.10. Single-stranded DNA was isolated from a single isolate. Using this DNA as template, site-directed mutagenesis was carried out with oligonucleotide AR15 as mutagenic primer, as described in section 2.16. This oligonucleotide directs the alteration of six bases immediately upstream of the ATG start site for the *atpE* gene, creating a recognition site for the enzyme *Bam*HI. Restriction analysis and DNA sequencing identified a clone with a *Bam*HI site introduced at the desired position. The clone was named M13mp18ε:AR15.

RF DNA from clone M13mp18ε:AR15 was digested with the enzyme *Bam*HI, and the 580bp fragment carrying the *atpE* gene was subcloned into the *Bam*HI site of plasmid pAN1132. Restriction analysis identified a clone with the *Bam*HI-*Bam*HI fragment inserted in the correct orientation into the vector for expression of the GST-ε fusion protein. This plasmid, which carries genes for the GST-ε fusion and the gene for the γ-subunit, was named pAN974 (see Figure 4.1), and used to transform strain AN3347 to create strain AN3830.

**4. 4 Analysis of the expression of the GST-spinach ε-subunit fusion and spinach γ-subunit from plasmids pAN787, pAN1132 and pAN974 using *in vitro* transcription/ translation.**

The expression of proteins from plasmids pAN787, pAN1132 and pAN974 was analysed using *in vitro* transcription/translation, as described in section 2.20. The gel autoradiographs from these experiments are shown in Figure 4.2. Plasmid pAN1132, carrying the gene for the mature γ-subunit but not the GST-ε fusion, expresses at very low levels a protein of approximately 36 kDa which is not expressed from plasmid pAN787. This is the approximate molecular mass of the spinach γ-subunit. The gel lane corresponding to plasmid pAN974, which carries genes for both the GST-ε fusion and the γ-subunit, shows proteins of approximately 40 kDa (the approximate size of the GST-ε fusion). A protein of the same molecular mass (~36 kDa) as that expressed from pAN1132 is also present, but appears to be present at a much higher level. This result suggests that the presence of the GST-ε fusion protects the γ-subunit from degradation by proteolytic enzymes that are presumably present in the *E. coli* S30 extract used in the *in vitro* transcription/ translation reactions, which is indicative of an interaction between the two proteins. Some degradation of the GST-ε-fusion

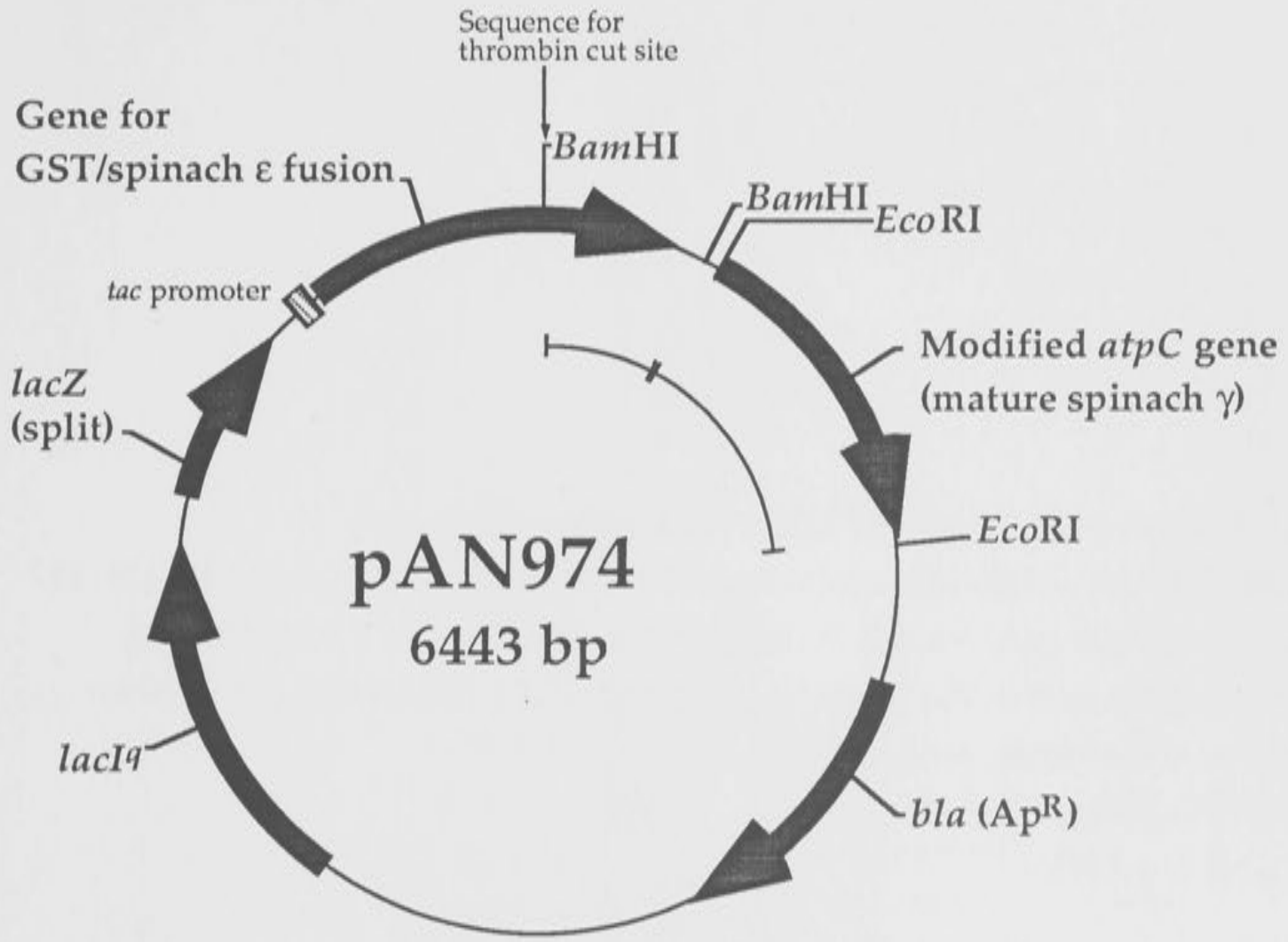


**Figure 4.1**: Plasmid pAN974, carrying the gene encoding a fusion protein of GST and the spinach chloroplast $F_OF_1$-ATPase ε-subunit, with the modified *atpC* gene encoding the mature γ-subunit. The *E. coli uncE* pregenic region occupies the 30 bases immediately upstream of the modified *atpC* gene.

**Figure 4.2**: Autoradiographs of SDS-PAGE gels with *in vitro* transcription/translation products from the vector pAN787, plasmid pAN1132 (which carries the gene for the mature spinach chloroplast γ-subunit) and pAN974 (which carries the genes for both the GST-ε fusion and the γ-subunit).

(a) Lane 1: Molecular weight markers
Lane 2: pAN787
Lane 3: pAN1132

(b) Lane 1: Molecular weight markers
Lane 2: pAN787
Lane 3: pAN974

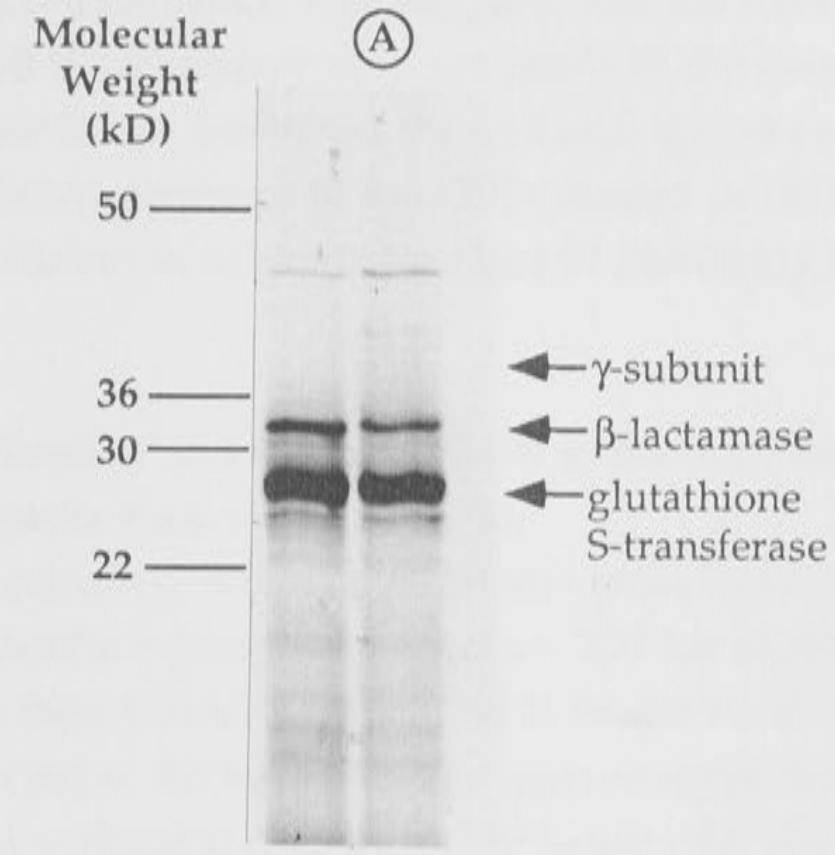
Molecular Weight (kD)
A
50
36
30
22
γ-subunit
β-lactamase
glutathione S-transferase

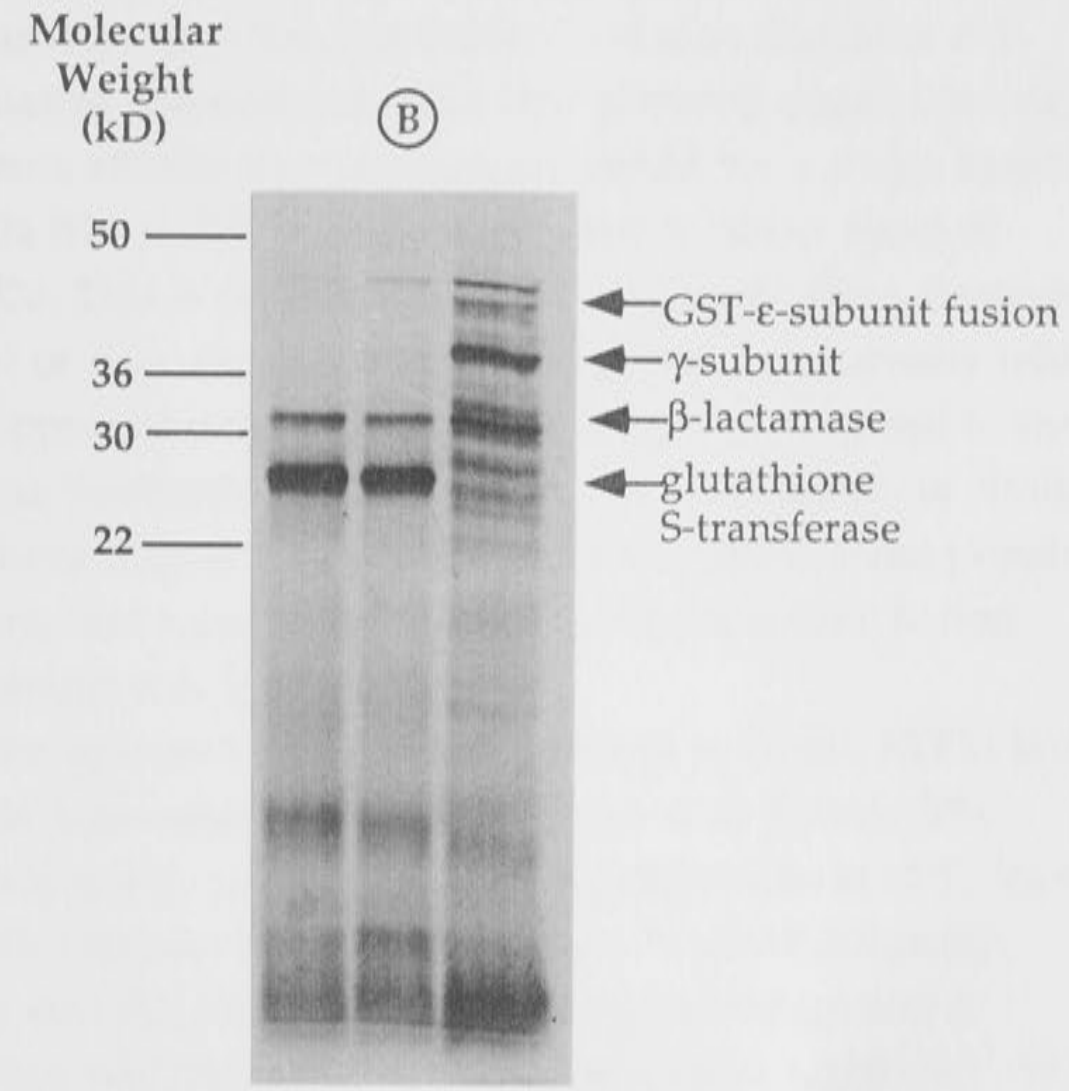
Molecular Weight (kD)
B
50
36
30
22
GST-ε-subunit fusion
γ-subunit
β-lactamase
glutathione S-transferase

protein appears to have occurred. This suggests that the interaction between the GST-ε fusion and the γ-subunit may not result in the formation of a stable complex. Other bands visible on the autoradiograph in the pAN974 lane may be degradation products of the GST-ε-fusion protein, one or more of which may be sufficient to achieve the effect of stabilising the structure of the γ-subunit.

**4.5 Attempted purification of a complex of the spinach chloroplast $F_OF_1$-ATPase γ-and ε-subunits from strain AN3830.**

A large scale culture of strain AN3830 was grown as described in section 2.23. The procedure described in section 2.25 for purification of GST fusion proteins was then followed, using STEM buffer in all steps.

Samples collected at the various steps were analysed by SDS-PAGE (see Figure 4.3.a). As with other gels described below, the sample of the pellet following the 39,000 x *g* centrifugation step was taken by scooping a small unmeasured amount into loading buffer, and was therefore not intended for quantitative comparisons. The lane showing protein bound to the glutathione agarose affinity chromatography beads has a major band of approximately 41kDa (the ε-GST fusion protein) and a fainter band of approximately 26 kDa. This is presumably free GST formed from cleavage of the fusion protein at or near the thrombin cleavage site by proteases within the cell. A band of approximately 35 kDa (which would correspond to the molecular mass of the γ-subunit) is also present, but other bands of similar intensity appear to have bound the beads non-specifically. It is not possible to conclude, therefore, that a stable complex between the ε-GST fusion protein and the γ-subunit was formed.

The glutathione agarose beads were suspended in 10 mL STEM buffer, and human thrombin was added to a concentration of 20 U/mL. The suspension was rocked gently in a 50 mL polypropylene tube at 25°C for two hours. Samples of the material bound to the beads (washed following thrombin digestion) and the supernatant following centrifugation to remove the beads were analysed by SDS-PAGE (see Figure 4.3.b). The 41kDa ε-GST fusion protein remains mostly undigested on the beads, and no trace of 14 kDa free ε-subunit appeared in the supernatant, although some appears to be associated with the beads following thrombin digestion. The ε-GST fusion protein appears therefore to have folded in such a way as to restrict access of thrombin to the cleavage site, rendering the protein largely resistant to thrombin digestion. The following sections describe attempts to overcome this problem.

**Figure 4.3 (a)**: SDS-PAGE analysis of samples collected at the various steps in the purification of a GST-spinach chloroplast ε-subunit fusion from strain AN3830:

Lane 1: Molecular weight markers

Lane 2: Pellet following 39,000 x g centrifugation of disrupted cells

Lane 3: Supernatant following 39,000 x g centrifugation of disrupted cells

Lane 4: Unbound material following exposure of supernatant (Lane 3) to glutathione agarose beads

Lane 5: Material bound to the glutathione agarose beads

Lane 6: Molecular weight markers

**Figure 4.3 (b)**: Effect of thrombin addition to material bound to the glutathione agarose beads:

Lane 1: Material bound to the glutathione agarose beads following incubation with 20 U/mL thrombin at 25°C for two hours

Lane 2: Material in supernatant following centrifugation to remove glutathione agarose beads

Lane 3: Molecular weight markers

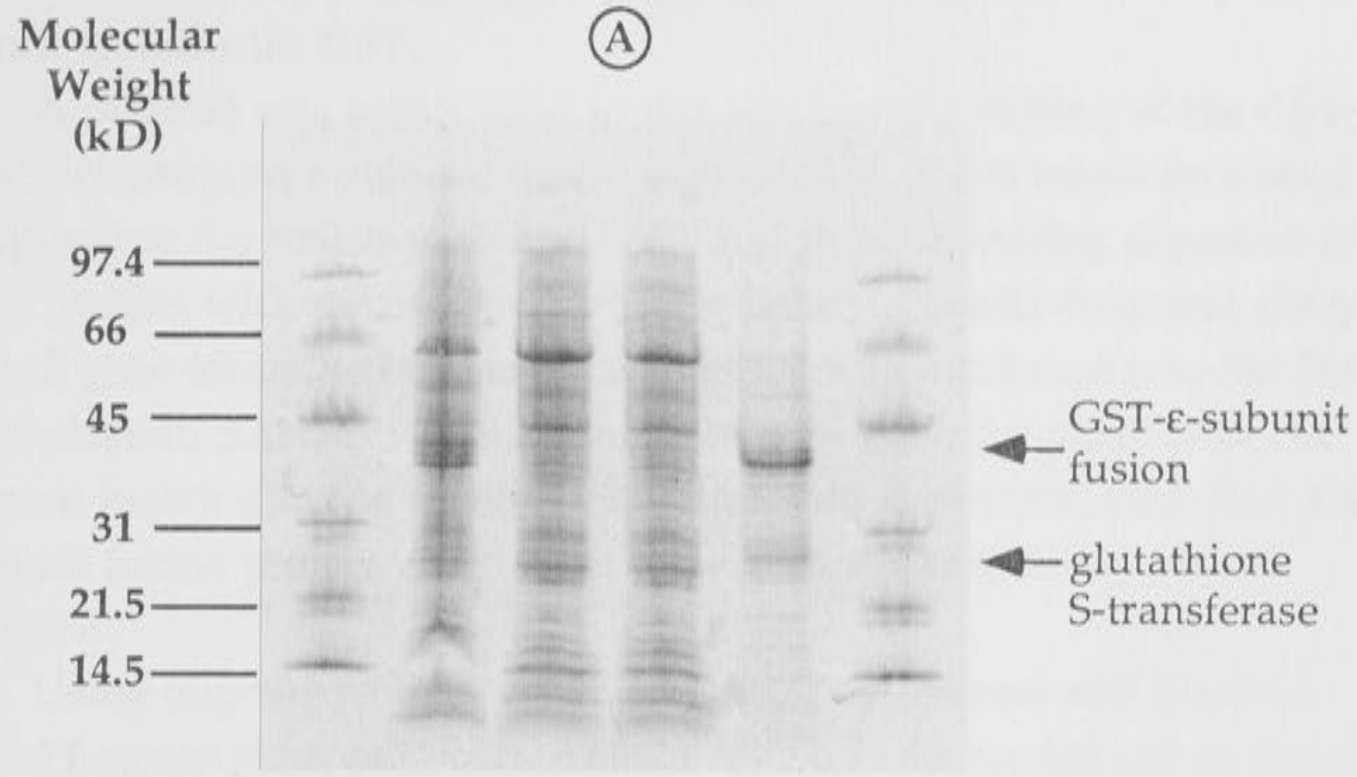
Molecular
Weight
(kD)
A
97.4
66
45
31
21.5
14.5
GST-ε-subunit
fusion
glutathione
S-transferase

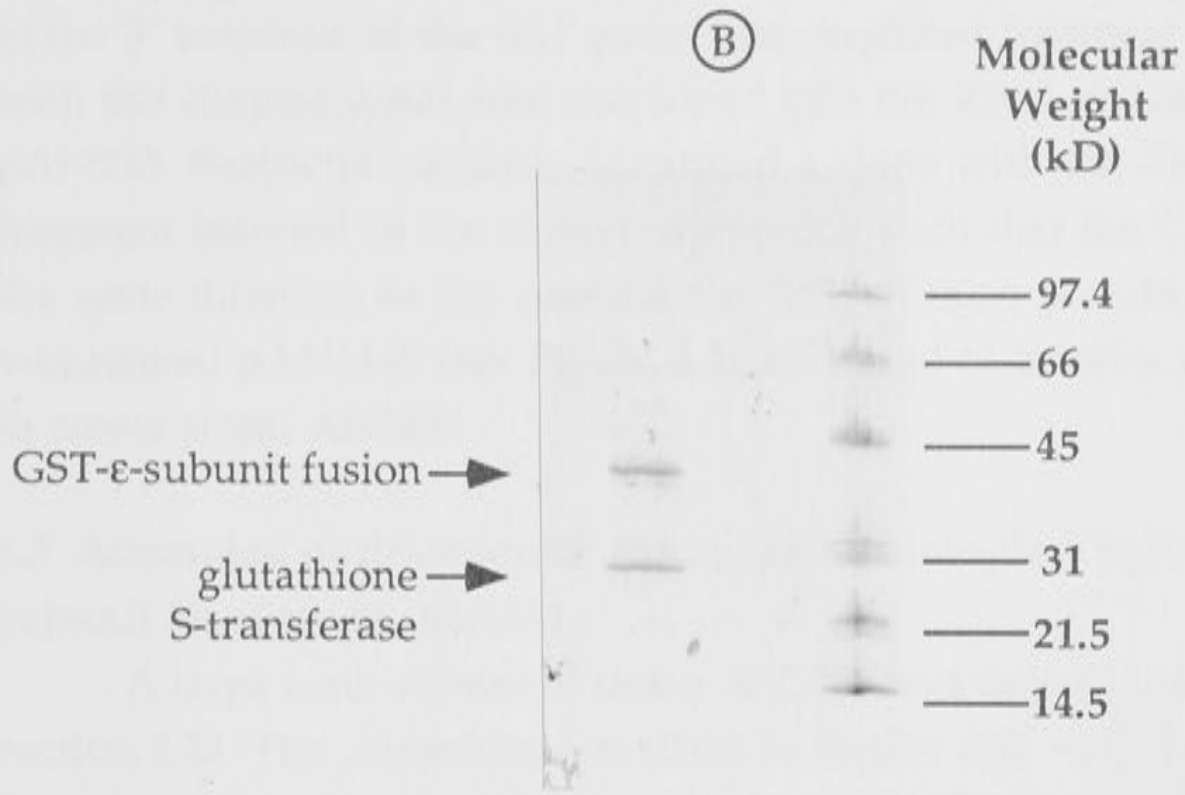
B
Molecular
Weight
(kD)
GST-ε-subunit fusion
glutathione
S-transferase
97.4
66
45
31
21.5
14.5

**4.6 Construction of a plasmid co-expressing a GST-spinach chloroplast ε-subunit fusion with GST.**

A plasmid was constructed to test whether the folding of the GST-spinach chloroplast ε-subunit fusion expressed in *E. coli* might be altered by co-expressing the fusion with free GST, and thus improving digestion of the fusion protein with thrombin. The 580bp *Bam*HI/*Bam*HI fragment carrying the *atpE* gene (described in section 4.2 above) was subcloned into the *Bam*HI site of plasmid pAN787. Restriction analysis identified a clone with the fragment inserted in the correct orientation into the vector, such that a GST-ε-subunit fusion protein may be expressed. This plasmid was named pAN925.

Using oligonucleotides AR16 and AR17 as primers and plasmid pGEX-2T as template, polymerase chain reaction was carried out as described in section 2.18 to amplify an 820bp fragment encoding the *Schistosoma japonicum* GST gene, along with preceding sequence including the *tac* promoter. The oligonucleotides AR16 and AR17 were identical to vector sequence 5′ of the GST gene and complementary to sequence 3′ of the GST gene respectively, except that a *Sma*I (*Xma*I) recognition sequence was incorporated into the sequence of AR16, and AR17 removes the *Bam*HI site at the 3′ terminus of the GST gene. The amplified fragment was digested with the enzyme *Xma*I, and subcloned into the *Xma*I site of plasmid pAN925. Restriction analysis identified a clone with the *Xma*I-*Xma*I fragment inserted in the correct orientation such that the GST gene runs in the same direction as the gene for the GST-ε fusion protein. This plasmid was named pAN1149 (see Figure 4.4), and used to transform strain AN3347 to create strain AN3832.

**4.7 Attempted purification of the spinach chloroplast $F_OF_1$-ATPase ε-subunit from strain AN3832.**

A large scale culture of strain AN3832 was grown as described in section 2.23. The procedure described in section 2.25 for purification of GST fusion proteins was then followed, using STEM buffer in all steps.

Samples collected at the various steps were analysed by SDS-PAGE (see Figure 4.5.a). The lane showing protein bound to the glutathione agarose affinity chromatography beads has two major bands of approximately 41 kDa (the GST-ε-subunit fusion protein) and 26 kDa (free GST). Approximately equal amounts of these proteins have bound to the

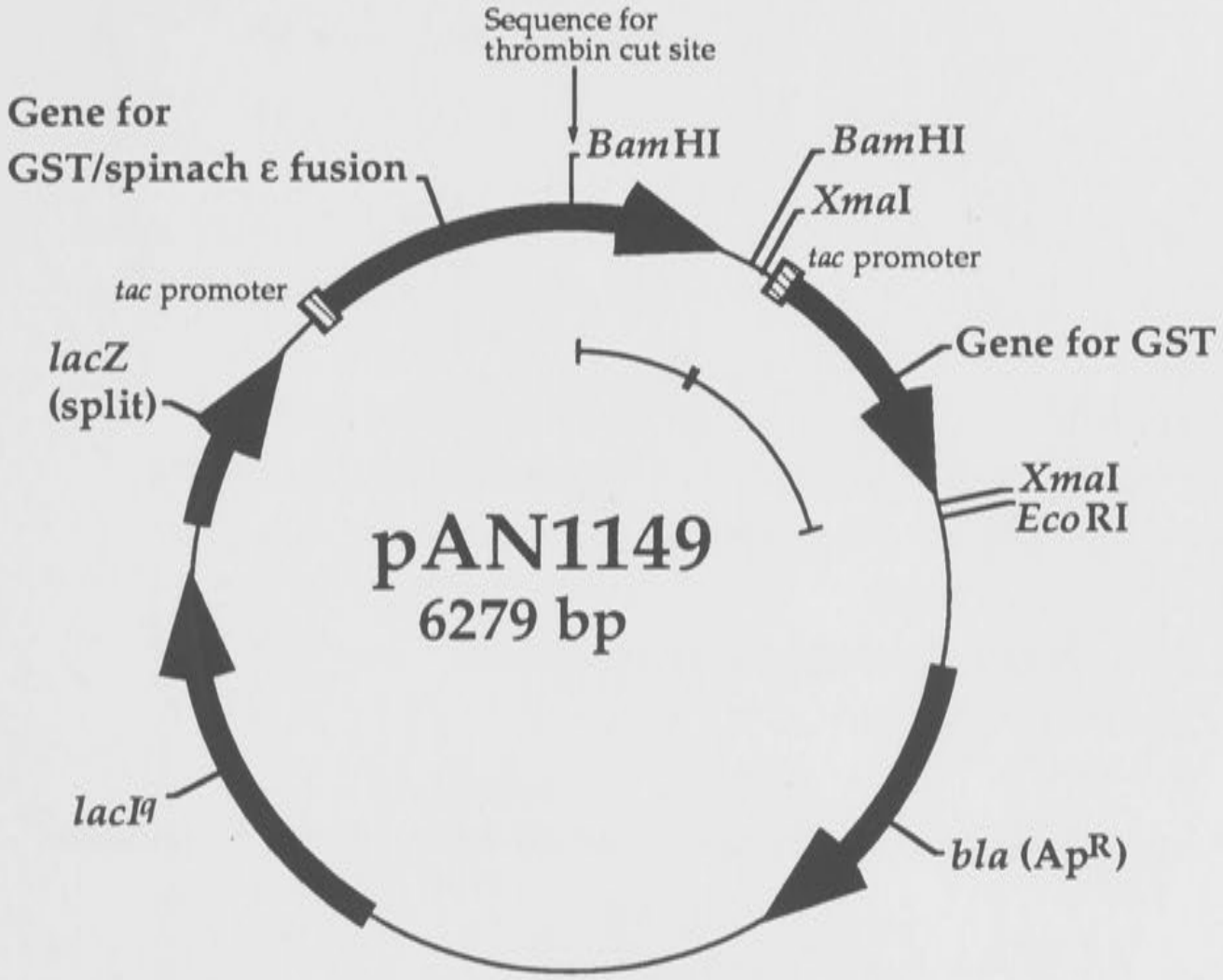


**Figure 4.4**: Plasmid pAN1149, which carries genes for a fusion protein of GST and the spinach chloroplast $F_OF_1$-ATPase ε-subunit and GST.

**Figure 4.5 (a)**: SDS-PAGE analysis of samples collected at the various steps in the purification of a GST-spinach chloroplast ε-subunit from strain AN3832:
Lane 1: Molecular weight markers
Lane 2: Pellet following 39,000 x g centrifugation of disrupted cells
Lane 3: Supernatant following 39,000 x g centrifugation of disrupted cells
Lane 4: Unbound material following exposure of supernatant (Lane 3) to glutathione agarose beads
Lane 5: Material bound to the glutathione agarose beads
Lane 6: Molecular weight markers

**Figure 4.5 (b)**: Effect of thrombin addition to material bound to the glutathione agarose beads:
Lane 1: Molecular weight markers
Lane 2: Material bound to the glutathione agarose beads following incubation with 20 U/mL thrombin at 25°C for two hours
Lane 3: Material in supernatant following centrifugation to remove glutathione agarose beads

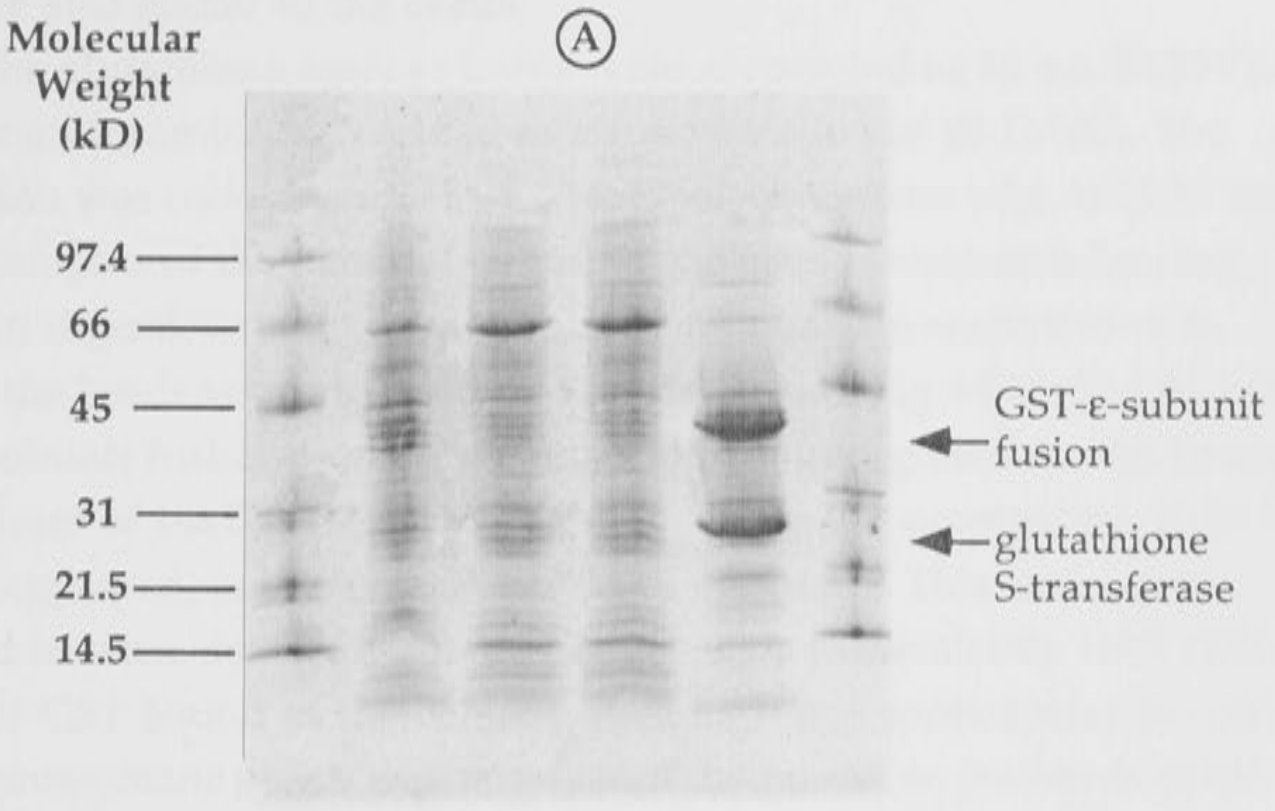
Molecular Weight (kD)
A
97.4
66
45
31
21.5
14.5
GST-ε-subunit fusion
glutathione S-transferase

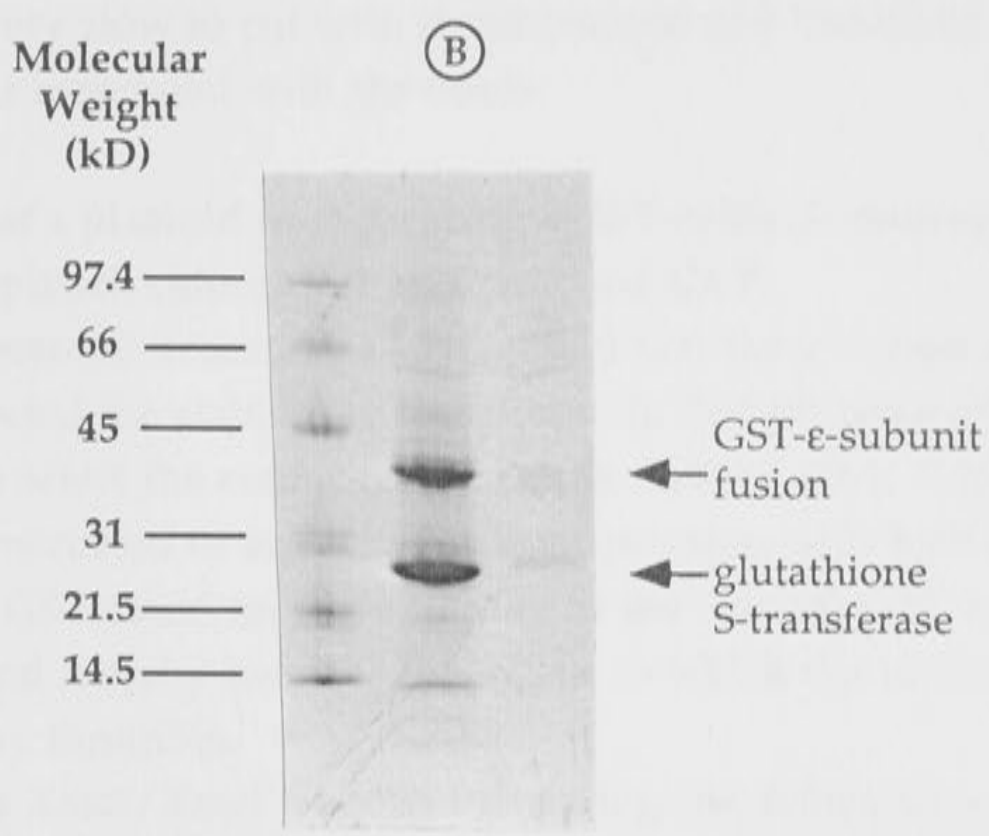
Molecular Weight (kD)
B
97.4
66
45
31
21.5
14.5
GST-ε-subunit fusion
glutathione S-transferase

beads. A 14 kDa protein is one of many others of varying molecular masss that have also bound to the beads.

The glutathione agarose beads were suspended in 10 mL STEM buffer, and human thrombin was added to a concentration of 20 U/mL. The suspension was rocked gently in a 50 mL polypropylene tube at 25 °C for two hours. Samples of the material bound to the beads (washed following thrombin digestion) and the supernatant following centrifugation to remove the beads were analysed by SDS-PAGE (see Fig 4.5.b). The 41 kDa GST-ε-subunit fusion protein remained mostly undigested on the beads, and no trace of 14kDa free ε-subunit appeared in the supernatant. A 14 kDa protein appeared, however, still bound to the beads. This may have occurred because the free ε-subunit associates non-covalently with GST-ε fusion or GST bound to the column. Although this protein may be residual of the contaminant which was observed to be bound to the beads prior to the thrombin digestion, the amount of it relative to the fusion is increased, and it is probably therefore ε-subunit. This suggests, by comparison with the results presented in section 4.5, that the co-expression of the free GST did not alter the folding or conformation of the GST-ε-fusion significantly. The GST-ε-fusion is very slow to cut with thrombin and any free ε-subunit produced remains associated with the beads.

**4.8 Construction of a plasmid co-expressing a GST-spinach chloroplast ε fusion with the spinach chloroplast γ-subunit and GST.**

Results presented in section 4.4 suggested that the presence of the GST-ε fusion affected the stability of the γ-subunit. The presence of the γ-subunit may also affect the conformation of the GST-ε fusion. A plasmid was therefore constructed to test whether co-expression with both the γ-subunit and free GST could improve folding of the spinach GST ε-subunit fusion protein, and thereby increase the extent to which the fusion protein may be cleaved by thrombin.

The 820 bp *Xma*I/*Xma*I fragment encoding the *Schistosoma japonicum* GST gene, along with preceding sequence including the *tac* promoter (described in section 4.5 above) was cloned into the *Xma*I site in plasmid pAN974 (described in section 4.2 above). Restriction analysis identified a clone with the *Xma*I-*Xma*I fragment inserted in the correct orientation such that the GST gene runs in the same direction as the genes for the GST-ε fusion and the γ-subunit. This plasmid was named pAN1024 (see Figure 4.6), and used to transform strain AN3347 to create strain AN3833.

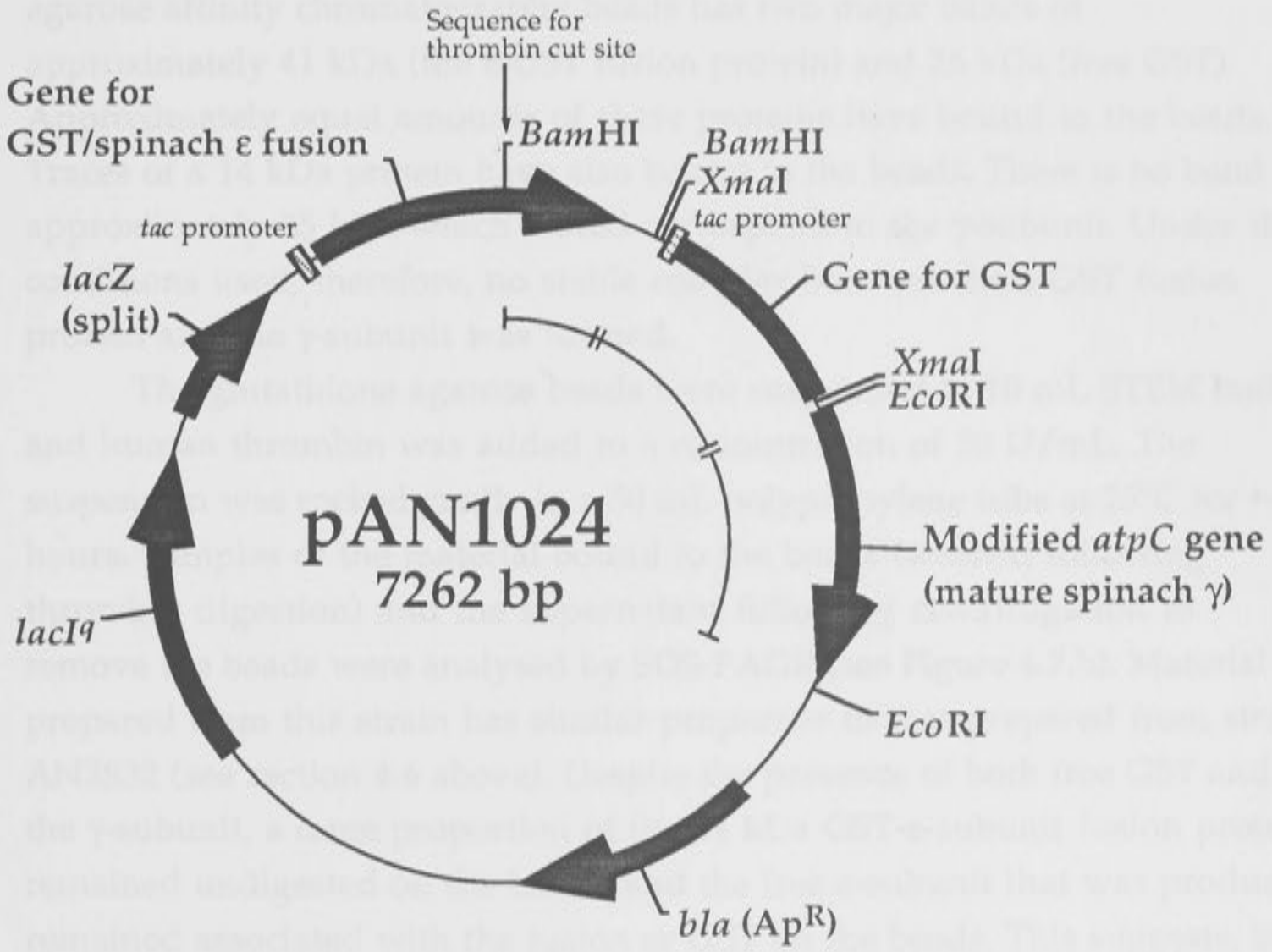


**Figure 4.6:** Plasmid pAN1024, which co-expresses a fusion protein of GST and the spinach chloroplast $F_oF_1$-ATPase ε-subunit with GST and the mature γ-subunit.

**4.9 Attempted purification of a complex of the spinach chloroplast $F_0F_1$-ATPase γ-and ε-subunits from strain AN3833.**

A large scale culture of strain AN3833 was grown as described in section 2.23. The procedure described in section 2.25 for purification of GST fusion proteins was then followed, using STEM buffer in all steps.

Samples collected at the various steps were analysed by SDS-PAGE (see Figure 4.7.a). The lane showing protein bound to the glutathione agarose affinity chromatography beads has two major bands of approximately 41 kDa (the ε-GST fusion protein) and 26 kDa (free GST). Approximately equal amounts of these proteins have bound to the beads. Traces of a 14 kDa protein have also bound to the beads. There is no band of approximately 35 kDa which would correspond to the γ-subunit. Under the conditions used, therefore, no stable complex between the ε-GST fusion protein and the γ-subunit was formed.

The glutathione agarose beads were suspended in 10 mL STEM buffer, and human thrombin was added to a concentration of 20 U/mL. The suspension was rocked gently in a 50 mL polypropylene tube at 25°C for two hours. Samples of the material bound to the beads (washed following thrombin digestion) and the supernatant following centrifugation to remove the beads were analysed by SDS-PAGE (see Figure 4.7.b). Material prepared from this strain has similar properties to that prepared from strain AN3832 (see section 4.6 above). Despite the presence of both free GST and the γ-subunit, a large proportion of the 41 kDa GST-ε-subunit fusion protein remained undigested on the beads, and the free ε-subunit that was produced remained associated with the fusion or GST on the beads. This suggests, by comparison with the results presented in section 4.7, that the co-expression of the γ-subunit did not alter the folding or conformation of the GST-ε-fusion. The apparent absence of a band for the γ-subunit on the gels may be due to proteolysis.

**4.10 Construction of a plasmid co-expressing a GST-spinach chloroplast γ fusion with the spinach chloroplast ε-subunit and GST.**

Since it was not possible to purify the free ε-subunit from a GST-ε fusion, a plasmid was constructed to express a GST-γ-subunit fusion along with the free ε-subunit and GST. Plasmids expressing the homologous *E. coli* subunits from genes arranged in this order have successfully been used to demonstrate the formation of a complex between a GST-γ-subunit fusion and the ε-subunit (Cox *et al.*, 1993). The vector upon which this plasmid was based was pAN990 (constructed by G. Ewart in this laboratory). This vector

**Figure 4.7 (a)**: SDS-PAGE analysis of samples collected at the various steps in the purification of a GST-spinach chloroplast ε-subunit from strain AN3833:
Lane 1: Molecular weight markers
Lane 2: Pellet following 39,000 x g centrifugation of disrupted cells
Lane 3: Supernatant following 39,000 x g centrifugation of disrupted cells
Lane 4: Unbound material following exposure of supernatant (Lane 3) to glutathione agarose beads
Lane 5: Material bound to the glutathione agarose beads
Lane 6: Molecular weight markers

**Figure 4.7 (b)**: Effect of thrombin addition to material bound to the glutathione agarose beads:
Lane 1: Molecular weight markers
Lane 2: Material bound to the glutathione agarose beads following incubation with 20 U/mL thrombin at 25°C for two hours
Lane 3: Material in supernatant following centrifugation to remove glutathione agarose beads

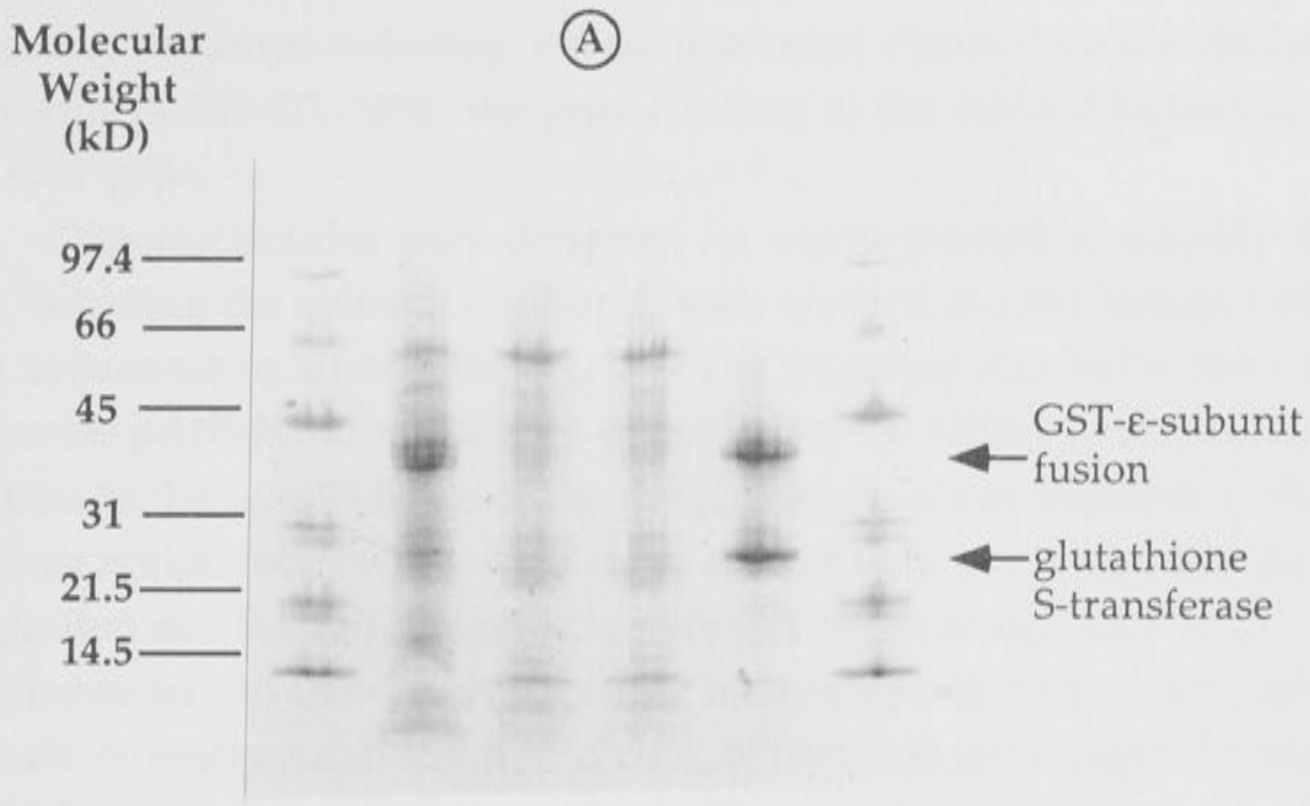
A
Molecular Weight (kD)
97.4
66
45
31
21.5
14.5
GST-ε-subunit fusion
glutathione S-transferase

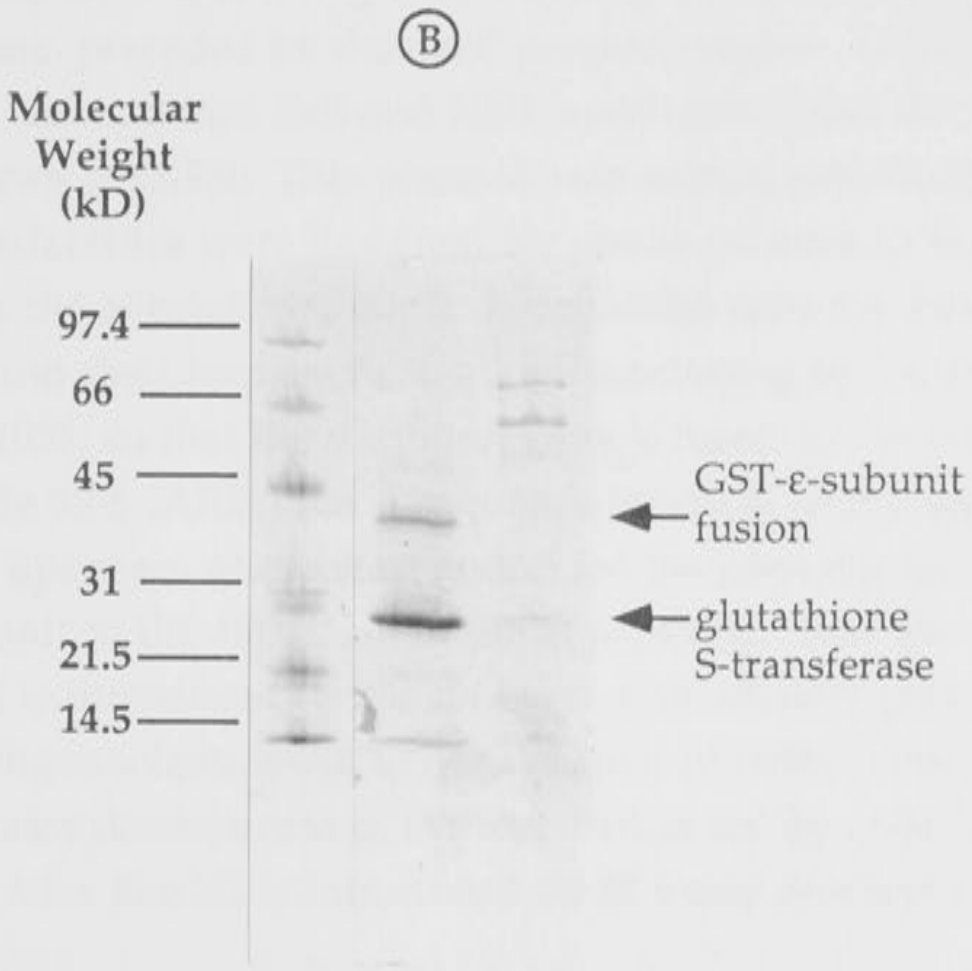
B
Molecular Weight (kD)
97.4
66
45
31
21.5
14.5
GST-ε-subunit fusion
glutathione S-transferase

carries a second copy of the *Schistosoma japonicum* GST gene, along with preceding sequence including the *tac* promoter, cloned into the *Aat*I site of the vector pGEX-4T1, with the gene running in the same direction as the first GST gene.

Oligonucleotides were designed for use as primers to amplify the gene encoding the spinach ε-subunit, with restriction sites incorporated into their sequences to allow subcloning of the fragment into convenient sites in the vector pAN990. The 3′ end of oligonucleotide AR18 has a sequence identical to the first 18 bases of the gene. Preceding this sequence is the *uncE* pregenic region (see section 4.1 above), altered only to incorporate the recognition site for *Sal*I. Oligonucleotide AR19 has a sequence complementary to the region from one base upstream of the stop codon to 33 bases downstream of the stop codon, except that the recognition sequence for *Not*I is introduced 8-16 bases downstream of the stop codon.

Using plasmid pAN420 (see section 4.2 above) as template and oligonucleotides AR18 and AR19 as primers, the polymerase chain reaction was used to amplify a 478bp fragment carrying the entire coding sequence for the *atpE* gene, preceded by the *uncE* pregenic region. This fragment was digested with the enzymes *Sal*I and *Not*I, and ligated into the *Sal*I and *Not*I sites of the vector pAN990. This plasmid was named pAN1051.

Oligonucleotides were designed for use as primers to amplify the gene encoding the spinach γ-subunit. Recognition sites for *Bam*HI were incorporated into their sequences to allow subcloning of the fragment into plasmid pAN1051, so that the γ-subunit gene is fused to the gene for GST. Oligonucleotide 93-5 (AR20) has a sequence identical to the region extending from 25 bases upstream of the start codon for the gene encoding the mature spinach γ-subunit to the 16th base in the gene, except that the recognition site for *Bam*HI is introduced in the six bases immediately preceeding the start codon. Oligonucleotide AR21 has a sequence complementary to the region 12-51 bases downstream of the stop codon for the gene, except that a recognition site for *Bam*HI is introduced 26-32 bases downstream of the stop codon.

Plasmid pAN1131 carries a 1.1kb fragment covering the entire modified *atpG* gene, encoding the mature spinach γ-subunit, cloned into the *Sph*I and *Bam*HI sites of pUC19 (see section 3.20). Using this plasmid as template and oligonucleotides AR20 and AR21 as primers, the polymerase chain reaction was used to amplify a 1.0 kb fragment. This fragment was digested with the enzyme *Bam*HI, and ligated into the *Bam*HI site in the

plasmid pAN1051. Restriction analysis identified a clone with the fragment inserted in the correct orientation for the γ-subunit to be expressed as a fusion protein with GST. This plasmid was named pAN1052 (see Figure 4.8) and used to transform AN3347 to create strain AN3831.

**4.11 Attempted purification of a complex of the spinach chloroplast γ- and ε-subunits from strain AN3831.**

A large scale culture of strain AN3831 was grown as described in section 2.23. Samples collected at various steps in the procedure for purification of the GST fusion protein were analysed by SDS-PAGE (see Figure 4.9.a). The lane with material from the pellet following the 39,000 x *g* centrifugation step has a strong band at the molecular mass predicted for the GST-γ-subunit fusion (62kDa), indicating that at least some of this protein is insoluble and may form inclusion bodies. Only a trace of the 62 kDa protein bound to the glutathione agarose beads following exposure to the supernatant. There was, however, very little present in the supernatant and it is therefore difficult to assess the proportion of soluble GST-γ-subunit fusion which binds to the beads.

The solubilisation of the γ-GST fusion protein from the pellet from the 39,000 x *g* centrifugation step was attempted. The insoluble material was suspended in four 10 mL aliquots of STEM buffer in 50mL polypropylene tubes. To each aliquot was added one of four non-denaturing detergents, to the following concentrations (at least double the relevant critical micelle concentration): 1% Triton X-114, 2% CHAPS, 2% sucrose monolaurate, 2% lauryl maltoside. The tubes were rocked gently at 4°C overnight, then centrifuged at 39,000 x *g* for 30 minutes to sediment unsolubilised material. Glutathione agarose affinity chromatography beads were then added to the supernatants in 50mL polypropylene tubes, which were rocked gently at 4°C for 2 hours. The beads were then washed thoroughly in STEM buffer.

From each of the four experiments, samples of the pellet following the 39,000 x *g* centrifugation step, unbound material in the supernatant following exposure to the beads and material bound to the beads were analysed by SDS-PAGE (see Fig 4.9.b and c). No 62kDa protein bound to the beads in any of the experiments, indicating that none of the four detergents had solubilised any of the γ-GST fusion protein in a form that would bind to the beads.

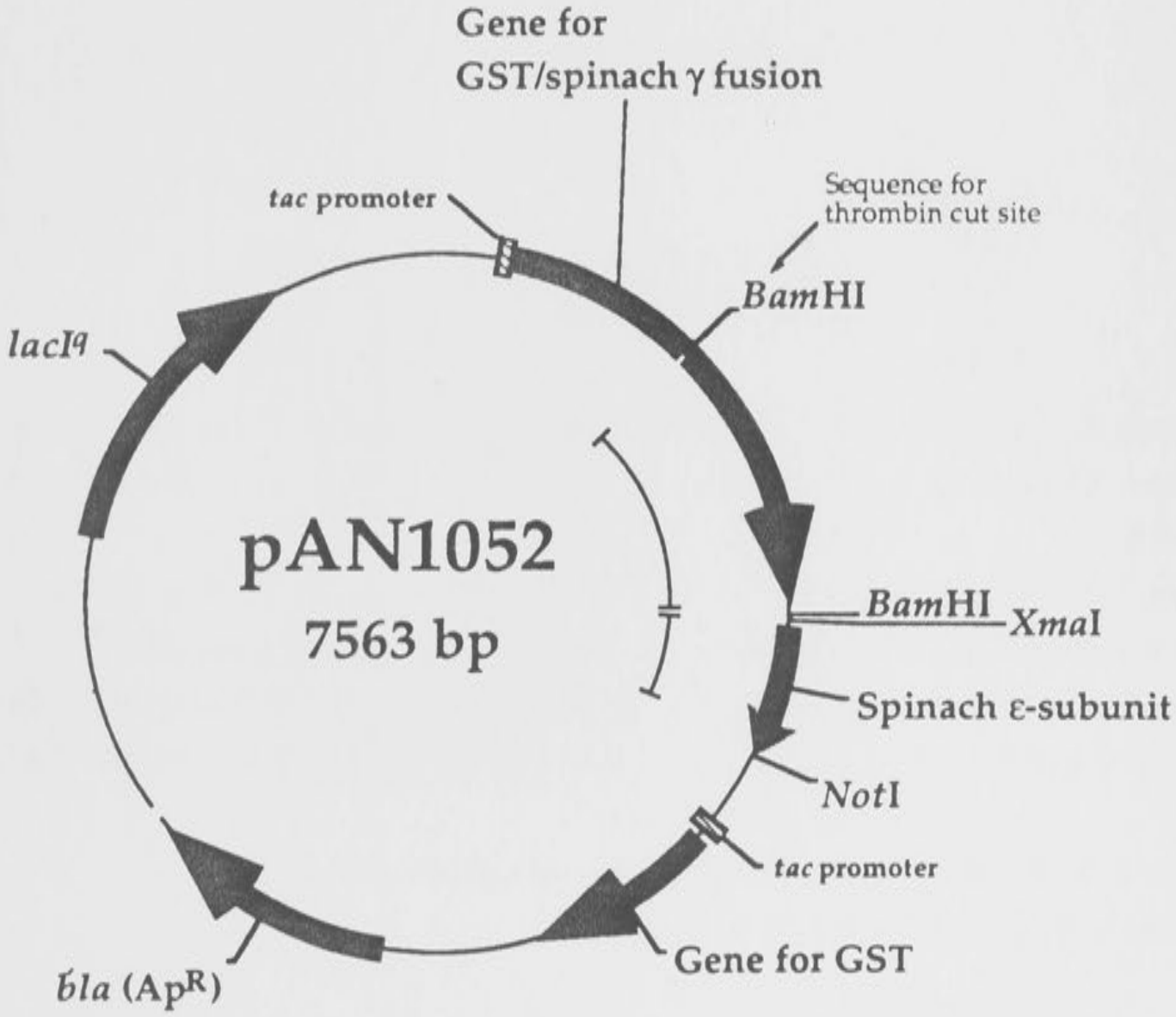


**Figure 4.8**: Plasmid pAN1052, which carries genes for a GST- spinach γ-subunit fusion, the free spinach ε-subunit and GST.

**Figure 4.9 (a)**: SDS-PAGE analysis of samples collected at the various steps in the purification of a GST-spinach chloroplast γ-subunit fusion from strain AN3831:

Lane 1: Molecular weight markers

Lane 2: Pellet following 39,000 x g centrifugation of disrupted cells

Lane 3: Supernatant following 39,000 x g centrifugation of disrupted cells

Lanes 4 and 5: Unbound material following exposure of supernatant (Lane 3) to glutathione agarose beads

Lane 6: Material bound to the glutathione agarose beads

Lane 7: Molecular weight markers

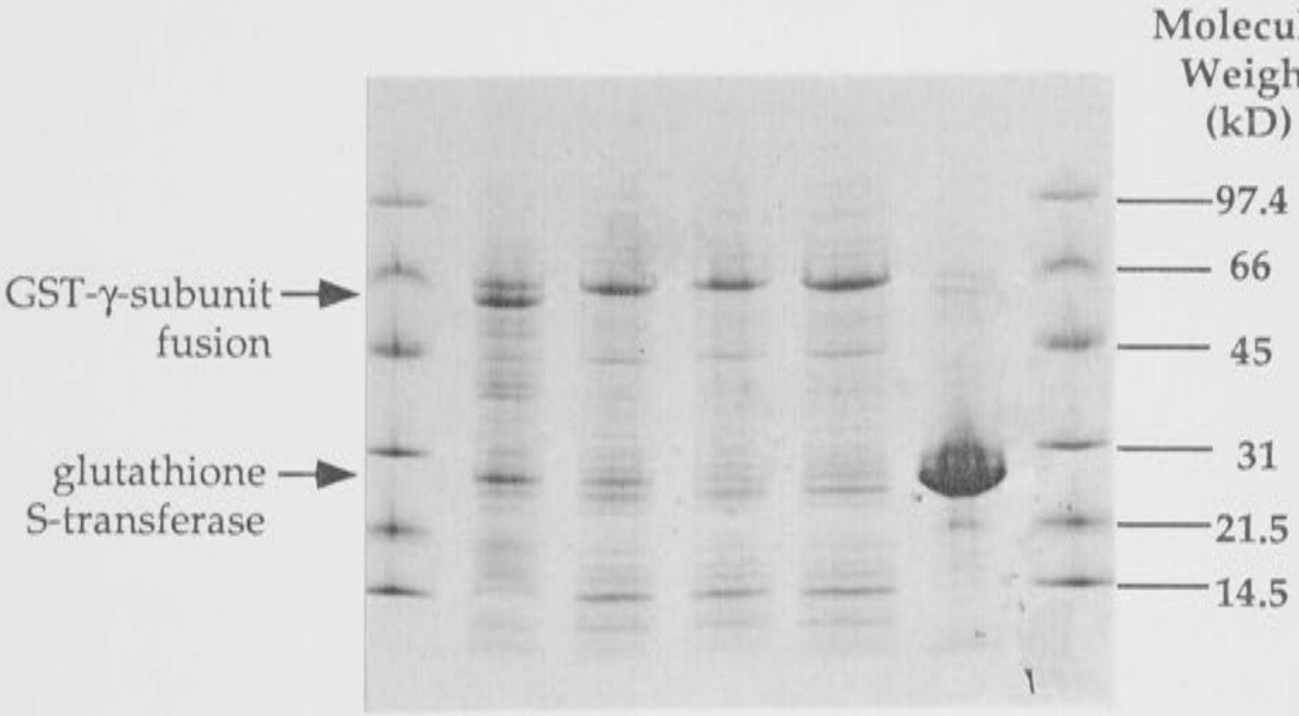
Molecular Weight (kD)
97.4
66
45
31
21.5
14.5
GST-γ-subunit fusion
glutathione S-transferase

**Figure 4.9 (b)**: Attempted extraction of the GST-spinach chloroplast γ-subunit fusion from the pellet following the 39,000 x g centrifugation of disrupted AN3842 cells using non-ionic detergents. Following extraction, the 39,000 x g centrifugation step was repeated, and the supernatant exposed to glutathione-agarose beads:

LANES 1, 2, 3 and 4: Extraction with 2% sucrose monolaurate:
Lane 1: Molecular weight markers
Lane 2: Pellet following 39,000 x g centrifugation of extract.
Lane 3: Unbound material following exposure of supernatant to glutathione agarose beads.
Lane 4: Material bound to the glutathione agarose beads

LANES 5, 6, 7 and 8: Extraction with 2% lauryl maltoside:
Lane 1: Molecular weight markers
Lane 2: Pellet following 39,000 x g centrifugation of extract.
Lane 3: Unbound material following exposure of supernatant to glutathione agarose beads.
Lane 4: Material bound to the glutathione agarose beads

**Figure 4.9 (c)**: Attempted extraction of the GST-spinach chloroplast γ-subunit fusion from the pellet following the 39,000 x g centrifugation of disrupted cells using non-ionic detergents. Following extraction, the 39,000 x g centrifugation step was repeated, and the supernatant exposed to glutathione-agarose beads:

LANES 1, 2, 3 and 4: Extraction with 1% Triton X-114:
Lane 1: Molecular weight markers
Lane 2: Pellet following 39,000 x g centrifugation of extract.
Lane 3: Unbound material following exposure of supernatant to glutathione agarose beads.
Lane 4: Material bound to the glutathione agarose beads

LANES 5, 6, 7 and 8: Extraction with 2% CHAPS:
Lane 5: Molecular weight markers
Lane 6: Pellet following 39,000 x g centrifugation of extract.
Lane 7: Unbound material following exposure of supernatant to glutathione agarose beads.
Lane 8: Material bound to the glutathione agarose beads

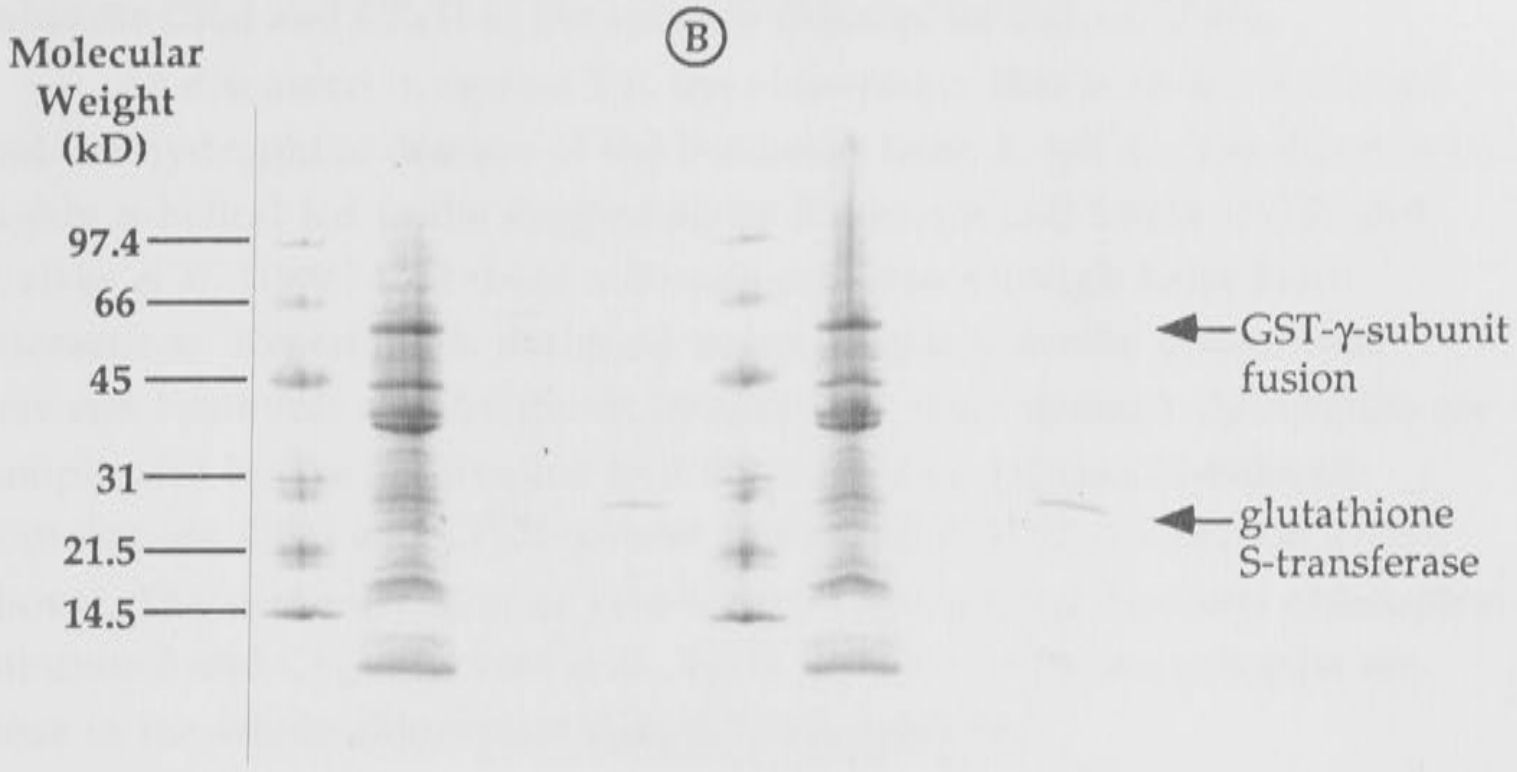
Molecular Weight (kD)
97.4
66
45
31
21.5
14.5
GST-γ-subunit fusion
glutathione S-transferase

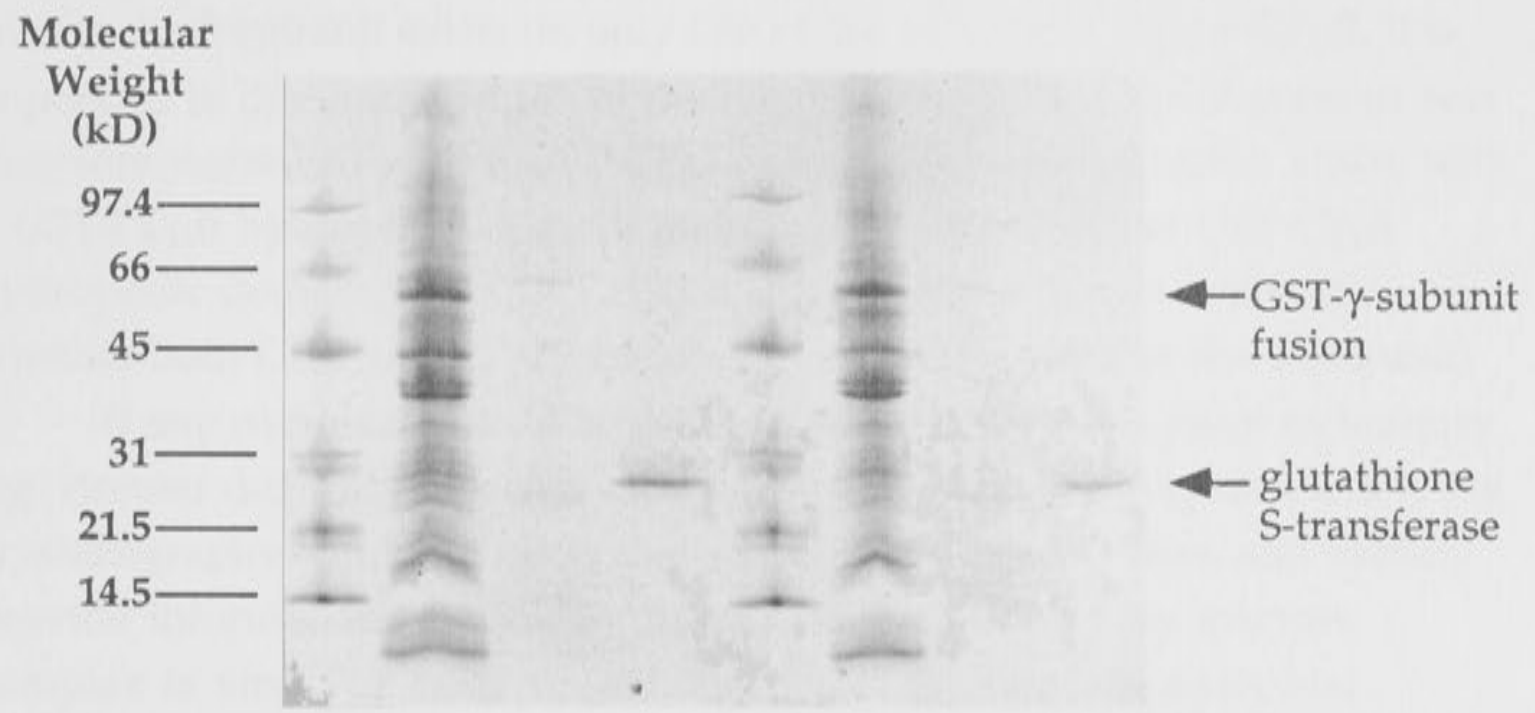
Molecular Weight (kD)
97.4
66
45
31
21.5
14.5
GST-γ-subunit fusion
glutathione S-transferase

**4.12 Background to studies on the δ-subunit and the hydrophilic portions of subunits $CF_oI$ and $CF_oII$ of the spinach chloroplast $F_oF_1$-ATPase.**

As discussed in section 1.6, the observation that both the δ-subunit and the hydrophilic domain of the *b*-subunit from *E. coli* are predicted to be highly α-helical led to the suggestion by Sternweis and Smith (1977) and Walker *et al.* (1984) that these subunits combine through helix-helix interactions. Experiments designed to investigate possible interactions between *b*-subunit and δ-subunit homologues from spinach chloroplast are complicated by the observation that there are two apparent *b*-subunit homologues, $CF_oI$ and $CF_oII$ (Glaser and Norling, 1992; see section 1.4.5 above). The demonstration of zero-length cross-linking between chloroplast subunits δ and $CF_oI$ (Beckers *et al.*, 1992) indicate that these subunits are close in the whole chloroplast $F_oF_1$-ATPase complex.

Plasmids were constructed from which a fusion of GST and the hydrophilic portion of one of the *b*-subunit homologues is expressed along with the δ-subunit, and in one case the other *b*-subunit hydrophilic portion homologue also. The purification of fusion proteins was attempted with the aim of detecting interactions between the hydrophilic portions of subunits $CF_oI$ and/or $CF_oII$ and the δ-subunit from spinach chloroplast. If a binding site for the δ-subunit exists on only one of the subunits $CF_oI$ or $CF_oII$, it is important to determine which of the two carries the site. The δ-subunit was therefore expressed with a GST-$CF_oI$ hydrophilic domain fusion alone, with a GST-$CF_oII$ hydrophilic domain fusion alone, and with the GST-$CF_oI$ hydrophilic domain plus free $CF_oII$ hydrophilic domain to determine whether both $CF_oI$ and $CF_oII$ contribute to a binding site for the δ-subunit.

If any complexes could be purified, a number of analytical techniques (eg. circular dichroism spectroscopy, analytical ultracentrifugation and X-ray crystallography) could be employed to study structure *in vitro*, and thereby provide information relevant to the overall structure of the enzyme complex *in vivo*. For example, sedimentation equilibrium analytical ultracentrifugation could be used to study whether the hydrophilic portions of $CF_oI$ and $CF_oII$ form homo- or heterodimers in solution, a question relevant in assessing the likelihood that a heterodimer of $CF_oI$ and $CF_oII$ in the chloroplast enzyme is structurally and functionally equivalent to the two *b*-subunits of the *E. coli* $F_oF_1$-ATPase complex.

**4.13 Construction of a plasmid co-expressing a GST-spinach chloroplast subunit $CF_oI$ (hydrophilic portion) fusion and GST.**

A plasmid was constructed to co-express a GST-$CF_oI$ subunit (hydrophilic portion) fusion with GST. This required the introduction of a *Bam*HI site into the *atpF* gene at the position corresponding to the junction in the amino acid sequence between the hydrophobic (transmembrane) and hydrophilic (soluble) portions of the $CF_oI$ subunit.

Clone M13 mp19*atpF*AR1 carries a 1.67kb fragment with the modified *atpF* gene, encoding the mature form of spinach chloroplast subunit $CF_oI$, cloned into *Eco*RI and *Hin*dIII sites of M13 mp19 (see section 3.4). Using single-stranded DNA of clone M13mp19:*atpF*AR1 as template, site-directed mutagenesis was carried out using oligonucleotide AR22 to change the GTG codon of valine-31 to TCC (coding for serine), and thereby introduce a *Bam*HI site into the sequence at this position. RF DNA was prepared from several isolates, digested with *Bam*HI, and analysed by agarose gel electrophoresis. An isolate carrying the desired mutations was named mp19*atpF*AR22.

RF DNA of clone mp19*atpF*AR22 was digested with *Bam*HI and *Hin*dIII to produce a 1292bp fragment with the 3′ end of the *atpF* gene encoding the hydrophilic portion of $CF_oI$, and the 5′ end of the *atpA* gene encoding the first 270 amino acid residues of the $CF_1$-α subunit. This fragment was ligated into the *Bam*HI and *Sma*I sites of the vector pGEX-2T by incubating the ligation reaction to allow annealing of the *Bam*HI cohesive ends, end-filling 5′ overhangs with the Klenow fragment of DNA polymerase I and dNTPs, and incubating the reaction to allow ligation of blunt ends. This plasmid was named pAN753. The insert fragment was subcloned subsequently into the vector pAN990, which carries a second copy of the gene for GST (see section 4.1 above). Plasmid pAN753 was digested with *Bam*HI and *Eco*RI, and the fragments separated by agarose gel electrophoresis. The 1.3 kb fragment carrying the portion of the *atpF* gene encoding the hydrophilic portion of $CF_oI$ was ligated into the *Bam*HI and *Eco*RI sites of the vector pAN990. This plasmid, named pAN1158, carries genes for a GST-$CF_oI$ hydrophilic portion fusion and GST (see Figure 4.10), and was used to transform AN3347 to create strain AN3844.

The whole cell protein content of strain AN3844, before and after addition to a culture of 0.1 mM IPTG, was analysed by SDS-PAGE (see Figure 4. 11.a). The induction of the *tac* promoters results in the increased expression of proteins with approximate molecular masses of 41 kDa and 26 kDa, corresponding to the GST-$CF_oI$ hydrophilic portion fusion and the free

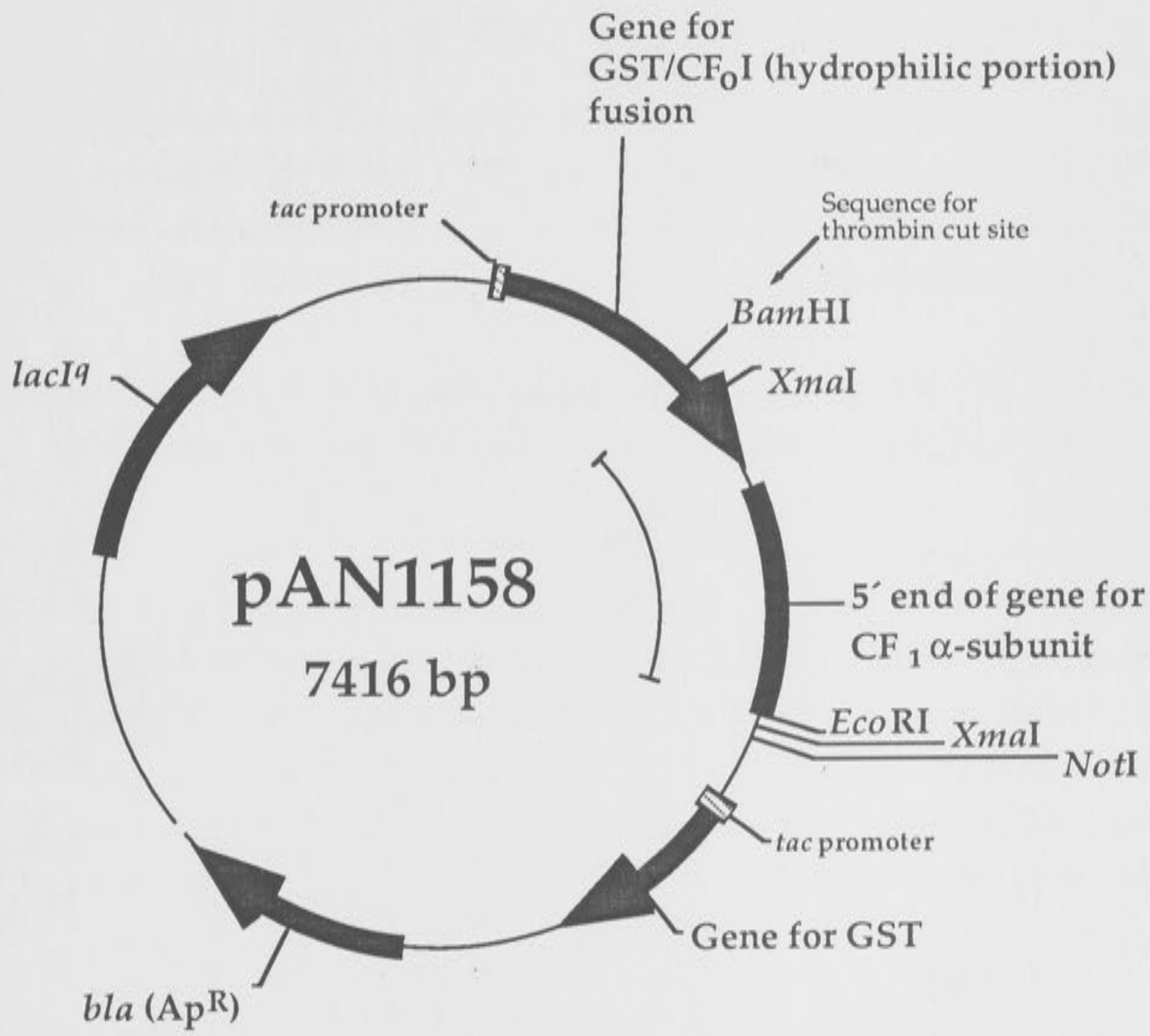


**Figure 4.10**: Plasmid pAN1158, which carries genes for a GST-spinach $CF_0I$ hydrophilic portion fusion and GST.

**Figure 4.11 (a)**: SDS-PAGE analysis of the whole cell protein content of strain AN3844, before and after addition to a culture of 0.1 mM IPTG. Induction increased expression of the GST-$CF_oI$ hydrophilic portion fusion and free GST from plasmid pAN1158, and the groEL protein from the plasmid pESL.

**Figure 4.11 (b)** : SDS-PAGE analysis of samples collected at the various steps in the attempted purification of the GST-$CF_oI$ hydrophilic portion fusion from strain AN3844:

Lane 1: Molecular weight markers
Lane 2: Pellet following 39,000 x g centrifugation of disrupted cells
Lane 3: Supernatant following 39,000 x g centrifugation of disrupted cells
Lane 4: Unbound material following exposure of supernatant (Lane 3) to glutathione agarose beads
Lane 5: Material bound to the glutathione agarose beads
Lane 6: Molecular weight markers

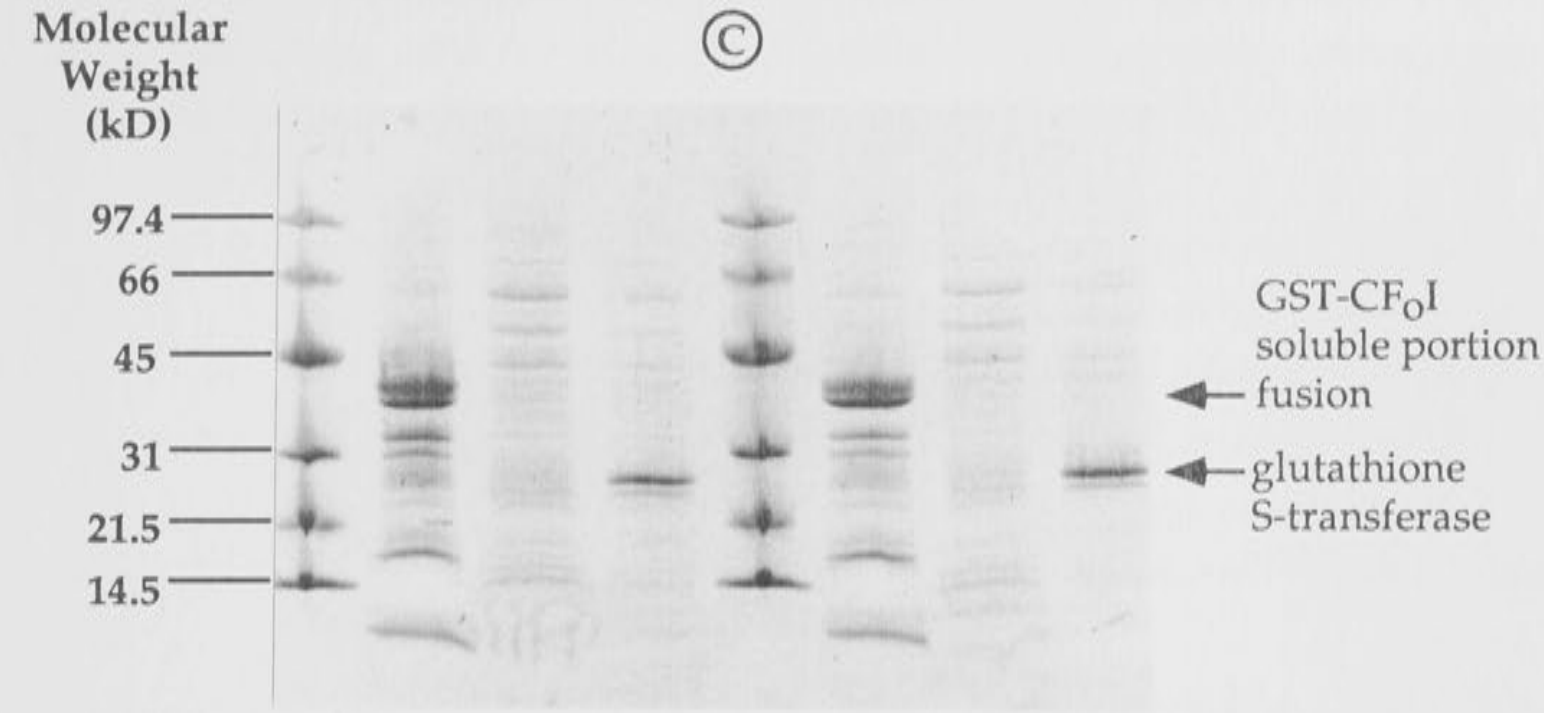
Molecular Weight (kD)
97.4
66
45
31
21.5
14.5
GST-CF$_O$I soluble portion fusion
glutathione S-transferase

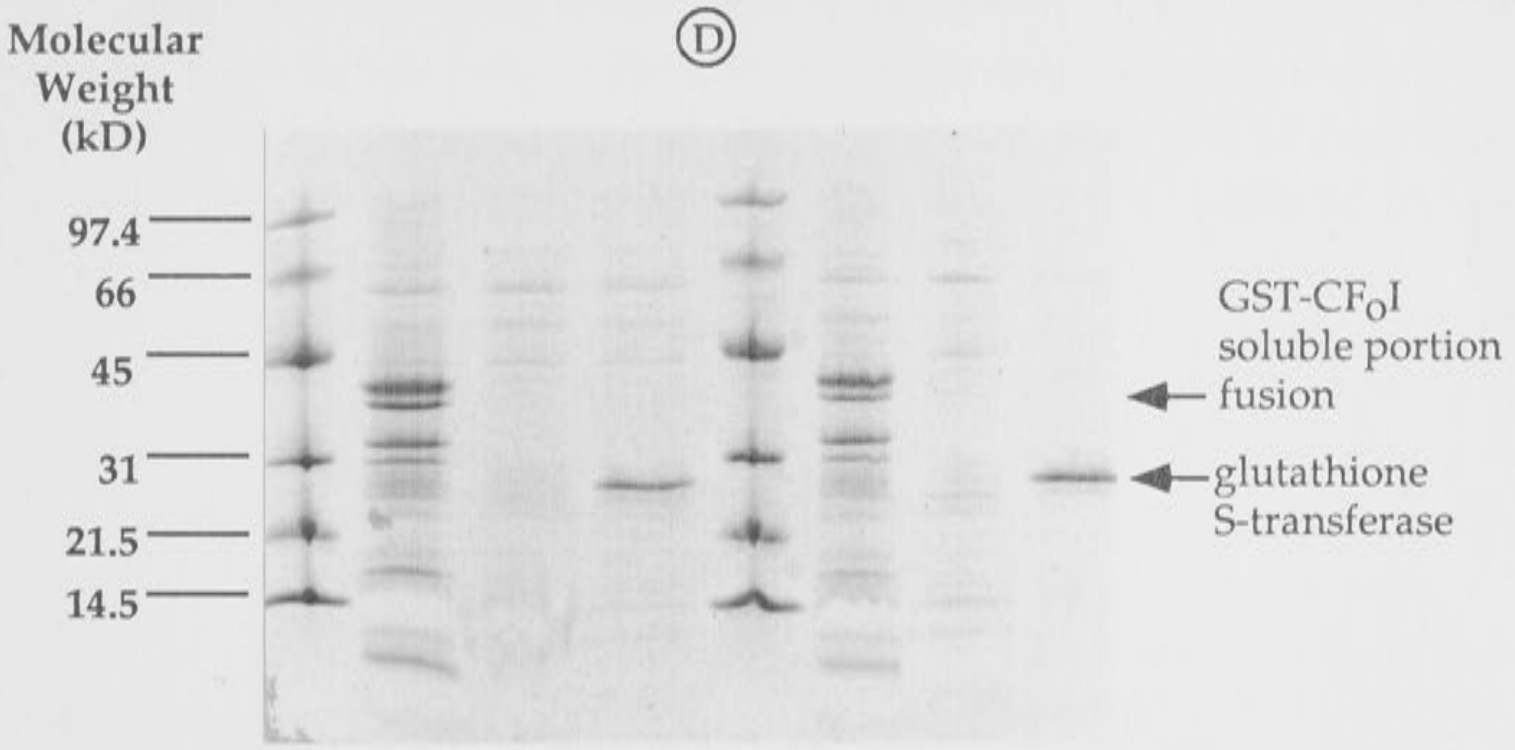
Molecular Weight (kD)
97.4
66
45
31
21.5
14.5
GST-CF$_O$I soluble portion fusion
glutathione S-transferase

**Figure 4.11 (c)**: Attempted extraction of the GST-$CF_oI$ hydrophilic portion fusion from the pellet following the 39,000 x g centrifugation of disrupted cells using non-ionic detergents. Following extraction, the 39,000 x g centrifugation step was repeated, and the supernatant exposed to glutathione-agarose beads:

LANES 1, 2, 3 and 4: Extraction with 2% sucrose monolaurate:
Lane 1: Molecular weight markers
Lane 2: Pellet following 39,000 x g centrifugation of extract.
Lane 3: Unbound material following exposure of supernatant to glutathione agarose beads.
Lane 4: Material bound to the glutathione agarose beads

LANES 5, 6, 7 and 8: Extraction with 2% lauryl maltoside:
Lane 1: Molecular weight markers
Lane 2: Pellet following 39,000 x g centrifugation of extract.
Lane 3: Unbound material following exposure of supernatant to glutathione agarose beads.
Lane 4: Material bound to the glutathione agarose beads

**Figure 4.11 (d)**: Attempted extraction of the GST-$CF_oI$ hydrophilic portion fusion from the pellet following the 39,000 x g centrifugation of disrupted cells using non-ionic detergents. Following extraction, the 39,000 x g centrifugation step was repeated, and the supernatant exposed to glutathione-agarose beads:

LANES 1, 2, 3 and 4: Extraction with 1% Triton X-114:
Lane 1: Molecular weight markers
Lane 2: Pellet following 39,000 x g centrifugation of extract.
Lane 3: Unbound material following exposure of supernatant to glutathione agarose beads.
Lane 4: Material bound to the glutathione agarose beads

LANES 5, 6, 7 and 8: Extraction with 2% CHAPS:
Lane 5: Molecular weight markers
Lane 6: Pellet following 39,000 x g centrifugation of extract.
Lane 7: Unbound material following exposure of supernatant to glutathione agarose beads.
Lane 8: Material bound to the glutathione agarose beads

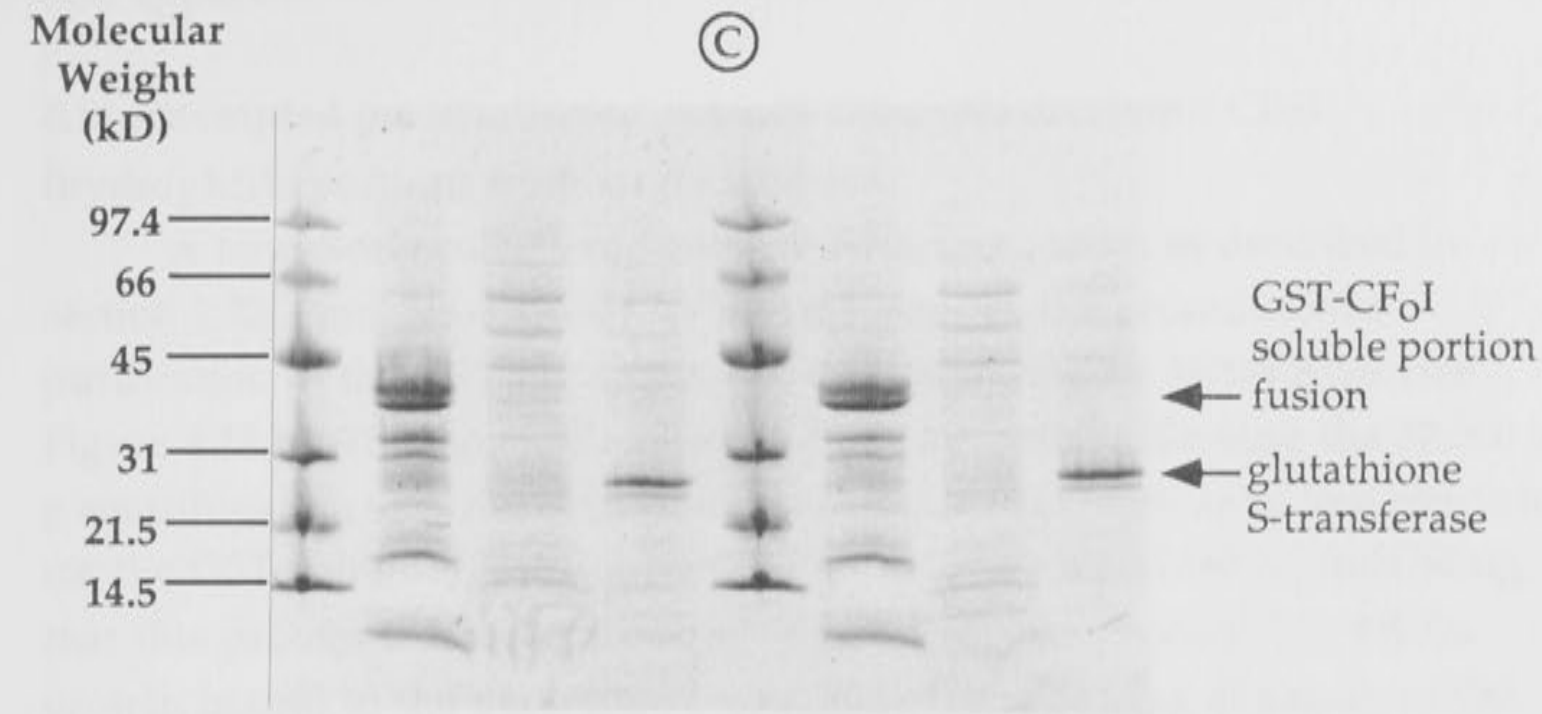
Molecular Weight (kD)
97.4
66
45
31
21.5
14.5
GST-CF$_O$I soluble portion fusion
glutathione S-transferase

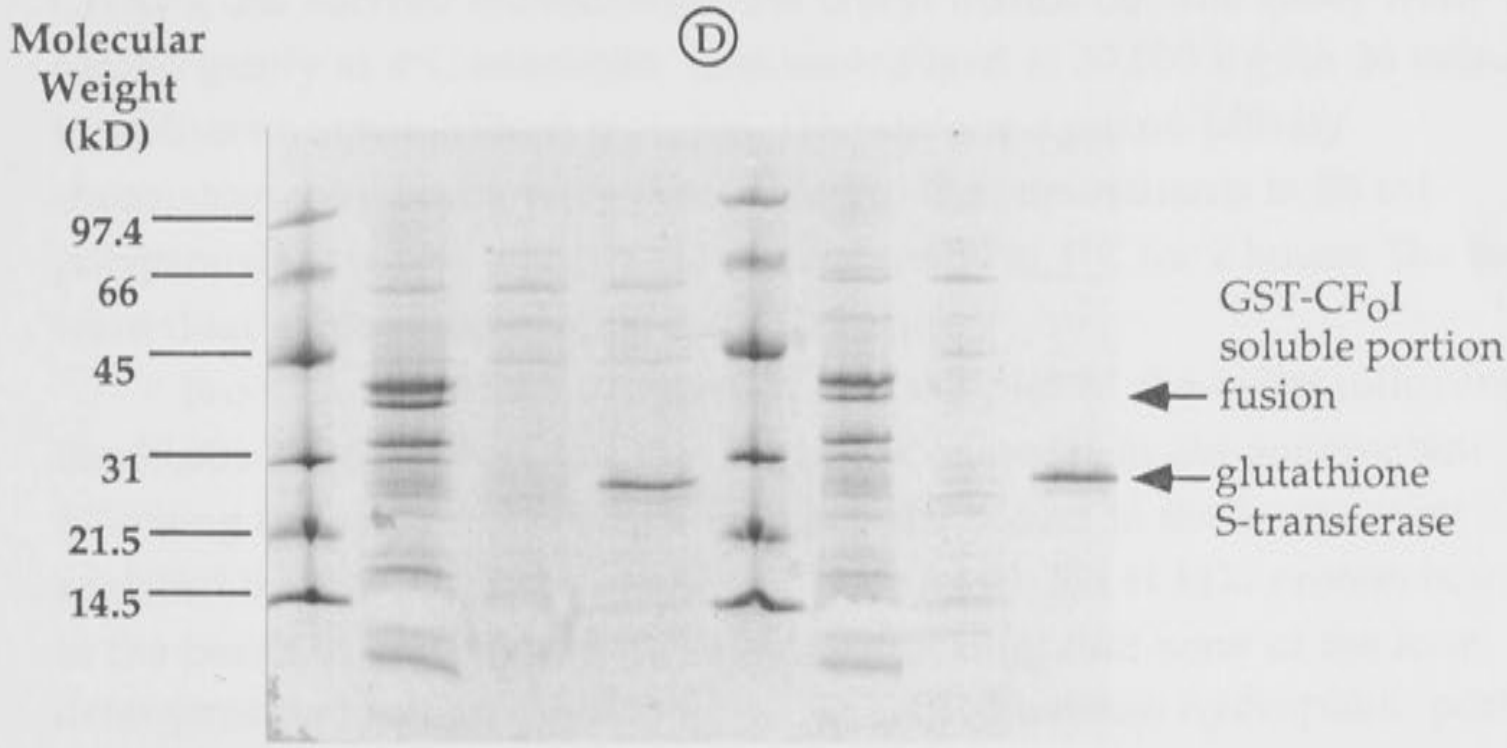
Molecular Weight (kD)
97.4
66
45
31
21.5
14.5
GST-CF$_O$I soluble portion fusion
glutathione S-transferase

GST. The induction of the 65 kDa groEL protein from the plasmid pESL is also apparent.

**4.14 Attempted purification of spinach chloroplast subunit $CF_0I$ (hydrophilic portion) from strain AN3844.**

A large scale culture of strain AN3844 was grown as described in section 2.23. Samples collected at various steps in the procedure for purification of the GST fusion protein were analysed by SDS-PAGE (see Figure 4.11.b). The lane with material from the pellet following the 39,000 x *g* centrifugation step has a band at a molecular mass similar to that predicted for the GST-subunit $CF_0I$ (hydrophilic portion) fusion (41kDa), indicating that this protein is insoluble and may form inclusion bodies. No 41kDa protein bound to the glutathione agarose beads following exposure to the supernatant.

The solubilisation of the GST-$CF_0I$ subunit hydrophilic portion fusion protein from the pellet from the 39,000 x *g* centrifugation step was attempted. The insoluble material was suspended in four 10 mL aliquots of STEM buffer in 50mL polypropylene tubes. To each aliquot was added one of four non-denaturing detergents, to the following concentrations (at least double the relevant critical micelle concentration): 1% Triton X-114, 2% CHAPS, 2% sucrose monolaurate, 2% lauryl maltoside. The tubes were rocked gently at 4°C overnight, then centrifuged at 39,000 x *g* for 30 minutes to sediment unsolubilised material. Glutathione agarose affinity chromatography beads were then added to the supernatants in 50 mL polypropylene tubes, which were rocked gently at 4°C for 2 hours. The beads were then washed thoroughly in STEM buffer.

From each of the four experiments, samples of the pellet following the 39,000 x *g* centrifugation step, unbound material in the supernatant following exposure to the beads and material bound to the beads were analysed by SDS-PAGE (see Figures 4.11.c and d). No 41 kDa protein bound to the beads in any of the experiments, indicating that none of the four detergents had solubilised any of the GST-$CF_0I$ subunit hydrophilic portion fusion protein in a form that would bind to the beads.

The next section describes the expression as a GST fusion of the hydrophilic portion of the second *b*-subunit homologue from chloroplasts, $CF_0II$, in the hope that this protein could be purified in soluble form.

**4.15 Construction of a plasmid co-expressing a GST-spinach chloroplast subunit $CF_oII$ (hydrophilic portion) fusion with the spinach chloroplast δ subunit and GST.**

To test whether a fusion of GST and the spinach chloroplast subunit $CF_oII$ (hydrophilic portion) could be purified as a soluble protein, and whether the δ-subunit would interact with this protein, a plasmid co-expressing a GST-spinach chloroplast subunit $CF_oII$ (hydrophilic portion) fusion with the spinach chloroplast δ-subunit and GST was constructed.

The polymerase chain reaction was used to amplify a fragment in which a *Bam*HI site at the 5′ terminus immediately precedes the coding region for the subunit $CF_oII$ hydrophilic portion, followed by the gene for the δ-subunit. For this purpose, oligonucleotide AR25 was designed to introduce a *Bam*HI site immediately preceding what would be aspartate-30 of the mature subunit $CF_oII$. Using oligonucleotide AR25 and the M13 reverse primer with plasmid pAN1165 as template, a 1.1 kb fragment was amplified. This fragment was digested with *Bam*HI and *Eco*RI, and ligated into the *Bam*HI and *Eco*RI sites of plasmid pAN990 to create pAN1156 (see Figure 4.12). This plasmid carries genes for a GST-spinach chloroplast subunit $CF_oII$ hydrophilic portion fusion, the δ-subunit and GST, and was used to transform strain AN3347 to create strain AN3842.

**4.16 Attempted purification of a complex of spinach chloroplast subunit $CF_oII$ hydrophilic portion and the δ-subunit from strain AN3842.**

A large scale culture of strain AN3842 was grown as described in section 2.23. Samples collected at various steps in the procedure for purification of the GST fusion protein were analysed by SDS-PAGE (see Figure 4.13.a). The lane with material from the pellet following the 39,000 x *g* centrifugation step has a band at a molecular mass similar to that predicted for the GST-subunit $CF_oII$ hydrophilic portion fusion (39 kDa), while no 39 kDa protein bound to the glutathione agarose beads following exposure to the supernatant, indicating that this protein is insoluble and may form inclusion bodies. The δ-subunit is not visible in sufficient amounts to be visible in any lane.

The solubilisation of the GST-subunit $CF_oII$ hydrophilic portion fusion protein from the pellet from the 39,000 x *g* centrifugation step was attempted. The insoluble material was suspended in four 10 mL aliquots of STEM buffer in 50 mL polypropylene tubes. To each aliquot was added one of four non-denaturing detergents, to the following concentrations: 1% Triton X-114, 2% CHAPS, 2% sucrose monolaurate, 2% lauryl maltoside.

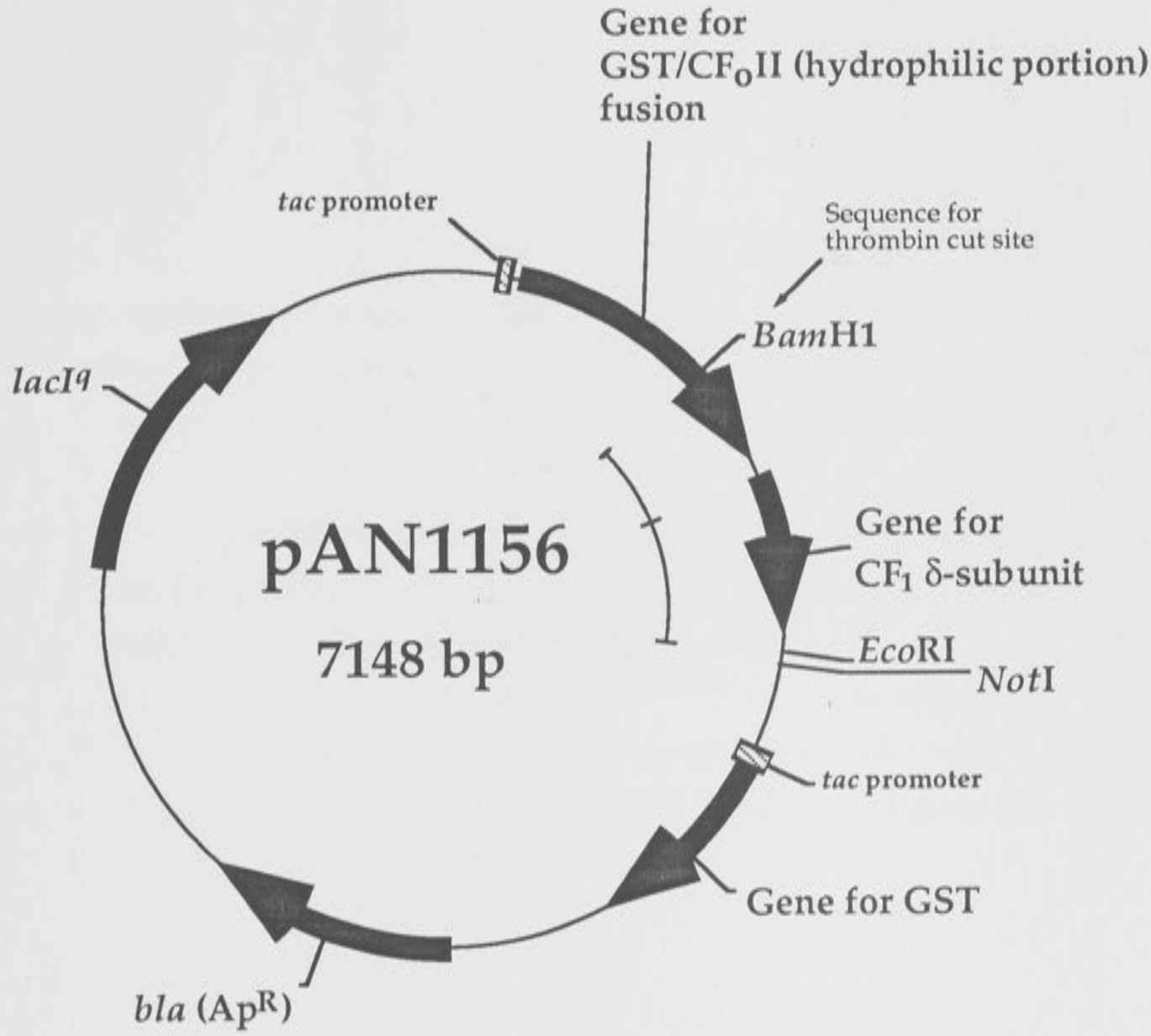


**Figure 4.12**: Plasmid pAN1156, which carries genes for a GST-spinach chloroplast subunit $CF_0II$ hydrophilic portion fusion, the spinach chloroplast δ-subunit and GST.

**Figure 4.13 (a)** : SDS-PAGE analysis of samples collected at the various steps in the attempted purification of the GST-$CF_oII$ hydrophilic portion fusion from strain AN3842:

Lane 1: Molecular weight markers

Lane 2: Pellet following 39,000 x g centrifugation of disrupted cells

Lane 3: Supernatant following 39,000 x g centrifugation of disrupted cells

Lane 4: Unbound material following exposure of supernatant (Lane 3) to glutathione agarose beads

Lane 5: Material bound to the glutathione agarose beads

Lane 6: Molecular weight markers

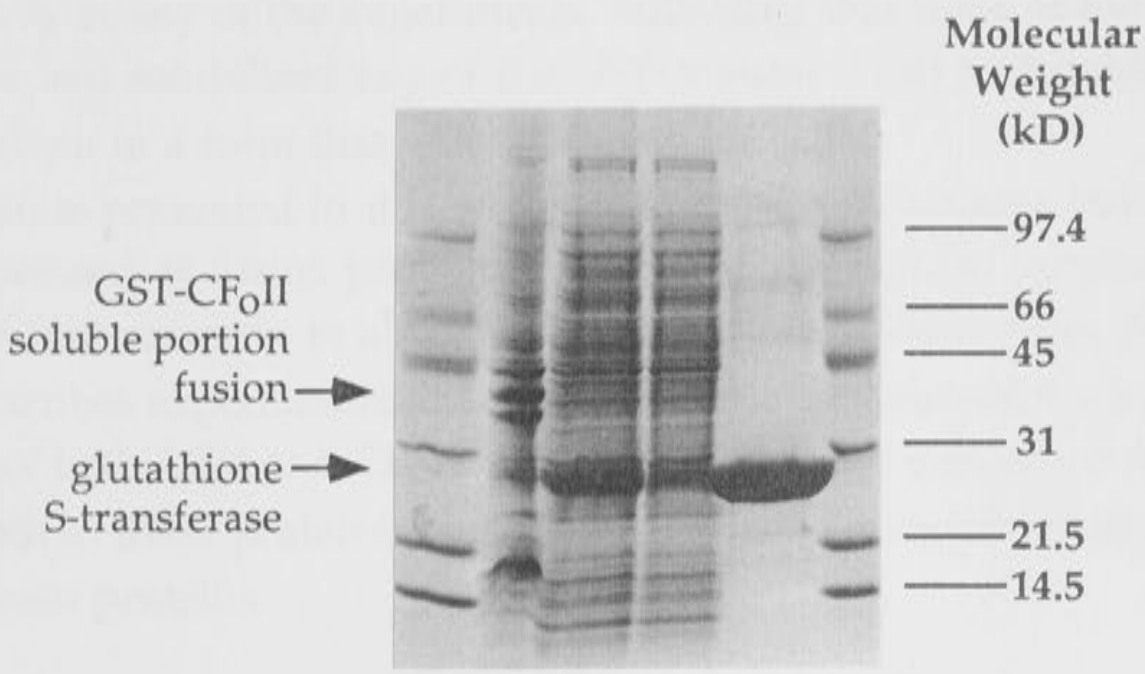
Molecular Weight (kD)
97.4
66
45
31
21.5
14.5
GST-CF$_O$II soluble portion fusion
glutathione S-transferase

The tubes were rocked gently at 4 °C overnight, then centrifuged at 39,000 x *g* for 30 minutes to sediment unsolubilised material. Glutathione agarose affinity chromatography beads were then added to the supernatants in 50 mL polypropylene tubes, which were rocked gently at 4 °C for 2 hours. The beads were then washed thoroughly in STEM buffer.

From each of the four experiments, samples of the pellet following the 39,000 x *g* centrifugation step, unbound material in the supernatant following exposure to the beads and material bound to the beads were analysed by SDS-PAGE (see Figures 4.13.b and c). No 40 kDa protein bound to the beads in any of the experiments, indicating that none of the four detergents had solubilised any of the GST-subunit $CF_oII$ hydrophilic portion fusion protein in a form that would bind to the beads.

Results presented in this section and section 4.10 above indicate that when expressed as fusion proteins, neither the hydrophilic portions of $CF_oI$ nor $CF_oII$ fold correctly to allow the expression in soluble form. The section below describes experiments to test whether the presence of the hydrophilic domains of both $CF_oI$ and $CF_oII$ are required to allow the correct folding of one or both of these proteins, and/or the binding of the δ-subunit to one or both of these proteins.

**4.17 Construction of a plasmid co-expressing a GST-spinach chloroplast subunit $CF_oI$ hydrophilic portion fusion with subunit $CF_oII$ hydrophilic portion, the δ-subunit and GST.**

To test whether the hydrophilic portions of both $CF_oI$ and $CF_oII$ must be expressed together for a soluble complex to form, and to test whether the δ-subunit might interact with this complex, a plasmid co-expressing a GST-spinach chloroplast subunit $CF_oI$ hydrophilic portion fusion with subunit $CF_oII$ hydrophilic portion, the δ-subunit and GST was constructed.

Polymerase chain reaction was used to amplify a fragment carrying a gene encoding a protein equivalent to the hydrophilic portion of $CF_oII$, immediately preceded by the *uncE* pregenic region. For this purpose, oligonucleotide AR23 was designed with a 30 bp 5´ sequence identical to the *uncE* pregenic region, preceded by an *Eco*RI site, and an 21 bp 3´ sequence identical to bases 565 to 582 of the gene for the mature $CF_oII$ (see section 3.6), except that the CTT codon for what would be leucine-29 in mature $CF_oII$ is replaced by the methionine codon ATG. Oligonucleotide AR24 was designed with a sequence complementary to a 35 bp region downstream of the *atpG* coding region except that an *Xba*I site was incorporated. Using plasmid pAN1140 as template (see section 3.7), and oligonucleotides AR23

**Figure 4.13 (b)**: Attempted extraction of the GST-$CF_oII$ hydrophilic portion fusion from the pellet following the 39,000 x g centrifugation of disrupted AN3842 cells using non-ionic detergents. Following extraction, the 39,000 x g centrifugation step was repeated, and the supernatant exposed to glutathione-agarose beads:

LANES 1, 2, 3 and 4: Extraction with 2% sucrose monolaurate:
Lane 1: Molecular weight markers
Lane 2: Pellet following 39,000 x g centrifugation of extract.
Lane 3: Unbound material following exposure of supernatant to glutathione agarose beads.
Lane 4: Material bound to the glutathione agarose beads

LANES 5, 6, 7 and 8: Extraction with 2% lauryl maltoside:
Lane 1: Molecular weight markers
Lane 2: Pellet following 39,000 x g centrifugation of extract.
Lane 3: Unbound material following exposure of supernatant to glutathione agarose beads.
Lane 4: Material bound to the glutathione agarose beads

**Figure 4.13 (c)**: Attempted extraction of the GST-$CF_oII$ hydrophilic portion fusion from the pellet following the 39,000 x g centrifugation of disrupted cells using non-ionic detergents. Following extraction, the 39,000 x g centrifugation step was repeated, and the supernatant exposed to glutathione-agarose beads:

LANES 1, 2, 3 and 4: Extraction with 1% Triton X-114:
Lane 1: Molecular weight markers
Lane 2: Pellet following 39,000 x g centrifugation of extract.
Lane 3: Unbound material following exposure of supernatant to glutathione agarose beads.
Lane 4: Material bound to the glutathione agarose beads

LANES 5, 6, 7 and 8: Extraction with 2% CHAPS:
Lane 5: Molecular weight markers
Lane 6: Pellet following 39,000 x g centrifugation of extract.
Lane 7: Unbound material following exposure of supernatant to glutathione agarose beads.
Lane 8: Material bound to the glutathione agarose beads

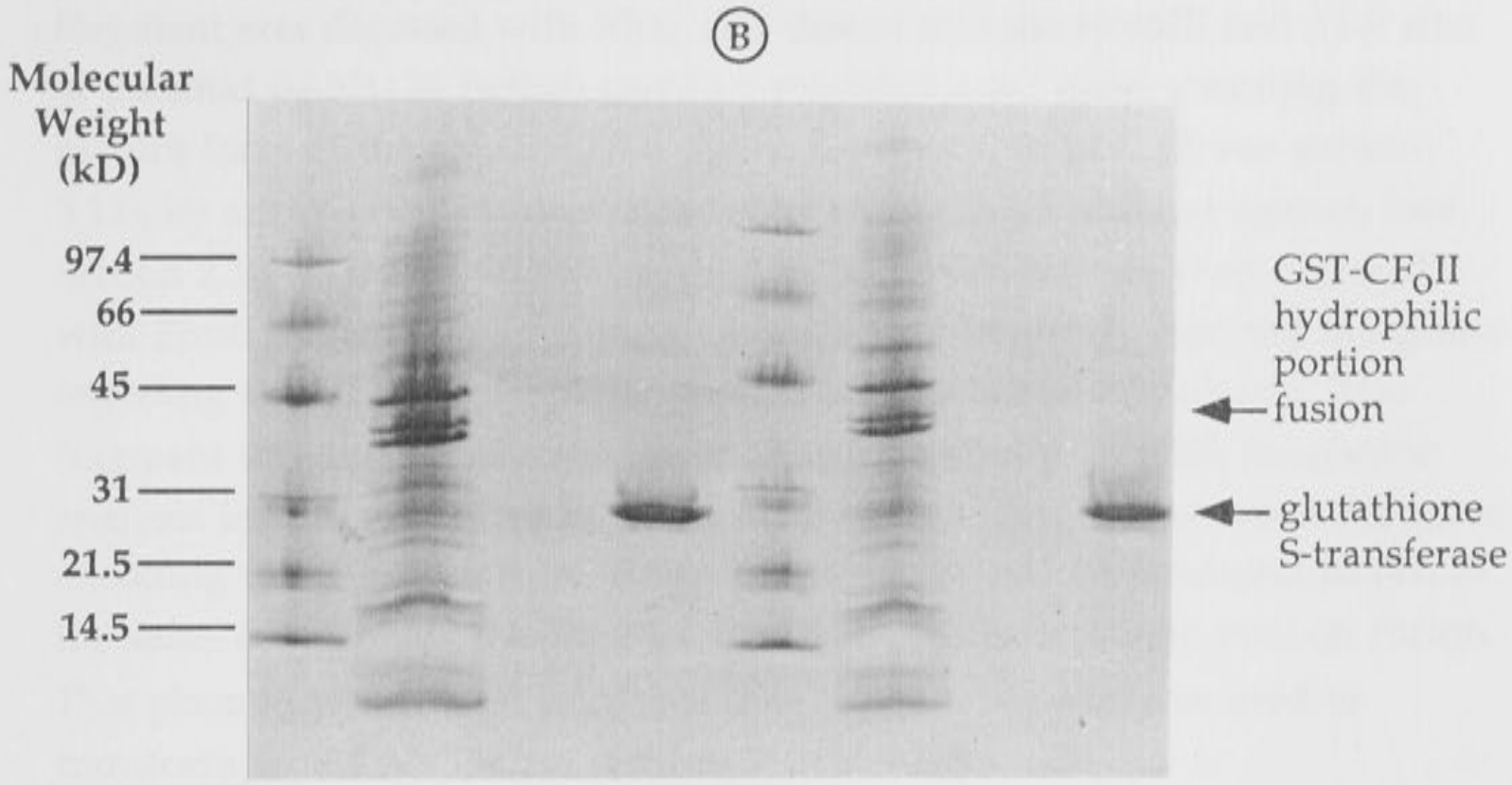
B
Molecular Weight (kD)
97.4
66
45
31
21.5
14.5
GST-CF$_o$II hydrophilic portion fusion
glutathione S-transferase

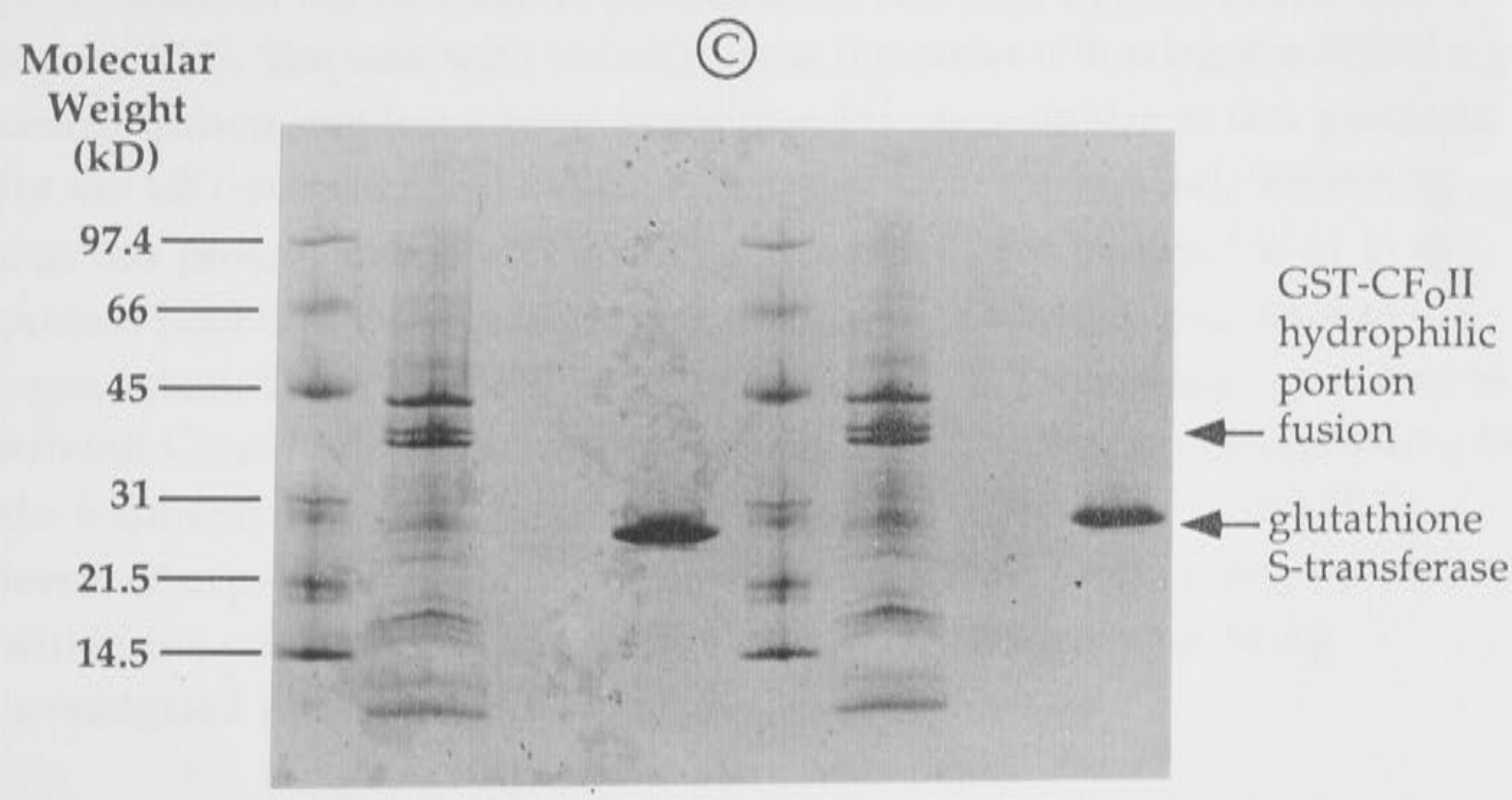
C
Molecular Weight (kD)
97.4
66
45
31
21.5
14.5
GST-CF$_o$II hydrophilic portion fusion
glutathione S-transferase

and AR24 as primers, an approximately 500 bp fragment was amplified. This fragment was digested with *Xba*I, and cloned into the *Hin*dIII and *Xba*I sites of plasmid pAN1126 (which carries a modified *atpD* gene, encoding the mature form of the spinach chloroplast δ-subunit, in pUC19; see section 3.15), by sticky-end ligation, followed by end-filling and blunt ligation (see section 2.10) to create plasmid pAN1165. This plasmid was then digested with *Eco*RI to generate an approximately 1.1 kb fragment, carrying the genes encoding the $CF_oII$ hydrophilic portion and the mature δ-subunit. This fragment was ligated into the *Eco*RI site of plasmid pAN1158. Restriction analysis identified a clone with the insert in the correct orientation for genes encoding the $CF_oII$ hydrophilic portion and the mature δ-subunit to run in the same direction as the gene for the GST-$CF_oI$ hydrophilic portion fusion. This plasmid was named pAN1164 (see Figure 4.14), and was used to transform strain AN3347 to create strain AN3850.

**4.18 Attempted purification of a complex of the spinach chloroplast subunit $CF_oI$ hydrophilic portion fusion with subunit $CF_oII$ hydrophilic portion and the δ-subunit from strain AN3850.**

A large scale culture of strain AN3850 was grown as described in section 2.23. Samples collected at various steps in the procedure for purification of the GST fusion protein were analysed by SDS-PAGE (see Figure 4.15). The lane with material from the pellet following the 39,000 x *g* centrifugation step has a band at a molecular mass similar to that predicted for the GST-subunit $CF_oI$ hydrophilic portion fusion (41kDa), indicating that this protein is insoluble and may form inclusion bodies. No 41 kDa protein bound to the glutathione agarose beads following exposure to the supernatant. There are no signs of either a 15 kDa protein corresponding to subunit $CF_oII$ hydrophilic portion or of a 20.5 kDa protein corresponding to the δ-subunit in any of the lanes. This may have been due to insufficient levels of expression of these proteins, or proteolysis of the foreign proteins within the cell, but time constraints prevented this question being investigated in more detail.

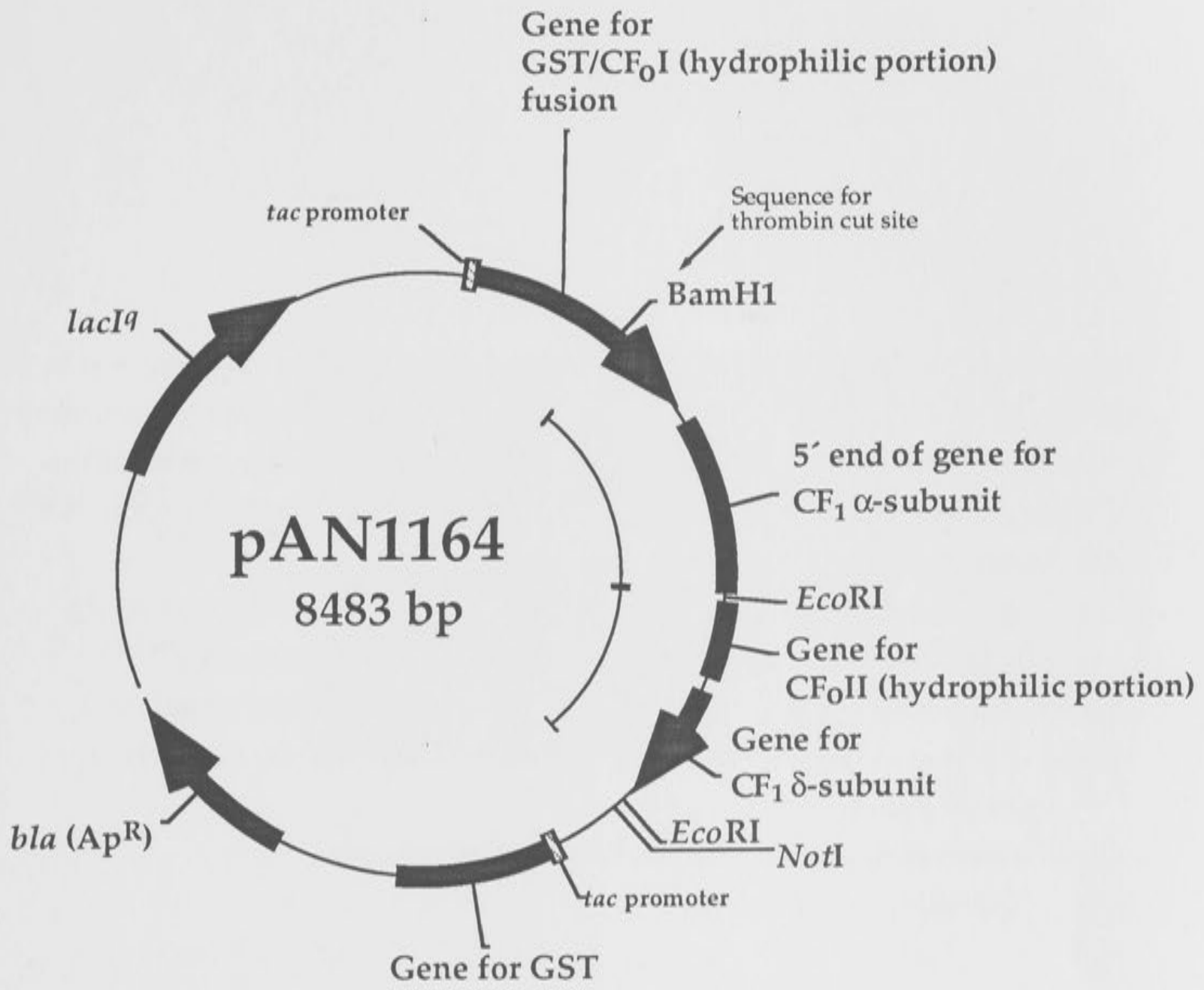


**Figure 4.14**: Plasmid pAN1164, which carries genes for a GST-spinach $CF_0I$ hydrophilic portion fusion, $CF_0II$ hydrophilic portion, the spinach chloroplast δ-subunit and GST.

**Figure 4.15** : SDS-PAGE analysis of samples collected at the various steps in the attempted purification of the GST-$CF_oI$ hydrophilic portion fusion from strain AN3850. This strain contains plasmid pAN1164, which carries genes for the GST-$CF_oI$ hydrophilic portion fusion, the $CF_oII$ hydrophilic portion and the mature spinach chloroplast δ-subunit.

Lane 1: Molecular weight markers

Lane 2: Pellet following 39,000 x g centrifugation of disrupted cells

Lane 3: Supernatant following 39,000 x g centrifugation of disrupted cells

Lane 4: Unbound material following exposure of supernatant (Lane 3) to glutathione agarose beads

Lane 5: Material bound to the glutathione agarose beads

Lane 6: Molecular weight markers

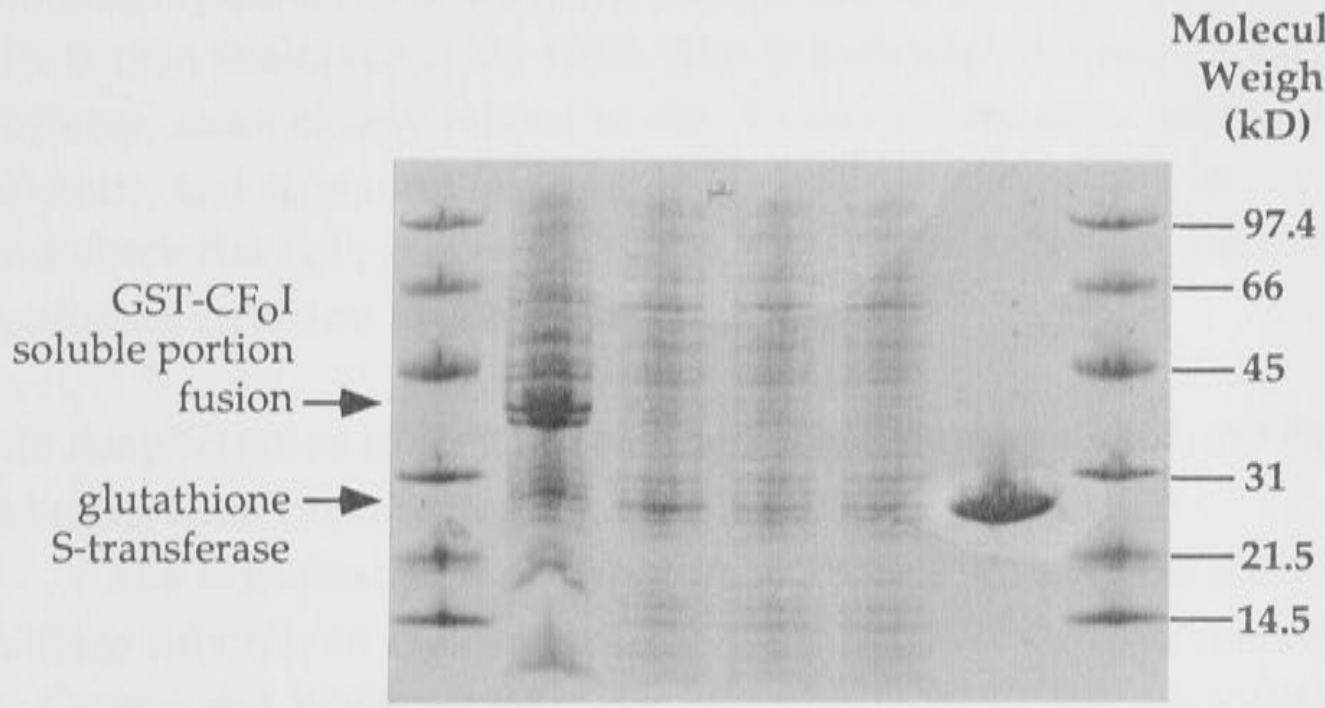
Molecular Weight (kD)
GST-CF$_O$I soluble portion fusion
glutathione S-transferase
97.4
66
45
31
21.5
14.5

## EXPRESSION OF *SYNECHOCOCCUS* R2 ATP SYNTHASE SUBUNITS AS FUSION PROTEINS WITH GLUTATHIONE-*S*-TRANSFERASE

Results presented in previous sections show that even when expressed as fusions with GST, a protein freely soluble in *E. coli*, and in the presence of the chaperonins groES and groEL, all spinach chloroplast proteins expressed were either insoluble, or in the case of the ε-subunit, possibly incorrectly folded. It was hoped, however, that the expression of homologous $F_OF_1$-ATPase subunits from cyanobacteria may be more successful. Judging by amino acid sequence homologies of $F_OF_1$-ATPase subunits, cyanobacteria are more closely related to *E. coli* than are higher plants (van Walraven *et al.*, 1993). The cyanobacterial subunits are, however, more closely related to the chloroplast subunits than to *E. coli* subunits, and structural information gained from the study of cyanobacterial $F_OF_1$-ATPase subunits may therefore be also useful in predicting structure in the chloroplast enzyme.

### 4.19 Amplification of genes encoding *Synechococcus* R2 $F_OF_1$-ATPase subunits from cyanobacterial genomic DNA

The organization and complete sequences of the genes for $F_OF_1$-ATPase subunits in the cyanobacterium *Synechococcus* 6301 were described by Cozens and Walker (1987). The genes for $F_OF_1$-ATPase subunits in *Synechococcus* 6301 are arranged in two clusters. The smaller cluster containing the genes encoding the β and ε subunits is separated from the other containing the genes encoding the *a*, *c*, *b´*, *b*, δ, α and γ subunits by at least 15 kb of DNA (Cozens and Walker, 1987).

Genomic DNA extracted from the closely related species *Synechococcus* R2 was provided as a kind gift from Dr. Dean Price, Research School of Biological Sciences, Australian National University. It was presumed that a very close similarity would exist between the nucleotide sequences of the two *Synechococcus* species, and that this would allow oligonucleotide primers designed from the published sequence of *Synechococcus* 6301 to be employed successfully in the amplification of genes for $F_OF_1$-ATPase subunits from *Synechococcus* R2 genomic DNA.

Two oligonucleotide primers were designed with the aim of amplifying a fragment carrying the *atpB* and *atpE* genes encoding the *Synechococcus* R2 $F_OF_1$-ATPase β- and ε- subunits. Oligonucleotide AR26 has a sequence identical to the region 73 to 39 bases 5´ of the start codon for the *atpB* gene, except that an *Eco*RI site is introduced at 57 to 51 bases 5´ of the start codon for the *atpB* gene. Oligonucleotide AR27 has a sequence

complementary to the region 2-35 bases 3′ of the stop codon for the *atpE* gene, except that an *Eco*RI site is introduced 16-22 bases 3′ of the stop codon for the *atpE* gene.

Using *Synechococcus* R2 genomic DNA as template and oligonucleotides AR26 and AR27 as primers, a 2019 bp fragment was amplified. This fragment was purified and digested with the enzyme *Eco*RI, and cloned into the *Eco*RI site of the vector pUC18. Restriction analysis identified a clone with insert in the correct orientation for expression of the *Synechococcus* R2 $F_OF_1$-ATPase β- and ε-subunits from the *lac* promoter of the vector. This plasmid was named pAN975.

PCR was used to amplify a fragment carrying the genes encoding the δ-, α- and γ-subunits of the *Synechococcus* R2 $F_OF_1$-ATPase. For this purpose, oligonucleotide AR28 was designed with a sequence identical to the region 56 to 23 bases upstream from the start codon of the gene for the *Synechococcus* 6301 δ-subunit, except that an *Xba*I site was introduced in bases 35 to 41 upstream from the δ-subunit start codon, and oligonucleotide AR29 was designed with a sequence complementary to the region 26-53 bases downstream of the *atpC* gene, which incorporates a pre-existing *Eco*RI site. Using *Synechococcus* R2 genomic DNA as template and oligonucleotides AR28 and AR29 as primers, the polymerase chain reaction was used to amplify an approximately 3.2kb fragment. This fragment was digested with the enzymes *Xba*I and *Eco*RI, and subcloned into the *Xba*I and *Eco*RI sites of the vector pUC19. Nucleotide sequencing of part of the insert and analysis of DNA digested with a variety of restriction enzymes confirmed that the 3.2kb insert carried the genes for the *Synechococcus* R2 $F_1$ subunits δ, α and γ. This plasmid was named pAN1035.

**4.20 Construction of a plasmid co-expressing a GST-*Synechococcus* R2 γ fusion with the *Synechococcus* R2 ε-subunit and GST.**

Although interaction between the γ- and ε-subunits from *E. coli* and chloroplast $F_OF_1$-ATPases has been established experimentally (Dunn, 1982; Cox *et al.*, 1993; McCarty, 1992), no such information is available regarding the properties of these subunits from cyanobacteria. The isolation of a complex of *Synechococcus* γ- and ε-subunits would therefore provide novel information on the subunit architecture in the cyanobacterial enzyme. If any complexes could be purified, a number of analytical techniques (eg. circular dichroism spectroscopy, analytical ultracentrifugation and X-ray crystallography) could be employed to study structure *in vitro*, and thereby

provide information relevant to the overall structure of the enzyme complex *in vivo*.

To test whether a complex between the *Synechococcus* R2 γ- and ε-subunits could be purified, a plasmid co-expressing a GST-*Synechococcus* R2 γ-subunit fusion with the *Synechococcus* R2 ε-subunit and GST was constructed. For this purpose, oligonucleotide AR30 was designed with a 20 base region at the 3′ end with a sequence identical to the first 20 bases of the *atpE* gene. Immediately preceding this region is the *uncE* pregenic region, modified to include a *Sal*I site. Oligonucleotide AR31 has a sequence at the 3′ end complementary to the last 20 bases of the *atpE* coding region, extending to 10 bases downstream of the *atpE* stop codon. This was preceded by a sequence including a *Not*I site.

Using oligonucleotides AR30 and AR31 as primers, and plasmid pAN975 as template, PCR was carried out to amplify the 480bp fragment with the gene for the ε-subunit, preceded by the *uncE* pregenic region. The fragment was digested with the enzymes *Sal*I and *Not*I, and ligated into the *Sal*I and *Not*I sites of the plasmid pAN990. This plasmid was named pAN1068.

The expression of the *Synechococcus* R2 $F_OF_1$-ATPase γ-subunit as a GST fusion protein required the gene for the γ-subunit to be cloned into the *Bam*HI and *Eco*RI sites of plasmid pAN1068. The presence of a *Bam*HI site within the coding sequence of the gene for the γ-subunit, 579 bases downstream from the start codon, complicated this procedure. In order to remove the internal *Bam*HI site, a two-step process using the polymerase chain reaction was carried out. Oligonucleotide AR32 was designed with a sequence identical to the region from 24 bases upstream of the start codon to 18 bases into the gene, except that a *Bam*HI site is introduced in the six bases immediately upstream of the start codon. Two oligonucleotides of complementary sequence, AR33 and AR34, were designed with a sequence straddling the internal *Bam*HI site, except that base 578 of the gene (G) is changed to A. This alters codon 193 from TTG to TTA, thus retaining leucine as the amino acid at this position.

Using plasmid pAN1035 as template (see section 4.19 above) and oligonucleotides AR32 and AR34 as primers, PCR was used to amplify a 618bp fragment encoding the 5′ end of the gene for the *Synechococcus* R2 γ-subunit. Using the same template, oligonucleotides AR33 and AR29 were then used to amplify a 431bp fragment encoding the 3′ end of the gene. The two amplification products were purified, mixed along with primers AR32

and AR29, heated to 94 °C, and cooled slowly to allow annealing of complementary regions at the ends of the fragments. The full length fragment lacking the internal *Bam*HI site was then amplified. This fragment was digested with the enzymes *Bam*HI and*Eco*RI, and subcloned into the *Bam*HI and*Eco*RI sites of plasmid pAN1068. This plasmid, named pAN1069, carries genes for a GST-*Synechococcus* R2 γ fusion, the *Synechococcus* R2 ε-subunit and GST(see Figure 4.16), and was used to transform strain AN3347 to create strain AN3827.

The whole cell protein content of strain AN3827, before and after addition to a culture of 0.1 mM IPTG, was analysed by SDS-PAGE (see Figure 4. 17). The induction of the *tac* promoters results in the increased expression of proteins with approximate molecular masss of 60 kDa, 15 kDa and 26 kDa, corresponding to the GST/γ fusion, the ε-subunit and the free GST.

**4.21 Attempted purification of a complex of the *Synechococcus* R2 γ- and ε-subunits from strain AN3827.**

A large scale culture of strain AN3827 was grown as described in section 2.23. Samples collected at various steps in the procedure for purification of the GST fusion protein were analysed by SDS-PAGE (see Fig 4.17a). The lane with material from the pellet following the 39,000 x *g* centrifugation step has a band at a molecular mass similar to that predicted for the γ-GST fusion (61 kDa), indicating that at least some of this protein is insoluble and may form inclusion bodies. Most of the fusion protein was soluble, but only a small proportion bound to the glutathione agarose beads following exposure to the supernatant, and the majority remained in the unbound fraction. A number of slightly smaller proteins, possibly degraded fusion protein, also bound to the beads. None of the ε-subunit (predicted molecular mass 14.8 kDa) appeared to bind, indicating that a complex of the γ- and ε-subunits was not formed.

The glutathione agarose beads were suspended in 10 mL STEM buffer, and human thrombin was added to a concentration of 20 U/mL. The suspension was rocked gently in a 50 mL polypropylene tube at 25 °C for two hours. Samples of the material bound to the beads following thrombin digestion and the supernatant following centrifugation to remove the beads were analysed by SDS-PAGE (see Figure 4.17.b). The supernatant contains, in addition to several higher molecular mass proteins of unknown identity, a protein of approximately 35 kDa which may be the *Synechococcus* R2 γ-subunit. Time constraints prevented the further characterisation of this protein.

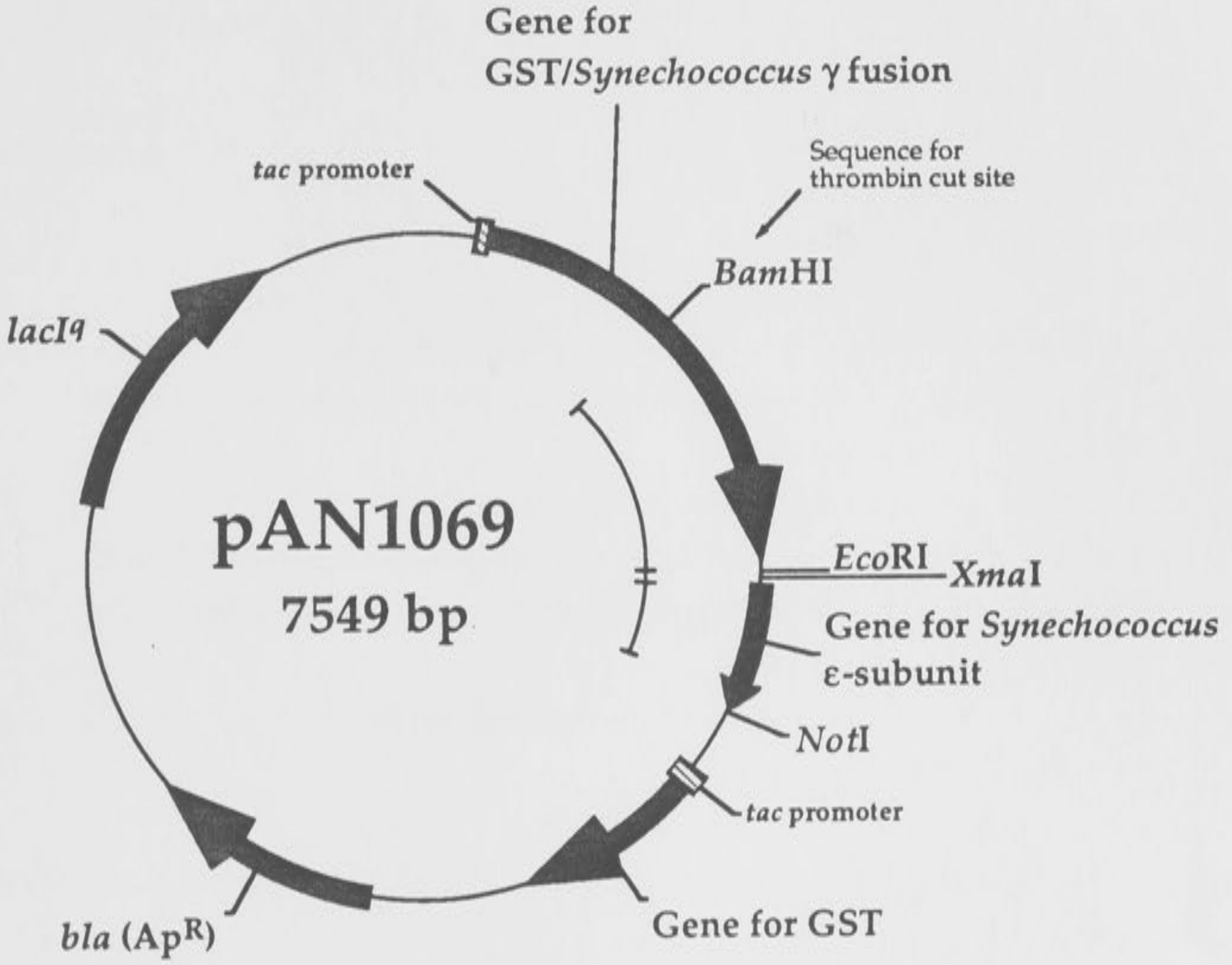


**Figure 4.16**: Plasmid pAN1069, which carries genes for a GST-*Synechococcus* γ-subunit fusion, the free *Synechococcus* ε-subunit and GST.

**Figure 4.17 (a)**:
Lanes 1-3: SDS-PAGE analysis of whole cell protein content of strain AN3827, before and after addition to a culture of 0.1 mM IPTG
Lane 1: Molecular weight markers
Lane 2: AN3827 whole cell protein content prior to IPTG addition
Lane 3: AN3827 whole cell protein content after IPTG addition

Lanes 4-9: SDS-PAGE analysis of samples collected at the various steps in the purification of a GST-*Synechococcus* R2 γ-subunit fusion from strain AN3827:
Lane 4: Molecular weight markers
Lane 5: Pellet following 39,000 x g centrifugation of disrupted cells
Lane 6: Supernatant following 39,000 x g centrifugation of disrupted cells
Lane 7: Unbound material following exposure of supernatant (Lane 6) to glutathione agarose beads
Lane 8: Material bound to the glutathione agarose beads
Lane 9: Molecular weight markers

**Figure 4.17 (b)**: Effect of thrombin addition to material bound to the glutathione agarose beads:
Lane 1: Material bound to the glutathione agarose beads following incubation with 20 U/mL thrombin at 25°C for two hours
Lane 2: Material in supernatant following centrifugation to remove glutathione agarose beads
Lane 3: Molecular weight markers

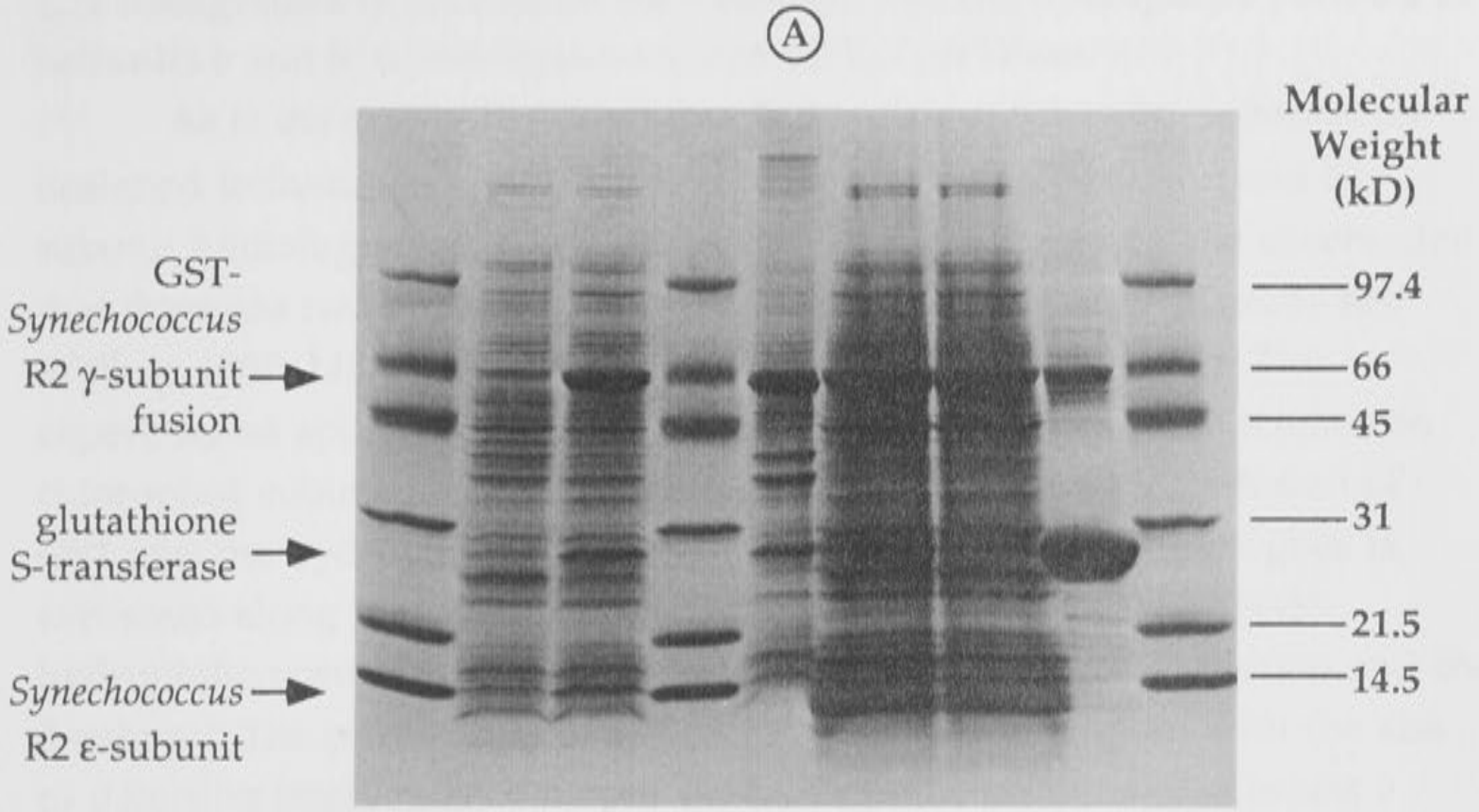
A
Molecular Weight (kD)
GST-Synechococcus R2 γ-subunit fusion
glutathione S-transferase
Synechococcus R2 ε-subunit
97.4
66
45
31
21.5
14.5

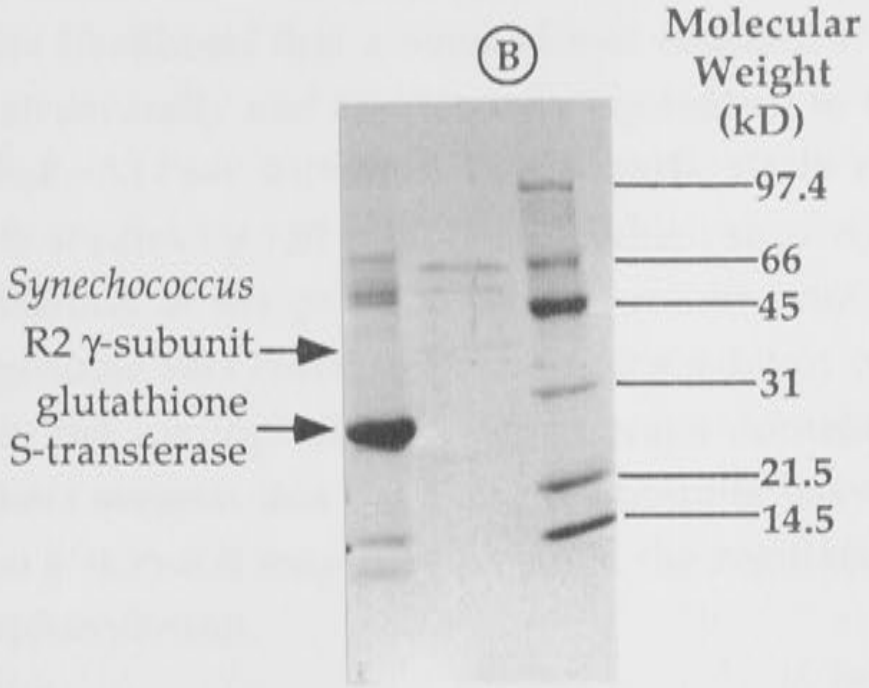
B
Molecular Weight (kD)
Synechococcus R2 γ-subunit
glutathione S-transferase
97.4
66
45
31
21.5
14.5

**4.22 Background to studies on the δ-subunit and the hydrophilic portions of subunits *b* and *b´* of the *Synechococcus* R2 $F_OF_1$-ATPase.**

As is the case with chloroplast $F_OF_1$-ATPase subunits, experiments designed to investigate possible interactions between *b*-subunit and δ-subunit homologues from cyanobacteria are complicated by the observation that there are two apparent *b*-subunit homologues, *b* and *b´* (Cozens and Walker, 1987; Lill and Nelson, 1991; van Walraven *et al.*, 1993). The experimental approach adopted was similar to that used in the studies on chloroplast subunits. Plasmids were constructed from which a fusion of GST and the hydrophilic portion of one of the *b*-subunit homologues is expressed along with the δ-subunit, and in one case a GST-*b*-subunit hydrophilic portion is expressed with the free *b´* hydrophilic portion and the δ-subunit. The purification of fusion proteins was attempted with the aim of detecting interactions between the hydrophilic portions of subunits *b* and/or *b´* and the δ-subunit from *Synechococcus* R2.

If any complexes could be purified, a number of analytical techniques (eg. circular dichroism spectroscopy, analytical ultracentrifugation and X-ray crystallography) could be employed to study structure *in vitro*, and thereby provide information relevant to the overall structure of the enzyme complex *in vivo*. For example, sedimentation equilibrium analytical ultracentrifugation could be used to study whether the hydrophilic portions of *b* and *b´* form homo- or heterodimers in solution, a question relevant in assessing the likelihood that a heterodimer of *b* and *b´* in the cyanobacterial enzyme is structurally and functionally equivalent to the two *b*-subunits of the *E. coli* $F_OF_1$-ATPase complex. This is particularly relevant following mutagenesis studies by Lill *et al.* (1994), which showed that although complete deletion of the gene for the *b´*-subunit from the *Synechocystis* sp. PCC 6803 genome was lethal to the cells, the subunit could be truncated leaving only the hydrophobic transmembrane domain with little effect. These workers suggest that the *b* and *b´*-subunits have different functions, and that the *b´*-subunit may play a role in the regulation of photophosphorylation.

**4.23 Attempted purification of a complex of the hydrophilic portions of the *Synechococcus* R2 *b*- and *b´*-subunits from strain AN3798.**

Plasmid pAN1007, constructed by Dr. Susan Howitt in this laboratory, has a gene for a fusion of the *Schistosoma japonicum* GST with the hydrophilic portion of the *Synechococcus* R2 *b*-subunit (amino acid residues

47-171, with leucine residues 47 and 48 replaced by glycine and serine, respectively), followed by the *uncE* pregenic region, followed by a gene for the hydrophilic portion of the *b´* subunit (amino acid residues 46-158, with lysine-46 replaced by methionine). This plasmid was constructed from the vector pAN990 (see section 4.9 above).

Plasmid pAN1007 (shown in Fig 4.18) was used to transform strain AN3347 to create strain AN3798. A large scale culture of strain AN3798 was grown as described in section 2.23. Proteins from samples collected at various steps in the procedure for purification of GST fusion proteins were analysed by SDS-PAGE (see Fig 4.19.a). The lane with material from the pellet following the 39,000 x *g* centrifugation step shows a band at a molecular mass similar to that predicted for the GST-*Synechococcus* R2 *b* -subunit hydrophilic portion fusion (40 kDa), indicating that at least some of this protein is insoluble and may form inclusion bodies. There was, however, some protein of this molecular mass in the supernatant following the centrifugation. The glutathione agarose beads exposed to the supernatant bound the 40 kDa protein in addition to the 27 kDa free GST also expressed from the plasmid. There was, however, no trace of any 12.5 kDa *Synechococcus* R2 *b´*- subunit hydrophilic portion having bound to the beads.

The glutathione agarose beads were suspended in 10 mL STEM buffer, and human thrombin was added to a concentration of 20 U/mL. The suspension was rocked gently in a 50mL polypropylene tube at 25 °C for two hours. Samples of the material bound to the beads following thrombin digestion and the supernatant following centrifugation to remove the beads were analysed by SDS-PAGE (see Figure 4.19.b). The digestion of the fusion protein is complete but the major cleavage product in the supernatant is much smaller than the 13.6 kDa *Synechococcus* R2 *b* -subunit hydrophilic portion (appears to be less than 8 kDa). Analysis of the amino acid sequence shows that there are no thrombin cleavage sites in the fusion protein other than that designed to separate the GST and the *Synechococcus* R2 *b* -subunit hydrophilic portion. There is therefore no apparent explanation for the degradation of the protein upon exposure to thrombin.

**4.24 Construction of a plasmid co-expressing a GST-*Synechococcus* R2 *b* subunit (hydrophilic portion) fusion with the *Synechococcus* R2 *b´* (hydrophilic portion) and δ-subunits, and GST.**

A plasmid was constructed to co-express a GST-*Synechococcus* R2 *b*-subunit hydrophilic portion fusion with the *Synechococcus* R2 *b´*-

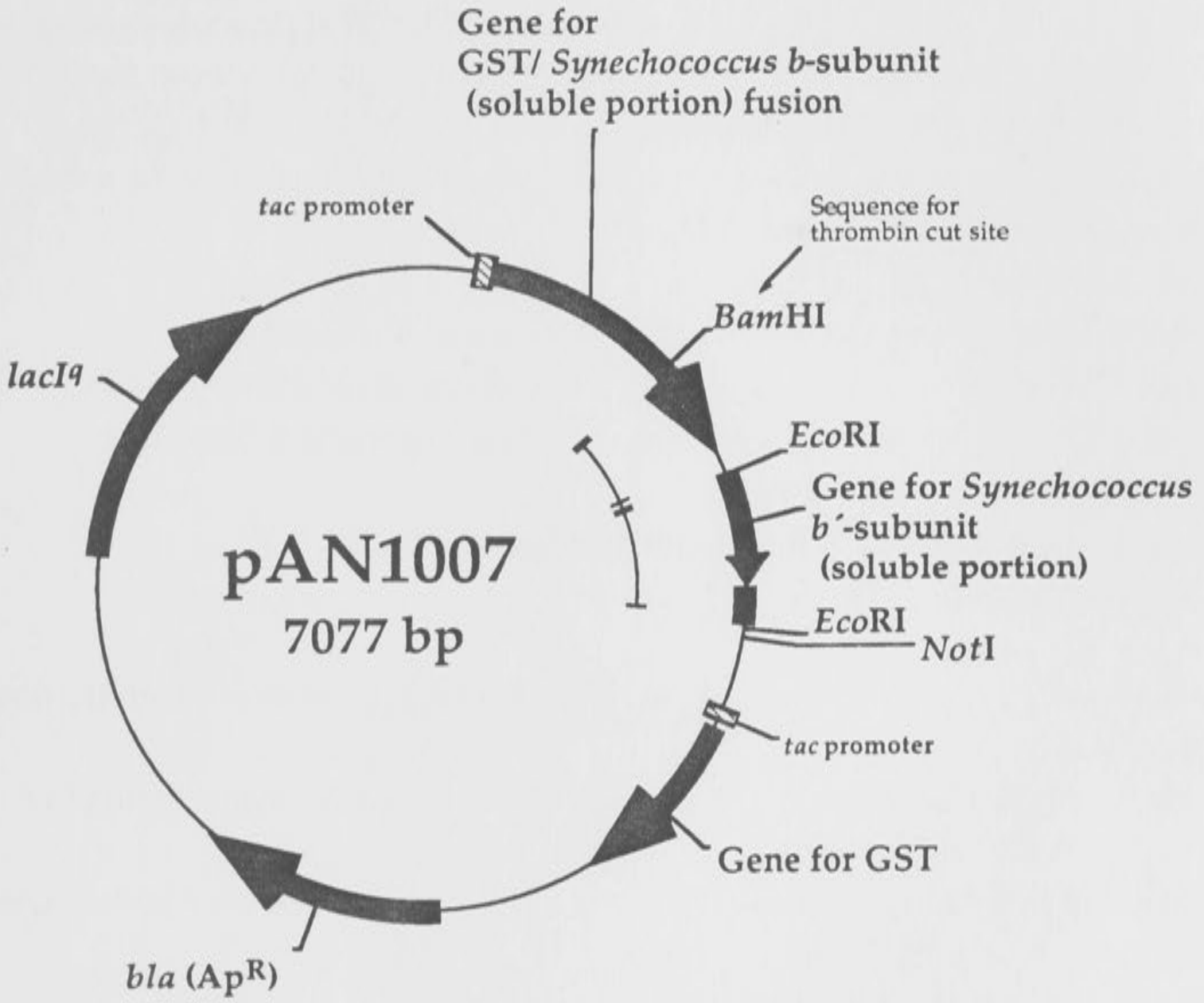


**Figure 4.18**: Plasmid pAN1007, which carries genes for a GST- *Synechococcus b*-subunit (soluble portion) fusion, the *Synechococcus b´*-subunit (soluble portion) and GST.

**Figure 4.19 (a)**: SDS-PAGE analysis of samples collected at the various steps in the purification of a GST-*Synechococcus* R2 *b* -subunit soluble portion fusion from strain AN3798. This strain contains plasmid pAN1007, which carries genes for a GST-*Synechococcus* R2 *b* -subunit soluble portion fusion, the soluble portion of the *b´* subunit, and GST.

Lane 1: Molecular weight markers

Lane 2: Pellet following 39,000 x g centrifugation of disrupted cells

Lane 3: Supernatant following 39,000 x g centrifugation of disrupted cells

Lane 4: Unbound material following exposure of supernatant (Lane 3) to glutathione agarose beads

Lane 5: Material bound to the glutathione agarose beads

Lane 6: Molecular weight markers

**Figure 4.19 (b)**: Effect of thrombin addition to material bound to the glutathione agarose beads:

Lane 1: Material bound to the glutathione agarose beads following incubation with 20 U/mL thrombin at 25°C for two hours

Lane 2: Material in supernatant following centrifugation to remove glutathione agarose beads

Lane 3: Molecular weight markers

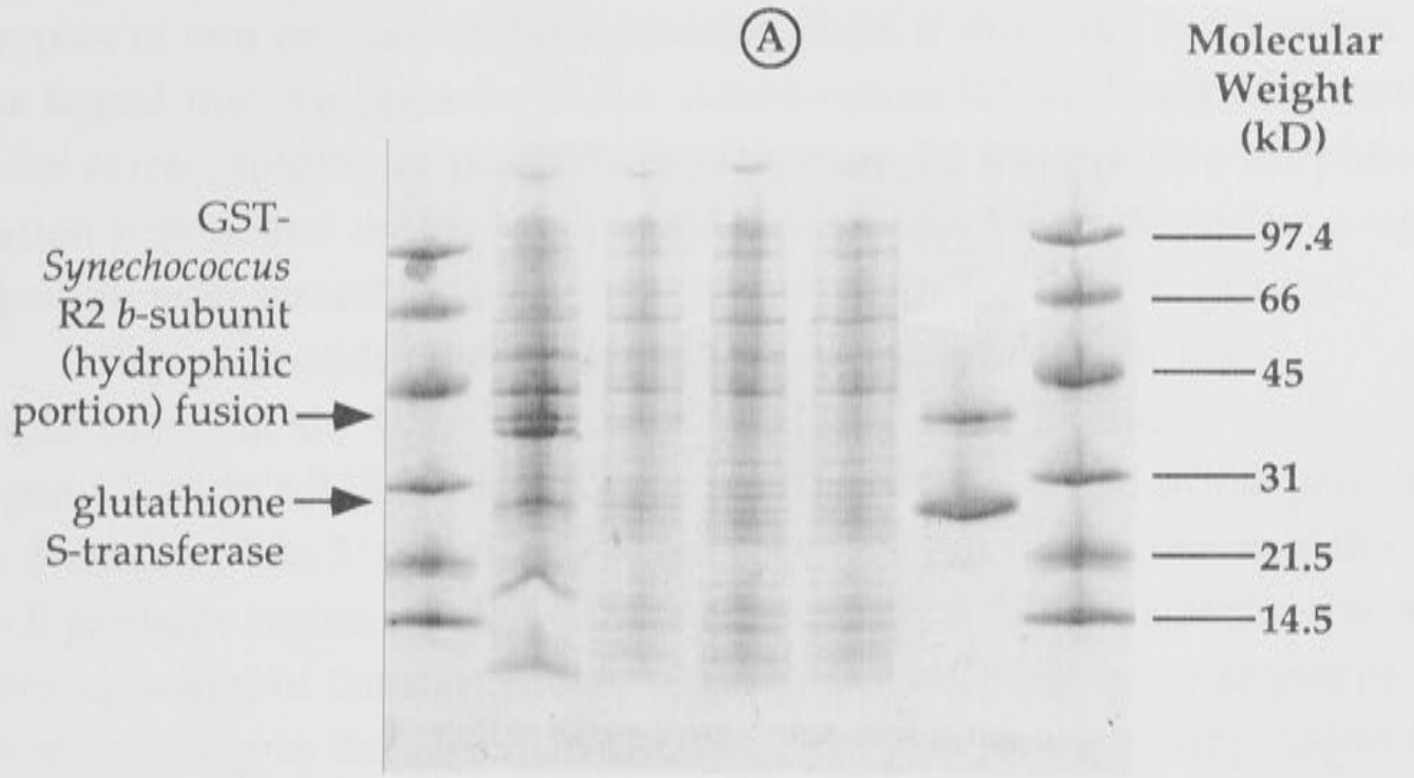
A
Molecular Weight (kD)
GST-Synechococcus R2 b-subunit (hydrophilic portion) fusion
glutathione S-transferase
97.4
66
45
31
21.5
14.5

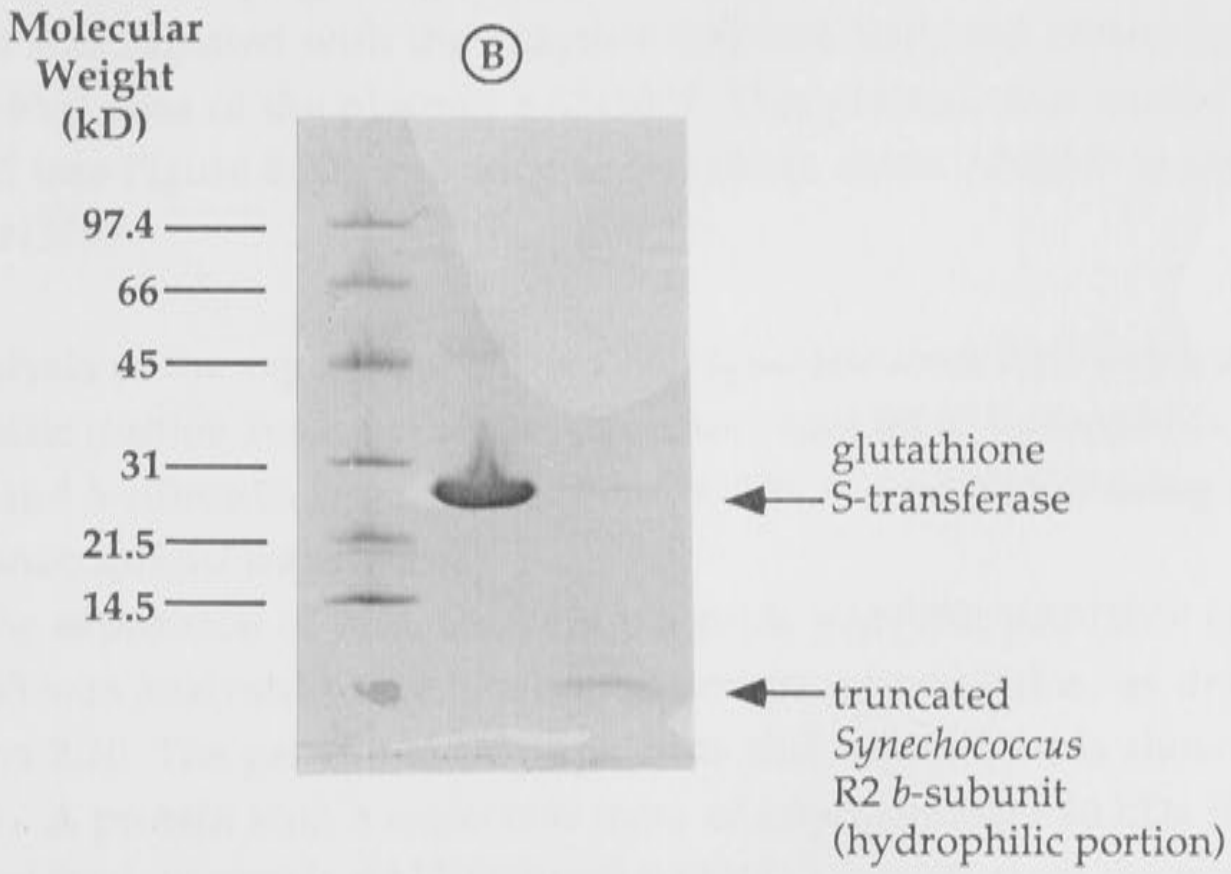
B
Molecular Weight (kD)
97.4
66
45
31
21.5
14.5
glutathione S-transferase
truncated Synechococcus R2 b-subunit (hydrophilic portion)

hydrophilic portion, the δ-subunit and GST, with the aim of purifying a complex of two or more of these proteins. Even if this were not possible, it was hoped that the presence of the *Synechococcus* R2 δ-subunit may assist in the correct folding of the GST-*Synechococcus* R2 *b*-subunit hydrophilic portion fusion, and render this protein less susceptible to degradation upon digestion with thrombin (see section above), allowing it to be purified.

Oligonucleotides were designed for use as primers for the amplification of the *Synechococcus* R2 δ-subunit. The 3´ end of oligonucleotide AR35 has a sequence identical to the 5´ end of the gene for the δ-subunit. The 5´ end of the oligonucleotide has the sequence of the *uncE* pregenic region, altered only to incorporate a *Sal*I recognition site 30-24 bases upstream of the start codon. Oligonucleotide AR36 has a sequence complementary to the region 26-67 bases downstream of the stop codon for the δ-subunit, except that a *Not*I recognition site is introduced 39-47 bases downstream of the stop codon. Using plasmid pAN1035 as template (see section 4.19 above) and oligonucleotides AR35 and AR36 as primers, polymerase chain reaction was carried out with *Pfu* polymerase to amplify a 655bp fragment carrying the gene for the *Synechococcus* R2 δ-subunit. This fragment was digested with the enzymes *Sal*I and *Not*I, and cloned into the *Sal*I and *Not*I sites of the plasmid pAN1007. This plasmid was named pAN1133 (see Figure 4.20), and used to transform strain AN3347 to create strain AN3797.

**4.25 Analysis of the expression of the GST-*Synechococcus* R2 *b* subunit hydrophilic portion fusion with the *Synechococcus* R2 *b´* hydrophilic portion and δ-subunits from plasmids pAN1007 and pAN1133 using *in vitro* transcription/ translation.**

The expression of proteins from plasmids pAN990, pAN1007 and pAN1133 was analysed using *in vitro* transcription/translation, as described in section 2.20. The gel autoradiograph from this experiment is shown in Fig. 4.21. A protein with a molecular mass of approximately 40 kDa is expressed from plasmids pAN1007 and pAN1133 (which carry the gene for the GST-*Synechococcus* R2 *b* subunit hydrophilic portion fusion) which is not expressed from the vector pAN990. This size is similar to the 41 kDa molecular mass predicted for the GST-*b* subunit hydrophilic portion fusion.

A protein with a molecular mass of approximately 20 kDa is expressed from plasmid pAN1133 (which carries the gene for the *Synechococcus* R2 δ-subunit) which is not expressed from the vector pAN990 or plasmid

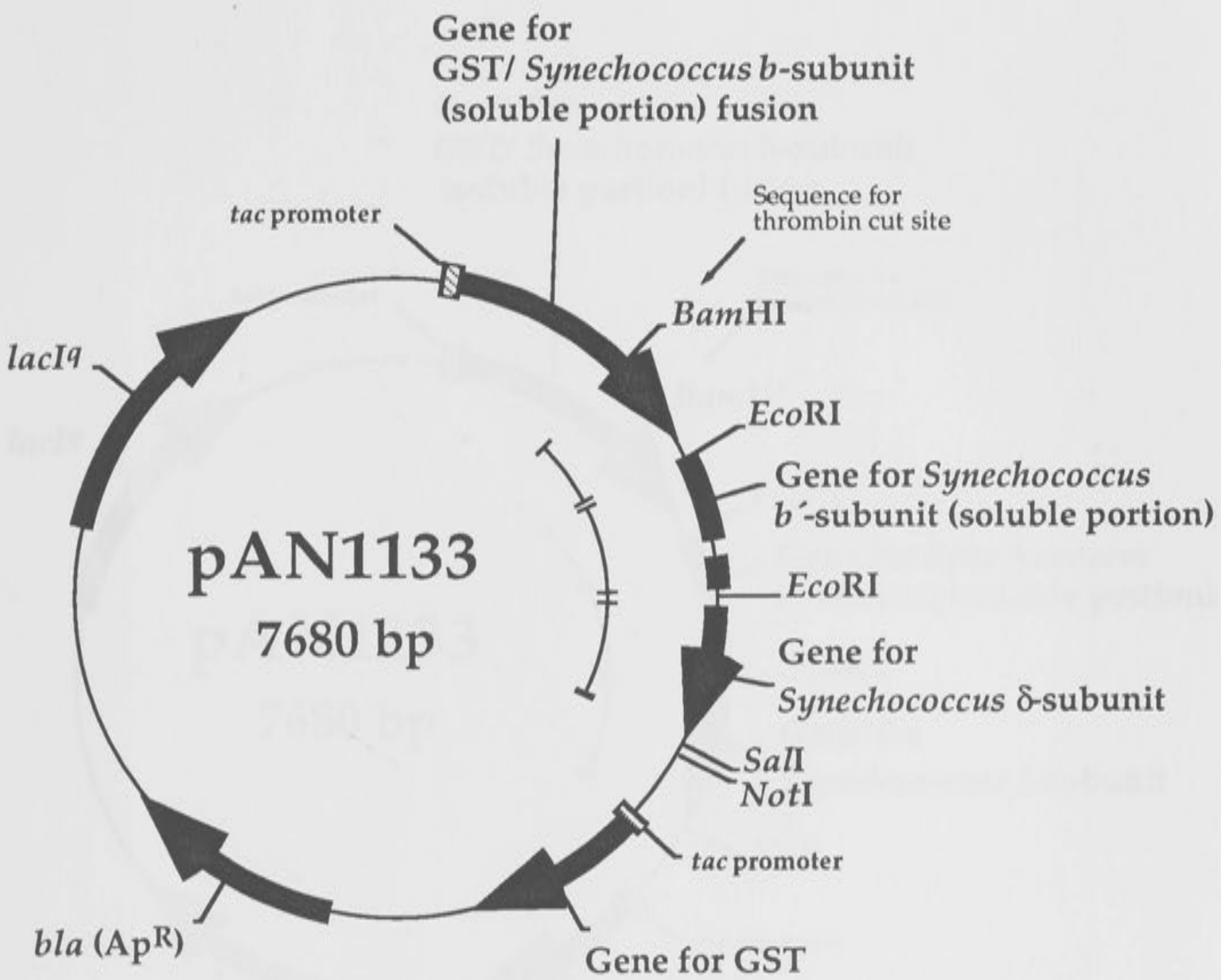


**Figure 4.20**: Plasmid pAN1133, which carries genes for a GST- *Synechococcus b*-subunit (soluble portion) fusion, the *Synechococcus b´*-subunit (soluble portion), the *Synechococcus* δ-subunit and GST.

**Figure 4.21**: Autoradiograph of an SDS-PAGE gel with *in vitro* transcription/translation products from the vector pAN990, plasmid pAN1007 (which carries genes for the GST-*Synechococcus* R2 *b* -subunit hydrophilic portion fusion, the *b´*-subunit hydrophilic portion and GST) and pAN1133 (which carries the genes for the GST-*Synechococcus* R2 *b*-subunit hydrophilic portion fusion, the *b´*-subunit hydrophilic portion, the δ-subunit and GST).

Lane 1: pAN990
Lane 2: pAN1007
Lane 3: pAN1133

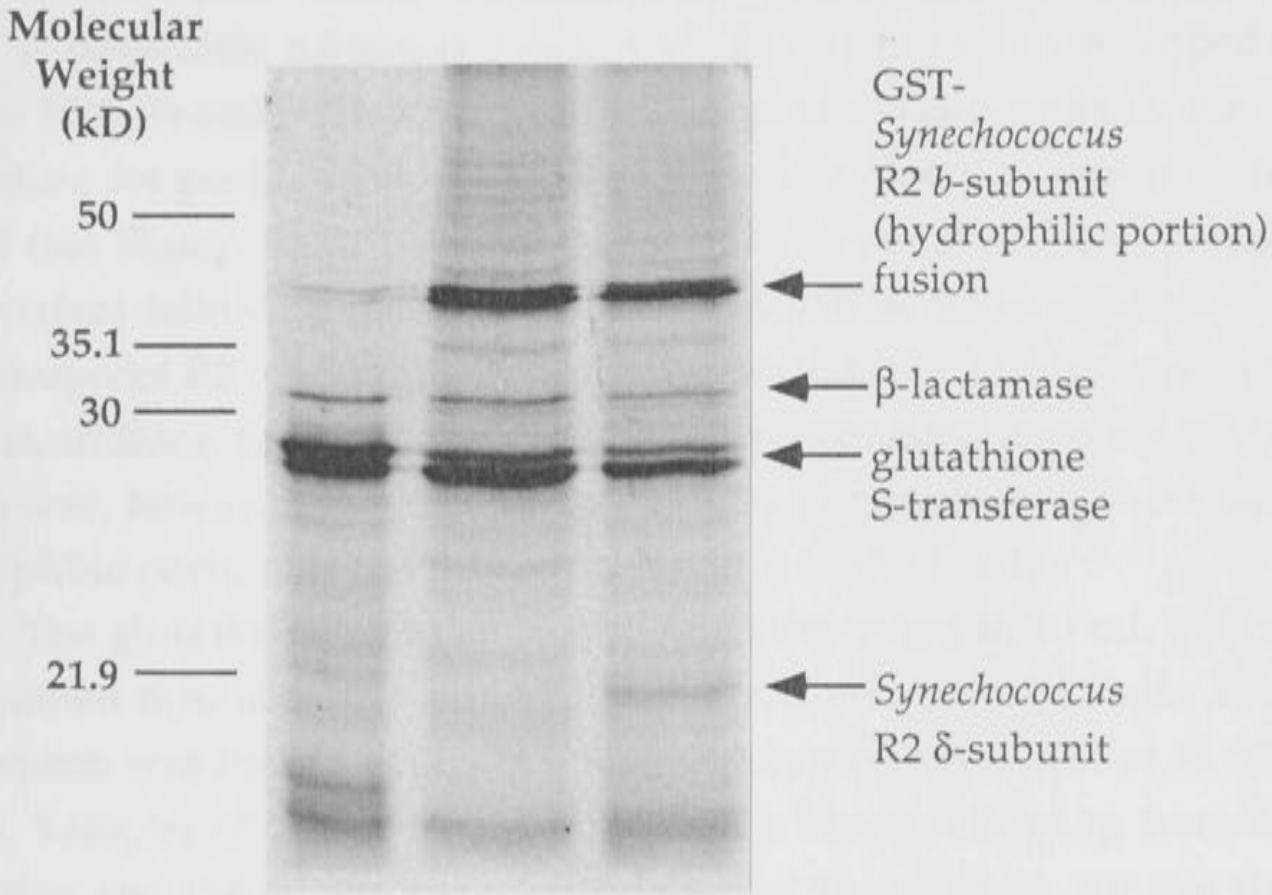
Molecular Weight (kD)
50
35.1
30
21.9
GST-
Synechococcus
R2 b-subunit
(hydrophilic portion)
fusion
β-lactamase
glutathione
S-transferase
Synechococcus
R2 δ-subunit

pAN1007. This size is similar to the 19.5kDa molecular mass predicted for the *Synechococcus* R2 δ-subunit.

The hydrophilic portion of the *Synechococcus* R2 $F_OF_1$-ATPase *b´* subunit does not contain methionine residues other than the formylated N-terminal residue. If this residue is cleaved in the *in vitro* transcription/ translation reaction, this may explain the absence of a band for this protein on the autoradiograph.

**4.26 Attempted purification of a complex of the hydrophilic portions of the *Synechococcus* R2 *b*- and *b´*- subunits and the δ-subunit from strain AN3797.**

A large scale culture of strain AN3798 was grown as described in section 2.23. Proteins from samples collected at various steps in the procedure for purification of GST fusion proteins were analysed by SDS-PAGE (see Figure 4.22). The glutathione agarose beads exposed to the supernatant following the 39,000 x *g* centrifugation step bound the *Synechococcus* R2 *b* -subunit hydrophilic portion-GST fusion protein (41 kDa) in addition to the 27 kDa free GST also expressed from the plasmid. There was, however, no trace of any 14 kDa *Synechococcus* R2 *b´*- subunit hydrophilic portion or the δ-subunit binding to the beads.

The glutathione agarose beads were suspended in 10 mL STEM buffer, and human thrombin was added to a concentration of 20 U/mL. The suspension was rocked gently in a 50 mL polypropylene tube at 25 °C for two hours. Samples of the material bound to the beads following thrombin digestion and the supernatant following centrifugation to remove the beads were analysed by SDS-PAGE (see Figure 4.22). A band at a molecular mass very similar to that predicted for the *b*-subunit hydrophilic portion (13.6 kDa) appears in the supernatant lane. This contrasts with the results from experiments involving strain AN3798 (see Fig. 4.19), which does not express the δ-subunit. Although the δ-subunit has not formed a complex with the *b*-subunit hydrophilic portion, the presence of the δ-subunit during the *in vivo* synthesis of the *b*-subunit hydrophilic portion appears to have assisted in its correct folding, such that it is no longer susceptible to degradation by thrombin during the incubation to cleave off the GST moiety of the fusion protein.

Due to time constraints, the further purification and characterisation of the *Synechococcus* R2 *b* -subunit hydrophilic portion was not attempted.

**Figure 4.22**: Lanes 1-4 show the SDS-PAGE analysis of samples collected at the various steps in the purification of a GST-*Synechococcus* R2 *b*-subunit (hydrophilic portion) fusion from strain AN3797. This strain contains plasmid pAN1133, which carries genes for a GST-*Synechococcus* R2 *b*-subunit (hydrophilic portion) fusion, the *Synechococcus* R2 *b´*-subunit (hydrophilic portion) and the *Synechococcus* R2 δ-subunit:

Lane 1: Molecular weight markers

Lane 2: Pellet following 39,000 x g centrifugation of disrupted cells

Lane 3: Supernatant following 39,000 x g centrifugation of disrupted cells

Lane 4: Unbound material following exposure of supernatant (Lane 3) to glutathione agarose beads

Lane 5: Material bound to the glutathione agarose beads

Lanes 6 and 7 show the effect of thrombin addition to material bound to the glutathione agarose beads:

Lane 6: Material bound to the glutathione agarose beads following incubation with 20 U/mL thrombin at 25°C for two hours

Lane 7: Material in supernatant following centrifugation to remove glutathione agarose beads

Lane 8: Molecular weight markers

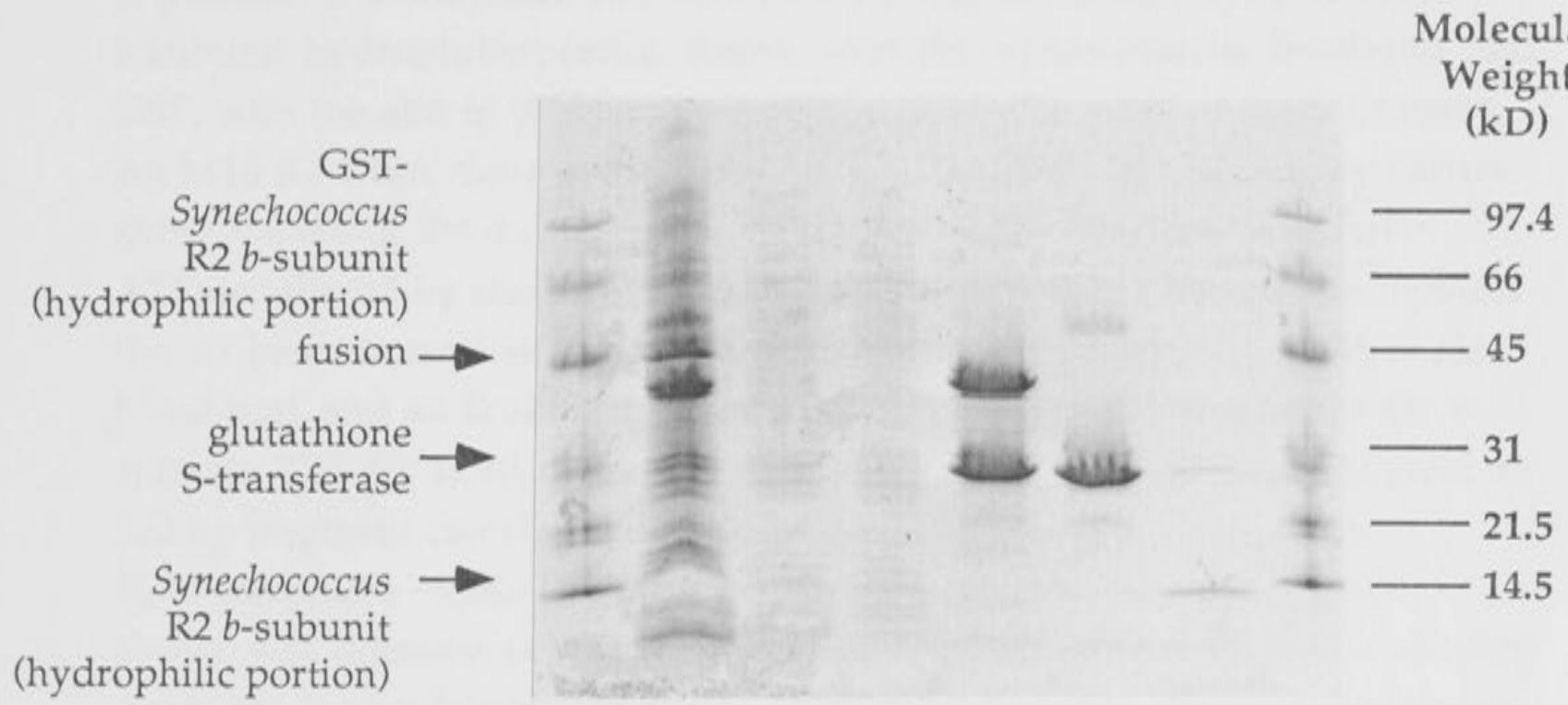
Molecular Weight (kD)
GST-
Synechococcus
R2 b-subunit
(hydrophilic portion)
fusion
glutathione
S-transferase
Synechococcus
R2 b-subunit
(hydrophilic portion)
97.4
66
45
31
21.5
14.5

**4.27 Construction of a plasmid co-expressing a GST-*Synechococcus* R2 *b´*-subunit (hydrophilic portion) fusion with the *Synechococcus* R2 δ-subunit and GST.**

As discussed in section 4.22 above, mutagenesis studies by Lill *et al.* (1994) suggest that the *Synechococcus* R2 *b*- and *b´*-subunits may play markedly different roles in the cyanobacterial $F_OF_1$-ATPase complex, with the *b´*-subunit possibly involved in regulation. It was therefore thought worthwhile to purify the *b´*-subunit in large amounts for detailed physical characterisation. The question of whether this subunit carries or contributes to a binding site for the δ-subunit was also thought worthy of investigation. A plasmid was therefore constructed to co-express a GST-*Synechococcus* *b´*subunit hydrophilic portion fusion with the *Synechococcus* δ-subunit and GST, with the aim of purifying a complex of two or more of these proteins. An M13 RF DNA clone constructed by R. Witham in this laboratory carries genes encoding the *a*-, *c*-, *b´*- and *b*-subunits of the *Synechococcus* $F_OF_1$-ATPase, altered by site-directed mutagenesis such that a *Bam*HI site replaces the six bases immediately preceding the codon for phenylalanine-48 of the *b´*-subunit, and an *Eco*RI site replaces codons 139-144 of the gene for the *b*-subunit. This RF DNA clone was digested with *Bam*HI and *Eco*RI to yield a 522 bp fragment carrying the gene for the hydrophilic portion of the *Synechococcus* *b´*-subunit. Plasmid pAN1133, described in section 4.21 above, was digested with *Bam*HI and *Eco*RI to remove the fragment carrying genes for the hydrophilic portions of the *Synechococcus* *b*- and *b´*-subunits. The 522 bp fragment was cloned into the purified remaining portion of the vector, which includes the gene for *Synechococcus* δ-subunit. The resulting plasmid, named pAN1160 (see Fig. 4.23), carries genes for a GST-*Synechococcus* *b´*subunit hydrophilic portion fusion, the *Synechococcus* δ-subunit and GST, and was used to transform strain AN3347 to create strain AN3846.

**4.28 Attempted purification of a complex of the hydrophilic portions of the *Synechococcus* R2 *b´*- and δ-subunits from strain AN3846.**

A large scale culture of strain AN3846 was grown as described in section 2.23. Proteins from samples collected at various steps in the procedure for purification of GST fusion proteins were analysed by SDS-PAGE (see Figure 4.24.a). The glutathione agarose beads exposed to the supernatant following the 39,000 x *g* centrifugation step bound the GST-*Synechococcus* R2 *b´*-subunit hydrophilic portion fusion (39 kDa) in

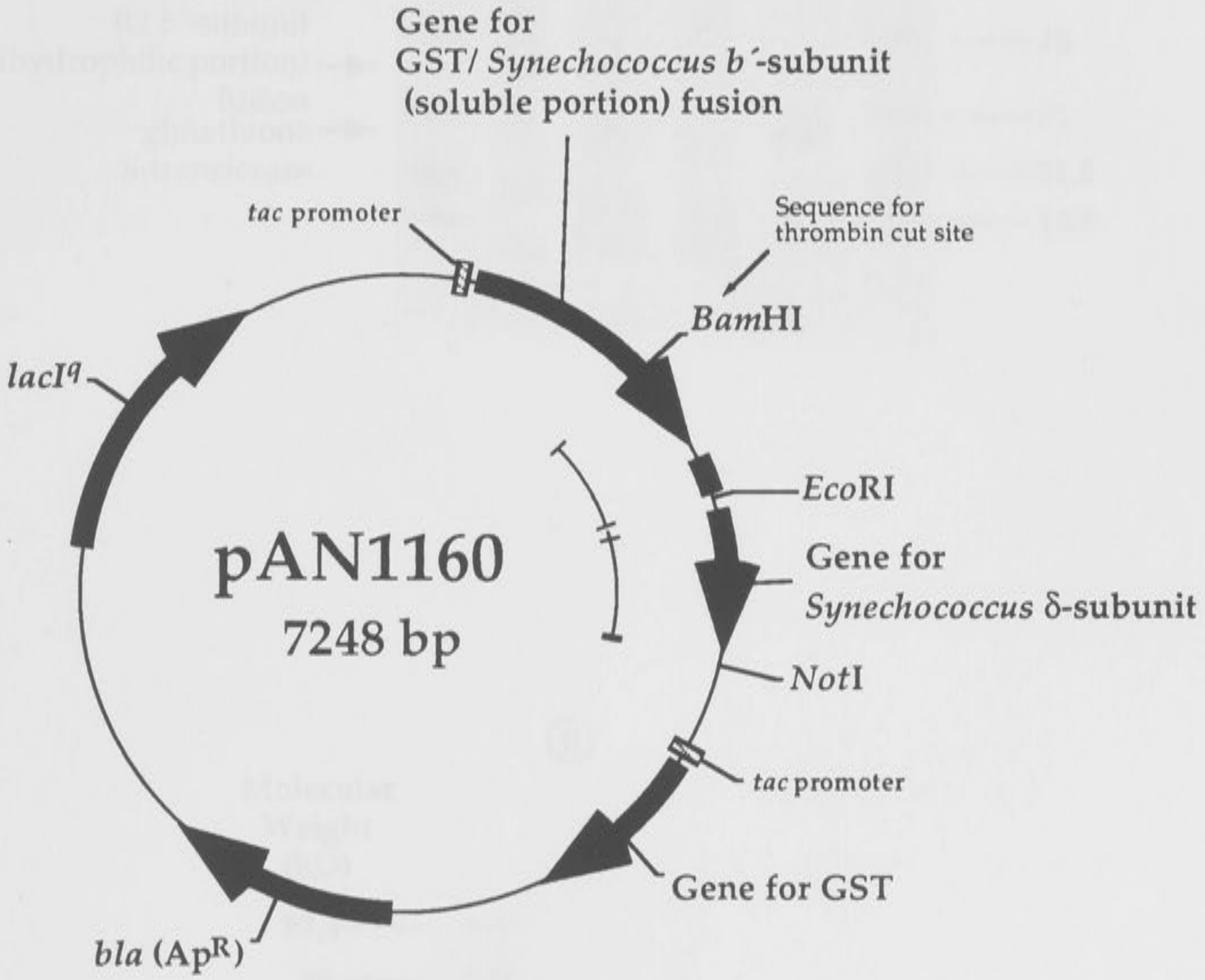


**Figure 4.23**: Plasmid pAN1160, which carries genes for a GST- *Synechococcus b´*-subunit (soluble portion) fusion, the *Synechococcus* δ-subunit and GST.

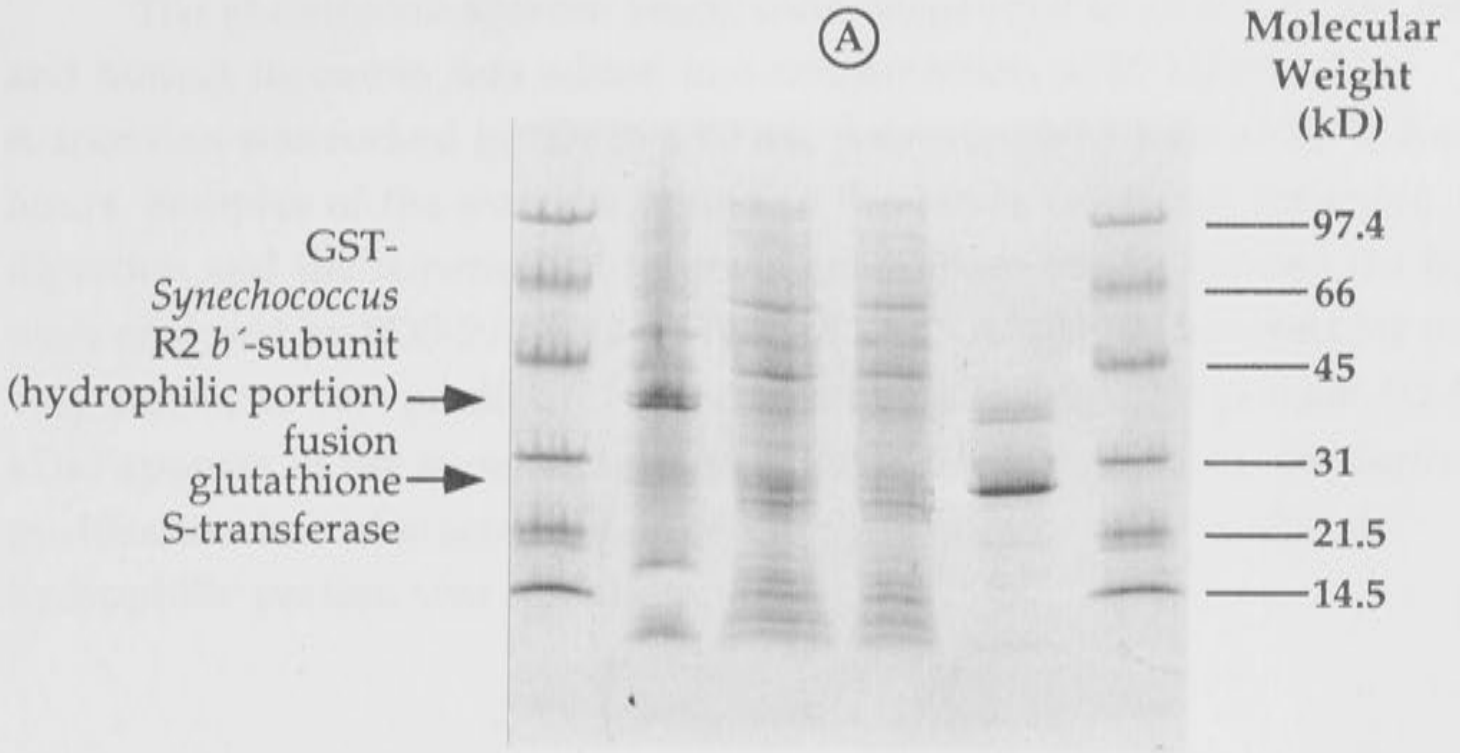
A
Molecular Weight (kD)
GST-
Synechococcus
R2 b´-subunit
(hydrophilic portion)
fusion
glutathione
S-transferase
97.4
66
45
31
21.5
14.5

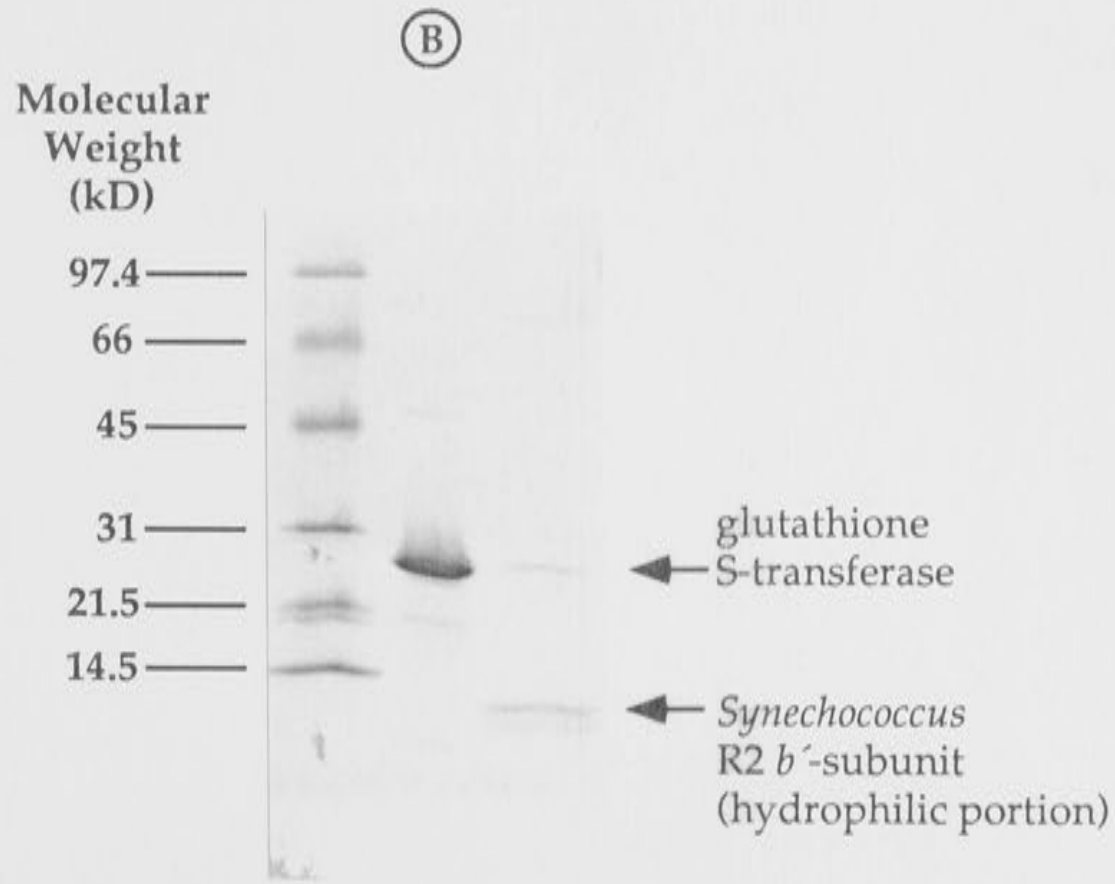
B
Molecular Weight (kD)
97.4
66
45
31
21.5
14.5
glutathione
S-transferase
Synechococcus
R2 b´-subunit
(hydrophilic portion)

addition to the 27 kDa free GST also expressed from the plasmid. There was, however, no trace of any of the δ-subunit binding to the beads.

The glutathione agarose beads were suspended in 10 mL STEM buffer, and human thrombin was added to a concentration of 20 U/mL. The suspension was rocked gently in a 50 mL polypropylene tube at 25 °C for two hours. Samples of the material bound to the beads following thrombin digestion and the supernatant following centrifugation to remove the beads were analysed by SDS-PAGE (see Figure 4.24.b). A band at a molecular mass very similar to that predicted for the *b´*-subunit hydrophilic portion (12.5 kDa) appears in the supernatant lane. Due to time constraints, the further purification and characterisation of the *Synechococcus* R2 *b´*-subunit hydrophilic portion was not attempted.

→ see back 2 pages

**Figure 4.24 (a)**: SDS-PAGE analysis of samples collected at the various steps in the purification of a GST-*Synechococcus* R2 *b´*-subunit (hydrophilic portion) fusion from strain AN3830. This strain contains plasmid pAN1160, which carries genes for a GST-*Synechococcus* R2 *b´*-subunit (hydrophilic portion) fusion, the *Synechococcus* R2 δ-subunit and GST:

Lane 1: Molecular weight markers

Lane 2: Pellet following 39,000 x g centrifugation of disrupted cells

Lane 3: Supernatant following 39,000 x g centrifugation of disrupted cells

Lane 4: Unbound material following exposure of supernatant (Lane 3) to glutathione agarose beads

Lane 5: Material bound to the glutathione agarose beads

Lane 6: Molecular weight markers

**Figure 4.24 (b)**: Effect of thrombin addition to material bound to the glutathione agarose beads:

Lane 1: Molecular weight markers

Lane 2: Material bound to the glutathione agarose beads following incubation with 20 U/mL thrombin at 25°C for two hours

Lane 3: Material in supernatant following centrifugation to remove glutathione agarose beads

**4.29 Discussion**

The goal of work described in this chapter was to isolate complexes of spinach chloroplast and cyanobacterial $F_OF_1$-ATPase subunits, and thereby gain information on the structural and functional relationships between subunits in the enzyme complex. Considering the large amount of work involved, the results overall were disappointing. However, results provided some evidence of intersubunit interactions.

Work with the spinach chloroplast $F_OF_1$-ATPase subunits highlighted a major problem often encountered when the expression of foreign proteins in *E. coli* is attempted. This relates to the insolubility of many foreign proteins when expressed in *E. coli* (Marston, 1986), and the formation in some cases of inclusion bodies in the cell. If this occurs, the recombinant protein must be solubilised from the inclusion bodies by denaturing detergents, or solubilised by chaotropic agents such as urea or guanidinium chloride, and refolded subsequently in the hope of regaining the native structure. In the studies described in this chapter, however, the expressed proteins have no enzymic activity which may be assayed, and it is therefore difficult to asses whether the native structure has been regained. Frangioni and Neel (1993) showed that the the anionic detergent sarkosyl (*N*-laurylsarcosine) can be used to solubilise many GST fusion proteins, and that subsequent treatment with a non-ionic detergent such as Triton X-100 allows the sarkosyl solubilised GST fusion protein to bind to glutathione agarose beads. These authors claim that fusion proteins purified in this way retain enzymatic activity. The solubilisation of the insoluble fusions of GST and the spinach chloroplast $F_OF_1$-ATPase subunits could be attempted, but it would be difficult to assess whether material solubilised by sarkosyl had retained native conformation.

The spinach chloroplast proteins studied in this work had a greater tendency to form inclusion bodies than was the case with the cyanobacterial proteins. This may be a reflection of the closer evolutionary relationship between *E. coli* and the cyanobacterium. Of all of the spinach chloroplast $F_OF_1$-ATPase subunits studied in this work, only the ε-subunit was soluble when expressed as a fusion with GST. However, digestion of the fusion protein by thrombin was very slow. Although digestion by thrombin of a GST-*E. coli* ε-subunit fusion is also rather slow (R. G. Solomon, personal communication), the poor cutting of the GST-chloroplast ε-subunit fusion may be due to the ε-subunit moiety of the fusion protein having folded in such a way as to prevent access by thrombin to its cleavage site at the junction with the GST moiety. The *E. coli* ε-subunit, with which the

conservative amino acid substitutions are taken into account (Zurawski *et al.*, 1982) appears to form an almost spherical globular shape (Sternweis and Smith, 1980). If the spinach chloroplast ε-subunit has a similar structure and is correctly folded, the ε-subunit moiety of a fusion protein would therefore be unlikely to restrict thrombin access to its cleavage site. It is therefore possible that the ε-subunit moiety has folded incorrectly, despite the fusion protein remaining soluble when expressed in *E. coli*. Incorrect folding of the GST-ε-subunit fusion may in part explain why the spinach chloroplast γ-subunit failed to bind to the GST-ε-subunit fusion when expressed from the same plasmid, although the presence of all or part the GST-ε-subunit was shown to stabilise the structure of the γ-subunit. An experiment which could provide more information would involve the construction of another plasmid in which a sequence encoding a short stretch of amino acids is inserted immediately downstream of the sequence encoding the thrombin cleavage site. If this stretch of amino acids were chosen specifically such that they would form an α-helical segment, this could serve to physically separate the GST and ε-subunit moieties, and possibly allow access of thrombin to its cleavage site. Alternatively, a plasmid could be constructed to allow expression of the ε-subunit with an N-terminal polyhistidine tag to facilitate purification by $Ni^{2+}$ affinity chromatography. In contrast to the GST, the polyhistidine region is small and does not need to form a particular conformation to bind the affinity column. Steric interference between the binding region and the complex may therefore be reduced. This approach could also solve the second problem observed with purification of the chloroplast ε-subunit. The small amount of free ε-subunit that was produced by cleavage of the GST fusion remained associated with the fusion protein or the glutathione agarose beads to which it was attached. Alternative methods of affinity chromatography may allow soluble chloroplast ε-subunit to be purified more efficiently.

The GST-γ-subunit fusion was not soluble and appears to have formed inclusion bodies in the *E. coli* cells in which it was expressed. It was hoped that if the fusion could be solubilised using non-denaturing detergents and purified by glutathione-agarose affinity chromatography, its interaction with the ε-subunit may be strong enough for the two proteins to be co-purified. The GST-γ-subunit fusion was, however, resistant to solubilisation by the four detergents used. The fusions of GST and the extramembranous domains of subunits $CF_oI$ and $CF_oII$ were also insoluble when expressed in *E. coli* cells. The fusion proteins were also resistant to solubilisation by the four non-denaturing detergents used. This prevented

any assessment of whether the δ-subunit could form complexes with the extramembranous domains of subunits $CF_oI$ and $CF_oII$, when expressed either alone or in combination. Future experiments will involve the use of concentrated urea to solubilise the insoluble fusion proteins GST-chloroplast γ, GST-$CF_oI$ and GST-$CF_oII$, the removal of the urea by dialysis, and hopefully the recovery of soluble proteins amenable to structural analysis.

Experiments with cyanobacterial $F_oF_1$-ATPase subunits appear to hold more promise for providing valuable structural information in the future. The GST-γ-subunit fusion, although soluble, appears not to bind glutathione agarose beads well. This may be due to the γ-subunit moiety of the fusion folding in such a way as to partially block the glutathione binding site on GST. The digestion with thrombin of material bound to the beads yields a protein with approximately the molecular mass of the γ-subunit, but further experiments are required to confirm its identity and investigate its physical properties. An experiment which could provide more information would involve the insertion of a stretch of amino acids predicted to form an α-helical segment to physically separate the GST and γ-subunit moieties (as discussed above for the spinach chloroplast ε-subunit).

Comparison of experiments involving the expression of a GST-*Synechococcus* R2 *b*-subunit hydrophilic portion fusion with the *Synechococcus* R2 *b´*-subunit hydrophilic portion with and without the δ-subunit suggest a possible role for the δ-subunit in assisting the correct folding of the *b*-subunit hydrophilic portion moiety. The δ-subunit did not co-purify with the *b*- subunit hydrophilic portion, and these proteins therefore do not appear to form a stable complex. The δ-subunit does appear, however, to allow the *b*-subunit hydrophilic portion to fold correctly, such that it is no longer susceptible to degradation by thrombin during the incubation to cleave off the GST moiety of the fusion protein. In this system, the δ-subunit may behave as a molecular chaperone, acting to stabilise the structure of the *b*-subunit hydrophilic portion as it is synthesised *in vivo* . According to this idea, the δ-subunit is capable of binding transiently to partly folded species of the *b*-subunit hydrophilic portion when these species are in isolation. When these proteins are packed within the native $F_oF_1$-ATPase complex, such interactions may form part of the multitude of intersubunit contacts which are doubtlessly involved in stabilising the structure of the whole enzyme.

Results from the purification of the hydrophilic portions of the *Synechococcus* R2 *b*- and *b´*-subunits raise interesting questions and provide many possibilities for further experimentation. Cleavage by thrombin of the GST-*Synechococcus* R2 *b*-subunit hydrophilic portion fusion purified from strain AN3797, which also carries genes for the *Synechococcus* R2 *b´*-subunit hydrophilic portion and the *Synechococcus* R2 δ-subunit, yields a single species of approximately 14 kDa, corresponding to the *b*-subunit hydrophilic portion. The *b´*-subunit hydrophilic portion is predicted to be 12.5 kDa in size, would be visible as a distinct band on the SDS-PAGE gel if it had bound to the *b*-subunit (hydrophilic portion) to form a heterodimer. This would indicate that either the *b*-subunit hydrophilic portion is present as a monomer or an aggregate of a single species (such as a homodimer), and suggests that if the whole *b*- and *b´*-subunits form a heterodimer in the $F_OF_1$-ATPase complex, formation of the dimer does not take place in the absence of other subunits or the transmembrane α-helix. Analysis of native molecular mass by sedimentation equilibrium analytical ultracentrifugation could be used to determine whether the purified *b*-subunit hydrophilic portion is present as a monomer or a higher polymer in solution. This technique could also be applied to the purified *b´*-subunit hydrophilic portion.

Comparisons between the structures of the *b*- and *b´*-subunits are particularly relevant following the mutagenesis studies by Lill *et al.* (1994), which showed the *b´*-subunit could be truncated leaving only the hydrophobic transmembrane domain with little effect on cell growth, and therefore suggest that the *b* and *b´*-subunits have different functions. These workers suggest that the *b´*-subunit may play a role in the regulation of photophosphorylation in the cyanobacterium. Detailed structural information on the *b´*-subunit is required to investigate this possibility further.

# CHAPTER 5

# STUDIES ON *ESCHERICHIA COLI* ATP SYNTHASE SUBUNITS EXPRESSED AS FUSION PROTEINS WITH GLUTATHIONE-*S*-TRANSFERASE

## 5.1 Introduction

As discussed in section 1.6, a model for the mechanism of the $F_OF_1$-ATPase (Cox *et al.*, 1984; 1986) proposed that an inner complex consisting of the two *b*-subunits, and the *a*-, γ-, δ- and ε-subunits rotated relative to an outer complex consisting of a ring of the *c*-subunits and the $\alpha_3\beta_3$ hexamer. According to this model, interactions between the *b*-subunit and the minor $F_1$ subunits (γ, δ and ε)are important to the binding of the $F_O$ and $F_1$ sectors of the enzyme, consistent with the role previously proposed for the *b*-subunit (Walker *et al.*, 1982; Perlin *et al.*, 1983; Senior, 1983). The aim of part of the work described in this chapter was therefore to co-express the soluble domain of the *b*-subunit with the γ-, δ- and ε-subunits, with the aim of purifying a complex consisting of two or more of these proteins. Particular attention was paid to isolating a complex of the δ-subunit and the soluble domain of the *b*-subunit. Both of these proteins are predicted from Chou-Fasman sequence analysis to be highly α-helical (Senior, 1983; Walker *et al.*, 1982b; 1984) and circular dichroism spectroscopy has been used to confirm that this is the case (Sternweis and Smith, 1977; Dunn, 1992). Suggestions have been made that these subunits form a complex via helix-helix interactions (Walker *et al.*,1984). In addition, results presented in the previous chapter suggested that the cyanobacterial δ-subunit may behave as a molecular chaperone, acting to stabilise the structure of the cyanobacterial *b* -subunit soluble portion when these proteins are expressed at high levels from the same plasmid.

The methodology employed in this work was to coexpress one or all of the minor $F_1$ subunits with a fusion of the *Schistosoma japonicum* GST and soluble domain of the *b*-subunit. The fusion protein was purified by affinity chromatography on glutathione-agarose, and analysed to investigate which if any of the minor $F_1$ subunits co-purified with it.

As discussed in section 1.3.8, an 'integrated membrane assembly pathway' proposed by Cox *et al.* (1981) provides a model for assembly *in vivo* of the *E. coli* $F_OF_1$-ATPase which prevents the formation of a proton permeable $F_O$ at any stage. Evidence for this comes from the study of mutants deficient in the α- and β-subunits. Two-dimensional SDS-PAGE of membrane proteins isolated from these strains revealed that the *b*-subunit was not incorporated into the membrane, and indicated that both the α- and β- subunits are required for this process (Cox *et al.*, 1981). These results clearly indicate that there are specific interactions between the *b*-subunit and the α- or β-subunits or both, at least during the assembly phase. The properties of a mutant strain affected in the *b*-subunit also indicate a specific interaction between the *b*-subunit and the α-subunit. The G9D mutation, encoded by the *uncF476* allele (Jans *et al.*, 1984), occurs in the N-terminal domain predicted to form a transmembrane α-helix (Walker *et al.*, 1982; Senior, 1983). The mutation prevents assembly of the *b*-subunit into the membrane when expressed in a haploid strain. This is not, however, caused by the thermodynamic barrier of inserting a charged residue into the membrane, since assembly does occur if the gene dosage is increased by expressing the mutant allele from a multicopy plasmid (Jans *et al.*, 1984). A partial revertant strain was isolated which retained the sequence of the *uncF476* allele, but carried a second mutation which, based on complementation analysis, was located in the *uncA* gene encoding the α-subunit. This indicated that the failure of the mutant *b*-subunit to assemble into the membrane was caused by altered interaction with the α-subunit (Jans *et al.*, 1984). Chemical cross-linking studies with the $F_OF_1$-ATPase produced a b-β dimer (Aris and Simoni, 1983), suggesting that these subunits are close in the whole enzyme. This chapter describes the co-expression of the hydrophilic domain of the *b*-subunit with the α- and β-subunits, with the aim of purifying a complex consisting of two or more of these proteins, which may correspond to an assembly intermediate *in vivo*.

**5.2 Construction of a plasmid co-expressing a GST-*E. coli* *b*-subunit hydrophilic portion fusion with the *E. coli* δ-subunit and GST.**

A plasmid was constructed to co-express a GST-*E. coli* *b*-subunit hydrophilic portion fusion with the *E. coli* δ-subunit and GST, with the aim of purifying a complex of two or more of these proteins.

Plasmid pAN736, constructed by B. Cromer in this laboratory, has a portion of the *uncF* gene (encoding the hydrophilic portion of the *E. coli* $F_OF_1$-ATPase *b*-subunit) fused to the gene for *S. japonicum* GST, and the *uncH* gene encoding the δ-subunit, in the vector pGEX-2T. The *uncH* gene is preceded by the 30 bp *uncE* pregenic region, inserted to enhance translation of the δ-subunit. (This plasmid has a *Bam*HI site in the six bases immediately preceding the codon for what would be leucine-29 in the full size *b*-subunit. When the *b*-subunit/GST fusion protein is purified from strains carrying this plasmid and digested with thrombin, the resulting *b*-subunit is therefore 131 amino acids long, and has glycine and serine preceding the leucine at the amino terminus). Plasmid pAN736 was digested to completion with *Bam*HI, then digested partially with *Eco*RI. The resulting fragments were separated by agarose gel electrophoresis. The 1.0 kb DNA fragment carrying the portion of the *uncF* gene encoding the hydrophilic portion of the *b*-subunit, and the *uncH* gene was excised from the gel and purified.

The vector pAN990 was digested with *Bam*HI and *Eco*RI. The 1.0 kb *Bam*HI/*Eco*RI fragment was ligated into the vector. The resulting plasmid, named pAN1157, carries genes for the GST-*E. coli* *b*-subunit hydrophilic portion fusion, the *E. coli* δ-subunit and GST (see Figure 5.1). Plasmid pAN1157 was used to transform strain AN3347 (genotype described in section 4.1) to create strain AN3843.

**5.3 Purification of the *E. coli* *b*-subunit hydrophilic portion from strain AN3843.**

A large scale culture of strain AN3843 was grown as described in section 2.23. Samples collected at various steps in the procedure for purification of the GST fusion protein (see section 2.25) were analysed by SDS-PAGE (see Figure 5.2.a). As with other gels described below, the sample of the pellet following the 39,000 x *g* centrifugation step was taken by scooping a small unmeasured amount into loading buffer, and was therefore not intended for quantitative comparisons. The δ-subunit and some of the GST-*b*-subunit hydrophilic portion fusion occurs in the pellet following the 39,000 x *g* centrifugation step, possibly due to the high

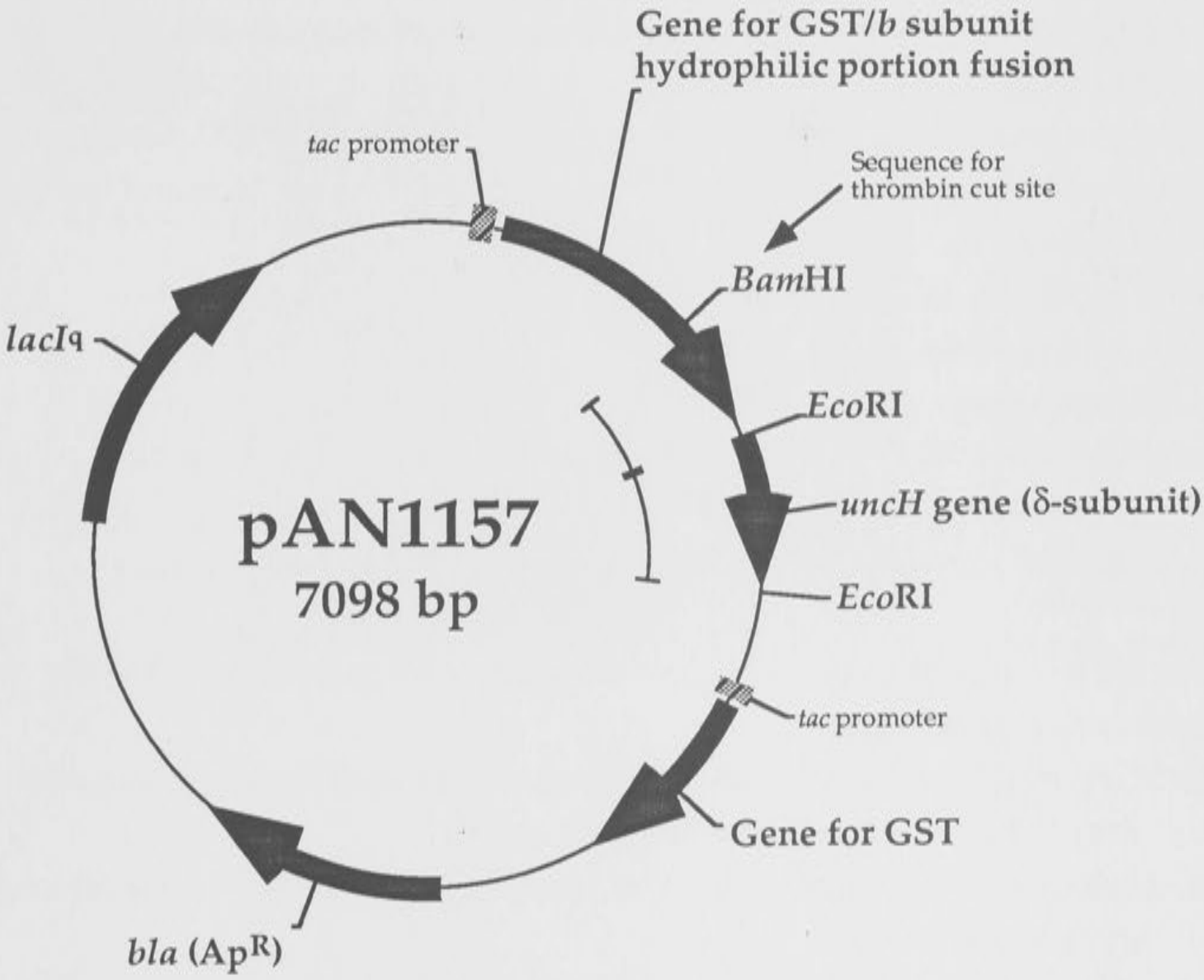


**Figure 5.1**: Plasmid pAN1157, which carries genes for a GST-*E. coli b*-subunit hydrophilic portion fusion, the δ-subunit and GST.

**Figure 5.2**: Lanes 1-4 show the SDS-PAGE analysis of samples collected at the various steps in the purification of a GST-*E. coli b*-subunit hydrophilic portion fusion from strain AN3843. This strain contains plasmid pAN1157, which carries genes for a GST-*E. coli b*-subunit hydrophilic portion fusion and the *E. coli* δ-subunit:

Lane 1: Molecular weight markers

Lane 2: Pellet following 39,000 x g centrifugation of disrupted cells

Lane 3: Supernatant following 39,000 x g centrifugation of disrupted cells

Lane 4: Unbound material following exposure of supernatant (Lane 3) to glutathione agarose beads

Lane 5: Material bound to the glutathione agarose beads

Lanes 6 and 7 show the effect of thrombin addition to material bound to the glutathione agarose beads:

Lane 6: Material bound to the glutathione agarose beads following incubation with 20 U/mL thrombin at 25°C for two hours

Lane 7: Material in supernatant following centrifugation to remove glutathione agarose beads

Lane 8: Molecular weight markers

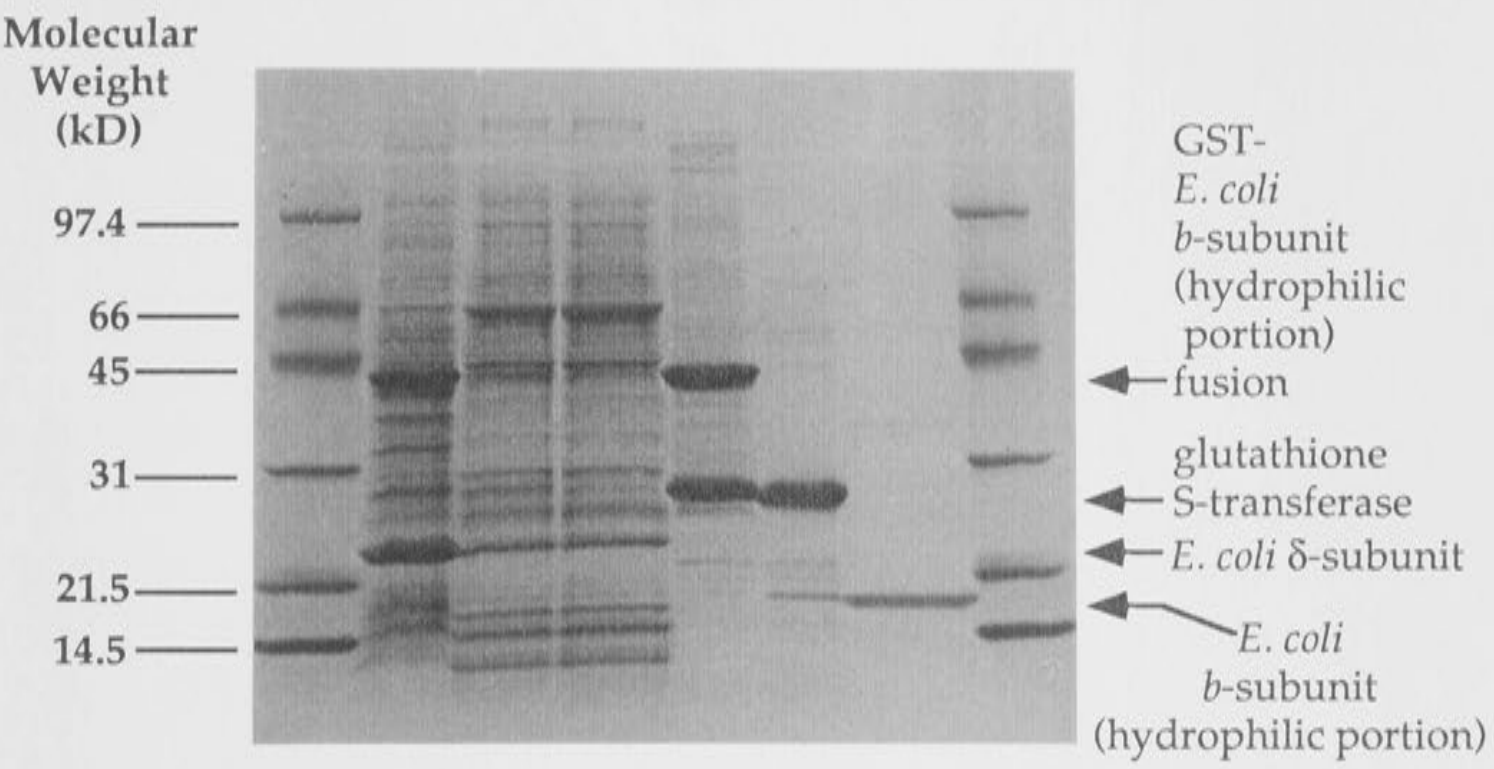
Molecular Weight (kD)
97.4
66
45
31
21.5
14.5
GST-
E. coli
b-subunit
(hydrophilic
portion)
fusion
glutathione
S-transferase
E. coli δ-subunit
E. coli
b-subunit
(hydrophilic portion)

**Figure 5.2 (b)**: Mass spectrometry analysis of a sample of the *E. coli* *b*-subunit (cytoplasmic portion), purified from strain AN3843, which co-expresses GST-*E. coli* *b*-subunit cytoplasmic portion fusion, the *E. coli* δ-subunit and GST. The crude preparation of the *b*-subunit cytoplasmic portion was purified to homogeneity on a gel-sieve HPLC prior to mass spectrometry analysis. The 7115 D and 14226 D peaks correspond to the doubly- and singly-protonated *E. coli* *b*-subunit (cytoplasmic portion) respectively. The 16948 D peak corresponds to the equine cardiac myoglobin standard.

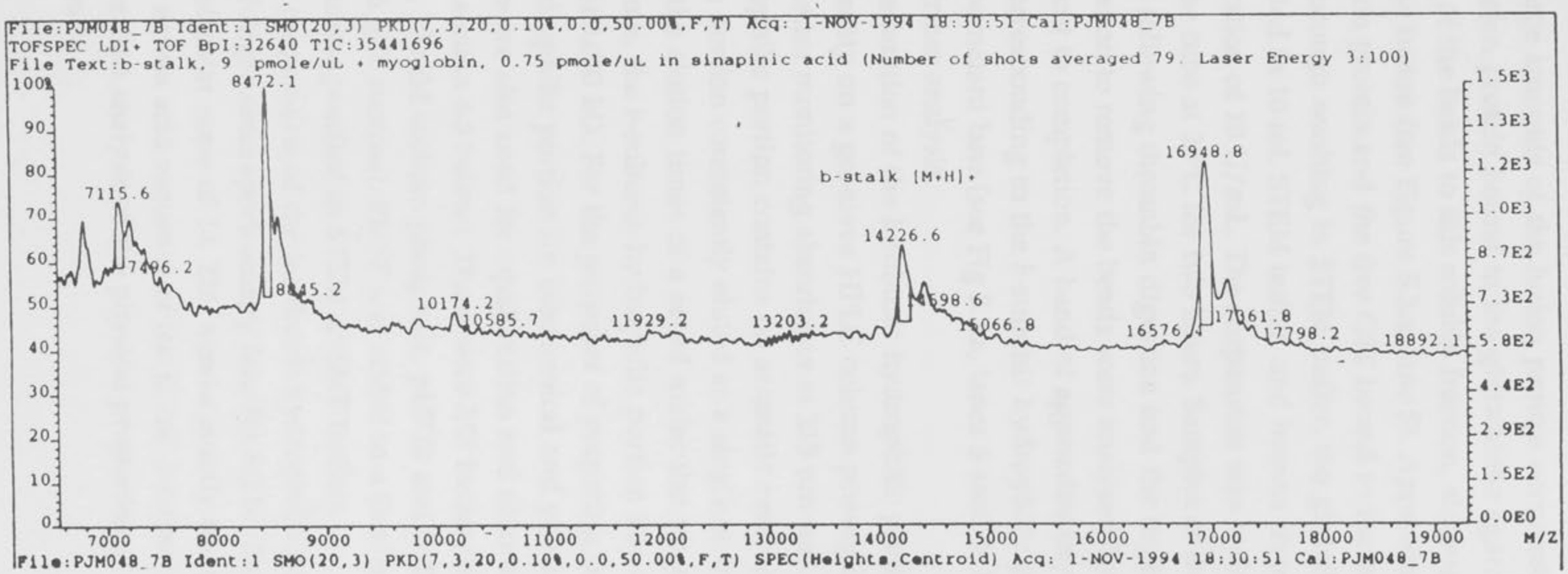
File:PJM048_7B Ident:1 SMO(20,3) PKD(7,3,20,0.10%,0.0,50.00%,F,T) Acq: 1-NOV-1994 18:30:51 Cal:PJM048_7B
TOFSPEC LDI+ TOF BpI:32640 TIC:35441696
File Text:b-stalk, 9 pmole/uL + myoglobin, 0.75 pmole/uL in sinapinic acid (Number of shots averaged 79. Laser Energy 3:100)
8472.1
7115.6
7406.2
8845.2
10174.2
10585.7
11929.2
13203.2
b-stalk [M+H]+
14226.6
14598.6
16066.8
16576
16948.8
17361.8
17798.2
18892.1
100
90
80
70
60
50
40
30
20
10
0
1.5E3
1.3E3
1.2E3
1.0E3
8.7E2
7.3E2
5.8E2
4.4E2
2.9E2
1.5E2
0.0E0
7000
8000
9000
10000
11000
12000
13000
14000
15000
16000
17000
18000
19000
M/Z
File:PJM048_7B Ident:1 SMO(20,3) PKD(7,3,20,0.10%,0.0,50.00%,F,T) SPEC(Heights,Centroid) Acq: 1-NOV-1994 18:30:51 Cal:PJM048_7B

expression level. Large amounts of the fusion protein occurred in the supernatant. The fusion protein bound to the glutathione agarose beads following exposure of the beads to this soluble fraction, although no δ-subunit bound to the fusion (see Figure 5.2.a, lane 5). Approximately equal amounts of the fusion protein and the free GST bound to the beads.

Following thorough washing in STEM buffer, the glutathione agarose beads were suspended in 10 mL STEM buffer, and human thrombin was added to a concentration of 10 U/mL. The suspension was rocked gently in a 50 mL polypropylene tube at 25°C for two hours. Samples of the material bound to the beads following thrombin digestion and the supernatant following centrifugation to remove the beads were analysed by SDS-PAGE. The fusion protein cut to completion. A band of approximately 15,000 molecular mass (corresponding to the *b*-subunit hydrophilic portion) appeared in the supernatant lane (see Fig 5.2.a, lanes 6 and 7). This sample was collected for further analysis.

The crude preparation of the *b*-subunit hydrophilic portion was purified to homogeneity on a gel-sieve HPLC column pre-equilibrated with STEM buffer. A detector monitoring absorbance at 215 nm was used because the *b*-subunit hydrophilic portion contains no aromatic residues. The *b*-subunit hydrophilic portion consistently eluted as a single sharp peak at 15.6 minutes. Based on the elution times of a set of molecular mass markers loaded on this column, the *b*-subunit hydrophilic portion has an apparent molecular mass of 160,000 kD. For the purposes of preparing large quantities of the *b*-subunit hydrophilic portion for biochemical and physical analysis, alternative buffers were also used for equilibration and elution from the HPLC column (see section 6.3 below). These were MP buffer (20 mM magnesium sulfate, 10 mM sodium phosphate, pH7.0) and SMP buffer (MP buffer containing 86 g/L sucrose). PMSF was added to a final concentration of 1 mM to preparations purified in STEM or SMP buffers.

The purified preparation of the *b*-subunit hydrophilic portion was analysed by time-of-flight mass spectrometry (see Fig 5.2.b). The protein was found to have a molecular mass of 14, 226, almost exactly the value predicted from the amino acid sequence of the *E. coli* *b*-subunit hydrophilic portion (14,223). Detailed analysis of the physical properties of this protein is described in Chapter 6.

**5.4 Construction of a plasmid co-expressing a GST-*b*-subunit hydrophilic portion fusion with the δ–subunit, the *b*-subunit hydrophilic portion, the γ-subunit, the ε-subunit and GST.**

To investigate whether the γ- and ε-subunits are required for the δ-subunit to interact with the *b*-subunit hydrophilic portion, a plasmid was constructed to co-express a GST-*b*-subunit hydrophilic portion fusion with the δ–subunit, the *b*-subunit hydrophilic portion, the γ-subunit, the ε-subunit and GST. The gene for the free *b*-subunit hydrophilic portion was included in case the GST moiety of the fusion protein were to interfere in the formation of a *b*-subunit hydrophilic portion dimer, which may be required for interaction with other subunits.

Plasmid pAN858, constructed by B. Cromer in this laboratory, has a portion of the *uncF*gene (encoding the hydrophilic portion of the *E. coli b*-subunit) fused to the gene for *S. japonicum* GST, the *uncH* gene encoding the δ-subunit, the portion of the *uncF*gene encoding the hydrophilic portion of the *b*-subunit, the *uncG* gene encoding the γ-subunit and the *uncC* gene encoding the ε-subunit, in the vector pGEX-2T. The *uncH* gene is preceded by the 30 bp *uncE* pregenic region, inserted to enhance translation of the δ-subunit. Plasmid pAN858 confers upon strains AN2015 (*uncH241;* Humbert *et al.*, 1983), AN1273 (*uncG428;* Downie *et al.*, 1979) and AN802 (*uncC424;* Gibson *et al.*, 1977) the ability to grow on succinate as sole carbon source, indicating that functional δ-, γ- and ε-subunits are expressed. As with plasmid pAN815, plasmid pAN858 has a *Bam*HI site in the six bases immediately preceding the codon for what would be leucine-29 in the full size *b*-subunit. When the purified *b*-subunit/GST fusion protein is digested with thrombin, the resulting *b*-subunit is therefore 131 amino acids long, and has glycine and serine preceding the leucine at the amino terminus. Plasmid pAN858 was digested with *Bam*HI and *Xma*I, and the resulting fragments separated by agarose gel electrophoresis. The 2.7kb DNA fragment carrying the portion of the *uncF*gene encoding the hydrophilic portion of the *b*-subunit, the *uncH* gene, the portion of the *uncF*gene encoding the hydrophilic portion of the *b*-subunit, the *uncG* gene and the *uncC* gene was excised from the gel and purified.

The vector pAN990 was digested with *Bam*HI and *Xma*I. The 2.7 kb *Bam*HI/*Xma*I fragment was ligated into the vector. The resulting plasmid, named pAN1055, co-expresses a GST-*E. coli b*-subunit hydrophilic portion fusion with the *E. coli* δ subunit, the *E. coli b*-subunit hydrophilic portion, the *E. coli* γ subunit, the *E. coli* ε-subunit and GST (see Figure 5.3). Plasmid pAN1055 was used to transform strain AN3347 to create strain AN3840.

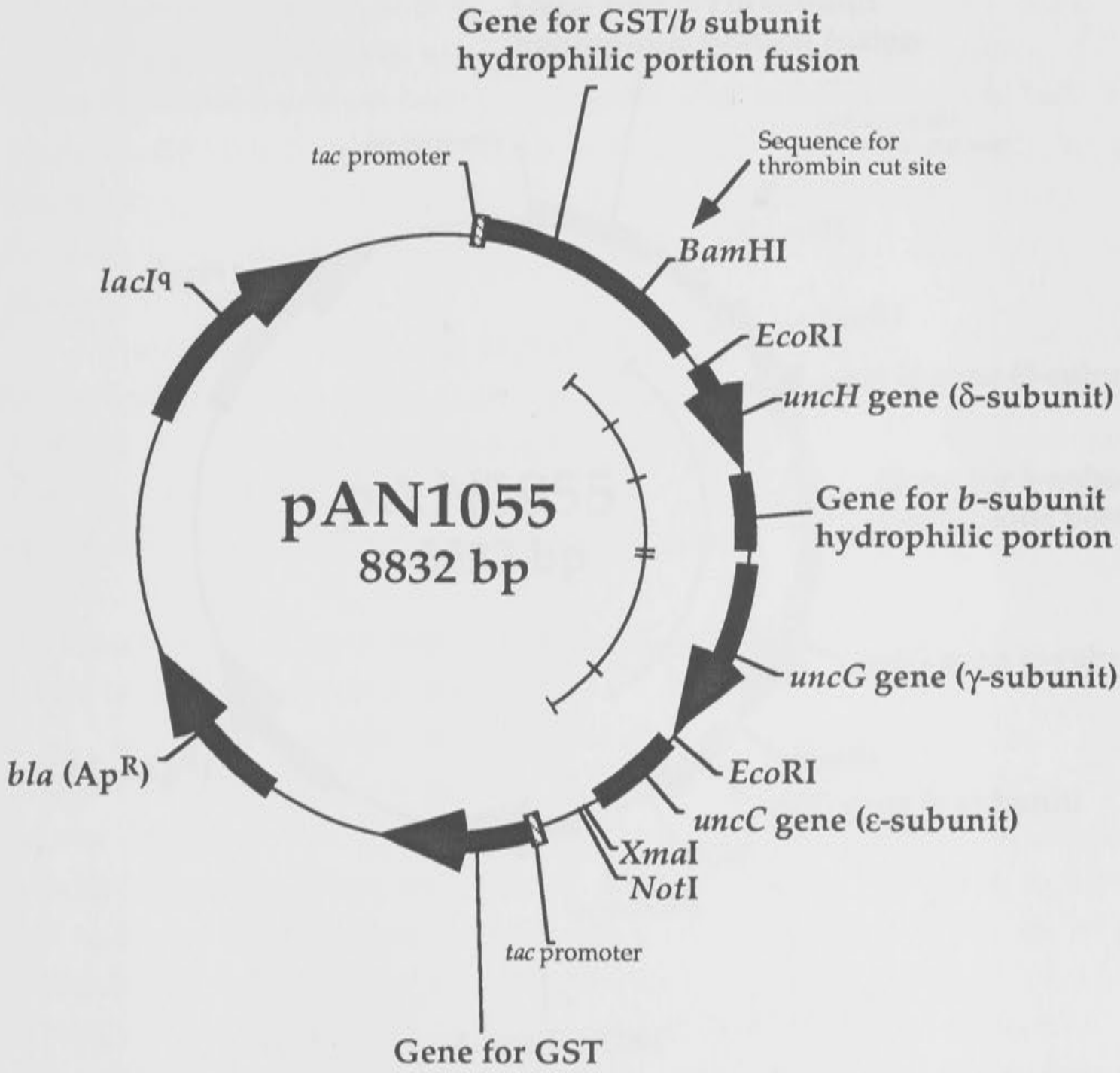


**Figure 5.3**: Plasmid pAN1055, which carries genes for a GST-*E. coli b*-subunit hydrophilic portion fusion, the δ-subunit, the *b*-subunit hydrophilic portion, the γ-subunit, the ε-subunit and GST.

**5.5 Attempted purification of complexes of *E. coli* ATP synthase subunits from strain AN3840.**

A large scale culture of strain AN3840 was grown as described in section 2.23. Samples collected at various steps in the procedure for purification of the GST fusion protein were analysed by SDS-PAGE (see Figure 5.4). Large amounts of the GST-*b*-subunit hydrophilic portion fusion and possibly the γ-subunit, the δ-subunit, the *b*-subunit hydrophilic portion and the ε-subunit occur in both the supernatant and unbound fractions. None of the fusion protein bound to the glutathione agarose beads following exposure of the beads to the soluble fraction (see Fig 5.4., lane 5). Since the GST-*b*-subunit fusion co-expressed only with the δ-subunit bound the beads readily (see section 5.3 above), co-expression with the γ- and ε-subunits has prevented the GST-*b*-subunit hydrophilic portion fusion from binding to the beads.

These observations suggest that a complex was formed by the GST-*b*-subunit hydrophilic portion fusion and one or more of the γ-, δ- and ε-subunits, such that the glutathione binding site on the GST moiety of the fusion protein was blocked. However, time constraints prevented attempts to identify or purify such a complex or complexes.

**5.6 Construction of a plasmid co-expressing a GST-*E. coli* *b*-subunit hydrophilic portion fusion and GST.**

Results presented in the previous chapter suggested that the cyanobacterial δ-subunit may assist in stabilising the structure of the cyanobacterial *b* -subunit soluble portion when these proteins are expressed at high levels from the same plasmid. Experiments were therefore carried out to test whether the presence of high levels of the *E. coli* δ-subunit in the cell during synthesis of the *E. coli b*-subunit hydrophilic portion fusion affects the folding of the *E. coli b*-subunit hydrophilic portion moiety. A plasmid was therefore constructed to co-express the GST-*E. coli* *b*-subunit hydrophilic portion fusion and GST without the *E. coli* δ-subunit.

Plasmid pAN1157 (described in section 5.2 above), was digested with *Bam*HI and *Eco*RI, and the resulting fragments separated by agarose gel electrophoresis. The 450 bp DNA fragment carrying the portion of the *uncF*gene encoding the hydrophilic portion of the *b*-subunit was excised from the gel and purified.

The vector pAN990 was digested with *Bam*HI and *Eco*RI. The 450 bp *Bam*HI/*Eco*RI fragment was ligated into the vector. The resulting plasmid, named pAN1053, co-expresses a GST-*E. coli* *b*-subunit hydrophilic portion

**Figure 5.4**: SDS-PAGE analysis of samples collected at the various steps in the attempted purification of a GST-*E. coli b*-subunit hydrophilic portion fusion from strain AN3840. This strain contains plasmid pAN1055, which co-expresses a GST-*b*-subunit hydrophilic portion fusion with the δ-subunit, the free *b*-subunit hydrophilic portion, the γ-subunit, the ε-subunit and GST.

Lane 1: Molecular weight markers
Lane 2: Pellet following 39,000 x g centrifugation of disrupted cells
Lane 3: Supernatant following 39,000 x g centrifugation of disrupted cells
Lane 4: Unbound material following exposure of supernatant (Lane 3) to glutathione agarose beads
Lane 5: Material bound to the glutathione agarose beads

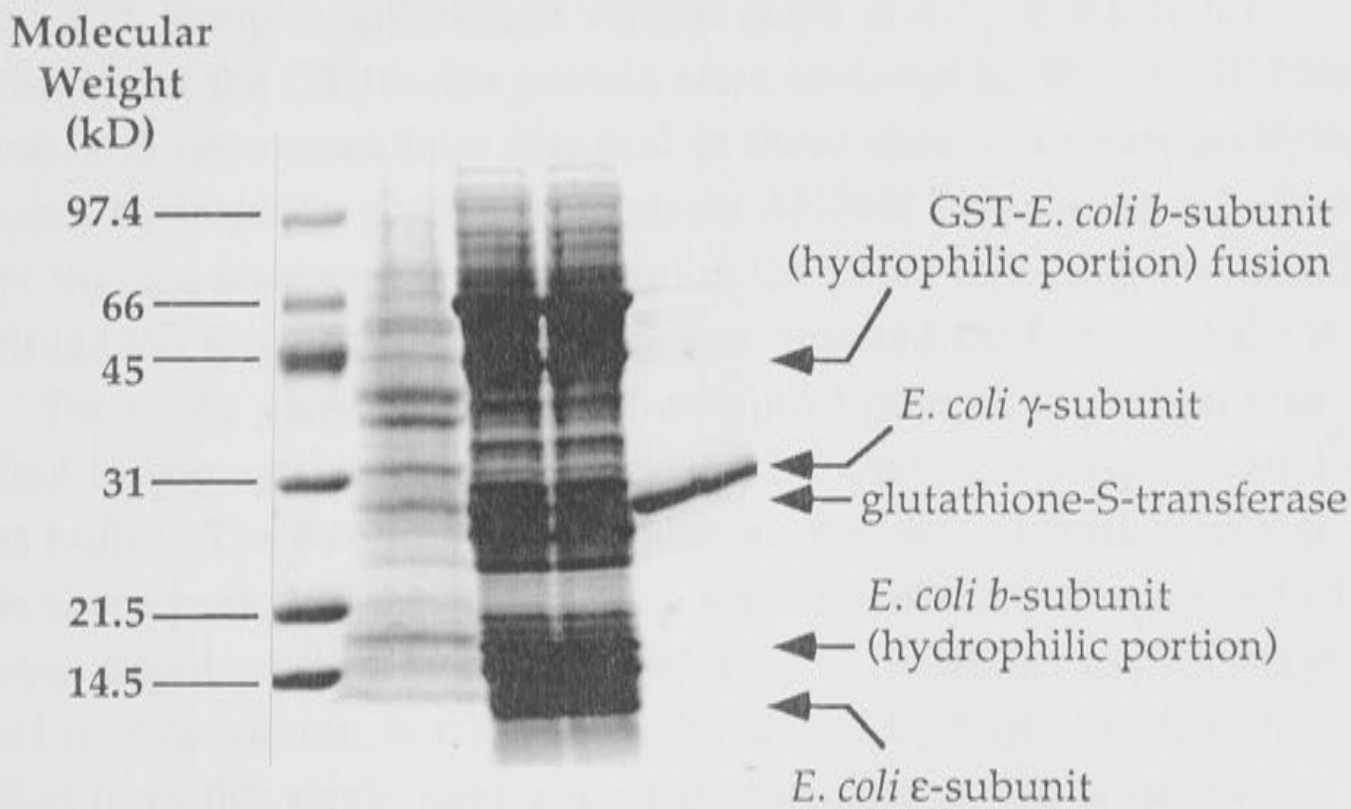
Molecular Weight (kD)
97.4
66
45
31
21.5
14.5
GST-E. coli b-subunit (hydrophilic portion) fusion
E. coli γ-subunit
glutathione-S-transferase
E. coli b-subunit (hydrophilic portion)
E. coli ε-subunit

fusion and GST (see Figure 5.5). Plasmid pAN1053 was used to transform strain AN3347 to create strain AN3826.

**5.7 Purification of the *E. coli* *b*-subunit hydrophilic portion from strain AN3826.**

A large scale culture of strain AN3826 was grown as described in section 2.23. Samples collected at various steps in the procedure for purification of the GST fusion protein were analysed by SDS-PAGE (data not shown), and were essentially identical to those observed when purifying the *b*-subunit hydrophilic portion from strain AN3843 (see section 5.3 above), except that the δ-subunit is not present in the pellet following the 39,000 x g centrifugation step. The final product was collected for further analysis.

The crude preparation of the *b*-subunit hydrophilic portion was purified to homogeneity on a gel-sieve HPLC column pre-equilibrated with STEM buffer. The *b*-subunit hydrophilic portion eluted consistently as a single sharp peak, but the elution time was variable in the range 16 to 18 minutes. Based on the elution times of a set of molecular mass markers loaded on this column, batches of the *b*-subunit hydrophilic portion purified from this strain have apparent molecular masss in the range 50,000 to 130,000. This variability indicates a significant difference in the properties of the *b*-subunit hydrophilic portion purified in the absence of the δ-subunit from those observed when the GST-*b*-subunit hydrophilic portion fusion was expressed from the same plasmid as the δ-subunit. The presence of high levels of the δ-subunit in the cell during synthesis of the *b*-subunit hydrophilic portion fusion appears therefore to have affected the folding of the *b*-subunit hydrophilic portion moiety, although further experiments are required to characterise this effect in more detail.

**5.8 Construction of a plasmid co-expressing a GST-*E. coli* *b*-subunit hydrophilic portion fusion with the *E. coli* δ- and β-subunits and GST.**

As described in section 5.1 above, an aim of the work described in this chapter involves the co-expression of the hydrophilic domain of the *b*-subunit with the α- and β-subunits, with the aim of purifying a complex consisting of two or more of these proteins, which may correspond to an assembly intermediate for the *E. coli* $F_OF_1$-ATPase *in vivo*. The first step in these experiments was the construction of a plasmid to co-express a GST-*E. coli* *b*-subunit hydrophilic portion fusion with the *E. coli* δ- and β-subunits and GST. Material was purified from a strain carrying this plasmid and analysed to allow comparisons with material purified from a strain

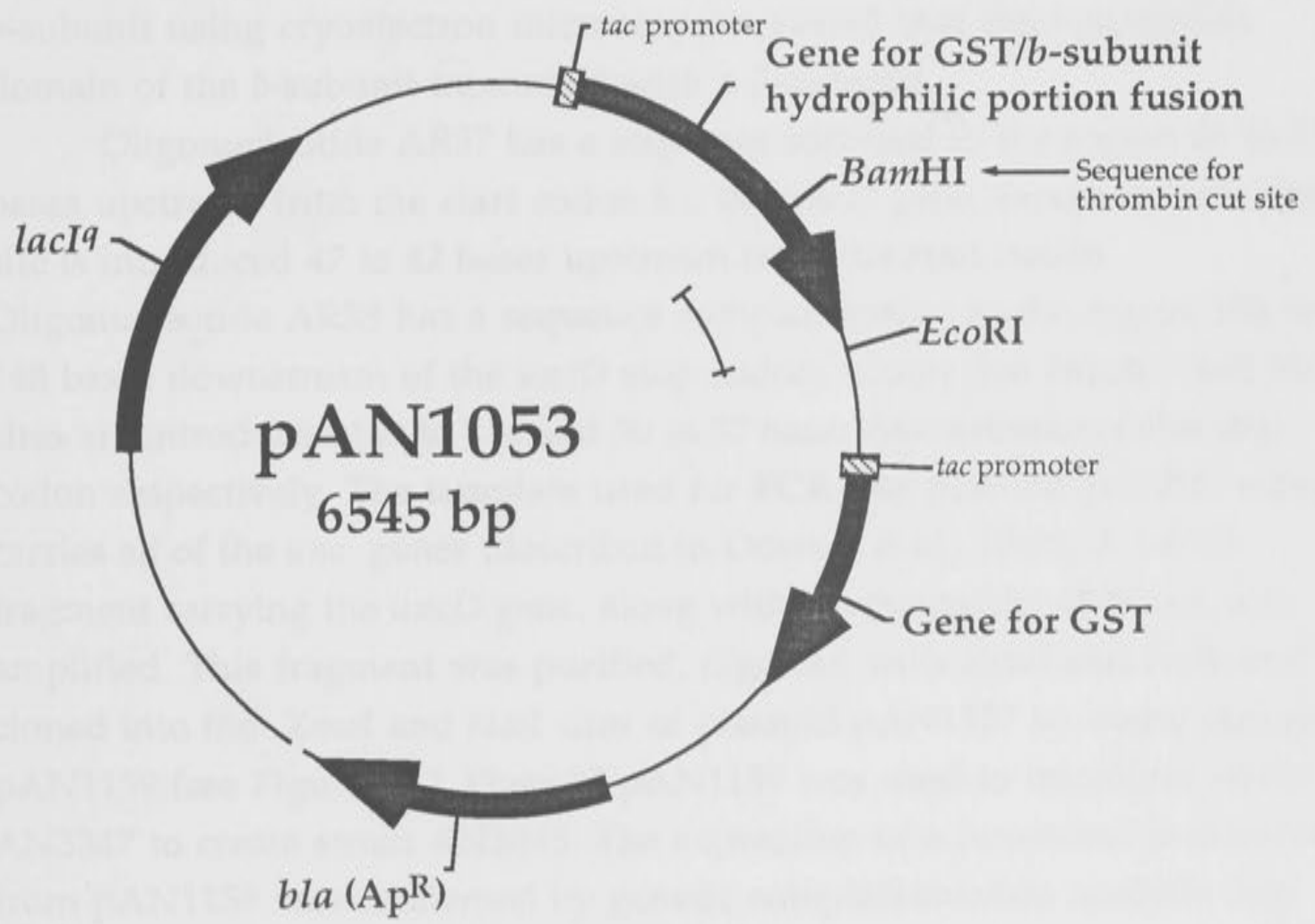


**Figure 5.5**: Plasmid pAN1053, which carries genes for a GST-*E. coli b*-subunit hydrophilic portion fusion and GST.

expressing the α-subunit also (see sections 5.10 and 5.11 below). The plasmid was constructed by cloning the *uncD* gene, which encodes the *E. coli* β-subunit, into plasmid pAN1157, which co-expresses a GST-*E. coli* *b*-subunit hydrophilic portion fusion with the *E. coli* δ-subunit and GST (see section 5.2 above). The gene for the β-subunit was chosen to be inserted into pAN1157 before the gene for the α-subunit because of recent experimental evidence suggesting specific interactions between the *b*-subunit hydrophilic portion and the β-subunit. Examination by Wilkens *et al.* (1994) of a complex formed between the *E. coli* $F_1$-ATPase and a truncated form of the *b*-subunit using cryoelectron microscopy revealed that the hydrophilic domain of the *b*-subunit interacted with a β-subunit.

Oligonucleotide AR37 has a sequence identical to the region 65 to 33 bases upstream from the start codon for the *uncD* gene, except that an *Xma*I site is introduced 47 to 42 bases upstream from the start codon. Oligonucleotide AR38 has a sequence complementary to the region 100 to 148 bases downstream of the *uncD* stop codon, except that *Hin*dIII and *Not*I sites are introduced 109 to 114 and 30 to 37 bases downstream of the stop codon respectively. The template used for PCR was plasmid pAN45, which carries all of the *unc* genes (described in Downie *et al.*, 1980). A 1.6 kb fragment carrying the *uncD* gene, along with the preceding 45 bases, was amplified. This fragment was purified, digested with *Xma*I and *Not*I, and cloned into the *Xma*I and *Not*I sites of plasmid pAN1157 to create plasmid pAN1159 (see Figure 5.6). Plasmid pAN1159 was used to transform strain AN3347 to create strain AN3845. The expression of a functional β-subunit from pAN1159 was confirmed by genetic complementation analysis (see section 5.10 below).

**5.9 Attempted purification of a complex of the *E. coli* *b*-subunit hydrophilic portion fusion and the *E. coli* δ- and β-subunits from strain AN3845.**

A large scale culture of strain AN3845 was grown as described in section 2.23. Samples collected at various steps in the procedure for purification of the GST fusion protein (see section 2.25) were analysed by SDS-PAGE (see Fig 5.7). The δ-subunit, most of the β-subunit and some of the GST-*E. coli* *b*-subunit hydrophilic portion fusion occurs in the pellet following the 39,000 x *g* centrifugation step, possibly due to the high expression level. Large amounts of the fusion protein occurred in the supernatant. Both the fusion protein and the free GST bound to the glutathione agarose beads following exposure of the beads to this soluble fraction. Traces of the approximately 50,000 kDa molecular mass β-subunit

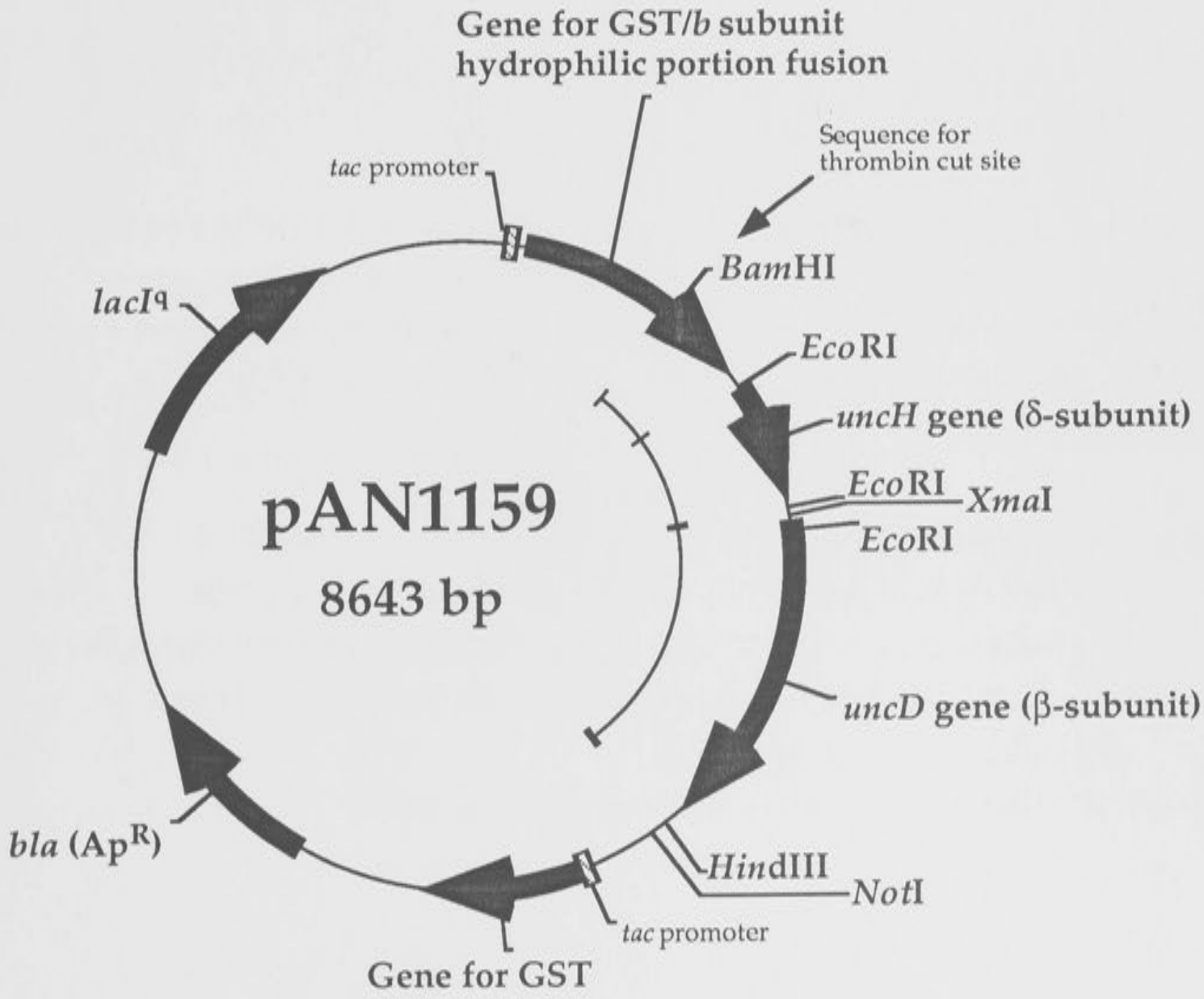


**Figure 5.6**: Plasmid pAN1159, which carries genes for a GST-*E. coli b*-subunit hydrophilic portion fusion, the δ-subunit, the β-subunit and GST.

**Figure 5.7**: SDS-PAGE analysis of samples collected at the various steps in the purification of a GST-*E. coli b*-subunit soluble portion fusion from strain AN3845. This strain contains plasmid pAN1159, which carries genes for a GST-*E. coli b*-subunit hydrophilic portion fusion, the *E. coli* δ-subunit, the *E. coli* β-subunit and GST:

Lane 1: Molecular weight markers
Lane 2: Pellet following 39,000 x g centrifugation of disrupted cells
Lane 3: Supernatant following 39,000 x g centrifugation of disrupted cells
Lane 4: Unbound material following exposure of supernatant (Lane 3) to glutathione agarose beads
Lane 5: Material bound to the glutathione agarose beads

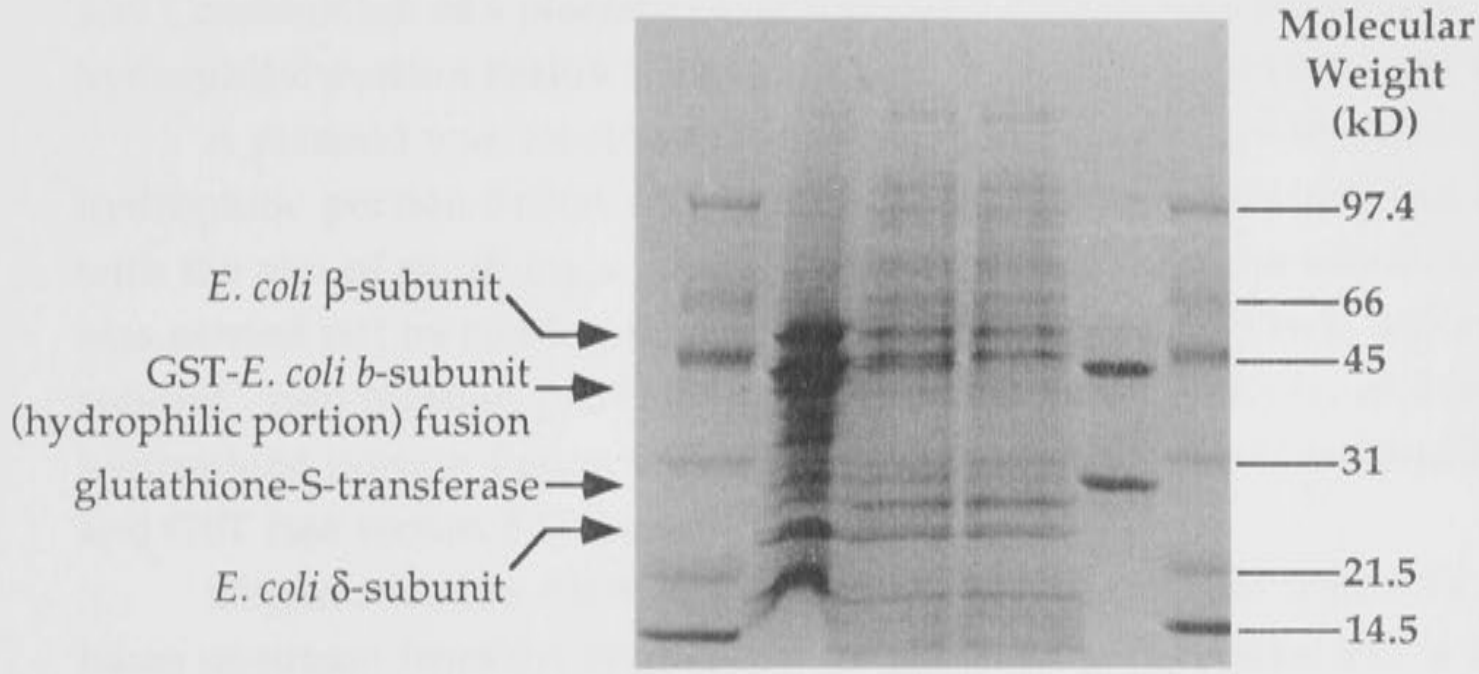
Molecular
Weight
(kD)
97.4
66
45
31
21.5
14.5
E. coli β-subunit
GST-E. coli b-subunit
(hydrophilic portion) fusion
glutathione-S-transferase
E. coli δ-subunit

appear to have bound to the fusion. Rather than pursuing further the purification of a complex, experiments involving co-expression of the α-subunit were carried out to test whether this could facilitate binding of the δ- and/or β-subunits to the *b*-subunit hydrophilic portion. This question is of particular interest because mutational analysis by Cox *et al.* (1981) showed that both the α- and β-subunits are required for insertion of the *b*-subunit into the membrane during assembly.

**5.10 Construction of a plasmid co-expressing a GST-*E. coli* *b*-subunit hydrophilic portion fusion with the *E. coli* δ-, β- and α-subunits and GST.**

A plasmid was constructed to co-express a GST-*E. coli* *b*-subunit hydrophilic portion fusion with the *E. coli* δ-, β- and α-subunits and GST, with the aim of purifying a complex of two or more of these subunits. This was carried out by cloning the *uncA* gene, which encodes the *E. coli* α-subunit , into plasmid pAN1159, which co-expresses a GST-*E. coli* *b*-subunit hydrophilic portion fusion with the *E. coli* δ subunit, the *E. coli* β-subunit and GST (see section 5.8 above).

Oligonucleotide AR39 has a sequence identical to the region 71 to 37 bases upstream from the start codon for the *uncA* gene, except that a *Hin*dIII site is introduced 60 to 55 bases upstream from the start codon. Oligonucleotide AR40 has a sequence complementary to the region 40 to 76 bases downstream of the *uncA* stop codon, except that a *Not*I site is introduced 52 to 59 bases downstream of the stop codon. Using plasmid pAN45 as template, PCR was carried out to amplify a 1.66 kb fragment carrying the *uncA* gene, along with the preceding 60 bases. This fragment was purified, digested with *Hin*dIII and *Not*I, and cloned into the *Hin*dIII and *Not*I sites of plasmid pAN1159 to create plasmid pAN1162 (see Figure 5.8). This plasmid was used to transform strain AN3347 to create strain AN3848.

The whole cell protein content of strain AN3848, before and after addition of IPTG (final concentration 0.1 mM) to a culture of this strain, was analysed by SDS-PAGE (see Figure 5.9.a). The induction of the *tac* promoters results in the increased expression of proteins with approximate molecular masss of 55,000, 50,000, 40,000 and 26,000, corresponding to the α-subunit, the β-subunit, the GST-*b*-subunit hydrophilic portion fusion and the free GST. It is noteworthy, however, that expression of the α-subunit is many fold weaker than the other induced proteins.

To confirm that the *uncD* gene is expressed from plasmid pAN1159, and that both the *uncD* and *uncA* genes are expressed from plasmid

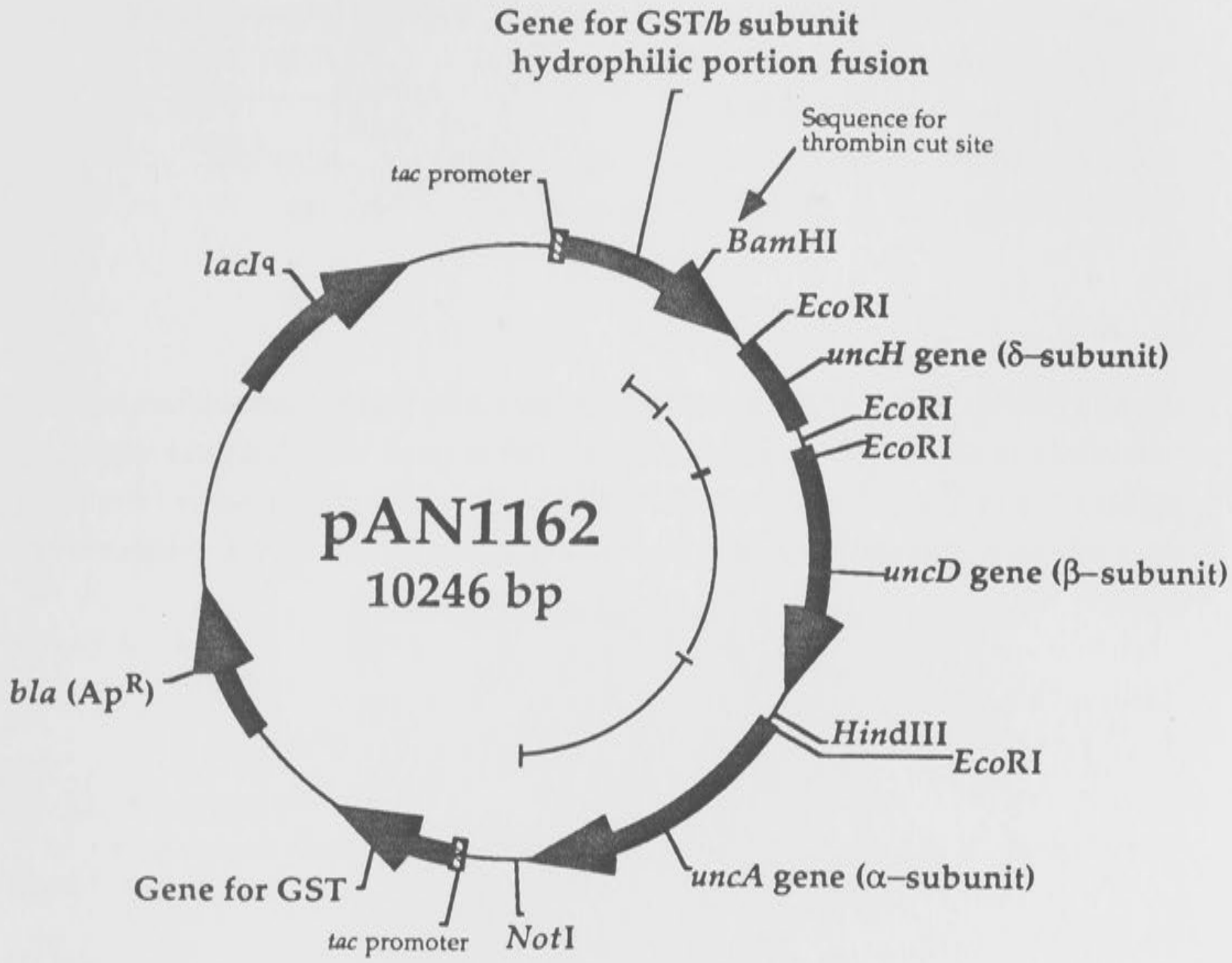


**Figure 5.8**: Plasmid pAN1162, which carries genes for a GST-*E. coli b*-subunit hydrophilic portion fusion, the δ-subunit, the β-subunit, the α-subunit and GST.

**Figure 5.9 (a)**: SDS-PAGE analysis of whole cell protein content of strain AN3848, before and after addition to a culture of 0.1 mM IPTG
Lane 1: Molecular weight markers
Lane 2: AN3848 whole cell protein content prior to IPTG addition
Lane 3: AN3848 whole cell protein content after IPTG addition

**Figure 5.9 (b)**: SDS-PAGE analysis of samples collected at the various steps in the purification of a GST-*E. coli b*-subunit soluble portion fusion from strain AN3848. This strain contains plasmid pAN1159, which carries genes for a GST-*b*-subunit soluble portion fusion, the δ-subunit, the β-subunit, the α-subunit and GST:

Lane 1: Molecular weight markers
Lane 2: Pellet following 39,000 x g centrifugation of disrupted cells
Lane 3: Supernatant following 39,000 x g centrifugation of disrupted cells
Lane 4: Unbound material following exposure of supernatant (Lane 3) to glutathione agarose beads
Lane 5: Material bound to the glutathione agarose beads

Effect of thrombin addition to material bound to the glutathione agarose beads:
Lane 6: Material bound to the glutathione agarose beads following incubation with 10 U/mL thrombin at 25°C for two hours
Lanes 7 and 8: Material in supernatant following centrifugation to remove glutathione agarose beads
Lane 9: Molecular weight markers

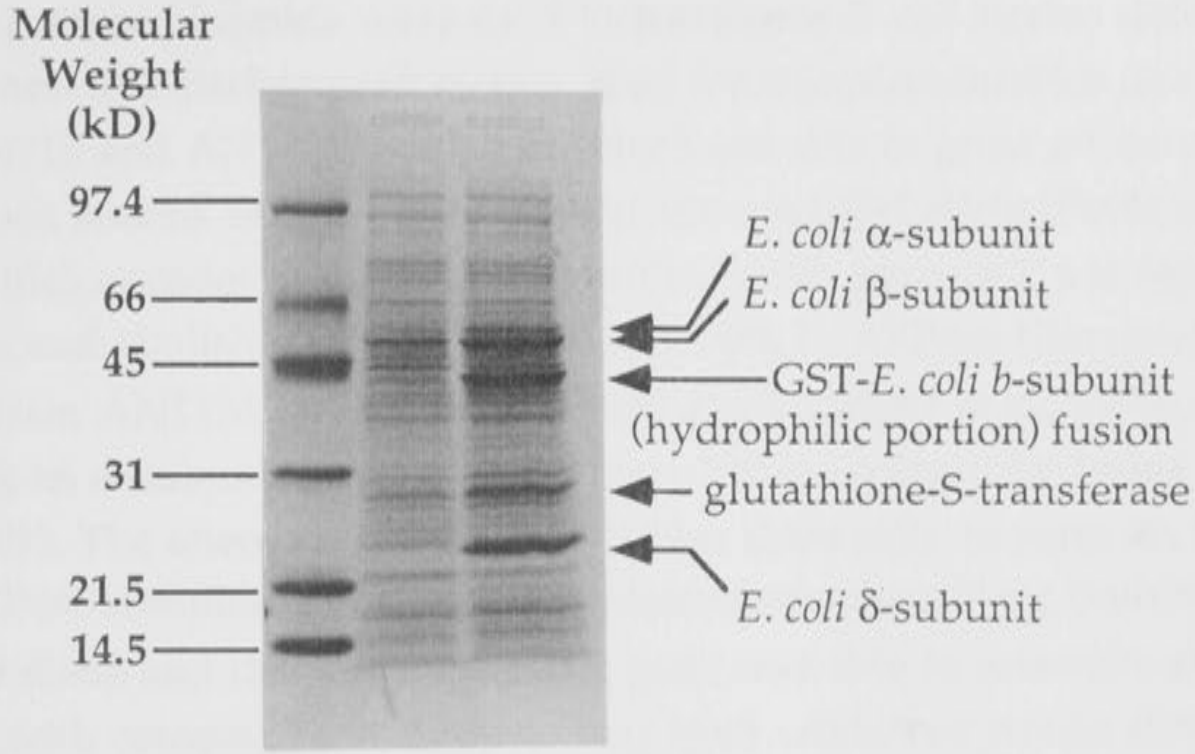
Molecular Weight (kD)
97.4
66
45
31
21.5
14.5
E. coli α-subunit
E. coli β-subunit
GST-E. coli b-subunit (hydrophilic portion) fusion
glutathione-S-transferase
E. coli δ-subunit

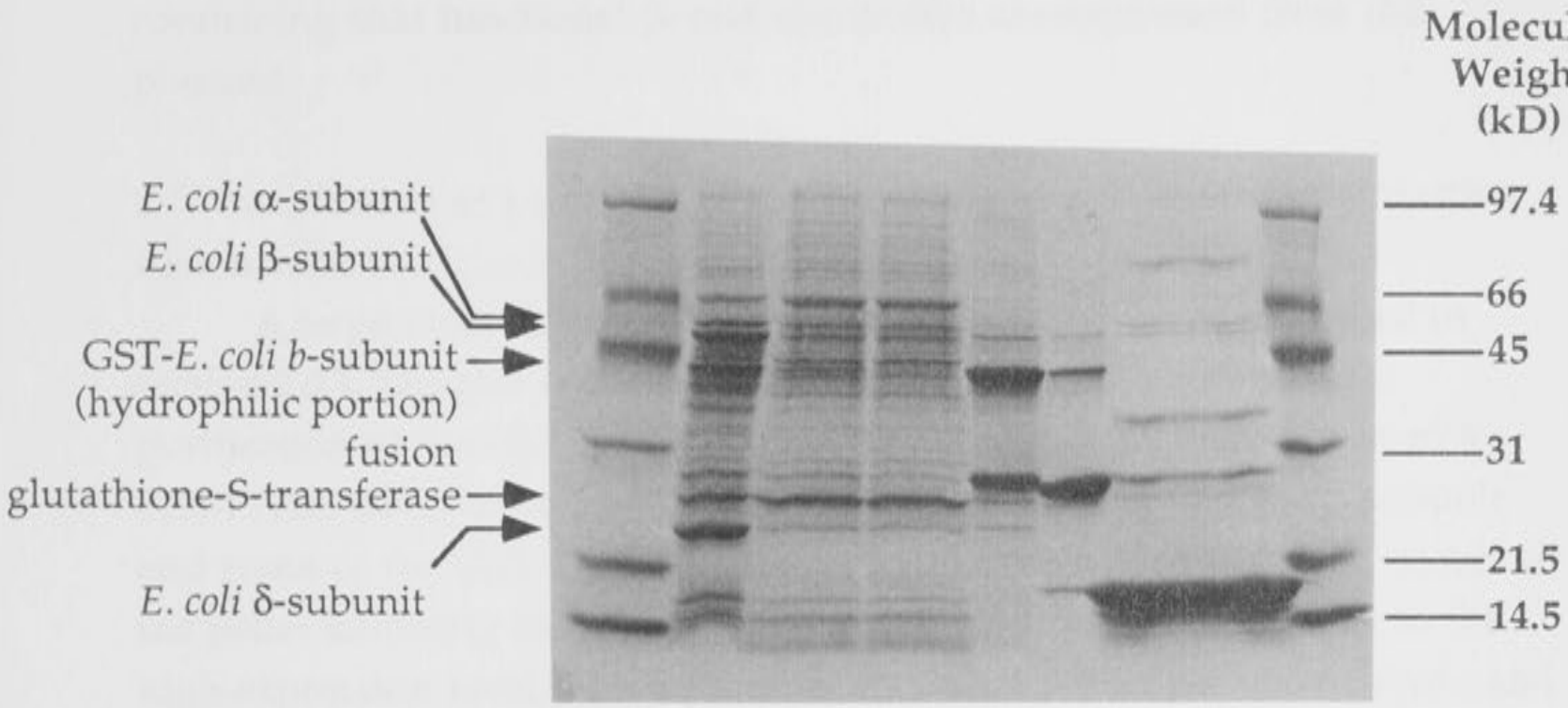
Molecular Weight (kD)
E. coli α-subunit
E. coli β-subunit
GST-E. coli b-subunit (hydrophilic portion) fusion
glutathione-S-transferase
E. coli δ-subunit
97.4
66
45
31
21.5
14.5

pAN1162, these plasmids were used to transform *E. coli* strains defective in these genes. The background strains used for complementation analysis were AN818 and AN1124, neither of which are able to grow on succinate as sole carbon source. Strain AN818 carries the *uncD409* allele (Fayle *et al.*, 1978), which encodes a mutant β-subunit in which glycine-214 is replaced by arginine, and abolishes normal assembly of the $F_1$-ATPase (Parsonage *et al.*, 1987). Strain AN1124 carries the *uncA450* allele (Senior *et al.*, 1979), encoding an α-subunit in which glutamate-299 is replaced by lysine (Maggio *et al.*, 1987). The altered α-subunit assembles aberrantly to form an inactive $F_OF_1$-ATPase complex, but a partial diploid strain containing both the *uncA450* allele and the wild-type *uncA* gene was able to assemble an enzyme with comparable activity to that from wild-type strains (Senior *et al.*, 1979). Transformation with plasmid pAN1159 conferred upon strain AN818 the ability to grow strongly on succinate as sole carbon source, confirming that a functional β-subunit is expressed from this plasmid. Transformation with plasmid pAN1162 conferred upon both strains AN818 and AN1124 the ability to grow strongly on succinate as sole carbon source, confirming that functional β- and α-subunits are expressed from this plasmid.

**5.11 Purification of a complex of the *E. coli* *b*-subunit hydrophilic portion fusion with the *E. coli* β- and α-subunits from strain AN3848.**

A large scale culture of strain AN3848 was grown as described in section 2.23. Samples collected at various steps in the procedure for purification of the GST fusion protein (see section 2.25) were analysed by SDS-PAGE (see Figure 5.9.b). The δ-subunit, the α-subunit, the β-subunit and some of the GST-*E. coli* *b*-subunit hydrophilic portion fusion occurs in the pellet following the 39,000 x *g* centrifugation step, possibly due to the high expression level. These proteins also occurred in the supernatant, and the fusion protein bound to the glutathione agarose beads following exposure of the beads to this soluble fraction. Significant amounts of the β-subunit, and a smaller amount of the α- and δ-subunits bound to the GST-*b*-subunit hydrophilic portion fusion, although these proteins are present in small amounts relative to the fusion (see Figure 5.9.b, lanes 2-5).

Following thorough washing in STEM buffer, the glutathione agarose beads were suspended in 10 mL STEM buffer, and human thrombin was added to a concentration of 10 U/mL. The suspension was rocked gently in a 50 mL polypropylene tube at 25°C for two hours. Samples of the material bound to the beads following thrombin digestion and the supernatant

following centrifugation to remove the beads were analysed by SDS-PAGE. A band of approximately 15,000 kDa molecular mass (corresponding to the *b*-subunit hydrophilic portion) appeared in the supernatant lane (see Figure 5.9.b, lanes 5 and 6). Both the α-subunit and the β-subunit remained bound to the *b*-subunit hydrophilic portion, although both of these proteins are present in small amounts relative to the *b*-subunit hydrophilic portion. Equal amounts of α- and β-subunits appear to bind to the final cut *b*-subunit hydrophilic portion.

Preliminary experiments aimed at the further purification of the complex of the *b*-subunit hydrophilic portion and the α- and β-subunits have been carried out using gel-sieve HPLC, and these indicate that the α/β/*b*-subunit hydrophilic domain complex is of similar molecular mass to the soluble $F_1$-ATPase. However, it must be stressed that these are only preliminary findings.

**5.12 Discussion**

Results presented in this chapter provide evidence for specific interactions between the soluble portion of the *b*-subunit and $F_1$ subunits of the *E. coli* $F_OF_1$-ATPase. These observations support a previously proposed role for the *b*-subunit in the binding of $F_1$ to $F_O$ (Walker *et al.*, 1982; Perlin *et al.*, 1983; Senior, 1983). However, no complexes with a defined stoichiometry were isolated during this work, and further experimentation is required.

The soluble portion of the *b*-subunit was purified from the cytoplasmic fractions of several strains using glutathione affinity chromatography. A sample of this protein prepared from strain AN3843 was purified to homogeneity using gel-sieve HPLC, allowing detailed physical characterisation to be carried out (described in the next Chapter of this thesis). Strain AN3843 expresses the δ-subunit along with the GST-*b*-subunit soluble portion fusion, but the δ-subunit was found to precipitate in the cell and did not co-purify with the fusion protein under the conditions used. Results presented in the previous chapter suggest that the cyanobacterial δ-subunit may act to stabilise the structure of the cyanobacterial *b* -subunit soluble portion when these proteins are expressed together. The elution profile of the GST-*E. coli b*-subunit soluble portion fusion from gel-sieve HPLC appeared to be reproducible when the fusion protein was co-expressed with the δ-subunit, and variable when not co-expressed with the δ-subunit. The δ-subunit therefore appears to influence the folding of the *b*-subunit, but its effects vary, presumably due to variations in the particular conditions used in each preparation. Further experimentation to investigate these effects are required.

Experiments with strain AN3840, which co-expresses a GST-*E. coli b*-subunit hydrophilic portion fusion with the *E. coli* δ-subunit, the *E. coli b*-subunit hydrophilic portion, the *E. coli* γ-subunit and the *E. coli* ε-subunit, indicate an interaction between the *b*-subunit hydrophilic portion and at least one of the minor $F_1$ subunits. When expressed with the δ-subunit alone (ie. in strain AN3843), the fusion binds to glutathione agarose beads, but when expressed with all three minor subunits the fusion does not bind to the beads. Given that the γ- and ε-subunits strongly bind in a complex (Dunn, 1982; Cox *et al.*, 1993), these subunits may both bind to the GST-*E. coli b*-subunit hydrophilic portion fusion in such a way as to block the binding of the fusion to the beads. This prevents the isolation of any putative complexes involving the *b*-subunit hydrophilic portion by glutathione agarose affinity chromatography, but the indication of

interactions with one or both of the γ- and ε-subunits raises the possibility for interesting further experiments. These observations are particularly significant in view of the fact that the rotational model of the mechanism of the $F_OF_1$-ATPase proposed by Cox *et al.* (1984) predicts that a stable complex formed by the *b*-, γ, δ- and ε-subunits. Alternative chromatographic procedures may allow purification of complexes from which useful physical structural data could be obtained. For example, plasmids could be constructed to allow expression of the *b*-subunit hydrophilic portion with an N-terminal polyhistidine tag to facilitate purification by $Ni^{2+}$ affinity chromatography. In contrast to the GST, the polyhistidine region is small and does not need to form a particular conformation to bind the affinity column. Steric interference between the binding region and the complex may therefore be reduced.

According to the integrated membrane assembly pathway proposed by Cox *et al.* (1981), the presence of both the α- and β-subunits is required for the incorporation of the *b*-subunit into the membrane. Experiments described in this chapter demonstrate that both the α- and β-subunits interact with the soluble portion of the *b*-subunit, as predicted by this model. Studies using strain AN3845, which co-expresses the GST-*E. coli* *b*-subunit hydrophilic portion fusion with β-subunit but not the α-subunit, indicate that traces of the β-subunit co-purified with the *b*-subunit hydrophilic portion. Studies using strain AN3848, which co-expresses the fusion with both the β- and α-subunits, indicate that both proteins co-purified with the *b*-subunit hydrophilic portion. It is noteworthy that although the β-subunit is expressed at far higher levels than the α-subunit from plasmid pAN1162, and that significantly more of the β-subunit than the α-subunit binds to the fusion protein, the final cut *b*-subunit hydrophilic portion binds equal amounts of α- and β-subunits. Interestingly, when co-expressed with the β- and α-subunits, the *b*-subunit hydrophilic portion binds significant amounts of the δ-subunit. This was not observed when the *b*-subunit hydrophilic portion was co-expressed with the β-subunit alone, and may indicate that during assembly *in vivo*, interaction with both the β- and α-subunits is required prior to the binding of the δ-subunit. This is consistent with the proposal that once an intermediate assembly complex with one α- and two β-subunits has been formed, the next step in the pathway involves the binding of one of the minor subunits (Cox and Gibson, 1987).

# CHAPTER 6

# PHYSICAL CHARACTERISATION OF WILD-TYPE AND MUTANT FORMS OF THE SOLUBLE PORTION OF THE *E. coli b*-SUBUNIT

## 6.1 Introduction

Results presented in the previous chapter are consistent with the predictions of previous workers (Walker *et al.*, 1982; Perlin *et al.*, 1983; Senior, 1983; Cox *et al.*, 1986) that the soluble portion of the *b*-subunit plays a central role in the binding of $F_1$ to $F_O$ in the *E. coli* $F_OF_1$-ATPase complex, and therefore in the mechanism of the coupling of proton transport to catalytic activity. Understanding of this mechanism requires detailed knowledge of the structure and function of this protein domain. Work described in this chapter involves the combined use of mutational and physical analysis to probe the structure of the soluble portion of the *b*-subunit, with the aim of improving the understanding of its role in the mechanism of the *E. coli* $F_OF_1$-ATPase.

As mentioned in section 5.1 above, the *b*-subunit mutation G9D, encoded by the *uncF476* allele, prevents assembly of the *b*-subunit into the membrane when expressed in a haploid strain, most likely because of altered interaction with the α-subunit (Jans *et al.*, 1984). A second *b*-subunit mutation, G131D (the *uncF515* allele; Jans *et al.*, 1985), also affects assembly of the $F_OF_1$-ATPase complex. Unlike haploid strains carrying the *uncF476* allele, strains carrying the *uncF515* allele have the *b*-subunit incorporated into the membrane, and a functional $F_O$ is formed (Jans *et al.*, 1985). The *uncF515* allele does not, therefore, disrupt interaction between the mutant *b*-subunit and the α-subunit. These two alleles (*uncF476* and *uncF515*) were found to partially complement one another (Jans *et al.*, 1985). Two-dimensional SDS-PAGE of membranes from mutant strains revealed that assembly in the strain carrying the *uncF476* allele was blocked at the 1α 1β stage (step 2 in Fig 1.6), whereas assembly in the strain carrying the *uncF515* allele was blocked at the 1α 2β stage (step 4 in Fig 1.6). Assembly in several strains, including those carrying the *uncG428* allele (Downie *et al.*, 1980), the *uncA450* allele (Senior *et al.*, 1979), several of the *uncD* alleles (Cox *et al.*, 1981) and a strain in which the *uncC* gene is inactivated by

Mu phage insertion, are also blocked at the 1α 2β stage (Cox *et al.*, 1981). This was suggested as being due to the inability of one or more of the minor subunits (γ, δ or ε) to bind to an intermediate complex at the 1α 2β stage (Cox and Gibson, 1987). In isolation the *uncF476* and *uncF515* alleles block the assembly pathway at different stages, but when expressed together, the two different mutant *b*-subunits are able to assemble with the other subunits to form a functional $F_OF_1$-ATPase complex.

Although the cytoplasmic domain of the *b*-subunit is extremely hydrophilic, G131 lies in a short stretch of hydrophobic residues (V124 to A132) near the C-terminus. This region is more highly conserved than the *b*-subunit as a whole (see discussion below), but is present only in organisms in which two identical *b*-subunits are incorporated into the $F_OF_1$-ATPase complex. Mutational analysis was carried out by Dr. S. M. Howitt (personal communication) to investigate the possibility that the hydrophobic domain rather than individual amino acids played a role in assembly. A series of mutants was constructed in which aspartic acid replaced each residue from V124 to A132. Each mutant plasmid was transformed into strain AN1440 (*uncF469)* which carries the chromosomal mutation Trp26→stop (Jans *et al.*, 1984). The substitutions V124D, A128D and G131D were found to have the most severe effects on function, while the substitutions I126D and A130D had very little effect and A125D, L127D or V129D had intermediate effects. These results indicate that the hydrophobic region is α-helical, since V124, A128 and G131 would lie on the same face of an α-helix, and that it is one surface of the domain that plays a key role in assembly. (Assays of the growth properties of the mutant strains described here, and the biochemical properties of membranes prepared from these strains, were carried out by Dr. S. M. Howitt in this laboratory, and detailed results are described in Appendix I of this thesis). The properties of the A128D mutant are very similar to those described previously for the G131D mutant (Jans *et al.*, 1985), in that membrane-bound ATPase activity was very low, but membranes were somewhat proton permeable, indicating that the $F_O$ sector was assembled. Because the residue A128 lies in the middle of the hydrophobic region, and because its replacement with aspartate causes as much a deleterious effect on $F_OF_1$-ATPase function as any of the mutants tested, the mutant *b*-subunit carrying the A128D mutation was chosen for detailed analysis.

Biochemical and physical analysis of the wild-type form of the hydrophilic portion of the *b*-subunit has been carried out previously (Dunn,

1992; Wilkens *et al.*, 1994). Analytical ultracentrifugation was used to show that this protein forms a dimer and has an extended shape in solution, and CD spectroscopy indicated a high α-helical content (Dunn, 1992). The protein was shown to bind the $F_1$-ATPase, albeit with low affinity (Dunn, 1992), and a complex of the hydrophilic portion of the *b*-subunit and the $F_1$-ATPase was visualised by cryoelectron microscopy (Wilkens *et al.*, 1994).

This chapter describes the use of biochemical and physical analysis techniques to probe the structure of the hydrophilic portion of the *b*-subunit, both in wild-type and mutant (A128D) form. For this purpose, the mutant form of the hydrophilic portion of the *b*-subunit was expressed as a fusion with GST and purified in a manner similar to that described for the wild-type form in the previous chapter. This allows direct comparison of the properties of the wild-type and mutant forms. It was hoped that a combination of the results of the *in vivo* biochemical experiments described above, and *in vitro* analysis of the biochemical and physical properties of the wild-type and mutant forms of the hydrophilic portion of the *b*-subunit could provide valuable information regarding the assembly, structure and function of the *E. coli* $F_OF_1$-ATPase.

**6.2 Construction of a plasmid co-expressing a GST-*b*-subunit hydrophilic portion (A128D) fusion with the δ-subunit and GST.**

A plasmid was constructed to co-express a GST-*b*-subunit hydrophilic portion (A128D) fusion with the δ-subunit and GST, with the aim of purifying large quantities of the mutant form of the *b*-subunit hydrophilic portion for biochemical and physical analysis.

Oligonucleotide AR41 was designed with a sequence identical to the *uncF* gene except that a *Bam*HI site is introduced in the six bases immediately preceding the codon for leucine-29, and oligonucleotide AR42 was designed with a sequence identical to the *uncF* gene except that the GCT codon for alanine-128 is replaced by the aspartate codon GAC. This laboratory possesses a plasmid with a 4.5kb fragment carrying the *unc* genes *B, E, F, H* and *A*, inserted into the *Hin*dIII site of the polylinker in M13mp19. Using single-stranded DNA of this clone as template, site-directed mutagenesis was carried out sequentially using oligonucleotides AR41 and AR42 as mutagenic primers, as described in section 2.16. The introduction of the mutations was confirmed by restriction analysis and DNA sequencing. RF DNA of the mutated clone was digested with *Bam*HI and *Eco*RI, and the 1.0 kb DNA fragment carrying the portion of the *uncF* gene encoding the hydrophilic portion of the *b*-subunit

(A128D) and the *uncH* gene was cloned into the *Bam*HI and *Eco*RI sites of the vector pAN990 as described in section 2.10. The resulting plasmid, named pAN1163, carries genes for the GST-*b*-subunit hydrophilic portion (A128D) fusion, the δ-subunit and GST. As with the wild-type form, when the mutant *b*-subunit/GST fusion protein is purified and digested with thrombin, the resulting *b*-subunit is 131 amino acids long, and has glycine and serine preceding the leucine at the amino terminus. Plasmid pAN1163 was used to transform strain AN3347 to create strain AN3849.

**6.3 Purification of the *E. coli* *b*-subunit hydrophilic portion (A128D) from strain AN3849.**

A large scale culture of strain AN3849 was grown as described in section 2.23. Samples collected at various steps in the procedure for purification of the GST fusion protein (see section 2.25) were analysed by SDS-PAGE (see Fig 6.1). Some of the GST-*b*-subunit hydrophilic portion fusion occurs in the pellet following the 39,000 x *g* centrifugation step, but large amounts of the fusion protein occurred in the supernatant. The fusion protein bound to the glutathione agarose beads following exposure of the beads to this soluble fraction (see Fig 6.1, lane 5). Approximately equal amounts of the fusion protein and the free GST bound to the beads.

Following thorough washing in STEM buffer, the glutathione agarose beads were suspended in 10 mL STEM buffer, and human thrombin was added to a concentration of 10 U/mL. The suspension was rocked gently in a 50 mL polypropylene tube at 25°C for two hours. Samples of the material bound to the beads following thrombin digestion and the supernatant following centrifugation to remove the beads were analysed by SDS-PAGE. The fusion protein cut to completion. A band of approximately 15,000 molecular weight (corresponding to the mutant (A128D)*b*-subunit hydrophilic portion) appeared in the supernatant lane (see Fig 6.1, lanes 6 and 7). This sample was collected for further analysis.

The crude preparation of the mutant *b*-subunit hydrophilic portion was purified to homogeneity on a gel-sieve HPLC column pre-equilibrated with STEM buffer. The mutant *b*-subunit hydrophilic portion eluted consistently as a single sharp peak at 16 $^3/_4$ minutes. Based on the elution times of a set of molecular weight markers loaded on this column, the mutant *b*-subunit hydrophilic portion has an apparent molecular weight of 85,000. For the purposes of preparing large quantities of the mutant *b*-subunit hydrophilic

**Figure 6.1**: Lanes 1-4 show the SDS-PAGE analysis of samples collected at the various steps in the purification of a GST-*E. coli b*-subunit hydrophilic portion fusion from strain AN3849. This strain contains plasmid pAN1163, which carries genes for a GST-*E. coli b*-subunit (mutant A128D) hydrophilic portion fusion and the *E. coli* δ-subunit:

Lane 1: Molecular weight markers

Lane 2: Pellet following 39,000 x g centrifugation of disrupted cells

Lane 3: Supernatant following 39,000 x g centrifugation of disrupted cells

Lane 4: Unbound material following exposure of supernatant (Lane 3) to glutathione agarose beads

Lane 5: Material bound to the glutathione agarose beads

Lanes 6 and 7 show the effect of thrombin addition to material bound to the glutathione agarose beads:

Lane 6: Material bound to the glutathione agarose beads following incubation with 20 U/mL thrombin at 25°C for two hours

Lane 7: Material in supernatant following centrifugation to remove glutathione agarose beads

Lane 8: Molecular weight markers

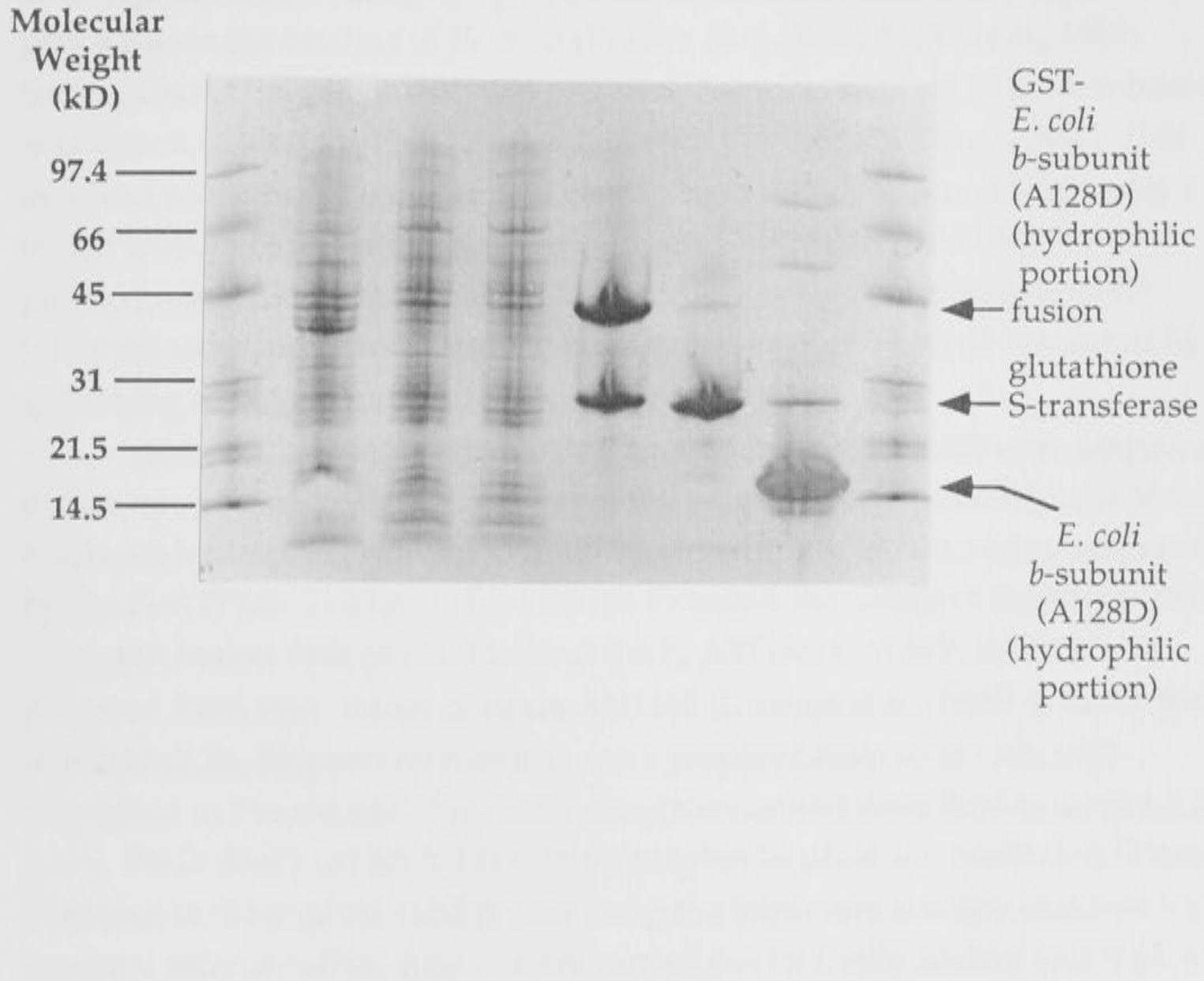
Molecular Weight (kD)
97.4
66
45
31
21.5
14.5
GST-
E. coli
b-subunit
(A128D)
(hydrophilic
portion)
fusion
glutathione
S-transferase
E. coli
b-subunit
(A128D)
(hydrophilic
portion)

portion for biochemical and physical analysis, alternative buffers were also used for equilibration and elution from the HPLC column (see sections 6.5, 6.6 and 6.7 below). These were MP buffer (20 mM magnesium sulfate, 10 mM sodium phosphate, pH7.0) and SMP buffer (MP buffer containing 86 g/L sucrose).

**6.4 Comparison of the ability of wild-type and mutant (A128D) forms of the *b*-subunit hydrophilic portion to bind the *E. coli* $F_1$-ATPase.**

From secondary structure predictions based on analysis of the amino acid sequence, the hydrophilic portion of the *b*-subunit has been proposed to play a role in the binding of $F_1$ to $F_O$ (Walker *et al.*, 1982; Perlin *et al.*, 1983; Senior, 1983). Consistent with this proposal, the polar domain of the *b*-subunit was shown to bind the $F_1$-ATPase, albeit with low affinity (Dunn, 1992). This involved two types of experiments. Firstly, the *b*-subunit polar domain was mixed with an $F_1$ preparation, and a complex ("six-subunit-ATPase") was purified using size-exclusion HPLC. Secondly, the *b*-subunit polar domain inhibited reconstitution of stripped membranes by $F_1$-ATPase as measured by quenching of quinacrine fluorescence (Dunn, 1992).

Atebrin fluorescence quenching assays (see section 2.26) were employed to measure and compare the abilities of the wild-type and mutant forms of the *b*-subunit hydrophilic portion to inhibit reconstitution of stripped membranes by the $F_1$-ATPase. The level of inhibition indicates the ability of each form of the *b*-subunit hydrophilic portion to bind the $F_1$-ATPase. Crude $F_1$-ATPase was prepared from membranes of strain AN1460 (Downie *et al.*, 1980) as described in section 2.24. Stripped membranes were prepared from strain AN2840 (described in Howitt and Cox, 1992) using the method described in section 2.24.

Preliminary experiments established that 50 µL of the crude $F_1$-ATPase preparation (33 mg/mL total protein) was the minimum amount required for maximal reconstitution. Assays were carried out by firstly adding to 500 µL of Hepes buffer (see section 2.26) 50 µL of $F_1$-ATPase and 500 µL of either the wild-type (2 mg/mL protein) or mutant (1.5 mg/mL protein) forms of the *b*-subunit hydrophilic portion, or 500 µL of STEM buffer as a control. The mixture was allowed to incubate at 30°C for 5 minutes in the quartz cuvette used for the atebrin fluorescence quenching assay. The cuvette was placed into the spectrofluorophotometer compartment. The machine was zeroed, and the recording of fluorescence was commenced. 30 µL of stripped membranes were added, the atebrin (quinacrine dihydrochloride) was added to a final

concentration of 5 μM, and the level of fluorescence was noted. NaCN and ATP were then added to concentrations of 2.5 mM and 1 mM respectively, and the contents of the cuvette were mixed thoroughly. The quenching of atebrin fluorescence upon ATP addition measures the electrochemical proton gradient that is formed across the membrane due to proton pumping coupled to ATP hydrolysis by the reconstituted $F_OF_1$-ATPase. When this quench reached its maximal level, the uncoupler CCCP (carbonyl cyanide *m*-chlorophenylhydrazone) was added to a final concentration of 4 mM, and fluorescence returned to its maximal level.

Traces from the atebrin fluorescence quenching experiments are shown in Figure. 6.2 (a-c). In the control experiment (Figure 6.2.c), where STEM buffer was incubated with $F_1$-ATPase prior to the reconstitution assay, ATP-dependent atebrin fluorescence quenching was 53% of the original fluorescence level. In the experiment where the wild-type form of the *b*-subunit hydrophilic portion was incubated with $F_1$-ATPase prior to the assay (Figure 6.2.a), ATP-dependent atebrin fluorescence quenching was 12% of the original fluorescence level. In the experiment where the mutant (A128D) form of the *b*-subunit hydrophilic portion was incubated with $F_1$-ATPase prior to the assay (Figure 6.2.b), ATP-dependent atebrin fluorescence quenching was 51% of the original fluorescence level. Doubling the added quantity of wild-type *b*-subunit hydrophilic portion reduced the observed ATP-dependent quench to 8% (from 12%), while doubling the added quantity of mutant *b*-subunit hydrophilic portion had no effect (still 51% ATP-dependent quench).

These results indicate that the wild-type form of the *b*-subunit hydrophilic portion strongly inhibited reconstitution of proton pumping activity coupled to ATP hydrolysis by the $F_1$-ATPase on stripped membranes, while the mutant form had negligible inhibitory effect as judged by comparison with the control. This suggests that the wild-type form of the *b*-subunit hydrophilic portion binds the $F_1$-ATPase to prevent attatchment of the $F_1$-ATPase to the $F_O$ on the membranes, confirming the observations of Dunn (1992). However, the mutant form of the *b*-subunit hydrophilic portion does not apparently bind the $F_1$-ATPase, as it does not prevent attachment of the $F_1$-ATPase to the $F_O$ on the membranes.

Additional atebrin fluorescence quenching assays were carried out to examine the effect of adding the wild-type form of the *b*-subunit hydrophilic portion to native membranes (those from which the stripped membranes used in the experiments described above were prepared). 30 μL of membranes were

**Figure 6.2:** Comparison of the abilities of the wild-type and mutant (A128D) forms of the *b*-subunit hydrophilic portion to inhibit reconstitution of ATP-dependent atebrin fluorescence quenching by the $F_1$-ATPase. 30 µL of stripped membranes were used.

A) Experiment in which the wild-type form of the *b*-subunit hydrophilic portion was incubated with $F_1$-ATPase prior to the reconstitution assay.

B) Experiment in which the mutant (A128D) form of the *b*-subunit hydrophilic portion was incubated with $F_1$-ATPase prior to the reconstitution assay.

C) The control experiment, in which STEM buffer was incubated with $F_1$-ATPase prior to the reconstitution assay.

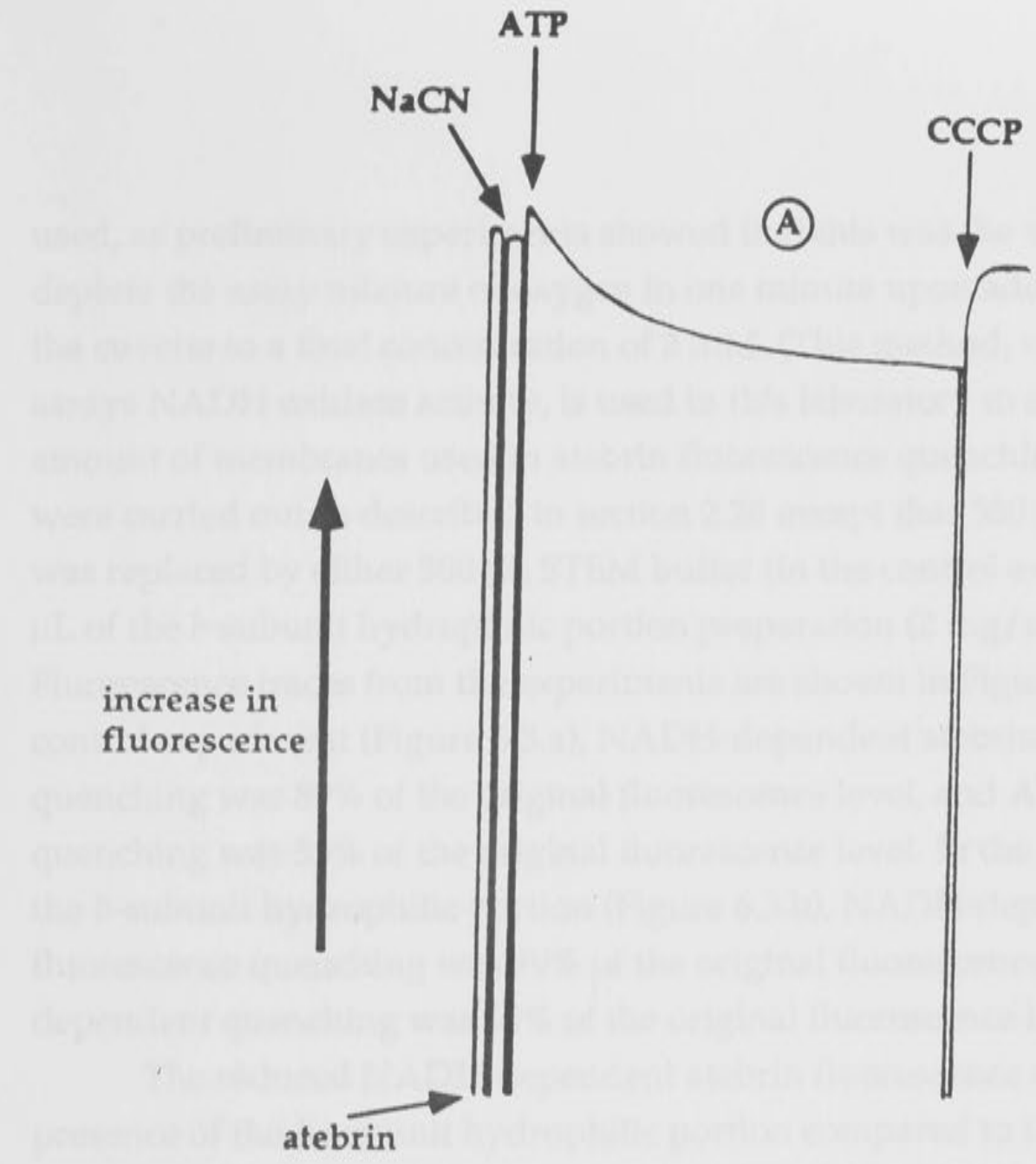
ATP
NaCN
CCCP
A
increase in
fluorescence
atebrin

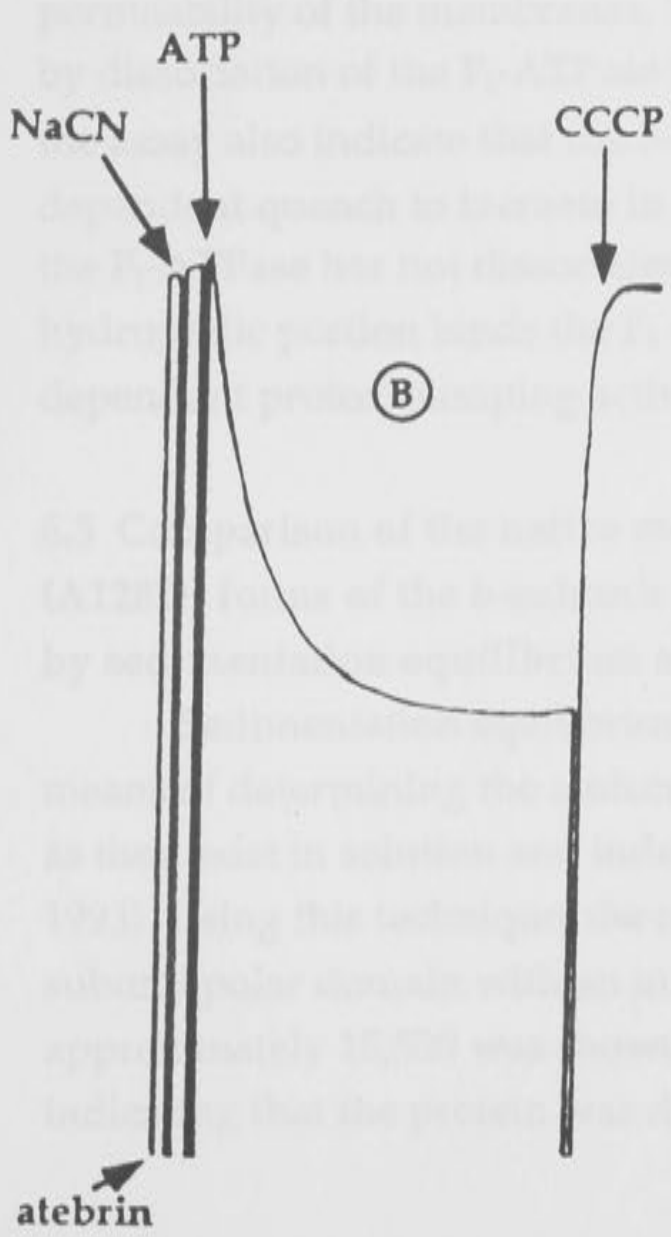
ATP
NaCN
CCCP
B
atebrin

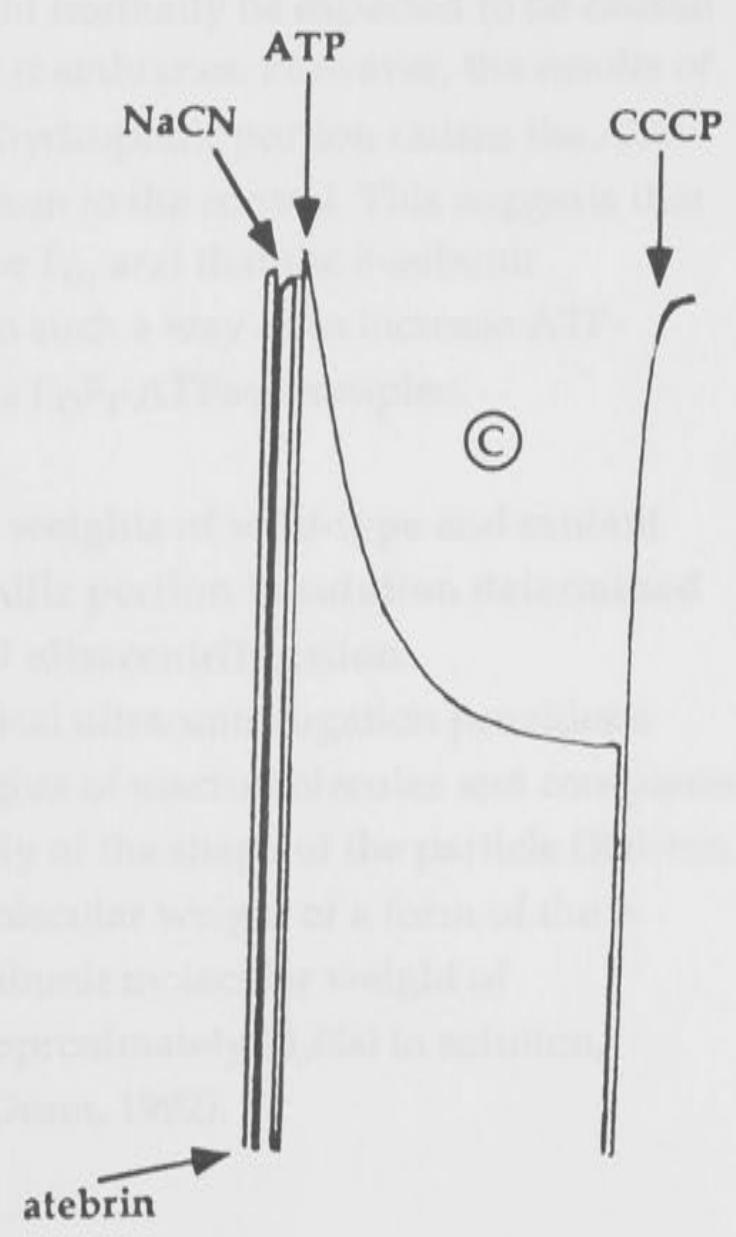
ATP
NaCN
CCCP
C
atebrin

used, as preliminary experiments showed that this was the volume required to deplete the assay mixture of oxygen in one minute upon addition of NADH to the cuvette to a final concentration of 2 mM. (This method, which indirectly assays NADH oxidase activity, is used in this laboratory to standardise the amount of membranes used in atebrin fluorescence quenching assays). Assays were carried out as described in section 2.26 except that 500 µL of Hepes buffer was replaced by either 500 µL STEM buffer (in the control experiment) or 500 µL of the *b*-subunit hydrophilic portion preparation (2 mg/mL protein). Fluorescence traces from the experiments are shown in Figure. 6.3. In the control experiment (Figure 6.3.a), NADH-dependent atebrin fluorescence quenching was 89% of the original fluorescence level, and ATP-dependent quenching was 55% of the original fluorescence level. In the experiment with the *b*-subunit hydrophilic portion (Figure 6.3.b), NADH-dependent atebrin fluorescence quenching was 79% of the original fluorescence level, while ATP-dependent quenching was 68% of the original fluorescence level.

The reduced NADH-dependent atebrin fluorescence quench in the presence of the *b*-subunit hydrophilic portion compared to the control experiment indicates that the protein has the effect of increasing proton permeability of the membranes. This might normally be expected to be caused by dissociation of the $F_1$-ATPase from the membranes. However, the results of the assay also indicate that the *b*-subunit hydrophilic portion causes the ATP-dependent quench to increase in comparison to the control. This suggests that the $F_1$-ATPase has not dissociated from the $F_O$, and that the *b*-subunit hydrophilic portion binds the $F_1$ moiety in such a way as to increase ATP-dependent proton pumping activity of the $F_OF_1$-ATPase complex.

**6.5 Comparison of the native molecular weights of wild-type and mutant (A128D) forms of the *b*-subunit hydrophilic portion in solution determined by sedimentation equilibrium analytical ultracentrifugation.**

Sedimentation equilibrium analytical ultracentrifugation provides a means of determining the molecular weights of macromolecules and complexes as they exist in solution and independently of the shape of the particle (Ralston, 1993). Using this technique, the native molecular weight of a form of the *b*-subunit polar domain with an inferred subunit molecular weight of approximately 15,500 was shown to be approximately 31,000 in solution, indicating that the protein was dimeric (Dunn, 1992).

**Figure 6.3:** Atebrin fluorescence quenching assays carried out to examine the effect of adding the wild-type form of the *b*-subunit hydrophilic portion to native membranes. 30 µL of membranes were used.

A) Assay carried out with 500 µL of Hepes buffer replaced by 500 µL STEM buffer (control experiment)

B) Assay carried out with 500 µL of Hepes buffer replaced by 500 µL *b*-subunit hydrophilic portion preparation (2 mg/mL protein)

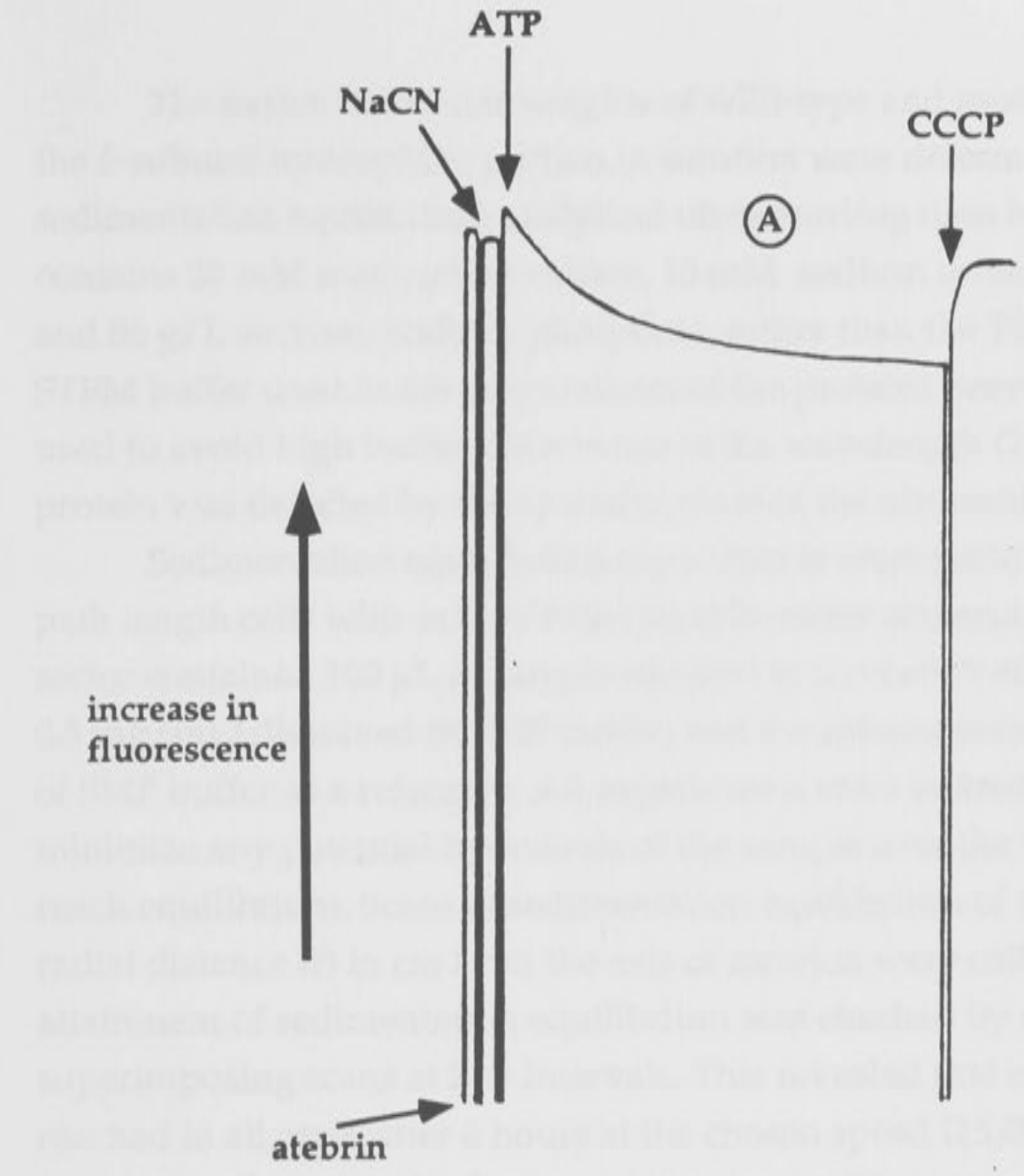
ATP
NaCN
CCCP
A
increase in
fluorescence
atebrin

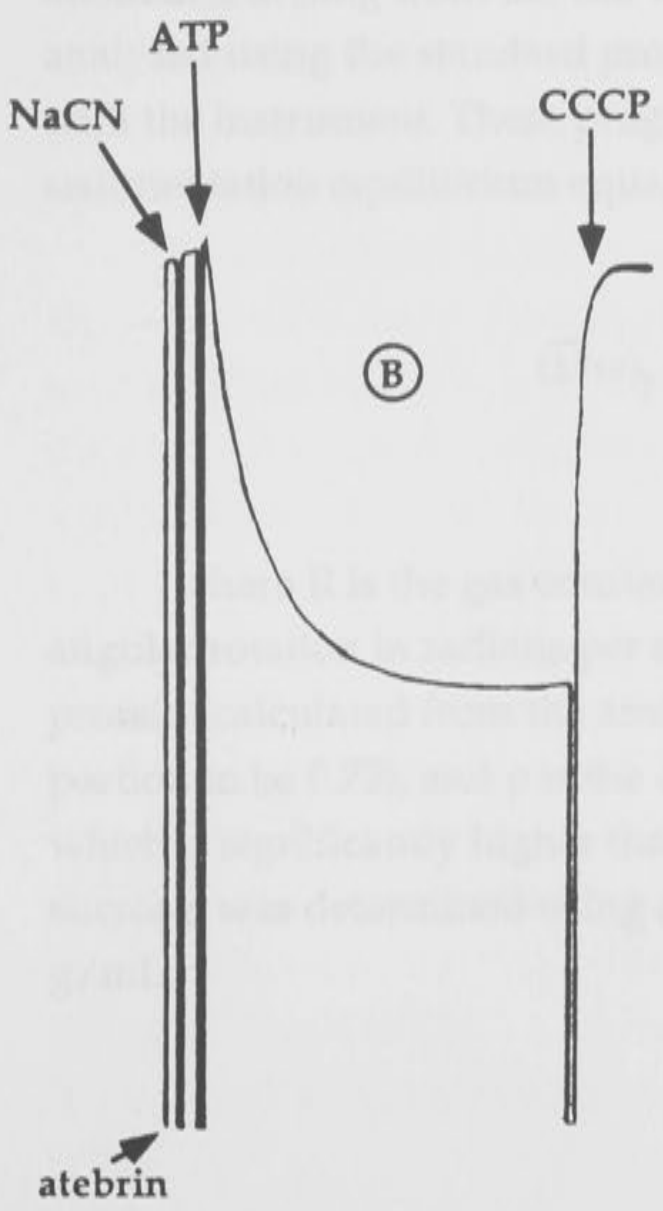
ATP
NaCN
CCCP
B
atebrin

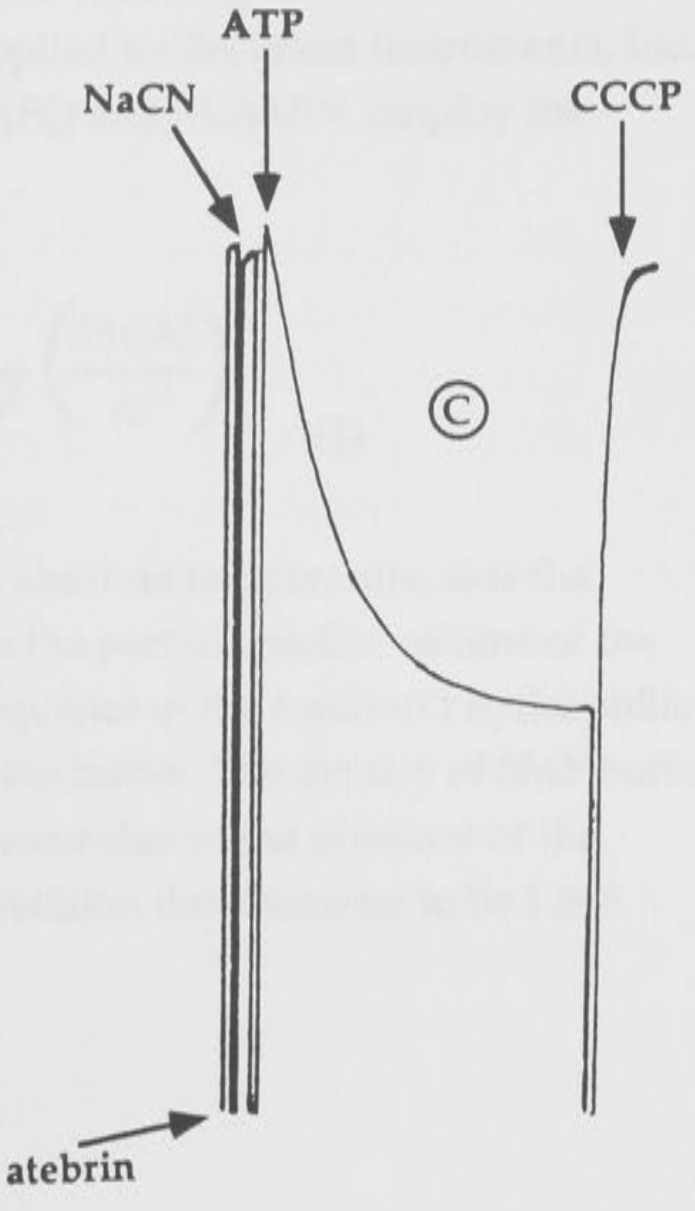
ATP
NaCN
CCCP
C
atebrin

The native molecular weights of wild-type and mutant (A128D) forms of the *b*-subunit hydrophilic portion in solution were determined by sedimentation equilibrium analytical ultracentrifugation in SMP buffer which contains 20 mM magnesium sulfate, 10 mM sodium orthophosphate (pH7.0), and 86 g/L sucrose. Sodium phosphate, rather than the TES present in the STEM buffer used in the preparations of the proteins previously described, was used to avoid high buffer absorbance at the wavelength (230 nm) at which the protein was detected by the optical system of the ultracentrifuge.

Sedimentation equilibrium experiments were performed using 12 mm path length cells with carbon-filled double-sector centrepieces. The solution sector contained 100 µL of sample (diluted to a concentration of approximately 0.5 mg/mL) dissolved in SMP buffer, and the solvent sector contained 110 µL of SMP buffer as a reference. All experiments were carried out at 4°C to minimize any potential hydrolysis of the sample over the time required to reach equilibrium. Scans at sedimentation equilibrium of absorbance (A) versus radial distance (r) in cm from the axis of rotation were collected at 230 nm. The attainment of sedimentation equilibrium was checked by collecting and superimposing scans at 2 hr intervals. This revealed that equilibrium had been reached in all cases after 6 hours at the chosen speed (15,000 rpm). Scans at 360 nm were collected and subtracted from the equilibrium scans to correct for anomalies arising from the cell windows. The resulting 'A' versus 'r' data were analysed using the standard programs supplied by Beckman Instruments, Inc. with the instrument. These programs, XLAEQ and XLAMW, employ the sedimentation equilibrium equation

$$(\overline{M}w)_r = \frac{2RT}{(1-\bar{\nu}\rho)\omega^2}\left(\frac{d\ln(A)}{dr^2}\right)_r \qquad (1)$$

where R is the gas constant, T is the absolute temperature, ω is the angular rotation in radians per second, $\bar{\nu}$ is the partial specific volume of the protein (calculated from the amino acid sequence of the *b*-subunit hydrophilic portion to be 0.73), and ρ is the density of the buffer. The density of SMP buffer, which is significantly higher than that of water due to the presence of the sucrose, was determined using a digital precision densitometer to be 1.048 g/mL.

For a homogeneous, thermodynamically ideal sample, equation (1) gives the molecular weight. If the sample is not homogeneous, $d\ln(A)/dr^2$ varies as a function of r (and hence concentration). Equation (1) then yields point weight average molecular weights, each being characteristic of the composition of the size mixture at that radial distance in the cell at which the slope has been evaluated.

Plots of ln(A) as a function of $r^2$ for the wild-type and mutant forms of the *b*-subunit hydrophilic domain were essentially linear (data not shown). These data were used to obtain the best-fit molecular weight for the relevant sample, employing the program XLAEQ, which assumes the sample is homogeneous and thermodynamically ideal. The molecular weight is evaluated corresponding to the best-fit straight line through the ln(A) versus $r^2$ plot. The native molecular weight of the wild-type *b*-subunit hydrophilic portion was found to be 28,000, while the mutant protein was found to have a molecular weight of 14,800. Since the subunit molecular weight of the *b*-subunit hydrophilic portion is approximately 14,200, these results indicate that the wild-type form of the protein is dimeric in solution (thus confirming the observation of Dunn (1992)), and that the mutant form exists as a monomer in solution.

**6.6 Comparison of the shapes of wild-type and mutant (A128D) forms of the *b*-subunit hydrophilic portion in solution determined by sedimentation velocity analytical ultracentrifugation.**

Sedimentation velocity experiments in the analytical ultracentrifuge allow the calculation of sedimentation and diffusion coefficients, the frictional ratio and Stokes radius of proteins. These data provide information regarding the size and shape of molecules (Ralston, 1993). Using this technique, the frictional ratio of a form of the *b*-subunit polar domain was shown to be approximately 2, indicating a highly extended structure for this protein (Dunn, 1992).

Sedimentation velocity experiments were carried out for both the wild-type and mutant forms of the *b*-subunit hydrophilic domain. The sample sector was almost filled with sample (diluted to a concentration of approximately 0.5 mg/mL) dissolved in SMP buffer, and the solvent sector contained a slightly higher volume of SMP buffer as a reference. Experiments were carried out at 50,000 rpm and at 20°C. Absorbance versus radial distance scans were collected automatically at 15 minute intervals at 230 nm. Plots of ln(r) as a function of

time were generated using the program XLAVEL, which was supplied with the instrument. The point 'r' is the point of inflection of the plot of absorbance versus radial distance at time 't' seconds. The sedimentation coefficient is evaluated from the equation

$$\ln(r) = \omega^2 st + C \qquad (2)$$

where $\omega$ is the angular velocity in radians per second, C is a constant and 's' is the sedimentation coefficient in Svedbergs when time 't' is expressed in seconds. A Svedberg is equivalent to $10^{-13}$ seconds. The program allows the experimenter to plot ln(r) as a function of time and fit a straight line by least squares to obtain the slope required to evaluate s. Values of s obtained in this way were corrected to the $s_{20,w}$ value using the equation

$$s_{20,w} = s_{T,b}\left(\frac{(1-\bar{\nu}\rho)_{20,w}}{(1-\bar{\nu}\rho)_{T,b}}\right)\left(\frac{\eta_{T,b}}{\eta_{20,w}}\right) \qquad (3)$$

where the subscript 20,w refers to the standard conditions (in water at 20°C), while T,b refers to the value obtained in the chosen buffer and at the temperature of the experiment. The viscosity, $\eta$, of SPM buffer was taken from a table showing the measured viscosities of sucrose solutions in water (Oncley, 1941). As mentioned above, the partial specific volume ($\bar{\nu}$) for the *b*-subunit hydrophilic portion is 0.73, and the density ($\rho$) of SPM buffer has been measured to be 1.048 g/mL.

Values for $s_{20,w}$ may be expressed as frictional ratios ($f/f_o$) by comparison with calculated tabulated values (Oncley, 1941) for $s_{20,w}$ of a perfectly spherical unhydrated particle of the same molecular mass, where $f/f_o$ is the ratio of the $s_{20,w}$ values of the hypothetical unhydrated spherical protein and the unhydrated sample protein.

The $f/f_o$ value may be expressed in terms of prolate (cigar-shaped) or oblate (discus-shaped) ellipsoids of revolution. However, consideration of the extended $\alpha$-helical structure of the *b*-subunit hydrophilic portion predicted from analysis of the amino acid sequence (Senior, 1983) would suggest that a prolate ellipsoid is more likely to accurately represent the shape of this protein. Calculated values of $f/f_o$ that differ from unity must be interpreted in terms of both a deviation from spherical shape and the amount of bound water (Oncley,

1941). If it is assumed that the *b*-subunit hydrophilic portion has an average amount of bound water (0.3 g/g protein; Oncley, 1941), the residual deviation of $f/f_o$ from unity may be expressed in terms of the axial ratio of the appropriate ellipsoid of revolution, based on tabulations of this data (Oncley, 1941). In the case of a prolate ellipsoid, this is a ratio of the values 'a' and 'b' as shown on the following diagram:

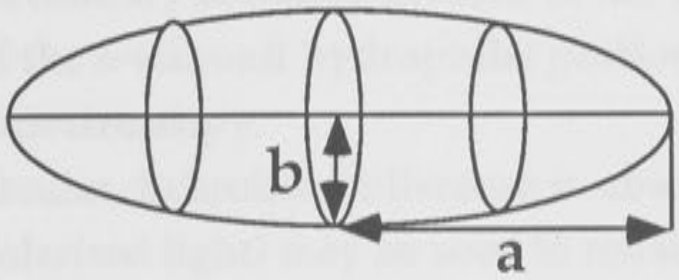


Results calculated from the measured sedimentation coefficients of the wild-type and mutant (A128D) forms of the *b*-subunit hydrophilic portion are shown in the table below. Calculations of $f/f_o$ and axial ratio are based on the wild-type and mutant forms possessing native molecular masses of 28,000 and 14,000 respectively, as measured by sedimentation equilibrium experiments described in the previous section.

| Protein | Wild-type form | Mutant form |
|---|---|---|
| $s_{20,w}$ | 2.0 | 1.7 |
| $f/f_o$ | 1.7 | 1.2 |
| Axial ratio | 8:1 | 3:1 |

Results from experiments with the wild-type form of the *b*-subunit hydrophilic portion are broadly consistent with the results of Dunn (1992), who reported a value for $f/f_o$ of 1.9, and concluded that the *b*-subunit hydrophilic portion dimer formed a highly extended structure.

The dimer of the wild-type form of the *b*-subunit hydrophilic portion, which possesses a native molecular mass of 28,000 Da, has an axial ratio of approximately 8:1, while the monomer mutant form, which possesses a native molecular mass of 14,000 Da, has an axial ratio of approximately 3:1. These results suggest that the wild-type protein forms a dimer by the end-to-end interaction of two extended structures (with axial ratios of approximately 4:1) to form a very highly extended native conformation (axial ratio 8:1). The

extended shapes of both the wild-type and mutant proteins suggest high levels of α-helical secondary structure. Circular dichroism spectroscopy, a technique which is used to predict secondary structure content, was used to assist in resolving this question.

**6.7 Comparison of the secondary structure content of the wild-type and mutant (A128D) forms of the *b*-subunit hydrophilic portion determined by circular dichroism (CD) spectroscopy.**

Measurement of circular dichroism (difference in absorbance between left and right circularly polarised light) may be used to reliably predict secondary structure of proteins and polypeptides in solution (Manavalan and Johnson, 1987). CD data can, however, only give statistically significant estimates of multiple classes of secondary structure if the scans are extended to wavelengths of 184 nm or less (Johnson, 1990). The CD scans of both the wild-type and mutant forms of the *b*-subunit hydrophilic portion were carried out over the wavelength range 182-260 nm at 20°C in a 0.1 cm path length quartz cell. The proteins were dissolved in MP buffer (SMP buffer, described above, without sucrose) because of the high absorbance of sucrose at far ultra-violet wavelengths. The baseline spectrum of MP buffer alone was subtracted from the data prior to analysis. Data were analysed by the computer program VARSLC1 written by W. Curtis Johnson and coworkers, Corvallis, Oregon, using the variable selection technique described by Johnson (1990).

The CD spectra of the wild-type and mutant forms of the *b*-subunit hydrophilic portion are shown in Figure 6.4. Using the data from which these graphs were plotted, computer analysis predicted that the wild-type form of the *b*-subunit hydrophilic portion had 100% α-helical content within experimental error. This is consistent with the finding of Dunn (1992), who reported that the *b*-subunit hydrophilic portion had a high α-helical content. Computer analysis predicted that the mutant (A128D) form of the *b*-subunit hydrophilic portion had 65% α-helical content. The computer program did not predict significant levels of any type of secondary structure other than α-helix in either the wild-type or mutant forms of the protein.

**Figure 6.4**: Circular dichroism spectra of the wild-type and mutant (A128D) forms of the *E. coli b*-subunit hydrophilic portion. Circular dichroism is expressed as mean residue ellipticity.

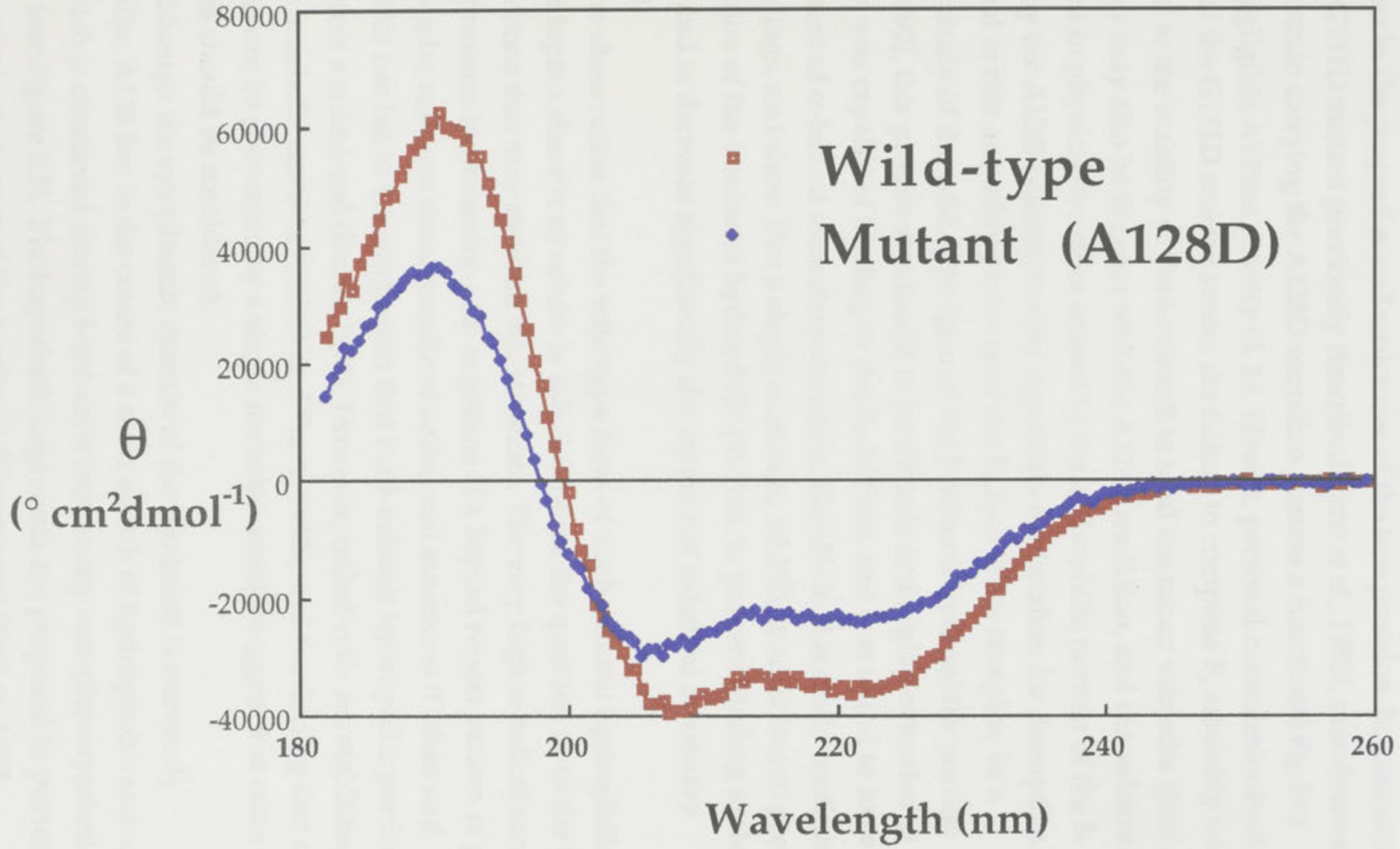
80000
60000
40000
20000
0
-20000
-40000
θ
(° cm²dmol⁻¹)
180
200
220
240
260
Wavelength (nm)
Wild-type
Mutant (A128D)

## 6.10 Discussion

The biochemical and physical analysis of the purified wild-type and mutant (A128D) forms of the *b*-subunit hydrophilic portion indicate profound differences in the properties and structures of the two proteins. In common with the G131D mutant previously described (Jans *et al.*, 1985), membranes from the strain carrying the A128D mutation possess a functional $F_O$, but exhibit negligible ATPase activity (S. M. Howitt, personal communication). In the case of the G131D mutant strain, the failure to complete $F_1$ assembly was attributed to the inability of the *b*-subunit to bind the minor subunits (Jans *et al.*, 1985). This may also be the case with the A128D mutation, and the substantial alterations in physical structure caused to the hydrophilic portion of the *b*-subunit by the A128D mutation offer a possible explanation for disruption of the normal *in vivo* assembly pathway of the $F_OF_1$-ATPase complex. In a previous study of the wild-type form of the *b*-subunit hydrophilic portion (Dunn, 1992), this protein was found to be dimeric and highly extended in structure, was capable of binding to the $F_1$-ATPase, and was found to have a high content of α-helical secondary structure. Results in this study confirm these findings, and show that a single mutation, A128D, is sufficient to prevent dimerisation of the *b*-subunit hydrophilic portion, to prevent binding to the $F_1$-ATPase, and to decrease significantly the amount of α-helical secondary structure.

The observation that the wild-type form of the *b*-subunit hydrophilic portion adopts a dimeric structure in solution raises the question as to the type of interactions that may stabilise this structure. The very high α-helical content, and the presence in the amino acid sequence of a heptad repeat pattern of polar and non-polar residues characteristic of coiled-coil structures (Cohen and Parry, 1990) has led to the suggestion that the *b*-subunit hydrophilic portion dimer forms a coiled-coil (Dunn, 1992). However, coiled-coils are stabilized by multiple interhelix contacts (Cohen and Parry, 1990), and the finding that dimer formation can be prevented by a single mutation would suggest that other structures should be considered.

Although the cytoplasmic domain of the *b*-subunit is extremely hydrophilic, A128 lies in the centre of a short stretch of hydrophobic amino acids which is conserved among *b*-subunits from many non-photosynthetic bacteria (see Figure 6.5). Photosynthetic organisms are proposed to possess two different homologues of the *b*-subunit (Cozens and Walker, 1987; Herrmann *et al.*, 1993) and this region is not present in either one of them. In

**Figure 6.5**: Hydropathy plots of *b*-subunits from different species. Hydropathy plots were calculated using the algorithm of Kyte and Doolittle (1982) and a window size of 9 amino acids. The hydrophobic region discussed in the text is underlined. Sequences used were from : *Escherichia coli* (Walker *et al.*, 1984), *Vibrio alginolyticus* (Krumholtz *et al.*, 1989), *Bacillus megaterium* (Brusilow *et al.*, 1989) and PS3 (Ohta *et al.*, 1988).

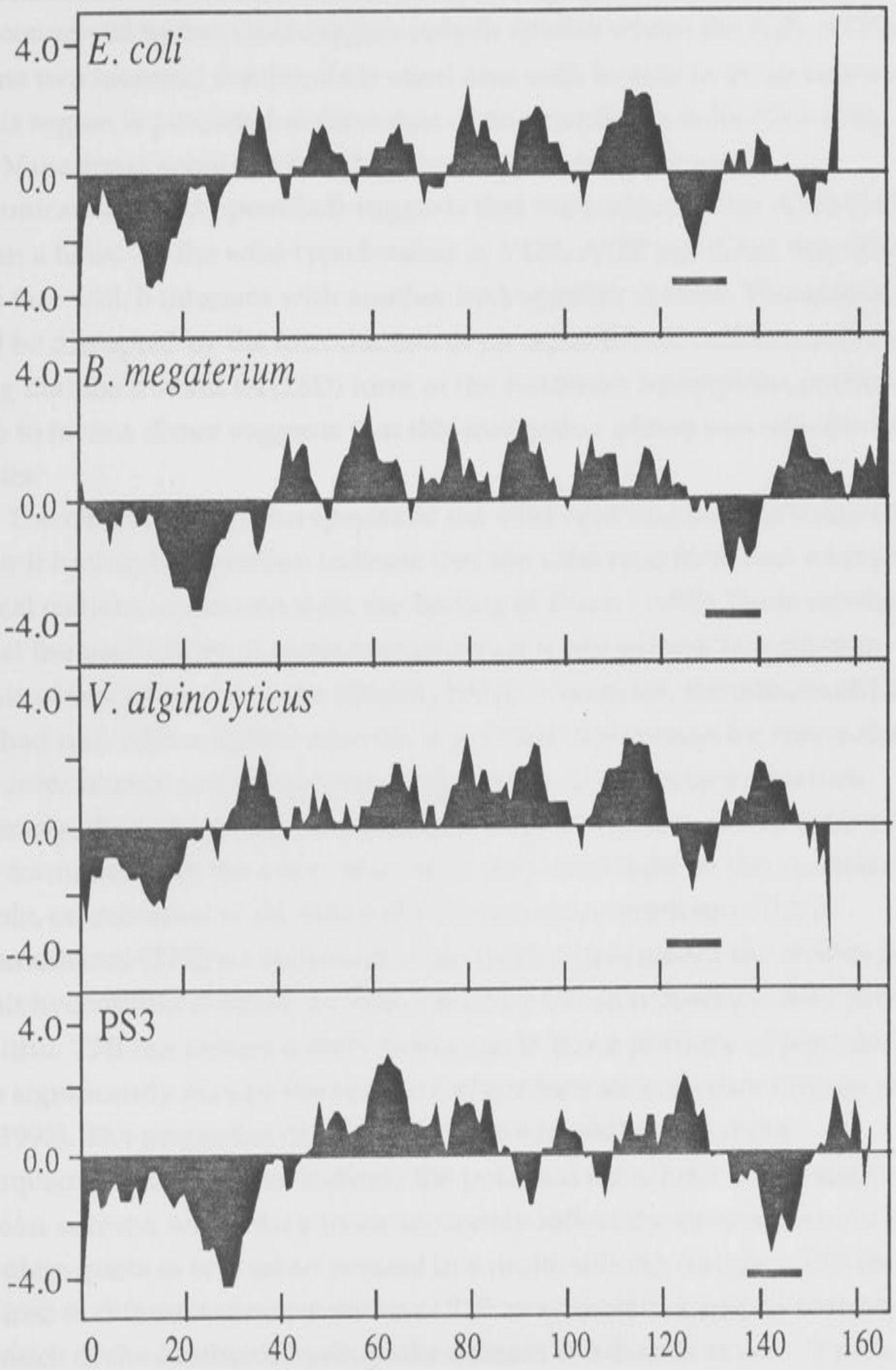
4.0
E. coli
0.0
-4.0
4.0
B. megaterium
0.0
-4.0
4.0
V. alginolyticus
0.0
-4.0
4.0
PS3
0.0
-4.0
0
20
40
60
80
100
120
140
160

these organisms, one of each of the two *b*-subunit homologues may replace the pair of identical *b*-subunits found in non-photosynthetic bacteria. The presence of the conserved hydrophobic region only in species where the $F_OF_1$-ATPase contains two identical *b*-subunits is consistent with its role in dimerisation. In *E. coli*, this region is predicted to form part of an extended α-helix (Cox *et al.*, 1984). Mutational analysis carried out by S. M. Howitt (personal communication; see Appendix I) suggests that the residues from A124 to G131 do form a helix. In the wild-type *b*-subunit, V124, A128 and G131 may form a helical face which interacts with another hydrophobic surface. This interaction would be disrupted by the introduction of an aspartic acid residue, and the finding that the mutant (A128D) form of the *b*-subunit hydrophilic portion is unable to form a dimer suggests that this interaction occurs between the two *b*-subunits.

The circular dichroism spectra of the wild-type and mutant forms of the *b*-subunit hydrophilic portion indicate that the wild-type form had a very high α-helical content, consistent with the finding of Dunn (1992). These results also support the predictions of secondary structure made using Chou-Fasman analysis of secondary structure (Senior, 1983). In contrast, the mutant (A128D) form had only 65% α-helical content. A possible explanation for this is that dimer formation is necessary for the stabilisation of secondary structure. Conversely, the formation of secondary structure may be required prior to dimer formation. Further experimentation may shed light on this question. For example, examination of the effect of different concentrations of 2,2,2-trifluoroethanol (TFE) on the α-helical secondary structure of the wild-type *b*-subunit hydrophilic domain, as determined by CD spectroscopy, may prove to be fruitful. TFE can induce α-helix formation in those portions of peptides which significantly occupy the α-region of conformational space (Dyson *et al.*, 1988; 1992). The properties of the *b*-subunit hydrophilic domain in TFE/aqueous mixtures may indicate the potential for α-helix formation in a less polar solvent, which may more accurately reflect the environment in which the protein exists *in vivo* when present in a multi-subunit complex. CD scans measured at different concentrations of TFE may therefore help in assessing how much of the *b*-subunit hydrophilic domain is α-helical *in vivo*. If such experiments are carried out in conjunction with determinations of native molecular weight by sedimentation equilibrium analytical ultracentrifugation, it may be possible to correlate the amounts and types of secondary structure present with propensity for dimer formation. Circular dichroism and

sedimentation equilibrium experiments could also be used to examine the effect of temperature on secondary structure content and dimer stability. The CD spectra of proteins with high α-helical content exhibit a characteristic intensely negative band at 222 nm (Hennesey and Johnson, 1981). With the wavelength fixed at this value, the CD of the wild-type *b*-subunit hydrophilic domain could be measured over a temperature range to determine the effect of temperature on α-helical secondary structure, while sedimentation equilibrium experiments could also be carried out over a range of temperatures to examine the effect of temperature on native molecular weight. This information would be valuable in assessing the strength of the interactions responsible for stabilising the *b*-subunit hydrophilic portion dimer. The dimerisation itself may play a role in stabilising secondary structure. As mentioned above, an effect *in vivo* of the G131D mutation (Jans *et al.*, 1985) and therefore probably the A128D mutation also, is to disrupt interaction between the *b*-subunit and the minor $F_1$ subunits during assembly. Aberrant folding of the mutant (A128D) *b*-subunit would be consistent with this proposal.

The observation that the dimeric wild-type *b*-subunit hydrophilic portion has an axial ratio approximately double that of the monomeric mutant form can only be rationally explained if the single *b*-subunits interact such that they are aligned end-to-end to form a very highly extended structure. This contradicts previously proposed models for the structure of the *b*-subunit which suggest that the hydrophilic portions of the two copies of the subunit are roughly parallel, and extend into the cytoplasm at an angle perpendicular to the plane of the membrane (Senior, 1983; Cox *et al.*, 1986). An alternative model which accomodates the results described in this chapter is discussed in Chapter 7.

The results of the reconstitution inhibition assays show that the wild-type form of the *b*-subunit hydrophilic portion, but not the mutant form, binds the $F_1$-ATPase to prevent attatchment of the $F_1$-ATPase to the $F_O$ on the membranes. Membranes prepared from a strain carrying the *b*-subunit A128D mutation showed negligible ATPase activity, but were permeable to protons when stripped (S. M. Howitt, personal communication; see Appendix I). This implies that the hydrophobic domains of the mutant *b*-subunits were correctly located in the $F_O$. The inability of the hydrophilic domains to dimerise may provide a rational explanation for the failure of the mutant strain to complete $F_1$ assembly, and if dimerisation is required for the *b*-subunit hydrophilic portion to interact with the $F_1$-ATPase, this could also explain why the mutant (A128D)

form of the protein fails to inhibit reconstitution of ATP-dependent proton pumping.

The addition of the wild-type form of the *b*-subunit hydrophilic portion to native unstripped membranes increased proton permeability of the membranes substantially as judged by the kinetics of NADH-dependent atebrin fluorescence quenching. This might normally be expected to be caused by dissociation of the $F_1$-ATPase from the membranes. However, the *b*-subunit hydrophilic portion also caused ATP-dependent quenching to increase significantly. This suggests that the $F_1$-ATPase has not dissociated from the $F_O$, and that the *b*-subunit hydrophilic portion binds the $F_1$ moiety in such a way as to increase ATP-dependent proton pumping activity of the $F_OF_1$-ATPase complex. This unexpected finding will be discussed in more detail in Chapter 7.

# CHAPTER 7

## GENERAL DISCUSSION

The purpose of this chapter is to summarise the findings presented in previous chapters, and to assess the extent to which the aims of the project have been achieved. An attempt will be made to show how results presented here may contribute to knowledge of the structure and function of $F_OF_1$-ATPases.

The aim of the first section of work described in this thesis was to test whether particular spinach chloroplast $F_OF_1$-ATPase subunits might be able to functionally replace the homologous *E. coli* subunits. It was hoped that at least one of the spinach chloroplast subunits would be able to replace the homologous *E. coli* subunit. Successful complementation would allow an experimental system involving genetic and biochemical analysis to be developed to probe the structure and function of the foreign subunit in the hybrid complex. Such a system would have the potential to provide a large amount of useful data. However, the failure of all of the chloroplast subunits to complement to any significant degree meant that the potential for gaining meaningful information was extremely limited. Given the very low level of sequence identity between the chloroplast and *E. coli* subunits involved in the complementation analysis, it is difficult to specify particular amino acid residues or sequence regions responsible for the failure of the experiment, and little insight into the structure and function of $F_OF_1$-ATPases is gained. The weak complementation of an *E. coli* mutant deficient in the δ-subunit by the chloroplast δ-subunit did not allow the development of a useful experimental system for analysing the δ-subunit because the ability to grow poorly on succinate was the only indicator of $F_OF_1$-ATPase function to suggest that the chloroplast subunit had assembled with the *E. coli* subunits to form a functional complex. Without measurable enzyme function as judged by other assays, such as growth performance on limiting glucose, membrane ATPase activity or ATP dependent atebrin fluorescence quenching, there would be little value in carrying out mutagenesis studies. A worthwhile outcome from the complementation analysis was the correction of a report in the literature claiming that

chloroplast subunit $CF_OI$ could functionally replace the *E. coli b*-subunit (Schmidt *et al.*, 1990). This was shown conclusively not to be the case.

The second aim of this project was to isolate complexes formed by subunits from the *E. coli*, chloroplast and cyanobacterial $F_OF_1$-ATPases, using a system involving expression of the subunits as fusions with the enzyme glutathione-S-transferase (GST). Studies on the spinach chloroplast subunits γ, $CF_OI$ and $CF_OII$ were hampered by the insolubility of the fusion proteins when expressed in *E. coli*. It was not possible to solubilise them using non-denaturing detergents, and the value of attempting to solubilise such proteins by denaturing means in the absence of an assayable enzymic acivity must be questioned. Although no stable complexes involving chloroplast or cyanobacterial $F_OF_1$-ATPase subunits could be identified, valuable information was gained. Firstly, it was shown that the hydrophilic portions of the *Synechococcus* R2 *b*- and *b´*-subunits are soluble when expressed as fusion proteins with GST. Although a complex of the GST-*b*-subunit fusion and the δ-subunit was not isolated, the δ-subunit was shown to assist in the correct folding of the *b*-subunit moiety since the fusion expressed in the presence of the δ-subunit was more resistant to proteolytic degradation during purification than was the case when the fusion was not expressed in the presence of the δ-subunit. Secondly, it was shown that the *Synechococcus* R2 γ-subunit is soluble when expressed as a fusion protein with GST. Only the preliminary stages of purification of the *Synechococcus* R2 *b*- and *b´*-subunits hydrophilic portions and the γ-subunit have been completed, but further refinement of the purification procedure should allow these proteins to be prepared in suitable amounts for analysis of their physical properties. Thirdly, it was shown that the chloroplast ε-subunit is soluble when expressed as a fusion protein with GST. Purification of the ε-subunit was prevented by the protein remaining bound to the beads following thrombin digestion, but further experimentation, possibly involving the purification of the ε-subunit using an alternative method of affinity chromatography, should allow this protein to be purified in large amounts for the purpose of carrying out analysis of its physical properties.

Studies involving the expression of *E. coli* $F_OF_1$-ATPase subunits did not result in the purification of any complexes with defined stoichiometry, but evidence for noteworthy intersubunit interactions was collected. When expressed from a strain which co-expresses a GST-*b*-subunit hydrophilic portion fusion with the δ-subunit, the free *b*-subunit hydrophilic portion, the γ-subunit and the ε-subunit, the GST-*b*-subunit hydrophilic portion fusion did not bind to glutathione agarose beads, but did bind when

expressed with the δ-subunit alone. This may be due to interactions involving the γ- and ε-subunits which block binding of glutathione to the GST moiety of the fusion protein, but analysis of the biochemical and physical properties of the purified *b*-subunit hydrophilic portion described in Chapter 6 offers an alternative explanation. The free *b*-subunit hydrophilic portion expressed in the strain would be expected, based on data from the sedimentation equilibrium analysis, to form a dimer with the *b*-subunit hydrophilic portion moiety of the fusion protein. The sedimentation velocity experiments show that the dimer is formed by two *b*-subunit hydrophilic portion proteins joining end-to-end to form a very highly extended structure, rather than aligning themselves side-by-side in parallel. This may bring the unfused copy of the *b*-subunit hydrophilic portion into close proximity with the GST moiety of the fusion, and thereby obstruct the glutathione binding site, preventing the fusion binding the beads. Further experiments are required to investigate this proposal. A plasmid could be constructed to express a GST-*b*-subunit hydrophilic portion fusion plus the free *b*-subunit hydrophilic portion without the other subunits, and the purification of the fusion attempted. If the fusion fails to bind glutathione agarose beads, this would support the proposal that formation of the very highly extended dimer is responsible for blocking the binding of the fusion to the beads, but if the fusion does bind to the beads this would indicate that the binding of one or more of the minor subunits to the *b*-subunit hydrophilic portion moiety is responsible for blocking the binding of the fusion to the beads when it is co-expressed with the δ-subunit, the free *b*-subunit hydrophilic portion, the γ-subunit and the ε-subunit.

The original rationale for pursuing the purification of a complex of the *b*-subunit hydrophilic portion and either or both of the α- and β-subunits was that such complexes may represent assembly intermediates in the integrated membrane assembly pathway (Cox *et al.*, 1981), which proposes that both the α- and β-subunits are required for incorporation of the *b*-subunit into the membrane. The α- and β-subunits were both found to copurify with the GST-*b*-subunit hydrophilic portion fusion, albeit in substoichiometric amounts. Interestingly, the α- and β-subunits bound in equal amounts to the isolated fusion protein, despite the β-subunit being expressed at significantly higher levels than the α-subunit from the plasmid. This may suggest that these subunits bind to the *b*-subunit hydrophilic portion in a cooperative fashion, but further experimentation is required to pursue this question. A plasmid could be constructed from the

one used in this study in which the *uncE* pregenic region is inserted to immediately precede the *uncA* gene, thereby increasing the efficiency of translation of the α-subunit. If the amounts of both the α- and β-subunits bound to the fusion increase relative to the amount of fusion, whilst retaining the 1:1 ratio of bound α- and β-subunits, it would indicate that the level of expression of the α-subunit from the original plasmid may have been limiting the amount of α/β/*b*-subunit hydrophilic portion complex formed. Preliminary experiments aimed at purifying this complex by size-exclusion HPLC indicate that the size of the complex is very similar to that of the whole $F_1$. This suggests that each *b*-subunit hydrophilic portion dimer may bind three copies each of the α- and β-subunits. Further refinement of the conditions for expression and purification of the complex will assist in the investigation of this question.

The observation that an α/β/*b*-subunit hydrophilic portion complex is formed should be interpreted with the results presented in Chapter 6 in mind. The addition of the wild-type form of the *b*-subunit hydrophilic portion to native unstripped membranes increased the proton permeability of the membranes while also increasing the ATP-dependent proton pumping activity of the $F_OF_1$-ATPase complex. These observations may only be rationally explained if the *b*-subunit hydrophilic portion is able to interact with an exposed surface of the enzyme, and argue against the idea that the *b*-subunit hydrophilic portion is buried within the bulk mass of $F_1$ subunits. This proposal is consistent with cryoelectron microscopy studies of the interaction of the *b*-subunit hydrophilic portion dimer with the $F_1$-ATPase (Wilkens *et al.*, 1994), which show that the *b*-subunit hydrophilic portion dimer interacts with one of the β-subunits but does not fill the central cavity within the $\alpha_3\beta_3$ hexamer.

Results from the analytical ultracentrifugation experiments indicate that the wild-type form of the *b*-subunit hydrophilic portion is a dimer with an axial ratio of approximately 8:1, and the mutant form is a monomer with an axial ratio of approximately 3:1. This is consistent with the elution profile of the two proteins from size-exclusion HPLC. Based on the elution times of standard proteins from the HPLC column, the wild-type form of the *b*-subunit hydrophilic portion had an apparent molecular weight of approximately 160,000 and the mutant form had an apparent molecular weight of approximately 85,000. These observations support the proposal that the dimerisation in the wild-type form is mediated by end-to-end interactions of the single subunit, with a short overlap. The overlapping sequence would be expected to comprise the short hydrophobic sequence

(residues V124 to A132) which includes residue A128. The mutation A128D prevented dimerisation, implicating this region in the interaction between the two *b*-subunits. It may be possible for the N-terminal hydrophobic regions predicted to traverse the membrane to extend at an angle perpendicular to the plane of the end-to-end structure. A computer-generated energy-minimised molecular model for the *b*-subunit hydrophilic portion dimer is shown in Figure 7.1.

A model for rotational catalysis was proposed by Cox *et al.* (1984; 1986) which proposes that $F_O$ assembles as a ring of *c*-subunits about a central core consisting of the *a*-subunit and the two *b*-subunits (see Figure 1.5), and that $F_1$ would consist of the minor subunits (γ, δ and ε) surrounded by the $\alpha_3\beta_3$ hexagon. In the assembled $F_OF_1$-ATPase complex, the movement of protons through $F_O$ would cause an inner core (the 'rotator', consisting of the the *a*-, *b*-, γ-, δ- and ε- subunits) to rotate relative to an outer complex (the 'stator') consisting of the *c*-, α- and β-subunits. The new proposed structure for the *b*-subunit described above is not consistent with this model, since it is not possible for the highly extended end-to-end structure of the *b*-subunit hydrophilic portion to form part of the complex proposed to rotate within the central cavity inside the $\alpha_3\beta_3$ hexamer. It is more likely that the *b*-subunit dimer forms part of the stator, and might therefore be expected to form interactions with the α- and β-subunits of the $F_1$ sector, and the *c*-subunits of the $F_O$ sector. The N-terminal hydrophobic segments of the *b*- would most likely be located at the rim of the $F_O$ complex, rather than within the ring of *c*-subunits as proposed by Cox *et al.* (1984). This is consistent with the results described in this work, which demonstrate specific interactions between the *b*-subunit hydrophilic portion and the α- and β-subunits, and the previous finding that both the α- and β-subunits are required for incorporation of the *b*-subunit into the membrane during assembly of the $F_OF_1$-ATPase complex (Cox *et al.*, 1981). Furthermore, the observation that addition of the *b*-subunit hydrophilic portion to native membranes influences the kinetics of proton translocation suggests interaction between the *b*-subunit hydrophilic portion and the outside of the complex. Although $F_1$ has been shown to protect the *b*-subunit from proteolysis by trypsin, the protective effect is not complete (Perlin *et al.*, 1983), and the possibility that the *b*-subunit may be afforded partial protection from proteolysis by interaction with the outside of the $F_1$ complex cannot be excluded.

The high resolution crystal structure of $F_1$ from bovine heart mitochondria reported by Abrahams *et al.* (1994) is consistent with the

**Figure 7.1**: An extended structure of the of the *b*-subunit hydrophilic portion was modelled and a β-turn constructed starting at residue 80 as predicted by the Chou-Fasman algorithm. The remainder of the sequence was converted to an α-helix and the resulting structure minimized to an RMS derivative of 0.06 kcal $mol^{-1}$ $Å^{-1}$. A copy of the minimized structure was made and laid on the original so that the structures were oriented at $180^{o}$ and the hydrophobic regions (residues 123 to 132) juxtaposed. The CPK residues show the hydrophobic regions and the N-termini of the models, the latter being pale blue.

Molecular modelling was carried out using the programs Insight and Discover (Biosym Technologies) on a Silicon Graphics workstation (Iris 4d/310GTX). The calculations for conjugate gradient minimizations of structures were carried out using the Fujitsu VP of the ANU Supercomputer Facility.

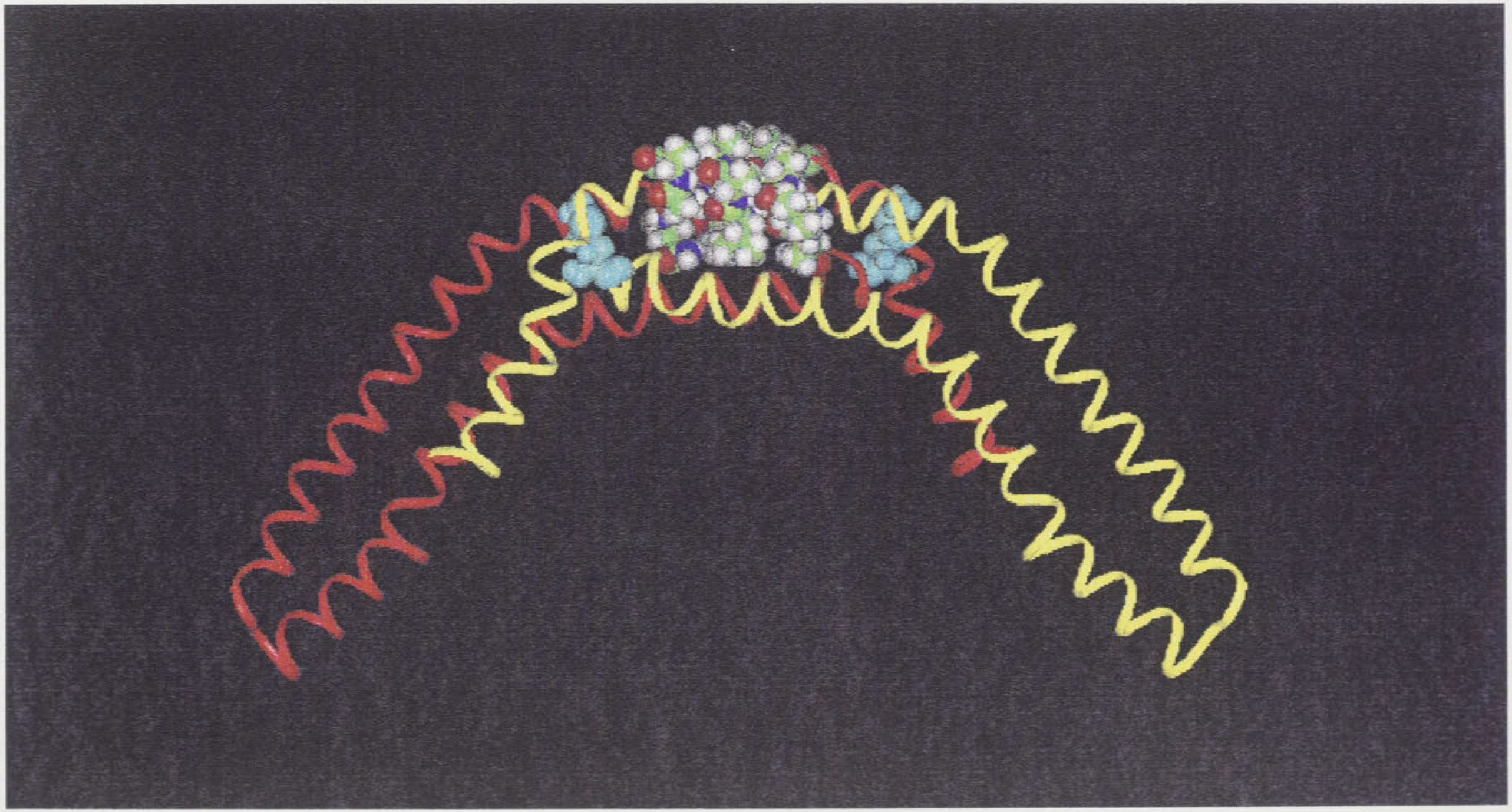

model of *b*-subunit structure proposed here. These workers suggest that rotation of the γ-subunit within the central cavity inside the $\alpha_3\beta_3$ hexamer may cause cyclical interconversion of the conformations of the catalytic sites. The crystal structure shows that space within the $\alpha_3\beta_3$ hexamer is limited, and appears mainly to be taken up by N- and C- terminal α-helices of the γ-subunit. There is little room available to accommodate the *b*-subunit hydrophilic domain, which therefore appears more likely to associate with the outside of the bulk mass of the $F_1$ formed by the $\alpha_3\beta_3$ hexamer. The lack of *b*-subunit missense mutations isolated relative to the number from other $F_O$ subunits (McCormick and Cain, 1993) may suggest that the *b*-subunit is not involved in tight packing with other subunits, where changes in the size and physical properties of amino acid side chains are more likely to have a deleterious effects. This would support the idea that the b-subunit contacts the outside, rather than the inside, of the $F_1$.

Electron spectroscopic images of cholate-solubilised $F_O$ complexes from *E. coli* observed by Birkenhäger *et al.* (1995) showed that $F_O$ has a deltoid-like structure with bilateral symmetry, or a trapezoidal shape, depending on the projection. This observation was interpreted by these workers as supporting a model for $F_O$ structure in which the *a*-subunit and the two copies of the *b*-subunit are located outside a *c*-subunit oligomer. The presence of a double lobe at the side of the trapezoidal images observed by Birkenhäger *et al.* (1995) is consistent with the model for the structure of the *b*-subunit proposed here. However, the suggestion by Birkenhäger *et al.* (1995) that the *a*-subunit is located outside the *c*-subunit oligomer appears to be inconsistent with other studies. 3-(trifluoromethyl)-3-(m-[$^{125}$I]-iodophenyl)diazirine ([$^{125}$I]-TID) labelling studies of proteoliposomes prepared from $F_O$ carried out by Steffens *et al.* (1987) compared the ([$^{125}$I]-TID) labelling of purified *c*-subunit reconstituted into liposomes alone to the labelling of the *a*- and *c*-subunits reconstituted together. The presence of the *a*-subunit completely blocked the labelling of some *c*-subunit residues. Since there is only one copy of the *a*-subunit, this implies that it is in contact with all of the *c*-subunits. Mutational analysis by Fimmel *et al.* (1985) showed that plasmid-borne expression of the mutant *c*-subunit A25T resulted in a mutant phenotype in an *uncE* mutant background strain, but a wild-type phenotype in a wild-type background strain. However, plasmid-borne expression of the mutant *c*-subunit A25Y resulted in a mutant phenotype in both mutant and wild-type background strains (Fimmel and Fordham,1989). The effect of the A25T mutation must be steric, because if it affected functional interaction between the *a*- and *c*-subunits, then one

mutant *c*-subunit per complex should result in the mutant phenotype. This implies that some mutant T25 *c*-subunits can be accommodated in the ring of *c*-subunits, but a ring composed entirely of T25 *c*-subunits cannot function, presumably because there is insufficient room for the *a*-subunit to function. Substituting A25 for a larger residue such as Y has a more deleterious effect, consistent with steric hindrance, in that not even a single copy of the mutant A25Y *c*-subunit can be accommodated within the ring of *c*-subunits.

The new proposal for the structure and function of the *b*-subunit described in this thesis opens up many avenues for further experimentation. The model for rotational catalysis proposed by Cox *et al.* (1986) is modified such that the *b*-subunit interacts with the α-, β- and *c*-subunits to form the stator, rather than forming part of the inner rotating complex with the *a*-, γ-, δ- and ε-subunits. A prediction of the new model is that the *a*-subunit should interact with the γ-, δ- and ε-subunits to form the rotator. This could be tested by using the approach described in this thesis, of co-expressing combinations of subunits and attempting to purify complexes. These experiments, along with further characterisation of the $\alpha/\beta/b$ complex already described will be important in providing support for the modified rotational hypothesis.

# APPENDIX 1

To investigate the role of the conserved hydrophobic region near the C-terminus of the *b*-subunit, a series of mutants was constructed in which aspartic acid replaced each residue from V124 to A132. Each mutant plasmid was transformed into strain AN1440 (*uncF469)* which carries the chromosomal mutation Trp26→stop. Membranes were prepared from each strain and the growth properties of the mutant strains and the ATPase activity and proton pumping activities of the membranes were determined. The results are shown in Table A1. The ability of each strain to grow on solid succinate medium is indicated as + or -. The values for the growth yield on 5 mM glucose and ATPase activity of each mutant are expressed as percentages, with the values for the coupled and uncoupled controls being set at 100% and 0, respectively. The ATPase activity of the coupled control was 0.8 mmol/min/mg protein. Atebrin fluorescence quenching activities are given as percentages of the maximum quench. The wild type values were 85% for NADH-dependent quenching activity and 92% for ATP-dependent quenching activity. Data was collected by Dr. S. M. Howitt.

The properties of the mutant strains suggests a helical periodicity for this region, with the most severely affected strains being those carrying the V124D and A128D mutations.

**Table A1.** Properties of mutants in which each residue in the conserved hydrophobic region is replaced by aspartic acid.

| Residue replaced by Asp : | $V_{124}$ | $A_{125}$ | $I_{126}$ | $L_{127}$ | $A_{128}$ | $V_{129}$ | $A_{130}$ | $G_{131}$ | $A_{132}$ |
|---|---|---|---|---|---|---|---|---|---|
| Mutant property | | | | | | | | | |
| Succinate growth | - | - | + | - | - | - | + | - | + |
| Growth yield (%) | 0 | 0 | 66 | 20 | 0 | 16 | 66 | 4 | 100 |
| ATPase activity (%) | 0 | 39 | 73 | 46 | 0 | 0 | 23 | 31 | ND |
| Atebrin quench | | | | | | | | | |
| -NADH-dependent | 60 | 81 | 81 | 65 | 61 | 65 | 85 | 66 | ND |
| -ATP-dependent | <5 | 24 | 46 | <5 | <5 | <5 | 36 | <5 | ND |

# REFERENCES CITED

**Abrahams, J. P., A. G. W. Leslie, R. Lutter and J. E. Walker (1994).** Structure at 2.8 Å resolution of $F_1$-ATPase from bovine heart mitochondria. *Nature* **370:** 621-628.

**Abrams, A., P. McNamara and F. B. Johnson (1960).** Adenosine Triphosphatase in Isolated Bacterial Cell Membranes. *J. Biol. Chem.* **235:** 3659-3662.

**Aggeler, R., Y. Z. Zhang and R. A. Capaldi (1987).** Labeling of the ATP synthase of *Escherichia coli* from the head-group region of the lipid bilayer. *Biochemistry* **26:** 7107-13.

**Aggeler, R. and R. A. Capaldi (1992).** Cross-Linking of the γ-Subunit of the *Escherichia coli* ATPase ($ECF_1$) via Cysteines Introduced by Site-Directed Mutagenesis. *J. Biol. Chem.* **267:** 21355-21359.

**Aggeler, R., S. X. Cai, J. F. W. Keana, T. Koike and R. A. Capaldi (1993).** The γ-subunit of the *Escherichia coli* $F_1$-ATPase Can Be Cross-Linked Near the Glycine-Rich Loop Region of a β-Subunit When ADP+$Mg^{2+}$ Occupies Catalytic Sites But Not When ATP+$Mg^{2+}$ Is Bound. *J. Biol. Chem.* **268:** 20831-20837.

**Alkjaersig, N., A. P. Fletcher and S. Sherry (1959).** *J. Biol. Chem.* **234:** 832-837.

**Alt, J., P. Winter, W. Sebald, J. G. Moser, R. Schedel, P. Westhoff and R. G. Herrmann (1983).** Localization and nucleotide sequence of the gene for the ATP synthase proteolipid subunit on the spinach plastid chromosome. *Current Genetics* **7:** 129-138.

**Altendorf, K., F. M. Harold and R. D. Simoni (1974).** Impairment and restoration of the energized state in membrane vesicles of a mutant of *Escherichia coli* lacking adenosine triphosphatase. *J. Biol. Chem.* **249:** 4587-4593.

**Amann, E., J. Brosius and M. Ptashne (1983).** Vectors bearing a hybrid *trp-lac* promoter useful for regulated expression of cloned genes in *Escherichia coli*. *Gene* **25:** 167-78.

**Andersson, B. and J. M. Anderson (1980).** Lateral heterogeneity in the distribution of chlorophyll-protein complexes of the thylakoid membranes of spinach chloroplasts. *Biochim. Biophys. Acta* **593:** 427-40.

**Andreo, C. S., W. J. Patrie and R. E. McCarty (1982).** Effect of ATPase activation and the δ-subunit of coupling factor 1 on reconstitution of photophosphorylation. *J. Biol. Chem.* **257:** 9968-75.

**Aris, J. P. and R. D. Simoni (1983).** Crosslinking and labeling of the *Escherichia coli* $F_1F_0$-ATP synthase reveal a compact hydrophilic portion of $F_0$ close to an $F_1$ catalytic subunit. *J. Biol. Chem* **258:** 14599-14609.

**Aris, J. P., D. J. Klionsky and R. D. Simoni (1985).** The $F_O$ subunits of the *Escherichia coli* $F_1F_O$-ATP synthase are sufficient to form a functional proton pore. *J. Biol. Chem.* **260:** 11207-15.

**Avron, M. (1963).** A coupling factor in photophosphorylation. *Biochim. Biophys. Acta* **77:** 699-702.

**Baird, B. A. and G. G. Hammes (1976).** Chemical cross-linking studies of chloroplast coupling factor 1. *J. Biol. Chem.* **251:** 6953-62.

**Beckers, G., R. J. Berzborn and H. Strotmann (1992).** Zero length crosslinking between subunits δ and I of the $H^+$-translocating ATPase of chloroplasts. *Biochim. Biophys. Acta* **1101:** 97-104.

**Biekmann, S. and J. Feierabend (1985).** Synthesis and degradation of unassembled polypeptides of the coupling factor of photophosphorylation $CF_1$ in 70S ribosome-deficient rye leaves. *Eur. J. Biochem.* **152:** 529-35.

**Bird, C. R., B. Koller, A. D. Auffret, A. K. Huttly, C. J. Howe, T. A. Dyer and J. C. Gray (1985).** The wheat chloroplast gene for $CF_O$ subunit I of ATP synthase contains a large intron. *EMBO J.* **4:** 1381-1388.

**Birkenhäger, R., M. Hoppert, G. Deckers-Hebestreit, F. Mayer and K. Altendorf (1995).** The $F_O$ complex of the *Escherichia coli* ATP synthase. Investigation by electron spectroscopic imaging and immunoelectron microscopy. *Eur. J. Biochem.* **230:** 58-67.

**Boekema, E. J., J. Xiao and R. E. McCarty (1990).** Structure of the ATP synthase from chloroplasts studied by electron microscopy. Localization of the small subunits. *Biochim. Biophys. Acta* **1020:** 49-56.

**Bouthyette, P. Y. and A. T. Jagendorf (1978).** The site of synthesis of pea chloroplast coupling factor 1. *Plant and Cell Physiol.* **19:** 1169-1174.

**Boyer, P. D., R. L. Cross and W. Momsen (1973).** A new concept for energy coupling in oxidative phosphorylation based on a molecular explanation of the oxygen exchange reactions. *Proc. Natl. Acad. Sci. U S A* **70:** 2837-9.

**Boyer, P. D. and W. E. Kohlbrenner (1981).** The present status of the binding change mechanism and its relation to ATP formation by chloroplasts. *Energy coupling in Photosynthesis.* Elsevier North Holland.

**Boyer, P. D. (1993).** The Binding Change Mechanism for ATP Synthase - Some Probabilities and Possibilities. *Biochim. Biophys. Acta* **1140:** 215-250.

**Bradford, M. M. (1976).** A rapid and sensitive method for the quantitation of microgram quantities of protein utilizing the principle of protein-dye binding. *Anal Biochem* **72:** 248-54.

**Bragg, P. D., P. L. Davies and C. Hou (1973).** Effect of removal or modification of subunit polypeptides on the coupling factor and hydrolytic activities of the $Ca^{2+}$ and $Mg^{2+}$-activated adenosine triphosphatase of *Escherichia coli*. *Arch. Biochem. Biophys.* **159:** 664-670.

**Bragg, P. D. and C. Hou (1975).** Subunit composition, function, and spatial arrangement in the $Ca^{2+}$-and $Mg^{2+}$-activated adenosine triphosphatases of *Escherichia coli* and *Salmonella typhimurium*. *Arch. Biochem. Biophys.* **167:** 311-21.

**Bragg, P. D. and C. Hou (1976).** Cross-linking of minor subunits in $Ca^{2+}$, $Mg^{2+}$-activated ATPase of *Escherichia coli*. *Biochem. Biophys. Res. Commun.* **72:** 1042-8.

**Bragg, P. D. and C. Hou (1980).** A cross-linking study of the $Ca^{2+}$, $Mg^{2+}$-activated adenosine triphosphatase of *Escherichia coli*. *Eur. J. Biochem.* **106:** 495-503.

**Bragg, P. D., H. Stan-Lotter and C. Hou (1981).** Affinity labeling of purified $Ca^{2+}$,$Mg^{2+}$-activated ATPase of *Escherichia coli* by the 2',3'-dialdehydes of adenosine 5'-di- and triphosphates. *Arch. Biochem. Biophys.* **207:** 290-9.

**Brusilow, W. S., R. P. Gunsalus, E. C. Hardeman, K. P. Decker and R. D. Simoni (1981).** *In vitro* synthesis of the $F_O$ and $F_1$ components of the proton translocating ATPase of *Escherichia coli*. *J. Biol. Chem.* **256:** 3141-4.

**Brusilow, W. S. (1987).** Proton leakiness caused by cloned genes for the $F_O$ sector of the proton-translocating ATPase of *Escherichia coli*: Requirement for $F_1$ genes. *J. Bacteriol.* **169:** 4984-90.

**Brusilow, W. S., M. A. Scarpetta, C. A. Hawthorne and W. P. Clark (1989).** Organization and sequence of the genes coding for the proton-translocating ATPase of *Bacillus megaterium*. *J. Biol. Chem.* **264:** 1528-33.

**Burkovski, A., H. G. Deckers and K. Altendorf (1990).** Expression of subunit III of the ATP synthase from spinach chloroplasts in *Escherichia coli*. *FEBS Lett.* **271:** 227-30.

**Burkovski, A., G. Deckershebestreit and K. Altendorf (1994).** Hybrid $F_O$ complexes of the ATP synthases of spinach chloroplasts and *Escherichia coli* - Immunoprecipitation and mutant analyses. *Eur. J. Biochem.* **225:** 1221-1228.

**Butlin, J. D., G. B. Cox and F. Gibson (1971).** Oxidative phosphorylation in *Escherichia coli* K12. Mutations affecting magnesium ion- or calcium ion-stimulated adenosine triphosphatase. *Biochem. J.* **124:** 75-81.

**Cain, B. D. and R. D. Simoni (1986).** Impaired proton conductivity resulting from mutations in the *a*-subunit of $F_1F_O$-ATPase in *Escherichia coli*. *J. Biol. Chem.* **261:** 10043-50.

**Cain, B. D. and R. D. Simoni (1988).** Interaction between Glu-219 and His-245 within the *a*-subunit of $F_1F_O$-ATPase in *Escherichia coli*. *J. Biol. Chem.* **263:** 6606-12.

**Cain, B. D. and R. D. Simoni (1989).** Proton translocation by the $F_1F_O$-ATPase of *Escherichia coli*. Mutagenic analysis of the *a*-subunit. *J. Biol. Chem.* **264:** 3292-300.

**Capaldi, R. A. (1994).** $F_1$-ATPase in a spin. *Nature Structural Biology* **1:** 660-663.

**Capaldi, R. A., R. Aggeler, P. Turina and S. Wilkens (1994).** Coupling between catalytic sites and the proton channel in $F_1F_O$-type ATPases. *Trends Biochem. Sci.* **19:** 284-289.

**Carmeli, C. and E. Racker (1973).** Partial resolution of the enzymes catalyzing photophosphorylation. XIV. Reconstitution of chlorophyll-deficient vesicles catalyzing phosphate-adenosine triphosphate exchange. *J. Biol. Chem.* **248:** 8281-7.

**Carr, N. G. and B. A. Whitton (1982).** *The Biology of Cyanobacteria*. Oxford, Blackwell Scientific Publications.

**Chang, A. C., H. A. Erlich, R. P. Gunsalus, J. H. Nunberg, R. J. Kaufman, R. T. Schimke and S. N. Cohen (1980).** Initiation of protein synthesis in bacteria at a translational start codon of mamalian cDNA: effects of the preceding nucleotide sequence. *Proc. Natl. Acad. Sci. U S A* **77:** 1442-6.

**Chang, J. Y. (1985).** Thrombin specificity. Requirement for apolar amino acids adjacent to the thrombin cleavage site of polypeptide substrate. *Eur. J. Biochem.* **151:** 217-24.

**Chen, Z., A. Spies, R. Hein, X. Zhou, B. C. Thomas, M. L. Richter and P. Gegenheimer (1995).** A Subunit Interaction in Chloroplast ATP Synthase Determined by Genetic Complementation between Chloroplast and Bacterial ATP Synthase Genes. *J. Biol. Chem.* **270:** 17124-17132.

**Chua, N. H. and G. W. Schmidt (1979).** Transport of proteins into mitochondria and chloroplasts. *J. Cell. Biol* **81:** 461-83.

**Codd, R., G. B. Cox, J. M. Guss, R. G. Solomon and D. Webb (1992).** The expression, purification and crystallization of the ε-subunit of the $F_1$ portion of the ATPase of *Escherichia coli*. *J. Mol. Biol.* **228:** 306-9.

**Cohen, C. and D. A. Parry (1990).** α-helical coiled coils and bundles: how to design an α-helical protein. *Proteins* **7:** 1-15.

**Cox, G. B., F. Gibson and L. McCann (1973).** Reconstitution of oxidative phosphorylation and the adenosine triphosphate-dependent transhydrogenase activity by a combination of membrane fractions from *uncA*$^-$ and *uncB*$^-$ mutant strains of *Escherichia coli* K12. *Biochem. J.* **134:** 1015-21.

**Cox, G. B., J. A. Downie, D. R. Fayle, F. Gibson and J. Radik (1978).** Inhibition, by a protease inhibitor, of the solubilization of the $F_1$-portion of the $Mg^{2+}$-stimulated adenosine triphosphatase of *Escherichia coli*. *J. Bacteriol.* **133:** 287-92.

**Cox, G. B., J. A. Downie, L. Langman, A. E. Senior, G. Ash, D. R. Fayle and F. Gibson (1981).** Assembly of the adenosine triphosphatase complex in *Escherichia coli*: assembly of $F_O$ is dependent on the formation of specific $F_1$ subunits. *J. Bacteriol.* **148:** 30-42.

**Cox, G. B., D. A. Jans, A. L. Fimmel, F. Gibson and L. Hatch (1984).** Hypothesis: The mechanism of ATP synthase. Conformational change by rotation of the *b*-subunit. *Biochim. Biophys. Acta* **768:** 201-208.

**Cox, G. B., A. L. Fimmel, F. Gibson and L. Hatch (1986).** The mechanism of ATP synthase: a reassessment of the functions of the *b*- and *a*-subunits. *Biochim. Biophys. Acta* **849:** 62-9.

**Cox, G. B. and F. Gibson (1987).** The assembly of $F_1F_0$-ATPase in *Escherichia coli*. *Curr. Top. Bioenerg.* **15:** 163-175.

**Cox, G. B., R. J. Devenish, F. Gibson, S. M. Howitt and P. Nagley (1992).** The structure and assembly of ATP synthase. *Molecular Mechanisms in Bioenergetics*. Elsevier Science Publishers B. V. 283-315.

**Cox, G. B., B. A. Cromer, J. M. Guss, I. Harvey, P. D. Jeffrey, R. G. Solomon and D. C. Webb (1993).** Formation *in vivo*, Purification and Crystallization of a Complex of the γ-subunit and ε-subunit of the $F_OF_1$-ATPase of *Escherichia coli*. *J. Mol. Biol.* **229:** 1159-1162.

**Cozens, A. L. and J. E. Walker (1987).** The organization and sequence of the genes for ATP synthase subunits in the cyanobacterium *Synechococcus* 6301. Support for an endosymbiotic origin of chloroplasts. *J. Mol. Biol* **194:** 359-383.

**Cross, R. L. (1981).** The mechanism and regulation of ATP synthesis by $F_1$-ATPases. *Ann. Rev. Biochem.* **50:** 681-714.

**Cross, R. L. and C. M. Nalin (1982).** Adenine nucleotide binding sites on beef heart $F_1$-ATPase. Evidence for three exchangeable sites that are distinct from three noncatalytic sites. *J. Biol. Chem.* **257:** 2874-81.

**Curry, K. A. and C. S. Tomich (1988).** Effect of ribosome binding site on gene expression in *Escherichia coli*. *DNA* **7:** 173-9.

**Dallmann, H. G., T. G. Flynn and S. D. Dunn (1992).** Determination of the 1-ethyl-3-[(3-dimethylamino)propyl]-carbodiimide- induced cross-link between the β- and ε- subunits of *Escherichia coli* $F_1$-ATPase. *J. Biol. Chem.* **267:** 18953-60.

**Das, A. and L. G. Ljungdahl (1993).** $F_O$ and $F_1$ Parts of ATP Synthases from *Clostridium thermoautotrophicum* and *Escherichia coli* Are Not Functionally Compatible. *FEBS Lett.* **317:** 17-21.

**Davies, P. L. and P. D. Bragg (1972).** Properties of a soluble $Ca^{2+}$- and $Mg^{2+}$ -activated ATPase released from *Escherichia coli* membranes. *Biochim. Biophys. Acta* **266:** 273-84.

**De Boer, H. A., L. J. Comstock and M. Vasser (1983).** The *tac* promoter: a functional hybrid derived from the *trp* and *lac* promoters. *Proc. Natl. Acad. Sci. U S A* **80:** 21-5.

**Deckers-Hebestreit, G. and K. Altendorf (1992).** Influence of Subunit-Specific Antibodies on the Activity of the $F_O$ Complex of the ATP Synthase of *Escherichia coli* .2. Effects of Subunit *c*-Specific Polyclonal Antibodies. *J. Biol. Chem.* **267:** 12370-12374.

**Deters, D. W., E. Racker, N. Nelson and H. Nelson (1975).** Partial resolution of the enzymes catalyzing photophosphorylation. XV. Approaches to the active site of coupling factor I. *J. Biol. Chem.* **250:** 1041-7.

**Dewey, T. G. and G. G. Hammes (1981).** Method for studying kinetics of light-induced transport across membranes. *Proc. Natl. Acad. Sci. U S A* **78:** 7422-5.

**Dilley, R. A., S. M. Theg and W. A. Beard (1987).** *Ann. Rev. Plant Physiol.* **38:** 347-389

**Doherty, A. and J. C. Gray (1980).** Synthesis of a dicyclohexylcarbodiimide-binding proteolipid by isolated pea chloroplasts. *Eur. J. Biochem.* **108:** 131-6.

**Dower, W. J., J. F. Miller and C. W. Ragsdale (1988).** High efficiency transformation of *E. coli* by high voltage electroporation. *Nucleic Acids Res.* **16:** 6127-45.

**Downie, J. A., A. E. Senior, G. B. Cox and F. Gibson (1979).** Solubilization of adenosine triphosphatase from membranes of *Escherichia coli*: Effect of *p*-aminobenzamidine. *J. Bacteriol.* **138:** 87-91.

**Downie, J. A., F. Gibson and G. B. Cox (1979).** Membrane adenosine triphosphatases of prokaryotic cells. *Ann. Rev. Biochem.* **48:** 103-31.

**Downie, J. A., A. E. Senior, F. Gibson and G. B. Cox (1979).** A fifth gene (*uncE)* in the operon concerned with oxidative phosphorylation in *Escherichia coli*. *J. Bacteriol.* **137:** 711-8.

**Downie, J. A., L. Langman, G. B. Cox, C. Yanofsky and F. Gibson (1980).** Subunits of the adenosine triphosphatase complex translated *in vitro* from the *Escherichia coli unc* operon. *J. Bacteriol.* **143:** 8-17.

**Downie, J. A., G. B. Cox, L. Langman, G. Ash, M. Becker and F. Gibson (1981).** Three genes coding for subunits of the membrane sector ($F_O$) of the *Escherichia coli* adenosine triphosphatase complex. *J. Bacteriol.* **145:** 200-10.

**Duncan, T. M. and A. E. Senior (1985).** The defective proton-ATPase of *uncD* mutants of *Escherichia coli*. Two mutations which affect the catalytic mechanism. *J .Biol. Chem* **260:** 4901-7.

**Duncan, T. M., D. Parsonage and A. E. Senior (1986).** Structure of the nucleotide-binding domain in the β-subunit of *Escherichia coli* $F_1$-ATPase. *FEBS Lett.* **208:** 1-6.

**Dunn, S. D. and M. Futai (1980).** Reconstitution of a functional coupling factor from the isolated subunits of *Escherichia coli* $F_1$ ATPase. *J. Biol. Chem.* **255:** 113-8.

**Dunn, S. D., L. A. Heppel and C. S. Fullmer (1980).** The $NH_2$-terminal portion of the α-subunit of *Escherichia coli* $F_1$ ATPase is required for binding the δ-subunit. *J. Biol. Chem.* **255:** 6891-6896.

**Dunn, S. D. and L. A. Heppel (1981).** Properties and functions of the subunits of the *Escherichia coli* coupling factor ATPase. *Arch. Biochem. Biophys.* **210:** 421-36.

**Dunn, S. D. (1982).** The isolated γ-subunit of *Escherichia coli* $F_1$-ATPase binds the ε-subunit. *J. Biol. Chem.* **257:** 7354-9.

**Dunn, S. D., V. D. Zadorozny, R. G. Tozer and L. E. Orr (1987).** Epsilon subunit of *Escherichia coli* $F_1$-ATPase: effects on affinity for aurovertin and inhibition of product release in unisite ATP hydrolysis. *Biochemistry* **26:** 4488-93.

**Dunn, S. D. and R. G. Tozer (1987).** Activation and inhibition of the *Escherichia coli* $F_1$-ATPase by monoclonal antibodies which recognize the ε-subunit. *Arch. Biochem. Biophys.* **253:** 73-80.

**Dunn, S. D. (1992).** The Polar Domain of the *b*-Subunit of *Escherichia coli* $F_1F_O$-ATPase Forms an Elongated Dimer That Interacts with the $F_1$ Sector. *J. Biol. Chem.* **267:** 7630-7636.

**Dyson, H. J., M. Rance, R. A. Houghten, P. E. Wright and R. A. Lerner (1988).** Folding of immunogenic peptide fragments of proteins in water solution. II. The nascent helix. *J. Mol. Biol.* **201:** 201-17.

**Dyson, H. J., G. Merutka, J. P. Waltho, R. A. Lerner and P. E. Wright (1992).** Folding of peptide fragments comprising the complete sequence of proteins. Models for initiation of protein folding. I. Myohemerythrin. *J. Mol. Biol.* **226:** 795-817.

**Ellis, R. J. (1977).** Protein synthesis by isolated chloroplasts. *Biochim. Biophys. Acta* **463:** 185-215.

**Engelbrecht, S., H. G. Deckers, K. Altendorf and W. Junge (1989).** Cross-reconstitution of the $F_OF_1$-ATP synthases of chloroplasts and *Escherichia coli* with special emphasis on subunit δ. *Eur. J. Biochem.* **181:** 485-91.

**Engelbrecht, S., H. G. Deckers, K. Altendorf and W. Junge (1989).** Cross-reconstitution of the $F_OF_1$-ATP synthases of chloroplasts and *Escherichia coli* with special emphasis on subunit δ. *Eur. J. Biochem.* **181:** 485-91.

**Engelbrecht, S. and W. Junge (1990).** Subunit δ of $H^+$-ATPases: at the interface between proton flow and ATP synthesis. *Biochim. Biophys. Acta* **1015:** 379-90.

**Evans, D. J. J. (1969).** Membrane adenosine triphosphatase of *Escherichia coli*: Activation by calcium ion and inhibition by monovalent cations. *J. Bacteriol.* **100:** 914-22.

**Evans, D. J. (1970).** Membrane $Mg^{2+}$-($Ca^{2+}$) activated adenosine triphosphatase of *Escherichia coli*: Characterisation in the membrane bound and solubilised states. *J. Bacteriol.* **104:** 1203-1212.

**Farron, F. and E. Racker (1970).** Studies on the mechanism of the conversion of coupling factor 1 from chloroplasts to an active adenosine triphosphatase. *Biochemistry* **9:** 3829-36.

**Farron, F. (1970).** Isolation and properties of a chloroplast coupling factor and heat-activated adenosine triphosphatase. *Biochemistry* **9:** 3823-8.

**Fayle, D. R., J. A. Downie, G. B. Cox, F. Gibson and J. Radik (1978).** Characterization of the mutant *uncD* gene product in a strain of *Escherichia coli* K12. An altered β-subunit of the magnesium ion-stimulated adenosine triphosphatase. *Biochem. J.* **172:** 523-31.

**Feng, Y. and R. E. McCarty (1990).** Subunit interactions within the chloroplast ATP synthase ($CF_O$-$CF_1$) as deduced by specific depletion of $CF_O$ polypeptides. *J. Biol. Chem.* **265:** 12481-5.

**Feng, Y. and R. E. McCarty (1990).** Chromatographic purification of the chloroplast ATP synthase ($CF_O$-$CF_1$) and the role of $CF_O$ subunit IV in proton conduction. *J. Biol. Chem* **265:** 12474-80.

**Fillingame, R. H., B. Porter, J. Hermolin and L. K. White (1986).** Synthesis of a functional $F_O$ sector of the *Escherichia coli* H+-ATPase does not require synthesis of the α- or β- subunits of $F_1$. *J. Bacteriol.* **165:** 244-51.

**Fimmel, A. L., D. A. Jans, L. Langman, L. B. James, G. R. Ash, J. A. Downie, A. E. Senior, F. Gibson and G. B. Cox (1983).** The $F_1F_O$-ATPase of *Escherichia coli*. Substitution of proline by leucine at position 64 in the *c*-subunit causes loss of oxidative phosphorylation. *Biochem. J.* **213:** 451-8.

**Fimmel, A. L. and S. A. Fordham (1989).** The $F_1F_O$-ATPase of *Escherichia coli*. The substitution of alanine by tyrosine at position 25 in the *c*-subunit affects function but not assembly. *Biochim. Biophys. Acta* **978:** 299-304.

**Foster, D. L. and R. H. Fillingame (1982).** Stoichiometry of subunits in the $H^+$-ATPase complex of *Escherichia coli*. *J. Biol. Chem.* **257:** 2009-2015.

**Fraga, D. and R. H. Fillingame (1989).** Conserved polar loop region of *Escherichia coli* subunit *c* of the $F_1F_O$ $H^+$-ATPase. Glutamine 42 is not absolutely essential, but substitutions alter binding and coupling of $F_1$ to $F_O$ *J. Biol. Chem* **264:** 6797-803.

**Fraga, D., J. Hermolin and R. H. Fillingame (1994).** Transmembrane helix-helix interactions in $F_O$ suggested by suppressor mutations to Ala24→Asp/Asp61→Gly mutant of ATP synthase subunit *c*. *J. Biol. Chem.* **269:** 2562-7.

**Frangioni, J. V. and B. G. Neel (1993).** Solubilization and purification of enzymatically active glutathione S-transferase (pGEX) fusion proteins. *Anal. Biochem.* **210:** 179-87.

**Friedl, P., C. Friedl and H. U. Schairer (1979).** The ATP synthetase of *Escherichia coli* K12: purification of the enzyme and reconstitution of energy-transducing activities. *Eur. J. Biochem.* **100:** 175-80.

**Friedl, P., C. Friedl and H. U. Schairer (1980).** $F_0$ of *Escherichia coli* ATP-synthase containing mutant and wild-type carbodiimide-binding proteins is impaired in $H^+$-conduction. *FEBS Lett.* **119:** 254-256.

**Fromme, P., P. Gräber and J. Salnikow (1987).** Isolation and identification of a fourth subunit in the membrane part of the chloroplast ATP-synthase. *FEBS Lett.* **218:** 27-30.

**Futai, M. (1977)**. Reconstitution of ATPase activity from the isolated α-, β-, and γ- subunits of the coupling factor, $F_1$, of *Escherichia coli*. *Biochem. Biophys. Res. Commun.* **79:** 1231-7.

**Futai, M., H. Kanazawa, K. Takeda and Y. Kagawa (1980)**. Reconstitution of ATPase from the isolated subunits of coupling factor $F_1$'s of *Escherichia coli* and thermophilic bacterium PS3. *Biochem. Biophys. Res. Commun.* **96:** 227-34.

**Futai, M. and H. Kanazawa (1983)**. Structure and function of proton-translocating adenosine triphosphatase ($F_OF_1$): biochemical and molecular biological approaches. *Microbiol. Rev.* **47:** 285-312.

**Futai, M., A. Iwamoto, H. Omote, Y. Orita, K. Shin, R. K. Nakamoto and M. Maeda (1992)**. *Escherichia coli* ATP synthase (F-ATPase): catalytic site and regulation of $H^+$ translocation. *J. Exp. Biol.* **172:** 443-9.

**Galmiche, J. M., S. Pezennec, R. B. Zhao, G. Girault and E. Baeuerlein (1994)**. The Prokaryotic Thermophilic $TF_1$-ATPase Is Functionally Compatible with the Eukaryotic $CF_O$-Part of the Chloroplast ATP-Synthase. *FEBS Lett.* **338:** 152-156.

**Gay, N. J. and J. E. Walker (1981)**. The *atp* operon: nucleotide sequence of the region encoding the α-subunit of *Escherichia coli* ATP-synthase. *Nucleic Acids Res.* **9:** 2187-94.

**Gay, N. J. and J. E. Walker (1981)**. The *atp* operon: nucleotide sequence of the promoter and the genes for the membrane proteins, and the δ-subunit of *Escherichia coli* ATP-synthase. *Nucleic Acids Res.* **9:** 3919-26.

**Gay, N. J. (1984)**. Construction and characterization of an *Escherichia coli* strain with a *uncI* mutation. *J. Bacteriol.* **158:** 820-5.

**Gibson, F., G. B. Cox, J. A. Downie and J. Radik (1977).** A mutation affecting a second component of the $F_O$ portion of the magnesium ion-stimulated adenosine triphosphatase of *Escherichia coli* K12. The *uncC424* allele. *Biochem. J.* **164:** 193-8.

**Gibson, F., G. B. Cox, J. A. Downie and J. Radik (1977).** Partial diploids of *Escherichia coli* carrying normal and mutant alleles affecting oxidative phosphorylation. *Biochem. J.* **162:** 665-70.

**Gibson, F., J. A. Downie, G. B. Cox and J. Radik (1978).** Mu-induced polarity in the *unc* operon of *Escherichia coli*. *J. Bacteriol.* **134:** 728-36.

**Gillham, N. W., J. E. Boynton and N. H. Chua (1978).** Genetic Control of Chloroplast Proteins. *Current Topics in Bioenergetics* **8:** 211-260.

**Girvin, M. E., J. Hermolin, R. Pottorf and R. H. Fillingame (1989).** Organization of the $F_O$ sector of Escherichia coli $H^+$-ATPase: the polar loop region of subunit *c* extends from the cytoplasmic face of the membrane. *Biochemistry* **28:** 4340-3.

**Glaser, E. and B. Norling (1991).** Chloroplast and plant mitochondrial ATP synthases. *Curr. Top. Bioenerg.* **16:** 223-263.

**Gogol, E. P., U. Lucken and R. A. Capaldi (1987).** The stalk connecting the $F_1$ and $F_O$ domains of ATP synthase visualised by electron microscopy of unstained specimens. *FEBS Lett.* **219:** 274-278.

**Gogol, E. P., R. Aggeler, M. Sagermann and R. A. Capaldi (1989).** Cryoelectron microscopy of *Escherichia coli* $F_1$ adenosinetriphosphatase decorated with monoclonal antibodies to individual subunits of the complex. *Biochemistry* **28:** 4717-24.

**Gogol, E. P., U. Lucken, T. Bork and R. A. Capaldi (1989).** Molecular architecture of *Escherichia coli* $F_1$ adenosinetriphosphatase. *Biochemistry* **28:** 4709-16.

**Gogol, E. P., E. Johnston, R. Aggeler and R. A. Capaldi (1990).** Ligand-dependent structural variations in *Escherichia coli* $F_1$-ATPase revealed by cryoelectron microscopy. *Proc. Natl. Acad. Sci. U S A* **87:** 9585-9.

**Gray, M. R., H. V. Colot, L. Guarente and M. Rosbash (1982).** Open reading frame cloning: identification, cloning, and expression of open reading frame DNA. *Proc. Natl. Acad. Sci. U S A* **79:** 6598-602.

**Green, C. D. and M. J. Hollingsworth (1994).** Tissue-specific expression of the large ATP synthase gene cluster in spinach plastids. *Plant Mol. Biol.* **25:** 369-376.

**Gresser, M. J., J. A. Myers and P. D. Boyer (1982).** Catalytic site cooperativity of beef heart mitochondrial $F_1$ adenosine triphosphatase. Correlations of initial velocity, bound intermediate, and oxygen exchange measurements with an alternating three-site model. *J. Biol. Chem.* **257:** 12030-8.

**Gromet-Elhanan, Z., D. Khananshvili, S. Weiss, H. Kanazawa and M. Futai (1985).** ATP synthesis and hydrolysis by a hybrid system reconstituted from the β-subunit of *Escherichia coli* $F_1$-ATPase and β-less chromatophores of *Rhodospirillum rubrum*. *J. Biol. Chem.* **260:** 12635-40.

**Guarente, L., G. Lauer, T. M. Roberts and M. Ptashne (1980).** Improved methods for maximizing expression of a cloned gene: a bacterium that synthesizes rabbit β-globin. *Cell* **20:** 543-53.

**Hackney, D. D. and P. D. Boyer (1978).** Subunit interaction during catalysis. Implications of concentration dependency of oxygen exchanges accompanying oxidative phosphorylation for alternating site cooperativity. *J. Biol. Chem.* **253:** 3164-70.

**Haddock, B. A. and J. A. Downie (1974).** The reconstitution of functional respiratory chains in membranes from electron-transport-deficient mutants of *Escherichia coli* as demonstrated by quenching of atebrin fluorescence. *Biochem. J.* **142:** 703-6.

**Hanahan, D. (1983).** Studies on transformation of *Escherichia coli* with plasmids. *J. Mol. Biol.* **166:** 557-80.

**Hansen, F. G., J. Nielsen, E. Riise and K. von Meyenburg (1981).** The genes for the eight subunits of the membrane bound ATP synthase of *Escherichia coli*. *Mol. Gen. Genet.* **183:** 463-72.

**Hanson, R. L. and E. P. Kennedy (1973).** Energy-transducing adenosine triphosphatase from *Escherichia coli*: purification, properties, and inhibition by antibody. *J. Bacteriol.* **114:** 772-81.

**Hartzog, P. E. and B. D. Cain (1994).** Second-site suppressor mutations at glycine 218 and histidine 245 in the *a*-subunit of $F_1F_O$ ATP synthase in *Escherichia coli*. *J. Biol. Chem.* **269:** 32313-32317.

**Hatch, L. P., G. B. Cox and S. M. Howitt (1995).** The essential arginine at position 210 in the *a*-subunit of the *Escherichia coli* ATP synthase can be transferred to position 252 with partial retention of activity. *J. Biol. Chem.* **270:** Issue #48.

**Hatefi, Y. (1985).** The mitochondrial electron transport and oxidative phosphorylation system. *Ann. Rev. Biochem.* **54:** 1015-69.

**Hauska, G., D. Samoray, G. Orlich and N. Nelson (1980).** Reconstitution of photosynthetic energy conservation. II. Photophosphorylation in liposomes containing photosystem-I reaction center and chloroplast coupling-factor complex. *Eur. J. Biochem.* **111:** 535-43.

**Hawthorne, C. A. and W. S. Brusilow (1986).** Complementation of mutants in the *Escherichia coli* proton-translocating ATPase by cloned DNA from *Bacillus megaterium*. *J. Biol. Chem.* **261:** 5245-8.

**Hazard, A. L. and A. E. Senior (1994).** Defective Energy Coupling in δ-subunit Mutants of *Escherichia coli* $F_1F_O$-ATP Synthase. *J. Biol. Chem.* **269:** 427-432.

**Hellmuth, K., G. Rex, B. Surin, R. Zinck and J. E. McCarthy (1991).** Translational coupling varying in efficiency between different pairs of genes in the central region of the *atp* operon of *Escherichia coli*. *Mol. Microbiol.* **5:** 813-24.

**Hermans, J., C. Rother, J. Bichler, J. Steppuhn and R. G. Herrmann (1988).** Nucleotide sequence of cDNA clones encoding the complete precursor for subunit δ of thylakoid-located ATP synthase from spinach. *Plant Mol. Biol.* **10:** 323-330.

**Hermolin, J., J. Gallant and R. H. Fillingame (1983).** Topology, organization and function of the psi subunit in the $F_0$ sector of the $H^+$-ATPase of *Escherichia coli*. *J. Biol. Chem.* **258:** 14550-14555.

**Hermolin, J. and R. H. Fillingame (1989).** $H^+$-ATPase activity of *Escherichia coli* $F_1F_O$ is blocked after reaction of dicyclohexylcarbodiimide with a single proteolipid (subunit *c*) of the $F_O$ complex. *J. Biol. Chem.* **264:** 3896-903.

**Hermolin, J. and R. H. Fillingame (1995).** Assembly of $F_O$ sector of *Escherichia coli* $H^+$ ATP synthase - Interdependence of subunit insertion into the membrane. *J. Biol. Chem.* **270:** 2815-2817.

**Herrmann, R. G., J. Steppuhn, G. S. Herrmann and N. Nelson (1993).** The Nuclear-Encoded Polypeptide $CF_OII$ from Spinach Is a Real, 9th Subunit of Chloroplast ATP Synthase. *FEBS Lett.* **326:** 192-198.

**Holton, T. A. and M. W. Graham (1991).** A simple and efficient method for direct cloning of PCR products using ddT-tailed vectors. *Nucleic Acids Res.* **19:** p1156

**Hoppe, J., H. U. Schairer and W. Sebald (1980).** The proteolipid of a mutant ATPase from Escherichia coli defective in $H^+$-conduction contains a glycine instead of the carbodiimide-reactive aspartyl residue. *FEBS Lett* **109:** 107-11.

**Hoppe, J., H. U. Schairer, P. Friedl and W. Sebald (1982).** An Asp-Asn substitution in the proteolipid subunit of the ATP-synthase from Escherichia coli leads to a non-functional proton channel. *FEBS Lett* **145:** 21-29.

**Hoppe, J. and W. Sebald (1984).** The proton conducting $F_O$-part of bacterial ATP synthases. *Biochim. Biophys. Acta* **768:** 1-27.

**Horstman, L. L. and E. Racker (1970).** Partial resolution of the enzyme catalyzing oxidative phosphorylation. XXII. Interaction between mitochondrial adenosine triphosphatase inhibitor and mitochondrial adenosine triphosphatase. *J. Biol. Chem.* **245:** 1336-44.

**Howitt, S. M., R. N. Lightowlers, F. Gibson and G. B. Cox (1990).** Mutational analysis of the function of the *a*-subunit of the $F_OF_1$-ATPase of *Escherichia coli*. *Biochim. Biophys. Acta* **1015:** 264-8

**Howitt, S. M. and G. B. Cox (1992).** 2nd-Site Revertants of an Arginine-210 to Lysine Mutation in the *a*-Subunit of the $F_OF_1$-ATPase from *Escherichia coli* - Implications for Structure. *Proc. Natl. Acad. Sci. USA* **89:** 9799-9803.

**Howitt, S. M., M. Cleeter, L. Hatch and G. B. Cox (1993).** Functional Stability of the *a*-Subunit of the $F_OF_1$-ATPase from Escherichia-coli Is Affected by Mutations in Three Proline Residues. *Biochim. Biophys. Acta* **1144:** 17-21.

**Hsu, S. Y., M. Senda, H. Kanazawa, T. Tsuchiya and M. Futai (1984).** Comparison of $F_1$'s of oxidative phosphorylation from *Escherichia coli* and *Salmonella typhimurium* and demonstration of interchangeability of their subunits. *Biochemistry* **23:** 988-93.

**Hudson, G. S., J. G. Mason, T. A. Holton, B. Koller, G. B. Cox, P. R. Whitfeld and W. Bottomley (1987).** A gene cluster in the spinach and pea chloroplast genomes encoding one $CF_1$ and three $CF_O$ subunits of the $H^+$-ATP synthase complex and the ribosomal protein S2. *J. Mol. Biol* **196:** 283-298.

**Humbert, R., W. S. Brusilow, R. P. Gunsalus, D. J. Klionsky and R. D. Simoni (1983).** *Escherichia coli* mutants defective in the *uncH* gene. *J. Bacteriol.* **153:** 416-22.

**Ishikawa, S. and A. L. Lehninger (1962).** Reconstitution of oxidative phosphorylation in preparations from *Micrococcus lysodeikticus*. *J. Biol. Chem.* **237:** 2401-2408.

**Issartel, J. P. and P. V. Vignais (1984).** Evidence for a nucleotide binding site on the isolated beta subunit from *Escherichia coli* $F_1$-ATPase. Interaction between nucleotide and aurovertin D binding sites. *Biochemistry* **23:** 6591-5.

**Iwamoto, A., M. Y. Park, M. Maeda and M. Futai (1993).** Domains near ATP γ-phosphate in the catalytic site of $H^+$-ATPase. Model proposed from mutagenesis and inhibitor studies. *J. Biol. Chem.* **268:** 3156-60.

**Jagendorf, A. T. and M. Smith (1962).** Uncoupling Phosphorylation in Spinach Chloroplasts by Absence of Cations. *Plant Physiol.* **37:** 135-141.

**Jans, D. A., A. L. Fimmel, L. Langman, L. B. James, J. A. Downie, A. E. Senior, G. R. Ash, F. Gibson and G. B. Cox (1983).** Mutations in the *uncE* gene affecting assembly of the *c*-subunit of the adenosine triphosphatase of *Escherichia coli*. *Biochem. J.* **211:** 717-26.

**Jans, D. A., A. L. Fimmel, L. Hatch, F. Gibson and G. B. Cox (1984).** An additional acidic residue in the membrane portion of the *b*-subunit of the energy-transducing adenosine triphosphatase of *Escherichia coli* affects both assembly and function. *Biochem. J.* **221:** 43-51.

**Jans, D. A., L. Hatch, A. L. Fimmel, F. Gibson and G. B. Cox (1985).** Complementation between *uncF* alleles affecting assembly of the $F_1F_O$-ATPase complex of *Escherichia coli*. *J. Bacteriol.* **162:** 420-6.

**Jennings, K. R. and G. G. Dolnikowski (1990).** Mass Analyzers. *Methods in Enzymology* **193:** 37-61.

**Johnson, W. C. (1990).** Protein secondary structure and circular dichroism: a practical guide. *Proteins: Structure, Function and Genetics* **7:** 205-214.

**Jounouchi, M., M. Takeyama, P. Chaiprasert, T. Noumi, Y. Moriyama, M. Maeda and M. Futai (1992).** *Escherichia coli* $H^+$-ATPase - Role of the δ-Subunit in Binding $F_1$ to the $F_O$ Sector. *Arch. Biochem. Biophys.* **292:** 376-381.

**Jounouchi, M., M. Maeda and M. Futai (1993).** The α-subunit of ATP Synthase ($F_OF_1$) - The Lys-175 and Thr-176 Residues in the Conserved Sequence (Gly-X-X-X-X-Gly-Lys-Thr/Ser) Are Located in the Domain Required for Stable Subunit-Subunit Interaction. *J. Biochem. Tokyo* **114:** 171-176.

**Junesch, U. and P. Gräber (1987).** Influence of the redox state and the activation of the chloroplast ATP synthase on proton-transport-coupled ATP synthesis/hydrolysis. *Biochim. Biophys. Acta* **893:** 275-288.

**Kaim, G. and P. Dimroth (1994).** Construction, expression and characterization of a plasmid-encoded $Na^+$-specific ATPase hybrid consisting of *Propionigenium modestum* $F_O$-ATPase and *Escherichia coli* $F_1$-ATPase. *Eur. J. Biochem.* **222:** 615-623.

**Kanazawa, H., K. Mabuchi, T. Kayano, T. Noumi, T. Sekiya and M. Futai (1981).** Nucleotide sequence of the genes for $F_O$ components of the proton-translocating ATPase from *Escherichia coli*: prediction of the primary structure of $F_O$ subunits. *Biochem. Biophys. Res. Commun.* **103:** 613-20.

**Kanazawa, H., T. Kayano, K. Mabuchi and M. Futai (1981).** Nucleotide sequence of the genes coding for α-, β- and γ-subunits of the proton-translocating ATPase of *Escherichia coli*. *Biochem. Biophys. Res. Commun.* **103:** 604-12.

**Kanazawa, H., K. Mabuchi, T. Kayano, F. Tamura and M. Futai (1981).** Nucleotide sequence of genes coding for dicyclohexylcarbodiimide-binding protein and the α-subunit of proton-translocating ATPase of *Escherichia coli*. *Biochem. Biophys. Res. Commun.* **100:** 219-25.

**Kanazawa, H., T. Kayano, T. Kiyasu and M. Futai (1982).** Nucleotide sequence of the genes for β- and ε-subunits of proton-translocating ATPase from *Escherichia coli*. *Biochem. Biophys. Res. Commun.* **105:** 1257-64.

**Kleid, D. G., D. Yansura, B. Small, D. Dowbenko, D. M. Moore, M. J. Grubman, P. D. McKercher, D. O. Morgan, B. H. Robertson and H. L. Bachrach (1981).** Cloned viral protein vaccine for foot-and-mouth disease: responses in cattle and swine. *Science* **214:** 1125-9.

**Kobayashi, H. and Y. Anraku (1972).** Membrane-bound adenosine triphosphatase of *Escherichia coli*. I. Partial purification and properties. *J. Biochem. Tokyo* **71:** 387-99.

**Koenen, M., U. Rüther and B. Müller-Hill (1982).** Immunoenzymatic detection of expressed gene fragments cloned in the *lacZ* gene of *E. coli*. *EMBO J.* **1:** 509-12.

**Koland, J. G., K. M. O'Brien and R. A. Cerione (1990).** Expression of epidermal growth factor receptor sequences as *E. coli* fusion proteins: applications in the study of tyrosine kinase function. *Biochem. Biophys. Res. Commun.* **166:** 90-100.

**Krumholz, L. R., U. Esser and R. D. Simoni (1989).** Nucleotide sequence of the *unc* operon of *Vibrio alginolyticus*. *Nucleic Acids Res.* **17:** 7993-4.

**Krupinski, J. and G. G. Hammes (1986).** Steady-state ATP synthesis by bacteriorhodopsin and chloroplast coupling factor co-reconstituted into asolectin vesicles. *Proc. Natl. Acad. Sci. U S A* **83:** 4233-7.

**Kuki, M., T. Noumi, M. Maeda, A. Amemura and M. Futai (1988).** Functional domains of ε-subunit of *Escherichia coli* $H^+$-ATPase ($F_OF_1$). *J. Biol. Chem.* **263:** 17437-42.

**Kyte, J. and R. F. Doolittle (1982).** A simple method for displaying the hydropathic character of a protein. *J. Mol. Biol.* **157:** 105-32.

**Laemmli, U. K. (1970)**. Cleavage of structural protein during the assembly of the head of bacteriophage T4. *Nature* **227:** 680-685.

**Laget, P. P. and J. B. Smith (1979)**. Inhibitory properties of the endogenous subunit ε in the *Escherichia coli* $F_1$-ATPase. *Arch. Biochem. Biophys.* **197:** 83-89.

**Laroe, D. J. and S. B. Vik (1992)**. Mutations at Glu-32 and His-39 in the ε-subunit of the *Escherichia coli* $F_1F_O$ ATP Synthase Affect Its Inhibitory Properties. *J. Bacteriol.* **174:** 633-637.

**Larson, R. J. and J. B. Smith (1977)**. Assembly of the catalytic unit of the *Escherichia coli* membrane ATPase *in vitro* requires the γ chain. *Biochemistry* **16:** 4266-70.

**Lee, C. and L. Ernster (1965)**. *Biochem. Biophys. Research Commun.* **18:** 523-529.

**Lewis, M. J., J. A. Chang and R. D. Simoni (1990)**. A topological analysis of subunit alpha from *Escherichia coli* $F_1F_O$-ATP synthase predicts eight transmembrane segments. *J. Biol. Chem.* **265:** 10541-50.

**Lien, S. and E. Racker (1971)**. Preparation and Assay of Chloroplast coupling factor $CF_1$. *Methods in Enzymology* **23:** 547-555.

**Lien, S., R. J. Berzborn and E. Racker (1972)**. Partial resolution of the enzymes catalyzing photophosphorylation. IX. Studies on the subunit structure of coupling factor 1 from chloroplasts. *J. Biol. Chem.* **247:** 3520-4.

**Lightowlers, R. N., S. M. Howitt, L. Hatch, F. Gibson and G. B. Cox (1987)**. The proton pore in the *Escherichia coli* $F_OF_1$-ATPase: a requirement for arginine at position 210 of the *a*-subunit. *Biochim. Biophys. Acta* **894:** 399-406.

**Lightowlers, R. N., S. M. Howitt, L. Hatch, F. Gibson and G. Cox (1988).** The proton pore in the *Escherichia coli* $F_OF_1$-ATPase: substitution of glutamate by glutamine at position 219 of the *a*-subunit prevents $F_O$-mediated proton permeability. *Biochim. Biophys. Acta* **933:** 241-8.

**Lill, H. and N. Nelson (1991).** The *atp1* and *atp2* operons of the cyanobacterium *Synechocystis* sp. PCC 6803. *Plant Mol. Biol.* **17:** 641-52.

**Lill, H., A. Burkovski, K. Altendorf, W. Junge and S. Engelbrecht (1993).** Complementation of *Escherichia coli unc* mutant strains by chloroplast and cyanobacterial $F_1$-ATPase subunits. *Biochim. Biophys. Acta* **1144:** 278-84.

**Lill, H., D. Steinemann and N. Nelson (1994).** Mutagenesis of the b'-Subunit of *Synechocystis* Sp PCC 6803 ATP-Synthase. *Biochim. Biophys. Acta* **1184:** 284-290.

**Linnane, A. W. and E. B. Titchener (1960).** Studies on the mechanism of oxidative phosphorylation: 6. A factor for coupled oxidation in the electron transport particle. *Biochim. Biophys. Acta* **39:** 469-478.

**Loo, T. W. and P. D. Bragg (1982).** The DCCD-binding polypeptide is close to the $F_1$ ATPase-binding site on the cytoplasmic surface of the cell membrane of *Escherichia coli*. *Biochem. Biophys. Res. Commun.* **106:** 400-6.

**Luck, D. N., J. K. Ngsee, F. M. Rottman and M. Smith (1986).** Synthesis of bovine prolactin in *Escherichia coli*. *DNA* **5:** 21-8.

**Lunardi, J., M. Satre, M. Bof and P. V. Vignais (1979).** Reactivity of the β-subunit of *Escherichia coli* adenosine triphosphatase with 4-chloro-7-nitrobenzofurazan. *Biochemistry* **18:** 5310-6.

**Lundberg, K. S., D. D. Shoemaker, M. W. Adams, J. M. Short, J. A. Sorge and E. J. Mathur (1991).** High-fidelity amplification using a thermostable DNA polymerase isolated from *Pyrococcus furiosus*. *Gene* **108:** 1-6.

**Lunsdorf, H., K. Ehrig, P. Friedl and H. U. Schairer (1984).** Use of monoclonal antibodies in immuno-electron microscopy for the determination of subunit stoichiometry in oligomeric enzymes. There are three alpha-subunits in the $F_1$-ATPase of *Escherichia coli*. *J. Mol. Biol.* **173:** 131-6.

**Luria, S. E. and J. W. Burrous (1957).** Hybridization between *Escherichia coli* and shigella. *J. Bacteriol.* **74:** 461-476.

**Mabuchi, K., H. Kanazawa, T. Kayano and M. Futai (1981).** Nucleotide sequence of the gene coding for the δ-subunit of proton translocating ATPase *of Escherichia coli. Biochem. Biophys. Res. Commun.* **102:** 172-9.

**Mackle, M. M. and B. A. Zilinskas (1994).** Role of signal peptides in targeting of proteins in cyanobacteria. *J. Bacteriol.* **176:** 1857-64.

**Maggio, M. B., J. Pagan, D. Parsonage, L. Hatch and A. E. Senior (1987).** The defective proton-ATPase of *uncA* mutants of *Escherichia coli.* Identification by DNA sequencing of residues in the α-subunit which are essential for catalysis or normal assembly. *J. Biol. Chem.* **262:** 8981-8984.

**Maggio, M. B., D. Parsonage and A. E. Senior (1988).** A mutation in the α-subunit of $F_1$-ATPase from *Escherichia coli* affects the binding of $F_1$ to the membrane. *J. Biol. Chem.* **263:** 4619-23.

**Manavalan, P. and W. C. J. Johnson (1987).** Variable selection method improves the prediction of protein secondary structure from circular dichroism spectra. *Anal. Biochem.* **167:** 76-85.

**Mares-Guia, M. and E. Shaw (1965).** Studies on the active center of trypsin: the binding of amidines and guanidines as models of the substrate side chain. *J. Biol. Chem* **240:** 1579-1585.

**Marston, F. A. (1986).** The purification of eukaryotic polypeptides synthesized in *Escherichia coli. Biochem. J.* **240:** 1-12.

**Mason, J. G. and P. R. Whitfeld (1990).** The γ-subunit of spinach chloroplast ATP synthase: isolation and characterisation of cDNA and genomic clones. *Plant Mol. Biol.* **14:** 1007-18.

**Matthijs, H. C. P. and H. J. Lubberding (1988).** Dark respiration in cyanobacteria. *Biochemistry of the algae and cyanobacteria.* Oxford, Clarendon Press. 131-145.

**McCarthy, J. E. (1988).** Expression of the *unc* genes in *Escherichia coli*. *J. Bioenerg. Biomembr.* **20:** 19-39.

**McCarty, R. E. and E. Racker (1966).** Effect of a coupling factor and its antiserum on photophosphorylation and hydrogen ion transport. *Brookhaven Symp Biol* **19:** 202-14.

**McCarty, R. E. and E. Racker (1967).** Partial resolution of the enzymes catalyzing photophosphorylation. 2. The inhibition and stimulation of photophosphorylation by N,N´-dicyclohexylcarbodiimide. *J. Biol. Chem.* **242:** 3435-3439.

**McCarty, R. E. and E. Racker (1968).** Partial resolution of the enzymes catalyzing photophosphorylation. 3. Activation of adenosine triphosphatase and $^{32}P$-labeled orthophosphate -adenosine triphosphate exchange in chloroplasts. *J. Biol. Chem.* **243:** 129-37.

**McCarty, R. E. (1992).** A Plant Biochemists View of $H^+$-ATPases and ATP Synthases. *J. Exp. Biol.* **172:** 431-441.

**Mendel-Hartvig, J. and R. A. Capaldi (1991).** Catalytic site nucleotide and inorganic phosphate dependence of the conformation of the ε-subunit in *Escherichia coli* adenosinetriphosphatase. *Biochemistry* **30:** 1278-84.

**Mendel-Hartvig, J. and R. A. Capaldi (1991).** Structure-function relationships of domains of the δ-subunit in *Escherichia coli* adenosine triphosphatase. *Biochim. Biophys. Acta* **1060:** 115-24.

**Mendiola-Morgenthaler, L. R., J. J. Morgenthaler and C. A. Price (1976).** Synthesis of coupling factor $CF_1$ protein by isolated spinach chloroplasts. *FEBS Lett.* **62:** 96-100.

**Merchant, S., S. L. Shaner and B. R. Selman (1983).** Molecular weight and subunit stoichiometry of the chloroplast coupling factor 1 from *Chlamydomonas reinhardi*. *J. Biol. Chem.* **258:** 1026-31.

**Miki, J., M. Maeda, Y. Mukohata and M. Futai (1988).** The γ-subunit of ATP synthase from spinach chloroplasts. Primary structure deduced from the cloned cDNA sequence. *FEBS Letters* **232:** 221-6.

**Mikuni, Y., S. Iwanaga and K. Konishi (1973).** A peptide released from plasma fibrin stabilzing factor in the conversion to the active enzyme by thrombin. *Biochem. Biophys. Res. Commun.* **54:** 1393-403.

**Miller, M. J., D. Fraga, C. R. Paule and R. H. Fillingame (1989).** Mutations in the conserved proline 43 residue of the *uncE* protein (subunit *c*) of *Escherichia coli* $F_1F_O$-ATPase alter the coupling of $F_1$ to $F_O$. *J. Biol. Chem* **264:** 305-11.

**Miller, M. J., M. Oldenburg and R. H. Fillingame (1990).** The essential carboxyl group in subunit *c* of the $F_1F_O$-ATP synthase can be moved and $H^+$-translocating function retained. *Proc. Natl. Acad. Sci. U S A* **87:** 4900-4.

**Mills, J. D., P. Mitchell and P. Schürmann (1980).** Modulation of coupling factor ATPase activity in intact chloroplasts: role of the thioredoxin system. *FEBS Lett.* **112:** 173-177.

**Mills, J. D. and P. Mitchell (1982).** Modulation of coupling factor ATPase activity in intact chloroplasts: reversal of thiol modulation in the dark. *Biochim. Biophys. Acta* **679:** 75-83.

**Mitchell, P. (1961).** Coupling of phosphorylation to electron and hydrogen transfer by a chemi-osmotic type of mechanism. *Nature* **191:** 144-148.

**Monod, J., G. Cohen-Bazire and M. Cohn (1951).** *Biochim. Biophys. Acta* **7:** 585-599.

**Moroney, J. V., C. S. Andreo, R. H. Vallejos and R. E. McCarty (1980).** Uncoupling and energy transfer inhibition of photophosphorylation by sulfhydryl reagents. *J. Biol. Chem.* **255:** 6670-4.

**Moroney, J. V., L. Lopresti, B. F. McEwen, R. E. McCarty and G. G. Hammes (1983).** The $M_r$ value of chloroplast coupling factor 1. *FEBS Lett.* **158:** 58-62.

**Mosher, M. E., L. K. White, J. Hermolin and R. H. Fillingame (1985).** $H^+$-ATPase of *Escherichia coli*. An *uncE* mutation impairing coupling between $F_1$ and $F_O$ but not $F_O$-mediated $H^+$ translocation. *J. Biol. Chem* **260:** 4807-14.

**Munn, A. L. (1988).** Expression of spinach chloroplast ATP synthase genes in *Escherichia coli* K12. PhD Thesis, Australian National University, Canberra, Australia.

**Munn, A. L., P. R. Whitfeld, W. Bottomley, G. S. Hudson, D. A. Jans, F. Gibson and G. B. Cox (1991).** The chloroplast β-subunit allows assembly of the *Escherichia coli* $F_O$ portion of the energy transducing adenosine triphosphatase [published erratum appears in *Biochim. Biophys. Acta* 1991 Dec 3;1098(1):127,129]. *Biochim. Biophys. Acta* **1060:** 82-8.

**Nagai, K. and H. C. Thogersen (1984).** Generation of β-globin by sequence-specific proteolysis of a hybrid protein produced in *Escherichia coli*. *Nature* **309:** 810-2.

**Nagley, P. (1988).** Eukaryote membrane genetics: the $F_O$ sector of mitochondrial ATP synthase. *Trends Genet* **4:** 46-51.

**Nakamaye, K. L. and F. Eckstein (1986).** Inhibition of restriction endonuclease *Nci*I cleavage by phosphorothioate groups and its application to oligonucleotide-directed mutagenesis. *Nucleic Acids Res* **14:** 9679-98.

**Nakamoto, R. K., M. Maeda and M. Futai (1993).** The γ-subunit of the *Escherichia coli* ATP Synthase - Mutations in the Carboxyl-Terminal Region Restore Energy Coupling to the Amino-Terminal Mutant γMet-23->Lys. *J. Biol. Chem.* **268:** 867-872.

**Nakamoto, R. K., M. K. Alshawi and M. Futai (1995).** The ATP synthase γ-subunit - Suppressor mutagenesis reveals three helical regions involved in energy coupling. *J. Biol. Chem.* **270:** 14042-14046.

**Nakamura, S., S. Iwanaga, T. Suzuki, Y. Mikuni and K. Konishi (1974).** Amino acid sequence of the peptide released from bovine factor XIII following activation by thrombin. *Biochem. Biophys. Res. Commun.* **58:** 250-6.

**Nechushtai, R. and N. Nelson (1981).** Photosystem I reaction centers from Chlamydomonas and higher plant chloroplasts. *J. Bioenerg. Biomembr.* **13:** 295-306.

**Nechushtai, R. and N. Nelson (1985).** Biogenesis of Photosystem I reaction centre during greening of oat, bean and spinach leaves. *Plant Mol. Biol.* **4:** 377-384.

**Nelson, N., D. W. Deters, H. Nelson and E. Racker (1973).** Partial resolution of the enzymes catalyzing photophosphorylation. 8. Properties of isolated subunits of coupling factor 1 from spinach chloroplasts. *J. Biol. Chem.* **248:** 2049-55.

**Nelson, N., B. I. Kanner and D. L. Gutnick (1974).** Purification and properties of $Mg^{2+}$-$Ca^{2+}$ adenosinetriphosphatase from *Escherichia coli*. *Proc. Natl. Acad. Sci. U S A* **71:** 2720-4.

**Nelson, N. (1976).** Structure and function of chloroplast ATPase. *Biochim. Biophys. Acta* **456:** 314-38.

**Nelson, N., H. Nelson and G. Schatz (1980).** Biosynthesis and assembly of the proton-translocating adenosine triphosphatase complex from chloroplasts. *Proc. Natl. Acad. Sci. USA* **77:** 1361-1364.

**Nelson, N. (1981).** Proton-ATPase of chloroplasts. *Curr. Top. Bioenerg.* **11:** 1-33.

**Nelson, N. and S. Cidon (1984).** New molecular aspects of energy-transducing protein complexes. *J. Bioenerg. Biomembr.* **16:** 11-36.

**Neumann, J. and A. T. Jagendorf (1964).** Light-induced pH changes related to phosphorylation by chloroplasts. *Arch. Biochem. Biophys.* **107:** 109-119.

**Nicholls, D. G. and S. J. Ferguson (1992).** *Bioenergetics* 2. Academic Press, London

**Nielsen, J., F. G. Hansen, J. Hoppe, P. Friedl and K. von Meyenburg (1981).** The nucleotide sequence of the *atp* genes coding for the $F_O$ subunits *a*, *b*, *c* and the $F_1$ subunit δ of the membrane bound ATP synthase of *Escherichia coli*. *Mol. Gen. Genet.* **184:** 33-9.

**Nielsen, J., B. B. Jorgensen, K. von Meyenburg and F. G. Hansen (1984).** The promoters of the *atp* operon of *Escherichia coli* K12. *Mol Gen Genet* **193:** 64-71.

**Nieuwenhuis, F. J., B. I. Kanner, D. L. Gutnick, P. W. Postma and K. van Dam (1973).** Energy conservation in membranes of mutants of *Escherichia coli* defective in oxidative phosphorylation. *Biochim. Biophys. Acta* **325:** 62-

**Nilsson, B., L. Abrahmsen and M. Uhlen (1985).** Immobilization and purification of enzymes with staphylococcal protein A gene fusion vectors. *EMBO J.* **4:** 1075-80.

**Norris, U., P. E. Karp and A. L. Fimmel (1992).** Mutational analysis of the glycine-rich region of the *c*-subunit of the *Escherichia coli* $F_OF_1$ ATPase. *J. Bacteriol.* **174:** 4496-9.

**Noumi, T., M. Maeda and M. Futai (1987).** Mode of inhibition of sodium azide on $H^+$-ATPase of *Escherichia coli*. *FEBS Lett.* **213:** 381-4.

**Ohta, S., M. Yohda, M. Ishizuka, H. Hirata, T. Hamamoto, H. Y. Otawara, K. Matsuda and Y. Kagawa (1988).** Sequence and over-expression of subunits of adenosine triphosphate synthase in thermophilic bacterium PS3. *Biochim. Biophys. Acta* **933:** 141-55.

**Omote, H., M. Maeda and M. Futai (1992).** Effects of Mutations of Conserved Lys-155 and Thr-156 Residues in the Phosphate-Binding Glycine-Rich Sequence of the $F_1$-ATPase β-subunit of *Escherichia coli*. *J. Biol. Chem.* **267:** 20571-20576.

**Omote, H., M. Y. Park, M. Maeda and M. Futai (1994).** The α/β Subunit Interaction in $H^+$-ATPase (ATP Synthase) - An *Escherichia coli* α-subunit Mutation (Arg-α 296→Cys) Restores Coupling Efficiency to the Deleterious β-subunit Mutant (Ser-β 174→Phe). *J. Biol. Chem.* **269:** 10265-10269.

**Oncley, J. L. (1941).** Evidence from physical chemistry regarding the size and shape of protein molecules from ultracentrifugation, diffusion, viscosity, dielectric dispersion and double refraction of flow. *Ann. N. Y. Acad. Sci.* **41:** 121-149.

**Park, M. Y., H. Omote, M. Maeda and M. Futai (1994).** Conserved Glu-181 and Arg-182 residues of *Escherichia coli* $H^+$-ATPase (ATP synthase) β-subunit are essential for catalysis: Properties of 33 mutants between β Glu-181 and β Lys-801 residues. *J. Biochem. Tokyo* **116:** 1139-1145.

**Parsonage, D., T. M. Duncan, M. S. Wilke, F. A. Kironde, L. Hatch and A. E. Senior (1987).** The defective proton-ATPase of *uncD* mutants of *Escherichia coli*. Identification by DNA sequencing of residues in the β-subunit which are essential for catalysis or normal assembly. *J. Biol. Chem.* **262:** 6301-7.

**Pati, S. and W. S. Brusilow (1989).** The roles of the α- and γ- subunits in proton conduction through the $F_O$ sector of the proton-translocating ATPase of *Escherichia coli*. *J. Biol. Chem.* **264:** 2640-4.

**Pati, S., D. Disilvestre and W. S. A. Brusilow (1992).** Regulation of the *Escherichia coli uncH* Gene by messenger RNA Secondary Structure and Translational Coupling. *Mol. Microbiol.* **6:** 3559-3566.

**Patrie, W. J. and R. E. McCarty (1984).** Specific binding of coupling factor 1 lacking the δ- and ε-subunits to thylakoids. *J. Biol. Chem.* **259:** 11121-8.

**Penefsky, H., A. Datta and M. E. Pullmann (1959).** *Federation Proc.* **23:** 533.

**Penefsky, H., M. E. Pullman, A. Datta and E. Racker (1960).** *J. Biol. Chem* **235:** 3330-3336.

**Perlin, D. S., D. N. Cox and A. E. Senior (1983).** Integration of $F_1$ and the membrane sector of the proton-ATPase of *Escherichia coli*. Role of subunit "*b*" (*uncF* protein). *J. Biol. Chem.* **258:** 9793-800.

**Perlin, D. S., L. R. Latchney, J. G. Wise and A. E. Senior (1984).** Specificity of the proton adenosinetriphosphatase of *Escherichia coli* for adenine, guanine, and inosine nucleotides in catalysis and binding. *Biochemistry* **23:** 4998-5003.

**Perlin, D. S., L. R. Latchney and A. E. Senior (1985).** Inhibition of *Escherichia coli* $H^+$-ATPase by venturicidin, oligomycin and ossamycin. *Biochim. Biophys. Acta* **807:** 238-44.

**Pinchot (1953).** *J. Biol. Chem* **205:** 65-74.

**Porter, A. C. G., C. Kumamoto, K. Aldape and R. D. Simoni (1985).** Role of the *b*-subunit of the *Escherichia coli* proton-translocating ATPase. A mutagenic analysis. *J. Biol. Chem* **260:** 8182-8187.

**Prairie, R. L., T. E. Conover and E. Racker (1963).** *Biochem. Biophys. Res. Commun.* **10:** 422-427.

**Pullmann, M. E., H. Penefsky and E. Racker (1958).** *Arch. Biochem. Biophys.* **76:** 227-230.

**Pullmann, M. E., H. S. Penefsky, A. Datta and E. Racker (1960).** Partial resolution of the enzymes catalyzing photophosphorylation. 1. Purification and properties of soluble, dinitrophenol-stimulated adenosine triphosphatase. *J. Biol. Chem.* **242:** 3435-3439.

**Racker, E. and L. L. Horstman (1967).** Partial resolution of the enzymes catalyzing oxidative phosphorylation. 13. Structure and function of submitochondrial particles completely resolved with respect to coupling factor. *J. Biol. Chem.* **242:** 2547-51.

**Ralston, G. (1993).** Introduction to Analytical Ultracentrifugation. *Beckman Instruments.*

**Rao, R., D. S. Perlin and A. E. Senior (1987).** The defective proton-ATPase of *unc*A mutants of *Escherichia coli*: ATP-binding and ATP-induced conformational change in mutant α-subunits. *Arch. Biochem. Biophys.* **255:** 309-15.

**Rex, G., B. Surin, G. Besse, B. Schneppe and J. E. G. Mccarthy (1994).** The mechanism of translational coupling in *Escherichia coli* - Higher order structure in the *atpHA* mRNA acts as a conformational switch regulating the access of *de novo* initiating ribosomes. *J. Biol. Chem.* **269:** 18118-18127.

**Richter, M. L., W. J. Patrie and R. E. McCarty (1984).** Preparation of the ε-subunit and ε-subunit-deficient chloroplast coupling factor 1 in reconstitutively active forms. *J. Biol. Chem.* **259:** 7371-3.

**Richter, M. L., Z. Gromet-Elhanan and R. E. McCarty (1986).** Reconstitution of the $H^+$-ATPase complex of *Rhodospirillum rubrum* by the β-subunit of the chloroplast coupling factor 1. *J. Biol. Chem.* **261:** 12109-13.

**Roisin, M. P. and A. Kepes (1972).** The membrane ATPase of *Escherichia coli*. I. Ion dependence and ATP-ADP exchange reaction. *Biochim. Biophys. Acta* **275:** 333-46.

**Roisin, M. P. and A. Kepes (1973).** The membrane ATPase of *Escherichia coli*. I. Release into solution, allotopic properties and reconstitution of membrane-bound ATPase. *Biochim. Biophys. Acta* **305:** 249-59.

**Rosing, J. and E. C. Slater (1972).** The value of G° for the hydrolysis of ATP. *Biochim. Biophys. Acta* **267:** 275-90.

**Rosing, J., C. Kayalar and P. D. Boyer (1977).** Evidence for energy-dependent change in phosphate binding for mitochondrial oxidative phosphorylation based on measurements of medium and intermediate phosphate-water exchanges. *J. Biol. Chem.* **252:** 2478-85.

**Rüther, U. and B. Müller-Hill (1983).** Easy identification of cDNA clones. *EMBO J.* **2:** 1791-4.

**Sambrook, J., E. F. Fritsch and T. Maniatis (1989).**Molecular cloning: a laboratory manual. *Cold Spring Harbour Laboratory Press.*

**Sanger, F., S. Nicklen and A. R. Coulson (1977).** DNA sequencing with chain-terminating inhibitors. *Proc. Natl. Acad. Sci. U S A* **74:** 5463-7.

**Saraste, M., N. J. Gay, A. Eberle, M. J. Runswick and J. E. Walker (1981).** The *atp* operon: nucleotide sequence of the genes for the γ-, β-, and ε-subunits of *Escherichia coli* ATP synthase. *Nucleic Acids Res.* **9:** 5287-96.

**Satre, M., G. Klein and P. V. Vignais (1978).** Isolation of *Escherichia coli* mutants with an adenosine triphosphatase insensitive to aurovertin. *J. Bacteriol.* **134:** 17-23.

**Satre, M., M. Bof and P. V. Vignais (1980).** Interaction of *Escherichia coli* adenosine triphosphatase with aurovertin and citreoviridin: inhibition and fluorescence studies. *J. Bacteriol.* **142:** 768-76.

**Satre, M., M. Bof, J. P. Issartel and P. V. Vignais (1982).** Chemical modification of $F_1$-ATPase by dicyclohexylcarbodiimide: application to analysis of the stoichiometry of subunits in *Escherichia coli* $F_1$. *Biochemistry* **21:** 4772-6.

**Sayers, J. R., W. Schmidt and F. Eckstein (1988).** 5'-3' exonucleases in phosphorothioate-based oligonucleotide-directed mutagenesis. *Nucleic Acids Res* **16:** 791-802.

**Sayers, J. R. and F. Eckstein (1990).** Properties of overexpressed phage T5 D15 exonuclease. Similarities with *Escherichia coli* DNA polymerase I 5'-3' exonuclease. *J. Biol. Chem.* **265:** 18311-7.

**Scarpetta, M. A., C. A. Hawthorne and W. S. Brusilow (1991).** Characterization of semi-uncoupled hybrid *Escherichia coli-Bacillus megaterium* $F_1F_O$ proton-translocating ATPases. *J. Biol. Chem.* **266:** 18567-72.

**Schauder, B., H. Blocker, R. Frank and J. E. McCarthy (1987).** Inducible expression vectors incorporating the *Escherichia coli atpE* translational initiation region. *Gene* **52:** 279-83.

**Schmid, R., N. Shavit and W. Junge (1976).** The coupling factor of photophosphorylation and the electric properties of the thylakoid membrane. *Biochim. Biophys. Acta* **430:** 145-53.

**Schmidt, G., A. J. W. Rodgers, S. M. Howitt, A. L. Munn, G. S. Hudson, T. A. Holten, P. R. Whitfeld, W. Bottomley, F. Gibson and G. B. Cox (1990).** The chloroplast $CF_OI$ subunit can replace the *b*-subunit of the $F_OF_1$-ATPase in a mutant strain of *Escherichia coli* K12 [retracted by Schmidt G., Rodgers A.J.W., Howitt S.M., Munn A.L., Hudson G.S., Holten T.A., Whitfeld P.R., Bottomley W., Gibson F., Cox G.B. In: *Biochim. Biophys. Acta* (1994) Jan 4;1183(3):563]. *Biochim. Biophys. Acta* **1015:** 195-9.

**Schmidt, G. (1992).** Expression of Subunit-II of Chloroplast $H^+$-ATPase in an *Escherichia coli* Mutant Lacking Subunit-*b* of Its $H^+$-ATPase. *Acta Physiol. Scand.* **146:** 275-278.

**Schneider, E. and K. Altendorf (1984).** Subunit *b* of the membrane moiety ($F_0$) of ATP synthase ($F_1F_0$) from *Escherichia coli* is indispensible for $H^+$-translocation and binding of the water-soluble $F_1$ moiety. *Proc. Natl. Acad. Sci. USA* **81:** 7279-7283.

**Schneider, E. and K. Altendorf (1985).** All three subunits are required for the reconstitution of an active proton channel ($F_0$) of *Escherichia coli* ATP synthase ($F_1F_0$). *EMBO J.* **4:** 515-518.

**Schneppe, B., G. Deckers-Hebestreit, J. E. McCarthy and K. Altendorf (1991).** Translation of the first gene of the *Escherichia coli unc* operon. Selection of the start codon and control of initiation efficiency. *J. Biol. Chem.* **266:** 21090-21098.

**Sebald, W., P. Friedl, H. U. Schairer and J. Hoppe (1982).** Structure and genetics of the $H^+$-conducting $F_O$ portion of the ATP synthase. *Ann. N. Y. Acad. Sci.* **402:** 28-44.

**Senior, A. E., D. R. Fayle, J. A. Downie, F. Gibson and G. B. Cox (1979).** Properties of membranes from mutant strains of *Escherichia coli* in which the β-subunit of the adenosine triphosphatase is abnormal. *Biochem. J.* **180:** 111-118.

**Senior, A. E., J. A. Downie, G. B. Cox, F. Gibson, L. Langman and D. R. Fayle (1979).** The *uncA* gene codes for the α-subunit of the adenosine triphosphatase of *Escherichia coli*. Electrophoretic analysis of *uncA* mutant strains. *Biochem. J.* **180:** 103-9.

**Senior, A. E. (1983).** Secondary and tertiary structure of membrane proteins involved in proton translocation. *Biochim. Biophys. Acta* **726:** 81-95.

**Senior, A. E., L. R. Latchney, A. M. Ferguson and J. G. Wise (1984).** Purification of $F_1$-ATPase with impaired catalytic activity from partial revertants of *Escherichia coli uncA* mutant strains. *Arch. Biochem. Biophys.* **228:** 49-53.

**Senior, A. E. (1988).** ATP synthesis by oxidative phosphorylation. *Physiol. Rev.* **68:** 177-231.

**Senior, A. E. (1990).** The proton-translocating ATPase of *Eschericia coli*. *Ann. Rev. Biophys. Biophys. Chem.* **19:** 7.

**Senior, A. E., S. Wilke-Mounts and M. K. Alshawi (1993).** Lysine-155 in β-Subunit Is a Catalytic Residue of *Escherichia coli* $F_1$-ATPase. *J. Biol. Chem.* **268:** 6989-6994.

**Shepard, H. M., E. Yelverton and D. V. Goeddel (1982).** Increased synthesis in *E. coli* of fibroblast and leukocyte interferons through alterations in ribosome binding sites. *DNA* **1:** 125-31.

**Shin, K., R. K. Nakamoto, M. Maeda and M. Futai (1992).** $F_OF_1$-ATPase γ-subunit Mutations Perturb the Coupling Between Catalysis and Transport. *J. Biol. Chem.* **267:** 20835-20839.

**Shine, J. and L. Dalgarno (1974).** The 3'-terminal sequence of *Escherichia coli* 16S ribosomal RNA: complementarity to nonsense triplets and ribosome binding sites. *Proc. Natl. Acad. Sci. U S A* **71:** 1342-6.

**Skakoon, E. N. and S. D. Dunn (1993).** Location of Conserved Residue Histidine-38 of the ε-subunit of *Escherichia coli* ATP Synthase. *Arch. Biochem. Biophys.* **302:** 272-278.

**Skakoon, E. N. and S. D. Dunn (1993).** Orientation of the ε-subunit in *Escherichia coli* ATP Synthase. *Arch. Biochem. Biophys.* **302:** 279-284.

**Smith, R. A., L. R. Latchney and A. E. Senior (1985).** Tight divalent metal binding to *Escherichia coli* $F_1$-adenosinetriphosphatase. Complete substitution of intrinsic magnesium by manganese or cobalt and studies of metal binding sites. *Biochemistry* **24:** 4490-4.

**Smith, D. B., K. M. Davern, P. G. Board, W. U. Tiu, E. G. Garcia and G. F. Mitchell (1986).** $M_r$ 26,000 antigen of *Schistosoma japonicum* recognized by resistant WEHI 129/J mice is a parasite glutathione S-transferase. *Proc. Natl. Acad. Sci. U S A* **83:** 8703-7.

**Smith, D. B. and K. S. Johnson (1988).** Single-step purification of polypeptides expressed in *Escherichia coli* as fusions with glutathione S-transferase. *Gene* **67:** 31-40.

**Soga, S., T. Noumi, M. Takeyama, M. Maeda and M. Futai (1989).** Mutational replacements of conserved amino acid residues in the α-subunit change the catalytic properties of *Escherichia coli* $F_1$-ATPase. *Arch. Biochem. Biophys.* **268:** 643-8.

**Solomon, A. K. (1962).** Ion transport in single cell populations. *Biophys. J.* **2:** 79-95.

**Solomon, K. A., D. K. Hsu and W. S. Brusilow (1989).** Use of *lacZ* fusions to measure *in vivo* expression of the first three genes of the *Escherichia coli unc* operon. *J. Bacteriol.* **171:** 3039-45.

**Soteropoulos, P., K. H. Süss and R. E. McCarty (1992).** Modifications of the γ-subunit of chloroplast coupling factor 1 alter interactions with the inhibitory ε-subunit. *J. Biol. Chem.* **267:** 10348-54.

**Soteropoulos, P., A. M. Ong and R. E. Mccarty (1994).** Alkylation of cysteine 89 of the γ-subunit of chloroplast coupling factor 1 with N-ethylmaleimide alters nucleotide interactions. *J. Biol. Chem.* **269:** 19810-19816.

**Stack, A. E. and B. D. Cain (1994).** Mutations in the δ-subunit Influence the Assembly of $F_1F_O$ ATP Synthase in *Escherichia coli*. *J. Bacteriol.* **176:** 540-542.

**Stanier, R. Y. and G. Cohen-Bazire (1977).** Phototrophic prokaryotes: the cyanobacteria. *Ann. Rev. Microbiol.* **31:** 225-74.

**Stanley, K. K. and J. P. Luzio (1984).** Construction of a new family of high efficiency bacterial expression vectors: identification of cDNA clones coding for human liver proteins. *EMBO J.* **3:** 1429-34.

**Steffens, K., J. Hoppe and K. Altendorf (1987).** $F_O$ part of the ATP synthase from *Escherichia coli*. Influence of subunits *a*, and *b*, on the structure of subunit *c*. *Eur. J. Biochem.* **170:** 627-630.

**Sternweis, P. C. and J. B. Smith (1977).** Characterization of the purified membrane attachment (δ) subunit of the proton translocating adenosine triphosphatase from *Escherichia coli*. *Biochemistry* **16:** 4020-5.

**Sternweis, P. C. (1978).** The ε-subunit of *Escherichia coli* coupling factor 1 is required for its binding to the cytoplasmic membrane. *J. Biol. Chem.* **253:** 3123-8.

**Süss, K. H. and O. Schmidt (1982).** Evidence for a $\alpha_3$, $\beta_3$, $\gamma$, I, II, $\varepsilon$, $III_5$ subunit stoichiometry of chloroplast ATP synthetase complex ($CF_1CF_O$). *FEBS Lett.* **144:** 213-218.

**Takabe, T. and G. G. Hammes (1981).** pH dependence of adenosine 5'-triphosphate synthesis and hydrolysis catalyzed by reconstituted chloroplast coupling factor. *Biochemistry* **20:** 6859-64.

**Takeda, K., M. Hirano, H. Kanazawa, N. Nukiwa, Y. Kagawa and M. Futai (1982).** Hybrid ATPase's formed from subunits of coupling factor $F_1$'s of *Escherichia coli* and thermophilic bacterium PS3. *J. Biochem. Tokyo* **91:** 695-701.

**Tang, C. L., S. Wilkens and R. A. Capaldi (1994).** Structure of the γ-subunit of *Escherichia coli* $F_1$-ATPase Probed in Trypsin Digestion and Biotin-Avidin Binding Studies. *J. Biol. Chem.* **269:** 4467-4472.

**Taylor, J. W., J. Ott and F. Eckstein (1985).** The rapid generation of oligonucleotide-directed mutations at high frequency using phosphorothioate-modified DNA. *Nucleic Acids Res* **13:** 8765-85.

**Taylor, J. W., W. Schmidt, R. Cosstick, A. Okruszek and F. Eckstein (1985).** The use of phosphorothioate-modified DNA in restriction enzyme reactions to prepare nicked DNA. *Nucleic Acids Res* **13:** 8749-64.

**Tittgen, J., J. Hermans, J. Steppuhn, T. Jansen, C. Jansson, B. Andersson, R. Nechushtai, N. Nelson and R. G. Herrmann (1986).** Isolation of cDNA clones for fourteen nuclear-encoded thylakoid membrane proteins. *Mol. Gen. Genet.* **204:** 258-265.

**Tozer, R. G. and S. D. Dunn (1987).** The ε-subunit and inhibitory monoclonal antibodies interact with the carboxyl-terminal region of the β-subunit of *Escherichia coli* $F_1$-ATPase. *J. Biol. Chem.* **262:** 10706-11.

**Tsuchiya, T. and B. P. Rosen (1975).** Energy transduction in *Escherichia coli*. The role of the $Mg^{2+}$ATPase. *J. Biol. Chem.* **250:** 8409-15.

**Turina, P. and R. A. Capaldi (1994).** ATP binding causes a conformational change in the γ-subunit of the *Escherichia coli* $F_1$ATPase which is reversed on bond cleavage. *Biochemistry* **33:** 14275-14280.

**Turina, P. and R. A. Capaldi (1994).** ATP Hydrolysis-Driven Structural Changes in the γ-Subunit of *Escherichia coli* ATPase Monitored by Fluorescence from Probes Bound at Introduced Cysteine Residues. *J. Biol. Chem.* **269:** 13465-13471.

**Vambutas, V. K. and E. Racker (1965).** Partial Resolution of the enzymes catalyzing Photophosphorylation I: Stimulation of photophosphorylation by a preparation of a latent $Ca^{++}$ dependent adenosine triphosphatase from chloroplasts. *J. Biol. Chem.* **240:** 2660-2667.

**Van Walraven, H. S., R. Lutter and J. E. Walker (1993).** Organization and Sequences of Genes for the Subunits of ATP Synthase in the Thermophilic Cyanobacterium-*Synechococcus* 6716. *Biochem. J.* **294:** 239-251.

**Verheijen, J. H., P. W. Postma and K. van Dam (1978).** Specific labelling of the ($Ca^{2+}$ + $Mg^{2+}$)-ATPase of *Escherichia coli* with 8-azido-ATP and 4-chloro-7-nitrobenzofurazan. *Biochim. Biophys. Acta* **502:** 345-53.

**Vieira, J. and J. Messing (1982).** The pUC plasmids, an M13mp7-derived system for insertion mutagenesis and sequencing with synthetic universal primers. *Gene* **19:** 259-68.

**Vik, S. B. and R. D. Simoni (1987).** $F_1F_O$-ATPase from *Escherichia coli* with mutant $F_O$ subunits. Partial purification and immunoprecipitation of $F_1F_O$ complexes. *J. Biol. Chem.* **262:** 8340-6.

**Von Meyenburg, K., B. B. Jorgensen, J. Nielsen and F. G. Hansen (1982).** Promoters of the *atp* operon coding for the membrane-bound ATP synthase of *Escherichia coli* mapped by Tn10 insertion mutations. *Mol. Gen. Genet.* **188:** 240-8.

**Walker, J. E., M. Saraste, M. J. Runswick and N. J. Gay (1982).** Distantly related sequences in the α- and β-subunits of ATP synthase, myosin, kinases and other ATP-requiring enzymes and a common nucleotide binding fold. *EMBO J.* **1:** 945-51.

**Walker, J. E., A. Eberle, N. J. Gay, M. J. Runswick and M. Saraste (1982).** Conservation of structure in proton-translocating ATPases of *Escherichia coli* and mitochondria. *Biochem. Soc. Trans.* **10:** 203-6.

**Walker, J. E. and N. J. Gay (1983).** Analysis of *Escherichia coli* ATP synthase subunits by DNA and protein sequencing. *Methods Enzymol.* **97:** 195-218.

**Walker, J. E., M. Saraste and N. J. Gay (1984).** The *unc* operon. Nucleotide sequence, regulation and structure of ATP-synthase. *Biochim. Biophys. Acta* **768:** 164-200.

**Walker, J. E., I. M. Fearnley, N. J. Gay, B. W. Gibson, F. D. Northrop, S. J. Powell, M. J. Runswick, M. Saraste and V. L. Tybulewicz (1985).** Primary structure and subunit stoichiometry of $F_1$-ATPase from bovine mitochondria. *J. Mol. Biol.* **184:** 677-701.

**Weber, J., S. Wilke-Mounts, R. S. F. Lee, E. Grell and A. E. Senior (1993).** Specific Placement of Tryptophan in the Catalytic Sites of *Escherichia coli* $F_1$-ATPase Provides a Direct Probe of Nucleotide Binding - Maximal ATP Hydrolysis Occurs with Three Sites Occupied. *J. Bio. Chem.* **268:** 20126-20133.

**Weber, J., S. Wilke-Mounts, E. Grell and A. E. Senior (1994).** Tryptophan Fluorescence Provides a Direct Probe of Nucleotide Binding in the Noncatalytic Sites of *Escherichia coli* $F_1$-ATPase. *J. Biol. Chem.* **269:** 11261-11268.

**Wernergrune, S., D. Gunkel, J. Schumann and H. Strotmann (1994).** Insertion of a "chloroplast-like" regulatory segment responsible for thiol modulation into γ-subunit of $F_OF_1$-ATPase of the cyanobacterium *Synechocystis* 6803 by mutagenesis of *atpC*. *Mol. Gen. Genet.* **244:** 144-150.

**Westhoff, P., N. Nelson, H. Bünemann and R. G. Herrmann (1981).** Localization of genes for coupling factor subunits on the spinach plastid chromosome. *Current Genetics* **4:** 109-120.

**Westhoff, P., J. Alt, N. Nelson and R. G. Herrmann (1985).** Genes and transcripts for the ATP synthase $CF_O$ subunits I and II from spinach thylakoid membranes. *Mol. Gen. Genet.* **199:** 290-299.

**Wetzel, C. M. and R. E. McCarty (1993).** Aspects of Subunit Interactions in the Chloroplast ATP Synthase .1: Isolation of a Chloroplast Coupling Factor 1-Subunit-III Complex from Spinach Thylakoids. *Plant Physiol* **102:** 241-249.

**Wetzel, C. M. and R. E. McCarty (1993).** Aspects of Subunit Interactions in the Chloroplast ATP Synthase .2: Characterization of a Chloroplast Coupling Factor 1-Subunit-III Complex from Spinach Thylakoids. *Plant Physiol.* **102:** 251-259.

**Whitehorn, E. A., K. J. Livak and S. R. J. Petteway (1985).** The effects of hybrid ribosome-binding-site variants on the expression of human interferon-β in *Escherichia coli*. *Gene* **36:** 375-9.

**Wilke-Mounts, S., J. Weber, E. Grell and A. E. Senior (1994).** Tryptophan-Free *Escherichia coli* $F_1$-ATPase. *Arch. Biochem. Biophys.* **309:** 363-368.

**Wilkens, S., S. D. Dunn and R. A. Capaldi (1994).** A cryoelectron microscopy study of the interaction of the *Escherichia coli* $F_1$-ATPase with subunit *b* dimer. *FEBS Lett.* **354:** 37-40.

**Winget, G. D., N. Kanner and E. Racker (1977).** Formation of ATP by the adenosine triphosphatase complex from spinach chloroplasts reconstituted together with bacteriorhodopsin. *Biochim. Biophys. Acta* **460:** 490-9.

**Wise, J. G., L. R. Latchney and A. E. Senior (1981).** The defective proton-ATPase of *uncA* mutants of *Escherichia coli*. Studies of nucleotide binding sites, bound aurovertin fluorescence, and labeling of essential residues of the purified $F_1$-ATPase. *J. Biol. Chem.* **256:** 10383-9.

**Wise, J. G., T. M. Duncan, L. R. Latchney, D. N. Cox and A. E. Senior (1983).** Properties of $F_1$-ATPase from the *uncD412* mutant of *Escherichia coli*. *Biochem. J.* **215:** 343-50.

**Wise, J. G., L. R. Latchney, A. M. Ferguson and A. E. Senior (1984).** Defective proton ATPase of *uncA* mutants of *Escherichia coli*. 5'-Adenylyl imidodiphosphate binding and ATP hydrolysis. *Biochemistry* **23:** 1426-32.

**Wise, J. G. and A. E. Senior (1985).** Catalytic properties of the *Escherichia coli* proton adenosinetriphosphatase: evidence that nucleotide bound at noncatalytic sites is not involved in regulation of oxidative phosphorylation. *Biochemistry* **24:** 6949-54.

**Wood, J. M., J. G. Wise, A. E. Senior, M. Futai and P. D. Boyer (1987).** Catalytic properties of the $F_1$-adenosine triphosphatase from *Escherichia coli* K-12 and its genetic variants as revealed by $^{18}O$ exchanges. *J. Biol. Chem.* **262:** 2180-6.

**Xiao, J. P. and R. E. McCarty (1989).** Binding of chloroplast coupling factor 1 deficient in the δ-subunit to thylakoid membranes. *Biochim. Biophys. Acta* **976:** 11121-11128.

**Xie, D. L., H. Lill, G. Hauska, M. Maeda, M. Futai and N. Nelson (1993).** The *atp2* Operon of the Green Bacterium *Chlorobium limicola*. *Biochim. Biophys. Acta* **1172:** 267-273.

**Xue, Z. X., C. G. Miller, J. M. Zhou and P. D. Boyer (1987).** Catalytic and noncatalytic nucleotide binding sites of chloroplast $F_1$ ATPase. Photoaffinity labeling and peptide sequencing. *FEBS Lett.* **223:** 391-4.

**Xue, Z. X., J. M. Zhou, T. Melese, R. L. Cross and P. D. Boyer (1987).** Chloroplast $F_1$ ATPase has more than three nucleotide binding sites, and 2-azido-ADP or 2-azido-ATP at both catalytic and noncatalytic sites labels the beta subunit. *Biochemistry* **26:** 3749-53.

**Yoshida, M., W. S. Allison, F. S. Esch and M. Futai (1982).** The specificity of carboxyl group modification during the inactivation of the *Escherichia coli* $F_1$-ATPase with dicyclohexyl[$^{14}$C]carbodiimide. *J. Biol. Chem.* **257:** 10033-7.

**Younis, H. M. and G. D. Winget (1977).** $CF_1$-dependent restoration of energy-linked reactions reconstituted with a hydrophobic protein from spinach chloroplasts. *Biochem. Biophys. Res. Commun.* **77:** 168-74.

**Zhang, Y., M. Oldenburg and R. H. Fillingame (1994).** Suppressor Mutations in $F_1$ Subunit ε Recouple ATP-Driven $H^+$ Translocation in Uncoupled Q42E Subunit *c* Mutant of *Escherichia coli* $F_1F_O$ ATP Synthase. *J. Biol. Chem.* **269:** 10221-10224.

**Ziegler, M., R. Xiao and H. S. Penefsky (1994).** Close Proximity of Cys64 and Cys140 in the δ-subunit of *Escherichia coli* $F_1$-ATPase. *J. Biol. Chem.* **269:** 4233-4239.

**Zurawski, G., W. Bottomley and P. R. Whitfeld (1982).** Structures of the genes for the β- and ε-subunits of spinach chloroplast ATPase indicate a dicistronic mRNA and an overlapping translation stop/start signal. *Proc. Natl. Acad. Sci. USA* **79:** 6260-6264.